Investigation of inducible nitric oxide synthase in an experimental model of chronic heart failure

Alyson Anne Miller

PhD-The University of Edinburgh-2001

I dedicate this thesis to my sister
Gillian with love

Declaration

I hereby declare that the work described in this thesis was performed entirely by myself, and that it has not been accepted in any previous application for a degree.

Alyson A. Miller

Acknowledgments

I would first of all like to thank my principal supervisor Dr. Gillian Gray for her continual advice and encouragement throughout my PhD. To Dr. Ian Megson, my second supervisor, I am thankful for his presence and source of motivation throughout my PhD, and not to forget his humour and vitality, not only in the laboratory but in the pub as well. Thank you to the Medical Research Council for their financial support. There are a number of people who I have worked within the laboratory that I would like to acknowledge, these include Pauline McEwan, Mark Miller, Isam Sharif, Mark Patrizio and Manuela Reicht, who have all helped in their special ways. Of course, my biggest thanks must go to Lorcan Sherry for his charm, wit and most importantly, his steadfast support over the past three years. Thank you to Darren Downing for his computing expertise and for all those Jack Daniels he bought me over the past three years.

Thank you to all my friends in Edinburgh and those who are no longer here. Eilis, Ian and Heather were always a source of distraction in those early days, thanks guys. A special thank you must go to my flatmate Hazel and to Catherine, Gillian, Elaine and Derek who have helped me through the past few months by simply being there. Finally, I would like to say thanks to my parents and sister for their constant support throughout my university career.

Abstract

Impaired nitric oxide (NO)-mediated vasodilatation has been implicated in the increased peripheral vascular resistance (PVR) associated with chronic heart failure (CHF). However, there is evidence that basal synthesis of NO may be preserved or even enhanced in CHF, perhaps due to the expression of the inducible NO synthase (iNOS). Increased superoxide production has been demonstrated in CHF and, since superoxide destroys NO, a reduction in NO bioavailability may be responsible for impaired NO-mediated relaxations and may also explain why PVR remains elevated despite increased NO production. Therefore, the aims of this thesis were to investigate the expression of iNOS in the cardiovascular system in rats with CHF following coronary artery ligation, to determine the functional significance of this potential source of NO on responsiveness of the peripheral vasculature and to investigate the role that superoxide plays in modulating vascular function.

Immunohistochemical studies revealed that iNOS was expressed in all cell types of small mesenteric arteries and in thoracic aortae from CHF rats. iNOS was also identified in coronary vascular and endocardial endothelial cells in hearts from CHF rats. Intense immunoreactive iNOS was also found throughout the viable left ventricular myocardium of hearts from CHF rats. No staining was found in arteries or hearts from sham-operated rats.

Prior to commencing functional studies, the pharmacological properties of the novel iNOS inhibitor, *N*-(3-(Aminomethyl) benzyl) acetamidine dihydrochloride (1400W), and the cell permeable superoxide dismutase mimetic, Mn [III] tetrakis [1-methyl-4-pyridyl] porphyrin (MnTMPyP) were investigated. Experiments revealed that 1400W was a selective iNOS inhibitor and that MnTMPyP was an effective SOD mimetic.

Despite the presence of iNOS, endothelium-intact small mesenteric arteries (300 – 350 μm) from CHF rats were hyperesponsive to phenylephrine (PE). Both 1400W and MnTMPyP reversed the hyperesponsiveness. Furthermore, the NOS substrate, L-arginine reduced responsiveness to PE of endothelium-denuded arteries

from CHF rats. None of these drugs altered responses to PE in arteries from sham-operated rats. Endothelium-dependent relaxations were impaired in arteries from CHF rats but were restored by MnTMPyP. These results suggest that substrate deficient, iNOS-derived superoxide may be responsible for this vascular dysfunction of small mesenteric arteries in this model of CHF.

In endothelium-intact thoracic aortic rings from CHF rats, 1400W has no significant effect on vascular responsiveness to norepinephrine (NE). Supplementation of endothelium-denuded aortic rings from CHF rats but not sham-operated rats with L-arginine, resulted in a significant reduction in responsiveness to NE. However, MnTMPyP had no significant effect on responsiveness of endothelium-intact aortic rings from CHF rats. These results suggest that despite being substrate deficient, iNOS plays no role in modulating vascular responsiveness in conductance arteries in this model of CHF.

The salient finding of this thesis is that iNOS is expressed in the peripheral vasculature and in the heart in this model of CHF. However, in small mesenteric arteries, which play a pivotal role in determining PVR, substrate deficient iNOS-derived superoxide is responsible for increased responsiveness of these arteries. In the thoracic aortae, however, iNOS appears to play no role in modulating vascular function. In conclusion, the findings of this thesis may represent an important mechanism for the raised PVR and endothelial dysfunction associated with CHF.

Publications

Abstracts and presentations:

MILLER, A.A., MEGSON, I.L. & GRAY, G.A. (1998). Vascular reactivity in conductance and resistance arteries in septic shock. Poster presentation at the 'Scottish Cardiovascular Forum', 2nd annual meeting, Edinburgh, September, 1998.

MILLER, A.A., MEGSON, I.L. & GRAY, G.A. (1999). Increased vascular responsiveness in a rat model of chronic heart failure, *Acta Physiologica Scandinavia*, **167**, Suppl 645. Poster presentation at the 'Biology of Nitric Oxide', 6th International Meeting, Stockholm, September 1999.

MILLER, A.A., MEGSON, I.L. & GRAY, G.A. (1999). Vascular Nitric Oxide System during Chronic Heart Failure. Oral presentation at the Scottish Nitric Oxide Workshop, 2nd Annual Meeting, St. Andrews, November 1999.

Full Paper

MILLER, A.A., MEGSON, I.L. & GRAY, G.A. (1999). Inducible nitric oxide synthase-derived superoxide contributes to hyporeactivity in small mesenteric arteries from a rat model of chronic heart failure, *British Journal of Pharmacology*, **131** (1), 29 – 36

Paper in Preparation

MILLER, A.A., REICHT, M., MEGSON, I.L. & GRAY, G.A. (2001). Investigation of the pharmacological selectivity of the novel inducible nitric oxide synthase inhibitor 1400W *in vitro*

Table of Contents

Table of Figures

List of Abbreviations

1400W	*N*-(3-(Aminomethyl)benzyl)acetamidine dihydrochloride
5-HT	5-hydroxytryptamine
ANOVA	analysis of variance
ACE	angiotensin converting enzyme
ACh	acetylcholine
ANP	atrial natriuretic peptide
AVP	arginine vasopressin
BH_4	(6R)-5,6,7,8-tetrahydrobiopterin
BNP	brain natriuretic peptide
BSA	bovine serum albumin
cAMP	cyclic 3', 5' adenosine monophosphate
CAD	coronary artery disease
CAL	coronary artery ligation
CHF	chronic heart failure
CRC	concentration response curve
cGMP	cyclic 3', 5' guanosine monophosphate
DETCA	detca diethyldithocarbamate
EDHF	endothelium-derived hyperpolarizing factor
EDRF	endothelium-derived relaxing factor
EDV	end-diastolic volume
eNOS	endothelial nitric oxide synthase

ET-1	endothelin-1
FAD	flavin adenine dinucleotide
FMN	flavin monophosphate
SGC	soluble guanylate cyclase
GTP	guanosine triphosphate
H_2O_2	hydrogen peroxide
iNOS	inducible nitric oxide synthase
IL-1	interleukin-1
IL-6	interleukin-6
IP_3	inositol 1,4,5-triphosphate
L-NAME	N^G-nitro-L-arginine methyl ester
L-NMMA	N^G-monomethyl-L-arginine
LPS	bacterial lipopolysaccharide
LV	left ventricular
MAP	mean arterial blood pressure
MI	myocardial infarction
MnTMPyP	Mn[III]tetrakis[1-methyl-4-pyridyl]porphyrin
NADP	nicotinamide adenine dinucleotide phosphate
NADPH	reduced nicotinamide adenine dinucleotide phosphate
nNOS	neuronal nitric oxide synthase
NO	nitric oxide
NO_2^-	nitrite
NO_3^-	nitrate
NE	norepinephrine

NYHA	New York Heart Association
$ONOO^-$	peroxynitrite
PBITU	S'S'-(1,3-phenylenebis(1,2 ethanediyl)bisisothiourea
PBS	phosphate buffered saline
pD_2	negative logarithm of the agonist concentration that results in a half maximal constriction or relaxation
PE	phenylephrine
PGI_2	prostacyclin
PKA	protein kinase A
PKB	protein kinase B
PKC	protein kinase C
PVR	peripheral vascular resistance
RAAS	renin-angiotensin-aldosterone system
TBS	tris-buffered saline
TGF-β	transforming growth factor-β
SNP	sodium nitroprusside
TNF-α	tumour necrosis factor-α
VSM	vascular smooth muscle

Chapter 1

General Introduction

1.1 The heart

1.1.1 Overview of Anatomy

The wall of the heart is composed of three layers, the inner endocardium which consists of a layer of endothelial cells, the middle layer, myocardium, which consists of cardiac muscle, and finally the pericardium, a two layered serous membrane enclosing the the whole heart. The myocardium is composed of various cells types including myocardial cells, specialised 'conducting' cells, endothelial cells, vascular smooth muscle (VSM) cells and connective tissue. The heart is divided into four chambers: the right and left ventricles and the right and left atria, with the right side of the heart being separated from the left side by a muscular wall called the interventricular septum. It is the myocardial cells in the ventricles that are responsible for pumping blood throughout the body.

Collagen is found in the extracellular space of the myocardium, and serves to support and align myocytes, blood vessels and lymphatic vessels, preserving the architecture of the myocardium. The network of collagen also prevents cardiac myocyte slippage and over stretching. The cardiac connective tissue also includes fibroblasts, which produce components of the extracellular matrix, namely collagen and fibronectin.

The blood being pumped through the heart chambers does not exchange nutrients and metabolic waste products with the myocardial cells. They, like the cells of all other organs, receive blood via arteries that branch off the aorta. Two major coronary arteries run from the base of the aorta to the left and right ventricles, respectively. These arteries then branch into smaller arteries, which run down the surface of the heart towards the apex. The major branch of the left coronary artery, which supplies blood to the left ventricle, is called the left anterior descending coronary artery (***Figure 1.1***). The control of the myocardial oxygen supply lies in the coronary arterioles, which keep branching until the very small, thin-walled capillaries are formed. It is here that transfer of oxygen from oxygenated arterial blood to the myocardial tissues occurs. Endothelial cells in the atrial and ventricular myocardium

form the lining of both coronary vessels and the fine coronary capillary network that runs throughout the myocardium, these endothelial cells being termed myoendothelial cells. At the level of the coronary microvasculature, there is close contact between endothelial cells and cardiac myocytes throughout the heart, with no cardiac myocyte being more that 2-3 μm from a coronary vascular endothelial cell (Shah & MacCarthy, 2000).

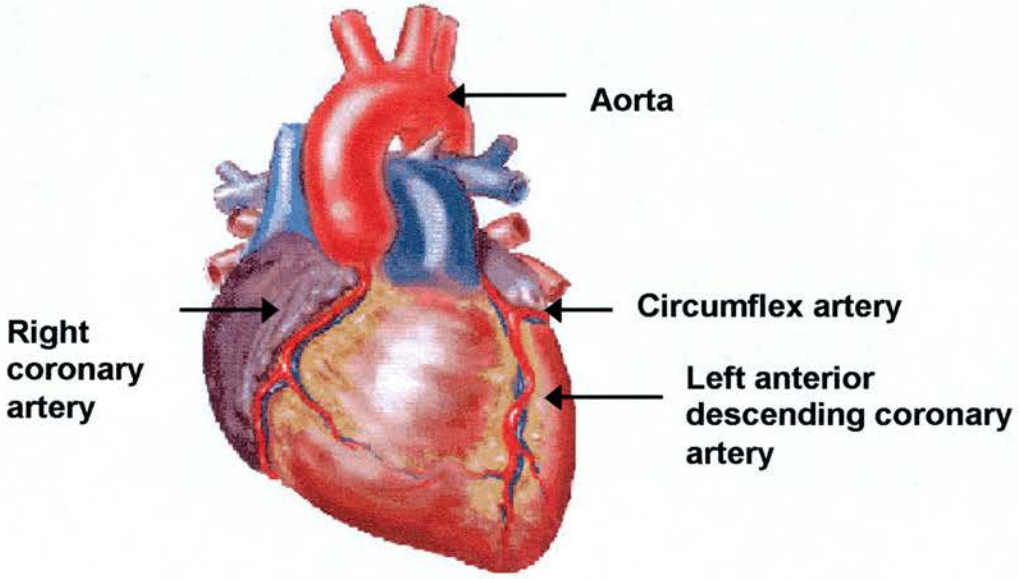

Figure 1.1 *Diagram of the heart showing major coronary blood vessels of the myocardium, including right coronary artery, left anterior descending coroanry artery and circumflex artery.*

1.1.2 The cardiac cycle

The cardiac events occurring from the beginning of one heartbeat to the beginning of the next constitute the *cardiac cycle*. In terms of mechanics, the cycle is divided into two major phases, both named after the events that occur in the ventricles: the period of ventricular contraction and blood ejection, **systole**, followed by a period of ventricular relaxation and blood filling, **diastole**. Each cycle is initiated by the spontaneous generation of an action potential in the sinoatrial node. The action

potential travels through the atrium, resulting in both atria contracting almost simultaneously. The action potential then travels through the atrioventricular (AV) node, the bundle of His and eventually via the Purkinje fibres. The Purkinje fibres rapidly distribute the impulse to the ventricles more or less simultaneously, ensuring a single coordinated contraction.

1.1.3 Control of the heart

Cardiac output is determined by the heart rate multiplied by the stroke volume. Heart rate is closely controlled by the autonomic nervous system; stimulation of the sympathetic nervous system increases heart rate, whereas the parasympathetic nervous system decreases heart rate. The stroke volume is regulated primarily by two opposing factors: the force with which the myocytes contract and the arterial pressure (afterload) against which they have to expel the blood.

The force of contraction of the myocyte is a variable, regulated quantity, and can be increased by two processes. Firstly, Frank-Starling's law states that the more a myocardial cell is stretched during diastole the greater the energy of the ensuing contraction. Thus, the amount of blood within the ventricle at the end of diastole (preload) will determine the force of contraction and hence stroke volume. The relationship between stroke volume and end-diastolic volume (EDV) is known as Starling's law of the heart. The physiological significance of this law is that venous return is an important determinant of stroke volume and hence cardiac output. The second mechanism for controlling stroke volume is the strength with which a myocyte contracts from a given initial stretch, 'or inotropic state'. This can be increased by the sympathetic nervous system and by hormonal influences (***Figure 1.2***).

The afterload has a negative effect on the stroke volume. This is because the immediate effect of contraction of the myocardium is not to produce ejection of blood but to raise the pressure within the ventricle. Ejection of blood can only occur when the pressure within the ventricle is greater than the pressure in the periphery,

and this consumes a substantial part of the energy available for each contraction. Therefore, if afterload is increased, more contractile energy is used to raise intraventricular pressure to that necessary to facilitate ejection.

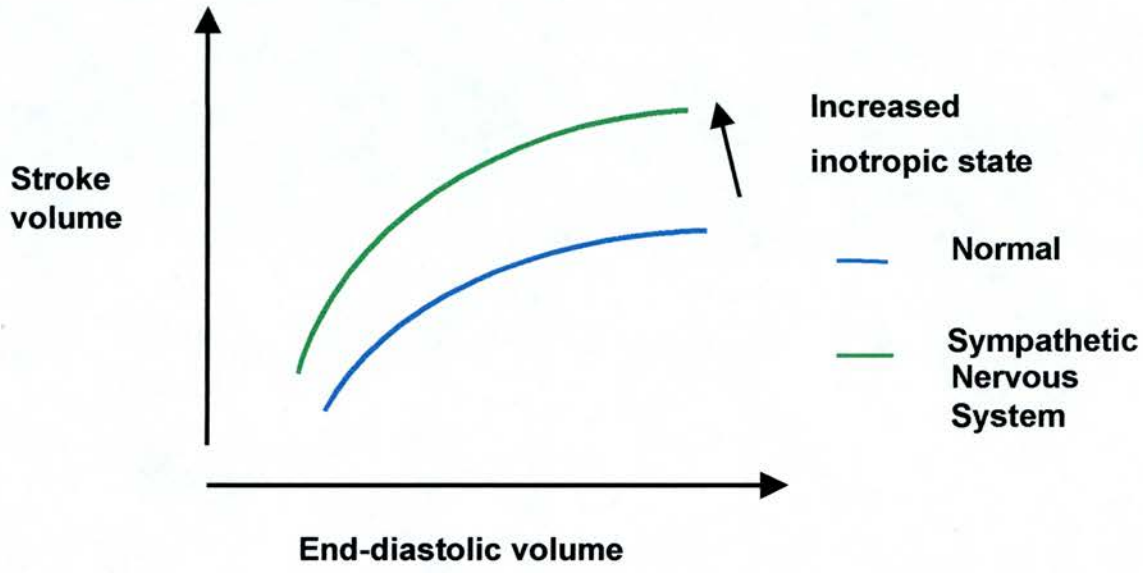

Figure 1.2 *Diagram showing the relationship between ventricular end-diastolic volume and stroke volume (Frank-Starling mechanism). Also shown is the effect of the sympathetic nervous system on this relationship (green).*

1.2 The circulation

1.2.1 Overview of anatomy

Blood vessels form a tubular network that permits blood to flow from the heart to all the living cells of the body and then back to the heart. The circulation is divided into the **pulmonary** and **systemic circulation**. In both the pulmonary and systemic circulation, arteries are responsible for the transportation of blood away from the heart, whereas veins are responsible for returning blood to the heart. Arteries, leaving the heart, branch extensively to form smaller microscopic vessels called arterioles, which subsequently branch into capillaries. Capillaries are the thinnest and most numerous of blood vessels and it is here that fluids, nutrients and waste products are exchanged between blood and tissue. Capillaries join with microscopic-sized veins, called post-capillary venules and venules, which deliver blood into the larger veins, which in turn return the blood to the heart.

On the basis of strictly morphological characteristics, and excluding capillaries, blood vessel anatomy is divided into three components (***Figure 1.3***). The **tunica intima** (endothelium) is the innermost layer of blood vessels and consists of flat endothelial cells adhering to an underlying layer of connective tissue. The endothelium acts as physical barrier to plasma proteins and cells, and also releases paracrine substances that modulate blood vessel tone (see Section **1.2.4**). The **tunica media** (VSM) is the middle layer of the blood vessel and is made up of spindle-shaped smooth muscle cells, embedded in matrix of elastin and collagen. The media provides mechanical strength and contractile power. The outermost layer is called the **tunica adventitia** (adventitia). The adventitia is a connective tissue sheath containing various cell types, including fibroblasts, tissue macrophages and schwann cells (Rhodin *et al.*, 1980). In addition, the adventita of larger arteries contain small blood vessels called vasa vasorum, which serve to nourish the thick media. Initially, it was thought that the adventitia served to hold the blood vessel loosely in place, however, it is now thought that the adventitia and its cellular components plays a role in modulating vascular function (Gutterman, 1999).

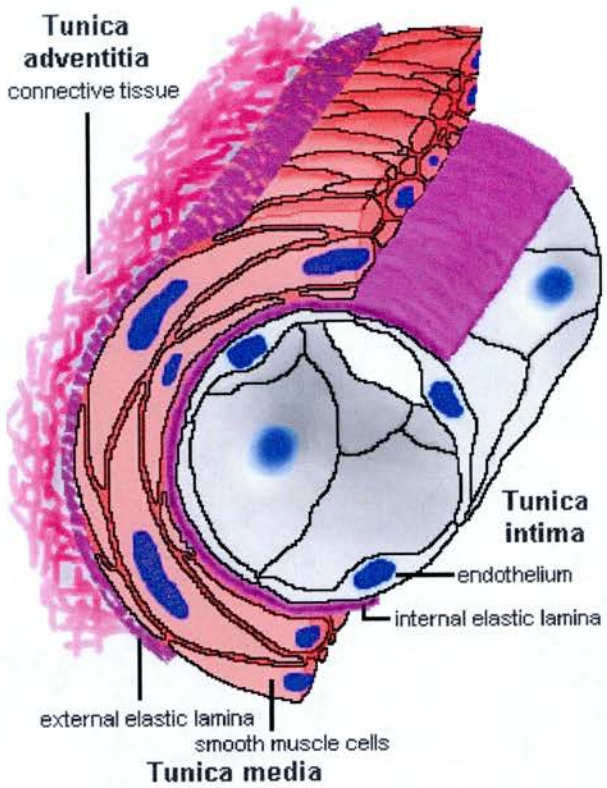

Figure 1.3 *Schematic diagram of the morphological characteristics of a blood vessel.*

1.2.2 The arterial circulation

The arterial circulation is constructed on the sound principal that each blood vessel must fulfil at least one other function in addition to the conduction of blood throughout the body. As a result the structure of blood vessels vary considerably to meet their functional roles. There are three main types of blood vessels in the arterial circulation: 1. **Elastic arteries** (eg aorta, carotid artery) have very distensible walls as a result of their media being rich in elastin, allowing them to expand an accomidate the blood from the heart (see Section **1.2.3**), 2. **Muscular arteries** are characterised by a thicker tunica media layer relative to the lumen diameter, and act as low-resistance conduits, 3. **Resistance arteries** have the thickest walls of all vessel types relative to their lumen. Their narrow lumens and thick muscular walls make these blood vessels the chief resistance to blood flow (see Section **1.2.3**).

1.2.3 Control of blood pressure

Arterial blood pressure is determined by the cardiac output multiplied by the total peripheral vascular resistance (PVR). As discussed in Section **1.1.3**, cardiac output can be altered by changes in heart rate and stroke volume. Total PVR is the sum of all the vascular resistances within the systemic circulation. The resistance to laminar flow arises exclusively from the internal friction between adjacent laminae of fluid and has nothing to do with friction between the tube and fluid. Nevertheless, resistance is greatly affected by tube geometry because the radius of the tube affects the rate of shear (sliding) of the laminae. The properties which determine resistance were elucidated in 1840 by Jean Leonard Marie Poiseuille. Poiseuille established that the resistance (**R**) to the steady laminar flow of fluid along a straight cyclindrical tube was proportional to tube length (**L**) and fluid viscosity (η); and inversely proportional to tube radius raised to the fourth power ($\mathbf{r}^4$):

$$R \propto L\eta / r^4$$

When physical constants are added to this relationship, rate of blood flow can now be calculated according to **Poiseuille's law**:

$$\text{Blood Flow} = \Delta P\, r^4\, (\pi)/\, \eta\, L\, (8)$$

Where: ΔP = driving force, ie. the difference in pressure between one end of the tube and the other

The physiological significance of this law is that resistance to blood flow is greatest in the arteries with the smallest diameter, ie small arteries and arterioles, and as a censequence these are the most important blood vessels in determining arterial blood pressure. The radius of arterioles is actively controlled by the tension of smooth muscle cells in its wall. Owing to the fourth-power effect on resistance, active changes in radius constitute an extremely powerful mechanism for regulating both the local blood flow downstream of the arteriole and the arterial pressure.

Larger arteries, while imposing little resistance to blood flow, serve two important functions in the arterial system. First, these arteries serve a conduit function, delivering an adequate supply of blood to smaller arteries and arterioles. The second important role of these arteries, which is complementary to the first, is to transform pulsatile flow generated by contraction of the ventricles into a continuous flow of blood in the periphery, sometimes referred to as a cushioning function. In this cushioning role, larger arteries play an important role in modulating arterial blood pressure (reviewed by London & Guerin, 1999). Briefly, large arteries distend to accomidate the entire blood volume ejected from the heart during systole. Arteries store part of the stroke volume and drain it during diastole. This transforms the pulsatile flow into an almost continuous blood flow in downstream arteries. Furthermore, it keeps the rise in arterial blood pressure to a minimum during systole thus protecting peripheral arteries from high pressures. In addition to their role in modulating arterial blood pressure, these arteries play an important role in the effciciency of the heart (Bank *et al.*, 1994). In particular, if the large arteries were not elastic then the heart would have to accelerate the entire volume of blood in the left

ventricle to the resistance arteries during early systole. Consequently, the heart would have to expend more energy in a shorter time. It is clear, therefore, that these arteries play an important role in the overall efficiency of the cardiovascular system.

1.2.4 The vascular endothelium

As described in Section **1.2.1**, the endothelium comprises the innermost layer of all blood vessels. Initially, it was thought that the endothelium served as physical barrier to plasma proteins and cells. However, it has been widely demonstrated that the endothelium plays a pivotal role in the regulation of vascular tone and in the modulation of various physiological processes, including inflammatory responses, mitogenesis, fibrinolysis, lipid transport and angiogenesis. The endothelium modulates the tone of underlying smooth muscle cells, and therefore blood flow and pressure, by producing a variety of paracrine substances that have vasoactive properties. Among these are endothelium-derived relaxing factor (EDRF), endothelin-1 (ET-1), prostacyclin (PGI_2), endothelium-derived hyperpolarizing factor (EDHF) and cyclooxygenase-derived contracting factors (***Figure 1.4***). Numerous stimuli can elicit the release of endothelium-derived factors, these include autocoids released from the tissue, circulating hormones, neurotransmitters, platelet products and mechanical changes within the blood vessel, eg. shear stress from the blood. (***Figure 1.4***).

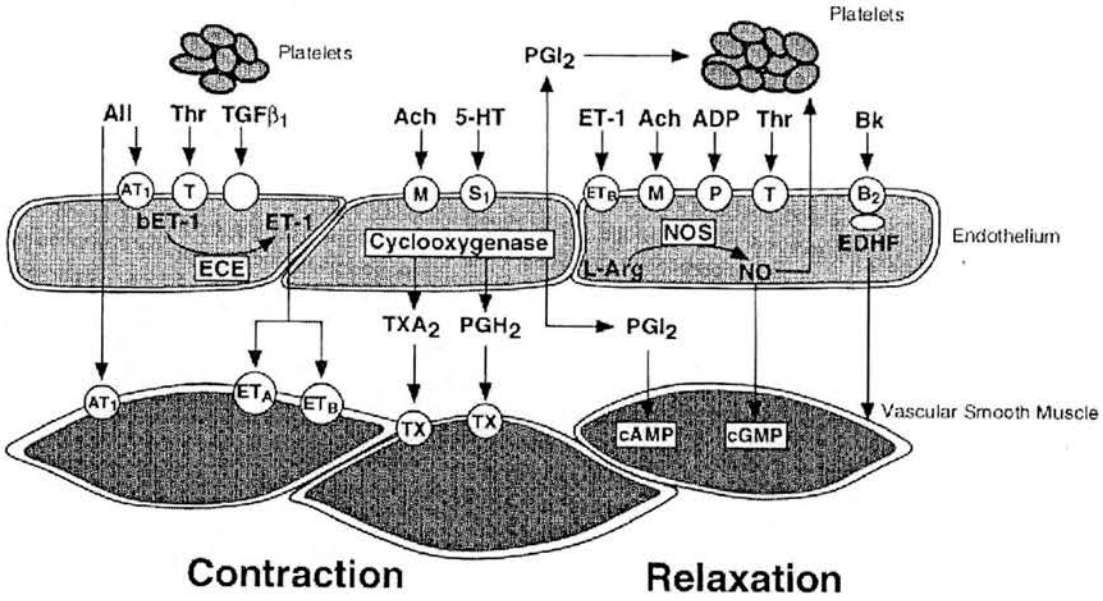

Figure 1.4 *Endothelium-derived vasoactive substances. The endothelium is a source of relaxing (right) and contracting factors (left).* ***AII****, angiotensin;* ***ACh****, acetylcholine;* ***ADP****, adenosine diphosphate;* ***AT_1****, angiotensin receptor 1;* ***Bk****, bradykinin;* ***B_2****, bradykinin receptor 2;* ***cAMP/cGMP****, cyclic adnosine/guanosine monophosphate;* ***ECE****, endothelin converting enzyme;* ***EDHF****, endothelium-derived hyperpolarizing factor;* ***5-HT****, 5-hydroxytryptamine;* ***bET-1****, big endothelin-1;* ***ET-1****, endothelin-1;* ***ET_A****, endothelin receptor A;* ***ET_B****, endothelin receptor B;* ***L-Arg****, L-arginine;* ***M****, muscarinic receptor;* ***NO****, nitric oxide; NOS, nitric oxide synthase;* ***P****, purinoceptor, PGH_2, prostaglandin H_2;* ***PGI_2****, prostacylin;* ***$TGF\beta_1$****, transforming growth factor β_1;* ***S_1****, serotonin receptor;* ***T****, thrombin receptor;* ***Thr****, thrombin;* ***TX****, thromboxane receptor;* ***TXA_2****, thromboxane A_2. Modified from The Endothelium in Cardiovascular Disease, Chapter 1, ed Lüscher, T.F., Springer.*

1.3 Nitric oxide

1.3.1 Discovery

The role of the endothelium as the source of a novel 'relaxing factor', EDRF, was first advanced by in 1980 by Furchgott and Zawadzki when they demonstrated that the vasorelaxant action of acetylcholine in isolated blood vessels was mediated by a diffusible factor released from the endothelium (Furchgott & Zawadzki, 1980). Early studies suggested that EDRF might be a product of the arachidonate pathway (Singer & Peach, 1983) or the cytochrome P-450 enzyme system (Pinto *et al.*, 1986). However, six years after his initial discovery, based on the similarities in the pharmacological properties of EDRF and **nitric oxide** (NO) generated from acidified NO_2^-, Furchgott suggested that EDRF might be NO. Within one year of this suggestion two groups had confirmed that the release of NO from the vascular endothelium accounts for the biological activity of EDRF (Ignarro *et al.*, 1987; Palmer *et al.*, 1987). It is still uncertain whether EDRF is free NO or labilie nitroso compound(s) from which NO is liberated, or both (see Section **1.3.6.2**; Myers *et al.*, 1990; Rubanyi *et al.*, 1991; Stamler *et al.*, 1992).

1.3.2 Nitric oxide synthases

Since the discovery of NO, it has been established that many cell types, besides endothelial cells, are capable of synthesizing NO. The enzymes responsible for the synthesis of NO are known as the **nitric oxide synthases** (NOS). In humans, three isoforms have been identified, neuronal NOS (nNOS), inducible NOS (iNOS) and endothelial (eNOS). Each isoform is the product of a separate gene and enzymes share 52% to 58% amino acid homology (Förstermann *et al.*, 1994). In general, the synthases are grouped into two broad categories: Ca^{2+}/calmodulin-dependent constitutive type (nNOS and eNOS) and an inducible isoform that is not dependent on Ca^{2+}/calmodulin (iNOS). Although, recent studies suggest that eNOS can also be activated in a Ca^{2+}-independent manner (Fleming *et al.*, 1999; Fisslthaler *et al.*, 2000).

nNOS was the first isoform to be purified and cloned from rat and porcine cerebellum (Bredt & Snyder, 1990; Mayer *et al.*, 1990). nNOS has since been localised to tissues and cells other than the brain, including, certain areas of the spinal cord, peripheral vasomotor nerves, skeletal muscle and cardiac neurons (Förstermann *et al.*, 1994). NO produced by this isoform of NOS has numerous roles throughout the nervous system, these include the regulation of synaptic plasticity (Schuman & Madison, 1991) and central and peripheral nervous control of the cardiovascular system (Cederqvist *et al.*, 1991; Huang *et al.*, 1995).

iNOS was first purified and cloned from an immunoactivated murine macrophage cell line (Lowenstein *et al.*, 1992; Xie *et al.*, 1992). The expression of iNOS in macrophages, and the subsequent production of large quantities of NO, plays a major role in the immunological defence against infection. (Nathan, 1992). Its expression can also be induced in almost any cell type, including vascular endothelial and smooth muscle cells (Schulz *et al.*, 1991; Balligand *et al.*, 1995; Fleming *et al.*, 1991) and cardiomyocytes (Brady *et al.*, 1992; Balligand *et al.*, 1994), by bacterial lipopolysaccharide (LPS) and inflammatory cytokines, such as tumour necrosis factor-α (TNF- α).

eNOS was originally purified and cloned from bovine vascular endothelial cells (Nishida *et al.*, 1992). In addition to its constitutive expression in arterial and venous vascular endothelial cells, eNOS is also expressed in cardiac myocytes (Seki *et al.*, 1996) and endocardial endothelial cells (Schulz *et al.*, 1991). eNOS-derived NO plays an important role in the control of the cardiovascular system (see Section **1.4**).

1.3.3 Synthesis of nitric oxide

The three isoforms of NOS exhibit a similar catalytic profile and composition. Each isoform of NOS catalyses the five-electron oxidation of the terminal guanido nitrogen of the amino acid, L-arginine, to form NO and L-citrulline, via the formation of N^{ω}-Hydroxyguanidine (NOHA) as an intermediate (Stuehr & Griffith, 1992; ***Figure 1.5***). The reaction is complex, involving oxygen and nicotanamide

adenine dinucleotide phosphate (NADPH) as co-substrates, and numerous other cofactors/coenzymes, including flavins, calmodulin and (6R)-5,6,7,8-tetrahydrobiopterin (BH_4).

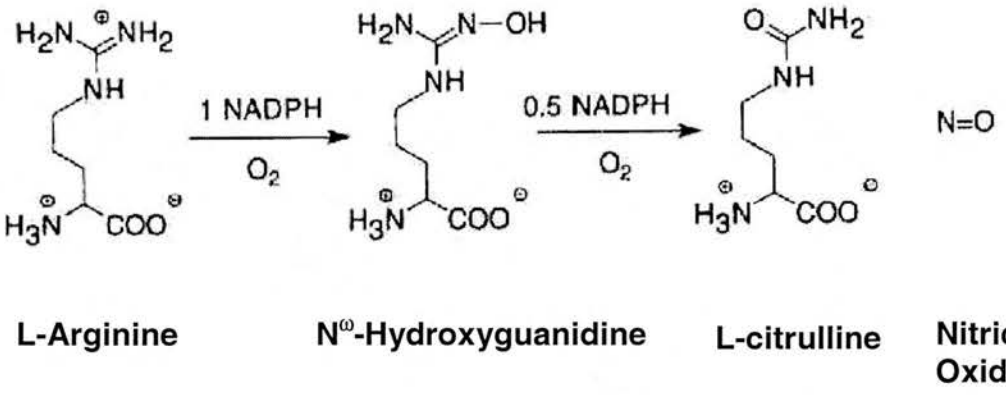

Figure 1.5 *Diagram showing the nitric oxide synthase catalysed reaction of L-arginine to nitric oxide*

All three isoforms of NOS consist of an active homodimer ranging in size from 130 – 162 kDa (Nathan & Xie, 1994). Each inactive monomer is made up of two parts, a C-terminal flavin-containing reductase domain and a N-terminal haem-containing oxygenase domain (***Figure 1.6***). The reductase domain contains regions that bind flavin mononucleotide (FMN) and flavin adenine dinucleotide (FAD) as prosthetic groups, as well as a binding site for NADPH. Furthermore, a site for phosphorylation by cAMP-dependent protein kinase A (PKA) is found in the reductase domain (Knowles & Moncada, 1994). The oxygenase domain contains a region for the binding of iron protoporphyrin IX (haem) as a prosthetic group, a binding site for L-arginine and BH_4. The binding site for calmodulin is generally thought to exist somewhere between the two domains (Bredt *et al.*, 1991; Ghosh & Stuehr, 1995; Gachhui *et al.*, 1996), although, a recent study demonstrated that eNOS also binds calmodulin in its oxygenase domain (Hellermann & Solomonson, 1997).

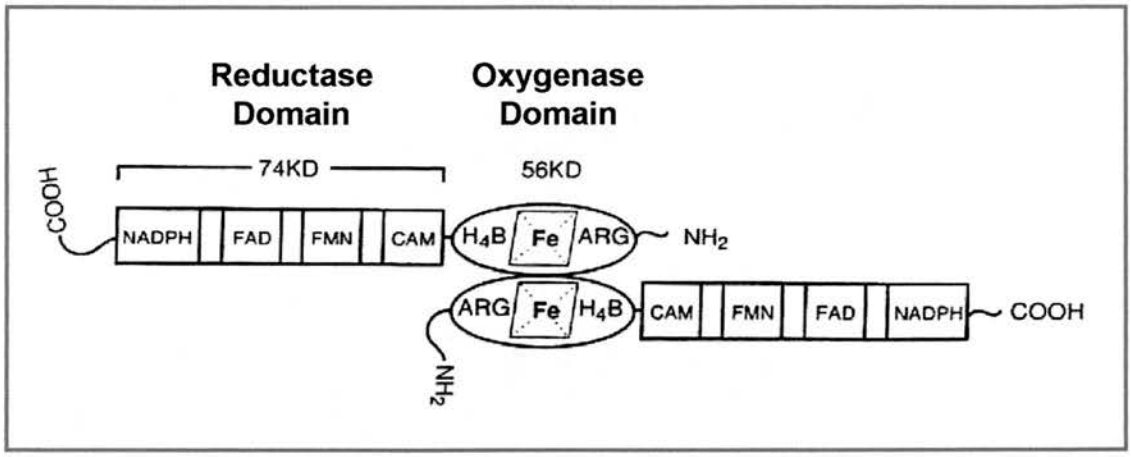

Figure 1.6 *General model of domain organisation of NOS subunits. Each subunit of NOS contains a reductase and oxygenase domain. Within the reductase domain binding sites for* ***NADPH****, flavin adenine dinucleotide (****FAD****), flavin mononucleotide (****FMN****), whereas the oxygenase domain contains sites for L-arginine (****ARG****), haem (****Fe****) and tetrahyrobiopterin (****H_4B****). Although the diagram shows the binding site for calmodulin (****CAM****) to be on the reductase domain, it is thought to be located somewhere between the two domains. During activation, the subunits are thought to be aligned head to head at the oxygenase domains, with the reductase domains attached as independent extensions. Modified from Stuehr: Annual Reviews of Pharmacology and Toxicology, 1997, 37: 339 – 359.*

Despite the structural similarities between the three isoforms, some differences exist. In contrast to nNOS and eNOS, where calmodulin binding is reversible, iNOS binds calmodulin extremely tightly (Cho *et al.*, 1992). Indeed, calmodulin remains bound to iNOS even after denaturing, suggesting that calmodulin is a constitutive part of this isoform (Cho *et al.*, 1992). The N-terminus of eNOS differs from both nNOS and iNOS, in that it is dually acylated by the fatty acids myristate and palmitate (Michel *et al.*, 1997). Both myristoylation (irreversible) and palmitylation (reversible) are required for targeting of eNOS to specialized plasmalemmal microdomains called caveolae (Feron *et al.*, 1998). Caveolin, the structural coat

protein of calveolae, interacts with eNOS and is thought to inhibit the enzyme in a reversible manner (Michel *et al.*, 1997; Ghosh *et al.*, 1998).

The detailed mechanism by which NOS synthesises NO remains to be established. However, a unified model has been proposed (Stuehr, 1999). The activity of all three isoforms is dependent on the dimerisation of the two monomers (Stuehr, 1999) and, in the case of eNOS, this dimerisation is preceded by its dissociation from caveolin in the caveolae (Michel *et al.*, 1997). Only the oxygenase domains appear necessary to form the dimer (McMillan & Masters, 1995). The precise mechanism by which dimerisation is induced is unclear. Studies suggest that Ca^{2+}/calmodulin binding to the oxygenase domain is essential for dimerisation of eNOS (Hellermann & Solomonson, 1997) and for its dissociation from caveolin in the caveolae (Feron *et al.*, 1998). Ca^{2+}/calmodulin is less important in the dimerisation of nNOS and plays no role in the dimerisation of iNOS. This is not surprising considering the constitutive manner in which calmodulin is bound to iNOS. The dimerisation of iNOS is dependent on the incorporation of haem, and the binding of L-arginine and BH_4 (Baek *et al.*, 1993). In nNOS and eNOS, haem incorporation is also important but BH_4 may not be an absolute requirement despite its ability to stabilise the dimers once they are formed (Klatt *et al.*, 1995; Venema *et al.*, 1997). A general model for the structure and domain composition of the dimeric form of NOS is shown in ***Figure 1.6***. It is has been postulated that the two subunits of NOS align head-to-head, with the oxygenase domains of each subunit interacting to form the dimer, and the reductase domains attached as independent extensions (Stuehr, 1999).

The flavin containing-reductase domain exhibits 56% homology to the dual-flavin enzymes NADPH-cytochrome P-450 reductase and the bacterial sulfite reductase (Bredt *et al.*, 1992). Because these enzymes all function to transfer electrons from NADPH to an endogenous or associated haem group, it is thought that the C-terminal reductase domain of NOS serves to transfer electrons from NAPDH to haem in the oxygenase domain (Stuehr, 1999). Therefore, the proposed model is as follows; NADPH-derived electrons, are transferred in a linear sequence across the two

domains, first entering the flavins and then passing to the haem in the oxygenase domain. Recent evidence suggests that this transfer of electrons may actually occur from the reductase domain in one monomer to the oxygenase domain in the other (Siddhanta *et al.*, 1998). Reduction of the haem moiety allows oxygen to bind and be reduced. Oxygen is then incorporated into the guanido group of L-arginine giving rise to the intermediate species, NOHA, which is then oxidised to give NO and L-citrulline.

1.3.4 Role of calmodulin and tetrahydrobiopterin in the synthesis of nitric oxide

Calmodulin is a Ca^{2+}-activated regulatory protein that binds to and regulates a number of enzymes known to respond to changes in intracellular [Ca^{2+}]. Calmodulin is considered to be one of the most important regulatory cofactors in the synthesis of NO by NOS. In addition to playing an allosteric role in synthesis of NO from eNOS, calmodulin also plays a catalytic role in all three isoforms. Indeed, Ca^{2+}/calmodulin is required for maximal activation of nNOS and eNOS. On the basis of electron flow studies, calmodulin is thought to act as a hinge between the reductase and oxygenase domains in each monomer (Abu-Soud *et al.*, 1994). When Ca^{2+}/calmodulin is not bound, the domains are not aligned, and the reductase domain cannot supply electrons to the haem. When Ca^{2+}/calmodulin is bound, the domains align and the enzyme is active. The precise mechanism by which Ca^{2+}/calmodulin activates electron transfer remains to be established, but, a recent study suggested that Ca^{2+}/calmodulin might induce a conformational change in the reductase domain that promotes electron transfer (Gachhui *et al.*, 1996). In addition to providing an electron 'bridge', it is thought that calmodulin may also promote electron transfer into the flavin domain from NADPH (Abu-Soud *et al.*, 1994).

The allosteric and catalytic roles of calmodulin in the synthesis of NO from nNOS and eNOS account for the Ca^{2+} dependence of these isoforms and also the insensitivity of iNOS to calcium. In iNOS, calmodulin is always bound, therefore the domains are aligned and the enzyme is active irrespective of the calcium concentration.

Tetrahydrobiopterin (BH_4) is a co-factor of many aromatic amino acid mono-oxygenases. BH_4 is an essential cofactor in the synthesis of NO by all isoforms of NOS (Mayer *et al.*, 1990). The precise role of BH_4 in NO synthesis is not fully understood. It has been suggested that cooperation exists between the binding sites of BH_4 and L-arginine, with BH_4 binding positively modulating the binding of L-arginine and vice versa (Klatt *et al.*, 1994; McMillan & Masters, 1995). Furthermore, recent studies reveal that BH_4 may play a crucial role in the coupling of electrons from the flavins to L-arginine (Xia *et al.*, 1998b). Haem-iron is approximately 80% reducible in the presence of NADPH and L-arginine (Siddhanta *et al.*, 1996), and reduction is further enhanced in the presence of BH_4 (Presta *et al.*, 1998). Binding of L-arginine to the oxygenase domain of NOS shifts the iron in haem from its low electron spin state to its higher spin state (McMillan & Masters, 1993). When BH_4 binds, the number of iron molecules with their electrons in high-spin state is increased further (Rodriguez-Crespo *et al.*, 1996; Salerno *et al.*, 1996). Therefore, BH_4 is probably not acting as an electron donor, but is acting with L-arginine to increase the reduction potential of the iron relative to the flavins and thus make electron transfer to the haem more thermodynamically favourable (Rodriguez-Crespo *et al.*, 1996).

1.3.5 Regulation of nitric oxide synthases

The generation of NO from eNOS and nNOS is generally assumed to be dependent on the binding of calmodulin to the enzyme, which is in turn dependent on the intracellular concentration of Ca^{2+}. Indeed, many receptor-dependent and -independent agonists stimulate the release of NO from eNOS and nNOS by elevating intracellular [Ca^{2+}]. However, it is now clear that eNOS and nNOS are also regulated by a Ca^{2+}/calmodulin-independent mechanism. For example, basal eNOS activity in native endothelial cells has been reported to occur at Ca^{2+} concentrations as low as 10 nM (Mülsch *et al.*, 1989). Furthermore, mechanical factors, such as fluid shear stress, and some receptor-dependent agonists are thought to increase the synthesis of NO from eNOS, in a Ca^{2+}/calmodulin-independent manner (Ayajiki *et al.*, 1996; Fisslthaler *et al.*, 2000, see Section **1.4.1.2**). It is postulated that the Ca^{2+}/calmodulin-

independent activation of eNOS is mediated by direct phosphorylation of eNOS. The precise mechanism by which phosphorylation of eNOS is induced is poorly understood. However, a number of phosphorlyating kinases have been implicated in the Ca^{2+}/calmodulin-independent activation of eNOS, including tyrosine kinases, PKA, cGMP-dependent protein kinases (PKG) and protein kinase B (PKB; Butt *et al.*, 2000; Fisslthaler *et al.*, 2000). Purified nNOS can also be phosphorylated by kinases. However, in contrast to eNOS, the activity of nNOS is downregulated by phosphorylation, suggesting a possible negative feedback regulatory mechanism (Bredt *et al.*, 1992).

In addition to the acute regulation of eNOS activity, NO production from eNOS can be modified chronically by altering the expression of the enzyme itself. An increase in shear stress within a blood vessel, not only increases endothelial release of NO acutely, but also upregulates the expression of eNOS (Miller & Vanhoutte, 1988). Indeed, a putative shear stress-responsive element has been described in the promotor sequence of eNOS (Marsden *et al.*, 1993). The inflammatory cytokine, tumour necrosis factor-α (TNF-α), down regulates the expression of eNOS in human umbilical vein endothelial cells (Yoshizumi *et al.*, 1993; Nathan & Xie, 1994). The mechanism of action of TNF-α has been ascribed to a destabilisation of mRNA for eNOS (Yoshizumi *et al.*, 1993).

iNOS is not constitutively expressed, but, its expression is transcriptionally regulated by various inflammatory cytokines and by bacterial LPS. Its activity is not dependent on Ca^{2+}/calmodulin. Therefore, once it is expressed, there are no regulatory mechanisms known for the activity of this enzyme.

1.3.6 Cellular interactions of nitric oxide

NO is capable of interacting with a variety of cellular molecules, including transition metals, molecular oxygen and superoxide (Stamler *et al.*, 1992). Each of the products of these reactions - metal-NO adducts, NO_x and peroxynitrite ($ONOO^-$) respectively - support additional nitrosative reactions, including S-nitrosation of thiol-containing proteins and the nitration of tyrosine residues. Not surprisingly, metal and thiol-containing proteins serve as major target sites for NO. Among these are signalling proteins (Lander *et al.*, 1993), ion channels receptors (Bolotina *et al.*, 1994) and enzymes (Gopalakrishna *et al.*, 1993; Stone & Marletta, 1994).

1.3.6.1 Metal-containing proteins

The interaction of NO with haem-containing proteins has been widely studied. The principal, but by no means exclusive, target for NO is iron in the haem group of soluble guanylate cyclase (sGC; Stone & Marletta, 1994). Indeed, many of the physiological effects of NO in the cardiovascular system, such as vasorelaxation and platelet inhibition, are mediated, in part, by the activation of sGC (see Section **1.4.1.1**). By binding to the haem group (Craven & DeRubertis, 1978), NO is thought to displace the trans-imidazole ligand, which attaches the haem to the enzyme (Traylor & Sharma, 1992). It is speculated that by displacing the trans-imidazole ligand for haem, sGC becomes free to undergo conformational changes that in essence, activate the enzyme (Traylor & Sharma, 1992). It is clear, however, that further studies are required to establish the precise mechanism by which sGC is activated. In addition to the activation of haem-containing proteins, NO can inhibit the activity of enzymes that use a haem prosthetic group as part of their catalysis. Examples include the cytochrome P-450 reductase enzymes (Stamler *et al.*, 1992). As discussed in Section **1.3.3**, the NOS family of isoenzymes contain haem as a prosthetic group. Therefore, it is not surprising that the haem of NOS readily binds NO. Binding of NO to the haem inhibits the activity of NOS in a reversible manner (Buga *et al.*, 1993), presumably by forming an iron-NO haem adduct and inhibiting the activity of the oxygenase domain. Thus, the interactions of NO with haem in NOS may serve as important autoregulatory feedback mechanism for NO synthesis.

Other haem containing proteins that are thought to be targets of NO include catalase (Brown, 1995) and cytochrome C (Giulivi, 1998).

NO also forms complexes with non-haem transition metal containing proteins. In particular, NO forms adducts with the iron-sulphur centres of the mitochondrial electron transport chain (complex I and complex II), which inhibits their activities (Clementi *et al.*, 1998).

1.3.6.2 Molecular oxygen

NO is vulnerable to oxidation by molecular oxygen, which results in the production of various nitrosating species, nitrogen dioxide (NO_2), dinitrogen trioxide (N_2O_3) and dinitrogen tetraoxide (N_2O_4) (collectively called NO_x). All three compounds are capable of nitrosating thiols, resulting in the formation of S-nitrosothiols. Thiol groups are found in many biological active compounds. The reaction of NO_x with cysteinyl sulhydryl moieties is now appreciated to be responsible for a wide range of protein modifications (Gaston, 1999). S-nitrosothiols, for example S-nitrosoglutathione, S-nitrosoalbumin and S-nitrosohaemoglobin, have been postulated to be putative intermediates of NO, some of which might be present in sufficient quantities to exert biological effects in their own right (Stamler *et al.*, 1992; Mayer *et al.*, 1998). S-nitrosothiols have been shown to be potent vasodilators and inhibitors of platelets (Ignarro *et al.*, 1981; Mellion *et al.*, 1983), and are considerably more stable than NO (Ignarro *et al.*, 1981). Furthermore, S-nitrosothiols may mediate some of their effects through activation of sGC (Mayer *et al.*, 1998). It is postulated that the production of S-nitrosothiols as intermediates of NO, serves to accentuate the biological effects of NO (Stamler *et al.*, 1992).

S-Nitrosation is thought to regulate the function of many other proteins. Examples include the down-regulation of Ca^{2+} currents through the NMDA glutamate receptor (Lipton *et al.*, 1993), inhibition of the activity of protein kinase C (Gopalakrishna *et al.*, 1993) and the opening of calcium-dependent potassium channels (Bolotina *et al.*, 1994). In a similar fashion to NO_x, S-nitrosothiols can readily transnitrosoate thiols in other proteins through the transfer of NO^+.

1.3.6.3 Superoxide

As discussed, NO is vulnerable to oxidation by molecular oxygen, however, this reaction is much slower than its reaction with superoxide. Indeed the reaction of NO with superoxide occurs at a diffusion-limited rate. The main source of superoxide in healthy cells is the mitochondrial electron transport chain, but most is inactivated by the family of isoenzymes, superoxide dimutase (SOD). However, in circumstances where cells produce increased amounts of superoxide production or have a decreased antioxidant capacity, NO will react with superoxide, under physiological pH conditions, to form peroxynitrite ($ONOO^-$). $ONOO^-$ may isomerise to yield NO_3^- (nitrate) or it may nitrate tyrosine residues on proteins (Ischiropoulos & al-Mehdi, 1995).

1.4 Nitric oxide and the cardiovascular system

1.4.1 Vascular tone

1.4.1.1 Cellular effects of nitric oxide in the vasculature

NO diffuses from the endothelium to underlying VSM cells where it causes smooth muscle relaxation. It is generally accepted that NO mediates smooth muscle relaxation via activation of the sGC/cGMP pathway, but, recent studies suggest that cyclic guanosine 3', 5' monophosphate (cGMP)-independent mechanisms may also be involved (Bolotina *et al.*, 1994; Gupta *et al.*, 1994; Mistry & Garland, 1998; Homer & Wanstall, 2000). Binding to sGC in VSM cells results in the conversion of guanosine triphosphate (GTP) to cGMP. It is generally accepted that cGMP triggers relaxation of VSM cells by initiating an intracellular cascade, which is ultimately dependent on the activation of cGMP-dependent protein kinases (PKG; Carvajal *et al.*, 2000). The precise mechanism by which PKG mediates VSM relaxation is poorly understood, however, two mechanisms have been proposed (Carvajal *et al.*, 2000). The first is a reduction in intracellular [Ca^{2+}] and the second is the reduction in the sensitivity of the contractile apparatus of VSM cells to Ca^{2+}.

Several investigators have shown in rat mesenteric artery, guinea pig and human trachea, isolated porcine tracheal smooth muscle cells and the Chinese Hamster ovary that activation of the cGMP-PKG pathway increases the activity Ca^{2+}-activated K^+ channels by phosphorylation of either the channel protein or a regulatory protein (Yamakage *et al.*, 1996; Zhou *et al.*, 1996; Mikawa *et al.*, 1998; Tanaka *et al.*, 1998). Similarly, studies have shown that PKG may activate the plasmalemmal and sacroplasmic reticulum (SR) Ca^{2+}/ATPase pump (Cornwell *et al.*, 1991; Rashatwar *et al.*, 1987; Furukawa *et al.*, 1988). Activation of Ca^{2+}-activated K^+ channels and the plasmalemmal Ca^{2+}/ATPase pump serve to increase Ca^{2+} efflux from the cell, whereas SR Ca^{2+}/ATPase pump increases the uptake of Ca^{2+} into the SR. Membrane voltage-dependent Ca^{2+} channels, which normally open in response to membrane depolarisation, can also be regulated by various protein kinases (Tewari & Simard, 1997). It has been suggested that PKG can phosphorylate the Ca^{2+} channel

or a closely associated regulatory protein, reducing the possibility that the channel remains in its open state (Tewari & Simard, 1997). Further to its effects on channels there is evidence to suggest that PKG can inhibit inositol triphosphate and its receptor (Lincoln & Cornwell, 1993; Komalavilas & Lincoln, 1996), which ultimately decrease the efflux of Ca^{2+} from the SR.

The mechanism of PKG-induced Ca^{2+} desensitisation is unknown, although several theories have been proposed. Studies using isolated smooth muscle cells have demonstrated that cGMP-PKG pathway results in an increase in the activity of myosin light chain phosphatase (MCLP; Wu *et al.*, 1996; Lee *et al.*, 1997). This is thought to decrease the phosphorylation of the contractile apparatus, resulting in a decrease in its sensitivity to Ca^{2+}. In cultured rat aortic smooth muscle cells, the cGMP-PKG pathway has been shown to inhibit protein kinase C (PKC) activation induced by angiotensin II and ET-1 (Kumar *et al.*, 1997). This supports a role for PKC inhibition as part of the decrease in Ca^{2+} sensitivity induced by cGMP (Kumar *et al.*, 1997), especially in those muscles in which PKC plays a role in smooth muscle contraction.

The cGMP-independent component of NO-induced smooth muscle relaxation is less well defined. Numerous studies have demonstrated that NO activates Ca^{2+}-dependent K^+ channels in a manner that is independent of the sGC/cGMP pathway (Bolotina *et al.*, 1994; Mistry & Garland, 1998). In isolated rabbit aorta, NO stimulated Na^+/K^+-ATPase by a mechanism that was not blocked by a GC inhibitor (Gupta *et al.*, 1994). Furthermore, a recent study demonstrated that the NO donor, spermine NONOate, resulted in cGMP-independent relaxation of isolated pulmonary arteries by a mechanism that involves activation of Na^+/K^+-ATPase, SR Ca^{2+}-ATPase and Ca^{2+}-activated K^+ channels (Homer & Wanstall, 2000). It is unclear if cGMP-independent mechanisms of NO-induced smooth muscle relaxation involve upstream secondary messengers. Interestingly, Bolotina *et al.* (1994) demonstrated that cGMP-independent activation of Ca^{2+}-dependent K^+ channels was dependent on the modification of sulphydryl groups within the channel, suggesting that NO-mediated S-nitrosation may be involved in the activation of these channels.

1.4.1.2 Basal release of nitric oxide

Mechanical forces are amongst the most important stimuli determining the release of NO. The endothelium is continuously exposed to shear stress, or viscous drag, from the blood and pulsatile stretching due to the beating of the heart. It has been widely demonstrated that these physical forces stimulate the release of NO from vascular endothelial cells (Hutcheson & Griffith, 1991; Ayajiki *et al.*, 1996; Fisslthaler *et al.*, 2000). The mechanisms by which the endothelium is able to sense changes in shear stress/pulsatile stretch on its luminal surface remain obscure. However, mechanical disruption/deformation of the endothelial cytoskeleton and subsequent transmission of the force from the cell surface to intracellular compartment has been suggested as a possible mechanism (Ingber, 1997).

There is some evidence that shear stress can increase intracellular [Ca^{2+}] by opening ion channels (Mo *et al.*, 1991). However, basal release of NO from the endothelium is evident in native endothelial cells at Ca^{2+} concentrations as low as 10 nM (Mülsch *et al.*, 1989). It has been suggested that shear stress/pulsatile stretch activates eNOS in a Ca^{2+}/calmodulin-independent manner, possibly by inducing phosphorylation of eNOS (Ayajiki *et al.*, 1996; Fisslthaler *et al.*, 2000; Nakano *et al.*, 2000).

As a result of the assiduous exposure of blood vessels to mechanical stress, NO is released from the endothelium in a continuous, basal fashion. Indeed, inhibition of eNOS reduces blood flow in virtually every arterial bed studied, including pulmonary and cardiac, demonstrating that NO plays an important role in maintaining blood flow through tissues (Lefroy *et al.*, 1993; Stamler *et al.*, 1994). Not surprisingly, the release of NO from resistance arteries plays a pivotal role in the regulation of total PVR and hence systemic arterial blood pressure. Indeed, systemic blockade of NO generation in humans using non-selective inhibitors of NOS, e.g. N^G-monomethyl-L-arginine (L-NMMA), results in an immediate rise in systemic arterial blood pressure (Haynes *et al.*, 1993; Stamler *et al.*, 1994). Knocking out the gene encoding eNOS in mice results in a significant hypertension (Huang *et al.*, 1995). Furthermore, the importance of eNOS-derived NO in the regulation of blood pressure and vascular homeostasis was further highlighted by the observation that a

missense variant of eNOS (Glu289Asp) in exon 7 of the eNOS gene is positively associated with essential hypertension and myocardial infarction (Miyamoto *et al.*, 1998).

As discussed in Section **1.2.3**, the main functional role of conductance arteries is to dampen the pressure oscillations that are caused by the intermittent nature of ventricular ejection. This cushioning effect is determined by the elastic properties of arterial walls (London & Guerin, 1999). There is substantial evidence that VSM tone plays a role in modulating the elastic properties of conductance arteries (Dobrin & Rovick, 1969; Wilson *et al.*, 1995; Bank, 1997; Joannides *et al.*, 1997). Furthermore, evidence suggests that the basal release of NO from the endothelium serves to increase arterial compliance (Bank *et al.*, 1994; Joannides *et al.*, 1997).

1.4.1.3 Agonist-stimulated release of NO

Many endogenous agonists can increase the release of NO from the endothelium, these include histamine, ADP, bradykinin, ET-1, thrombin and norepinephrine. It is generally accepted that these agonists act through specific receptors on the endothelial cell surface, to increase intracellular [Ca^{2+}] and thus activate eNOS. However, recent studies suggest that the effects of these agonists on eNOS, may be mediated, in part, by a Ca^{2+}/calmodulin-independent mechanism (Butt *et al.*, 2000). In a similar fashion to the effects of mechanical forces on eNOS activity, it is proposed that agonists, such as bradykinin, can also induce phosphorylation of eNOS and subsequent activation (Butt *et al.*, 2000).

1.4.2 Heart

1.4.2.1 Introduction

NO derived from the endothelium has the potential to indirectly influence cardiac function secondary to alterations in 1) arterial tone 2) venous return and hence left ventricular (LV0 filling volume, thereby modulating the cardiac output via the Frank-Starling mechanism and 3) coronary vascular tone and perfusion. In addition to these indirect effects, NO has direct actions on the functioning of cardiomyocytes.

Over the past decade, it has become apparent that complex, paracrine interactions exist between endothelial cells and cardiomyocytes in the heart, analogous to the paracrine crosstalk between endothelial cells and VSM cells. Two types of endothelial cells exist in the heart, namely endocardial endothelial cells (endocardium) and endothelial cells of the coronary vasculature. eNOS is expressed in the endocardium, the coronary endothelium (Schulz *et al.*, 1991), and at a much lower level in cardiomyocytes (Seki *et al.*, 1996). Furthermore, eNOS is expressed in the conducting system of the heart (Han *et al.*, 1996). In the intact mammalian heart, it is likely that NO released from the vascular endothelial cells is of greater physiological importance than the NO released from the endocardium. This is because no cardiac myocyte is more than 2-3 μm from a vascular endothelial cell, contrasting with the endocardium which lines the inner cavity surfaces, and is therefore likely to only influence subjacent myocytes (Shah & MacCarthy, 2000).

1.4.2.2 Regulation of nitric oxide release in the heart

Specific studies for eNOS activation in cardiomyocytes, coronary vascular endothelial cells and endocardial endothelial cells are lacking. However, as with the vascular endothelium, the most relevant physiological stimuli for the release of eNOS-derived NO in the heart are likely to be physical forces, i.e. flow-induced shear stress and mechanical deformation (stretch). During the cardiac cycle, these physical forces will oscillate, and it has been suggested that the release and action of NO in the heart may also be cyclic. Indeed, with the use of an NO sensor, Pinsky *et al.* (1997), demonstrated that there is a cyclical release of NO in the beating heart. Furthermore, there is a sharp rise in the release of NO during diastole. Conceivably, changes in workload of the heart, possibly even beat to beat, may be reflected in changes in the release of NO.

As with the vascular endothelium, the coronary vasculature and the endocardium are continuously exposed to the blood. Therefore, the activity of eNOS will be susceptible to regulation by circulating humoral factors. Furthermore, factors released from endothelial cells and cardiac myocytes may modulate the release of NO.

1.4.2.3 Cellular effects of nitric oxide in the heart

The effects of NO on cardiomyocytes are complex. A number of studies have been published concerning the cellular effects of NO on the heart, and multiple and complex contradictory actions have been reported. As in VSM cells, many of the cardiac effects of NO have been attributed to the elevation of intracellular cGMP, secondary to the activation of sGC. However, cGMP-independent mechanisms may also contribute. The main targets for cGMP are PKG and cGMP-stimulated and –inhibited cyclic nucleotide phosphodiesterases (cGsPDE and cGiPDE, respectively). However, it is possible that cGMP-activated phosphatases and cGMP-regulation of ion channels may be important. Reported actions of cGMP on cardiac myocytes include, 1) modulation of sacrolemmal Ca^{2+} influx through voltage-gated Ca^{2+} channels, 2) reduction in the sensitivity of the contractile apparatus to Ca^{2+}, 3) altered release of Ca^{2+} from SR, 4) changes in the action potential, 5) modulation of the cell volume, and 6) reduction in oxygen consumption (Shah & MacCarthy, 2000).

Some of the actions of NO in the myocardium may be mediated by cGMP-independent mechanisms. A recent study demonstrated that NO stimulates cyclic adenosine monophosphate (cAMP) in cardiomyocytes (Vila-Petroff *et al.*, 1999). Other possible cGMP-independent mechanisms include S-nitrosation of thiol groups and the formation of adducts with iron-sulphur containing proteins (see Section **1.3.6**). However, cGMP-independent effects may be more relevant when large amounts of NO are produced, for example as a result of iNOS expression (Shah & MacCarthy, 2000).

1.4.2.4 Effect of nitric oxide on systolic and diastolic function

While the role of NO in control vasomotor tone is well established, the physiological significance of eNOS-derived NO on the functioning of the heart is not fully understood. Many studies that have investigated the effects of NO on myocardial function have focused in the modulation of systolic function, i.e. inotropic state. However, in studies where full analysis of myocardial performance have been undertaken, NO has also been shown to exert significant effects on myocardial

relaxation and diastolic properties, often in the absence of changes in systolic function.

Using NO donors, recent studies have demonstrated that submicromolar concentrations of NO have a small positive inotropic effect on the basal contractile function of cultured rat myocytes (Kojda *et al.*, 1996; Vila-Petroff *et al.*, 1999). Similarly, in isolated human atrial myocytes, an NO donor (sodium nitroprusside; SNP) exerted positive inotropic effects (Kirstein *et al.*, 1995). In anaesthetised dogs, intra-aortic infusion of NOS-inhibitors induced a significant inotropic effect, despite an only moderate increase in mean aortic pressure and a lack of reduction of coronary blood flow (Klabunde *et al.*, 1991). This was interpreted as endogenous NO having a positive inotropic effect. A possible subcellular mechanism for the positive inotropic effects of NO may be via cGiPDE and a subsequent rise in intracellular cAMP levels (Kirstein *et al.*, 1995; Kojda *et al.*, 1996; Vila-Petroff *et al.*, 1999). In contrast to the effects of low concentrations of NO, higher (micromolar and above) doses of NO donors have been reported to induce negative inotropic effects (Brady *et al.*, 1993; Mohan *et al.*, 1996). Inhibition of endogenous NOS in isolated cardiomyocytes has been shown to have no effect on function, suggesting a lack of effect of NO on basal myocardial function and that endogenous myocardial NO may be derived from the endocardium and vascular endothelial cells.

In the isolated ferret papillary muscle preparation, exogenous donors of NO, substance P and a cGMP-analogue all resulted in an earlier and faster onset of LV relaxation and a reduction in the peak tension developed before systole (Smith *et al.*, 1991). An effect of NO and cGMP on twitch relaxation and diastolic properties has also been reported in isolated cardiac myocytes. In adult rat ventricular myocytes, a cGMP analogue caused an earlier onset of relaxation and an increase in diastolic cell length (Shah *et al.*, 1994). Furthermore, this effect was mediated without altering the intracellular $[Ca^{2+}]$. It was concluded that the effects of NO were mediated by a reduction in the sensitivity of the contractile apparatus (myofilaments) to Ca^{2+} probably via PKG (Shah *et al.*, 1994).

During diastole, filling of the LV with blood stretches the myofilaments of the myocytes, which ultimately determines the amount of blood that is ejected from the ventricle. It has been postulated that stretching of myocytes may be mediated by changes in myofilament responsiveness to Ca^{2+} (Shah & MacCarthy, 2000). Thus it is conceivable that the release of NO during diastole, serves to increase diastolic distensibilty by reducing Ca^{2+} sensitivity, and thus facilitate the Frank-Starling response of the whole heart. Furthermore, since the release of NO may be dependent on the amount of stretch imposed on the cardiac endothelium, NO may provide an acute autoregulatory feedback mechanism between LV workload and diastolic LV performance, thus optimising overall pump function. For example, during periods of increased LV workload, such as during exercise, the accompanying increases in heart rate, preload, contractility and coronary flow would result in increased stimuli for NO release (eg. increased fluid shear stress in the coronary vasculature and increased stretching of the endocardium and myocytes). The subsequent increase in NO synthesis could hasten LV relaxation, thus prolonging diastolic filling time and coronary perfusion. Furthermore, NO may increase the distensibility of the left ventricle, thus improving LV filling and, therefore, cardiac output. Indeed, intracoronary infusion of SNP in patients with angiographically normal coronary arteries and normal LV function resulted in: 1) an earlier onset of LV relaxation; 2) a concomitant reduction in peak and end-systolic LV pressure; 3) a fall in LV minimum diastolic pressure and LV end-diastolic pressure, with a rise in LV end-diastolic volume; and 4) a downward and rightward displacement of the LV diastolic pressure-volume relationship (Paulus *et al.*, 1994). Furthermore, a subsequent study by Paulus *et al.* (1995) reported similar effects of bicoronary infusion of substance P on LV relaxation and diastolic function in subjects with normal cardiac function. Thus, both exogenous and endogenous NO modulates myocardial relaxation and diastolic properties.

1.4.2.5 Interaction with the β-adrenergic pathway

Numerous studies have been carried out to investigate a possible role for NO in modulating β-adrenergic responses (Balligand *et al.*, 1993). Balligand *et al.* (1993) were the first to report that the inotropic response of adult rat ventricular myocytes to

the β-adrenergic agonist isoprenaline was enhanced by approximately 30% following application of an NOS inhibitor. However, these findings have not been universally confirmed. In isolated rat perfused hearts, the inotropic response to isoprenaline was unaffected by infusion of a NOS inhibitor (Ebihara & Karmazyn, 1996). In contrast to these studies with NOS inhibitors, most investigators have been able to demonstrate interactions between exogenous NO and β-adrenergic responses. For example, in isolated rat perfused hearts, the inotropic response to dobutamine was reduced by NO donors (Ebihara & Karmazyn, 1996). An interaction between endocardium-derived NO and β-adrenergic stimulation has also been demonstrated (Bartunek *et al.*, 1997). It is clear, therefore, that more research is needed to elucidate the precise role, if any, of NO in modulating β-adrenergic responses.

1.5. Heart Failure

1.5.1 Introduction

The understanding, investigation and treatment of chronic heart failure (CHF) in the medical profession, has improved substantially in the last 20 years. However, CHF is still a major cause of cardiovascular mortality and morbidity, accounting for 5% of acute hospital admissions in the UK (Sutton *et al.*, 1997). Furthermore, in USA it is the most common hospital-discharge diagnosis among patients older that 65 years (Lenfant, 1994). Once a patient has developed CHF, the quality of life and life expectancy is markedly reduced. Indeed, a recent study estimated a 6 year mortality rate of 84% for men and 77% for women (Croft *et al.*, 1999). The life expectancy of the population has increased substantially over the past 50 years, and it is projected that as the population ages, the incidence of CHF, and its resulting mortality, will markedly rise over the next decade. It is clear, therefore, that there is a need for extensive research into the pathogenesis of CHF and the development of novel therapeutic tools.

Traditionally, CHF is defined as a clinical syndrome typified by the inability of the heart to meet the metabolic requirements of the body. For the past 50 years the pathophysiology of this disease has largely been described in haemodynamic terms. According to this model, CHF follows damage to the heart, eg. after myocardial infarction (MI), which impairs its ability to eject blood; renal blood flow is reduced and subsequent sodium retention leads to pulmonary and peripheral oedema. Indeed, this focus on haemodynamics led to an increase in the use of digitalis to increase the inotropic state of the heart, and diuretics in the treatment of CHF (Packer, 1992). However, it is now well established that CHF is a disorder of the circulation, not merely a disease of the heart. For example, many patients have structural cardiac damage that adversely affects systolic and diastolic function, but they do not have CHF because compensatory mechanisms maintain cardiac output and peripheral perfusion. Therefore, CHF is not exlusively linked to heart damage but also requires failure of compensatory mechanisms that usually maintain cardiovascular

homeostasis. Indeed, it is now established that these compensatory mechanisms play a pivotal role in the pathophysiology of CHF (Packer, 1992). The progression from a compensated state to overt CHF, and the factors that are involved in this progression remains an important focus for medical research in the 21st century.

1.5.2 Chronic heart failure following myocardial infarction

CHF may occur as the result of myocardial damage caused by a number of disease processes such as coronary artery disease (CAD), hypertension, valvular disease, alcohol misuse and viral infection (myocarditis; Cowie *et al.*, 1997). Each disease holds its own complex pathology, but, they all result in irreversible impairment of myocardial function. Furthermore, impairment of LV function is the main cause of CHF, although right ventricular dysfunction also occurs. Impaired LV function may be global, as in hypertension, valvular disease, alcohol misuse and myocarditis, or regional as result of MI following CAD.

The most common cause of CHF in Western society is MI secondary to CAD (McMurray *et al.*, 1992). CAD most often results from atherosclerosis, where fat deposits on the inside of the coronary artery and leads to the formation of a plaque. The initial stage of this disease consists of an asymptomatic period where the non-obstructive plaque is formed with further progression dependant on associated risk factors. The obstructive stage, however, involves rapid rupturing of the plaque, thrombogenesis and the development of an occlusive or near occlusive thrombus (Falk *et al.*, 1996).

The size of the MI is dependent on the extent of the occlusion, its position within the coronary vasculature, the duration in which the artery remains occluded, LV oxygen consumption and collateral blood flow (Maroko *et al.*, 1971; Schaper & Pasyk, 1976). Initially, impaired coronary blood flow and oxygen supply to the affected area of the myocardium results in extensive biochemical and morphological changes in the myocardial cells (Poole-Wilson, 1989). Acute deprivation of oxygen to myocardial cells will, after 10-15 seconds, lead to a rapid decrease in oxygen and

high-energy phosphates, which ultimately result in a shift from aerobic to anaerobic metabolism. After a prolonged period of ischaemia, the accumulation of anaerobic waste products and a reduction in energy stores results in irreversible myocardial cell damage and death. In addition, there is experimental and clinical evidence that programmed cell death or apoptosis is a major source of myocardial cell death during myocardial ischaemia (Kajstura *et al.*, 1996; Saraste *et al.*, 1997).

Necrosis and/or apoptosis are followed by a process of degradation and clearance of damaged myocardial cells. This is thought to involve a complex interplay of inflammatory cells, such as neutrophils and macrophages (reviewed by Entman *et al.*, 1991). A scar, composed principally of collagen, then replaces the damaged myocardium (reviewed by Weber, 1997).

1.5.3 Acute response to cardiac injury

After MI, the heart is unable to sustain stroke volume due to a loss in myocardial cell mass and as result cardiac output falls. A complex interplay of haemodynamic and neurohormonal mechanisms are activated to maintain cardiovascular homeostasis.

Decreased stimulation of baroreceptors in the aortic arch, carotid sinus and the left ventricle, as a result of a reduced cardiac output, leads to an increase in sympathetic outflow from the autonomic nervous system. Increased sympathetic activation enhances the force and frequency of contraction of the non-injured myocardium and causes systemic vasoconstriction. Subsequent hypoperfusion and direct sympathetic innervation of the kidney activate the renin-angiotensin-aldosterone system (RAAS). Furthermore, stimulation of baroreceptors in the aortic arch and left ventricle promotes the release of arginine vasopressin (AVP) from the pituitary gland. All three systems serve to increase blood volume, total PVR and thus aid perfusion of organs.

Increased blood volume also results in an augmentation in venous return to the heart. As discussed in Section **1.1.3**, the stroke volume is dependent on the stretch of the

myofilaments, which in turn is dependent of the EDV. Therefore, during the acute response to cardiac injury, a greater EDV, as a result of increased venous return, will impose more stretch on the myocardium, resulting in an increase in the contractile state of the myocardium. This effectively shifts the Frank-Starling curve to the right, resulting in increased cardiac output.

In addition to the rapid activation of haemodynamic and neurohormonal compensatory mechanisms, the heart itself undergoes structural changes to compensate for the loss of viable myocardial cells. Increased total PVR and EDV increases the internal stretch exerted on the heart wall during diastole. This can dramatically distort its architecture and accelerate its energy expenditure. To prevent such adverse structural and functional effects, the heart undergoes a process called hypertrophy. The hypertrophied response is characterised by increased cardiomyocyte cell volume, proliferation of non-myocyte cells and increased myofibrillar protein expression (Rumberger, 1994). Stretching of cultured cardiac myocytes increased protein content by approximately 30% (Sadoshima *et al.*, 1992). Furthermore, analysis of cell signalling mechanisms shows that physical stress activates multiple signal transduction pathways, similar to those activated by growth factors (Swynghedauw, 1999). Indeed, a recent study provided evidence that cardiac hypertrophy *in vivo* is regulated by the stress-activated protein kinases, which belong to the mitogen-activated protein kinase family (Gabriel *et al.*, 1999). Although mechanical stretch is possibly the most common stimulus for hypertrophy, the sympathetic nervous system and RAAS may also play a role (Colucci, 1997). The subsequent increase in wall thickness reduces ventricular stress and restores the functioning of the heart without altering the stretch on the myocardial fibres (McKay *et al.*, 1986).

1.5.4 Chronic heart failure

Compensatory mechanisms serve to restore cardiovascular homeostasis, and may be sufficient for the patient to remain asymptomatic for some time. In general, however, with time these compensatory mechanisms appear to fail and may even become detrimental to the diseased heart. As a result, myocardial function declines further, cardiovascular homeostasis is no longer maintained and the patient develops symptoms of CHF. The pathological development of CHF translates into distinct, if overlapping, stages in clinical presentation and can be classified according to the New York Heart Association (NYHA) scaling system. Patients are categorised as NYHA Class I, II, III or IV (see ***Table 1***). Classes II, III and IV are regarded as mild, moderate and severe CHF respectively, while patients in Class I are regarded as very mild (Timms & Davies, 2000).

Class	Symptoms
I	Cardiac disease but without resulting limitation of physical activity.
II	Cardiac disease but with slight limitation of physical activity, comfortable at rest. Ordinary physical activity results in fatigue, palpitation, dyspnoea or anginal pain.
III	Cardiac disease resulting in marked limitation of physical activity but comfortable at rest. Less than ordinary physical activity causes fatigue, dyspnoea or anginal pain.
IV	Cardiac disease resulting in the inability to perform any physical activity without discomfort, often discomfort at rest. If any physical activity is undertaken, discomfort is increased.

Table 1 *NYHA classification of chronic heart failure*

In practice, CHF may be diagnosed whenever a patient develops signs or symptoms of low cardiac output, pulmonary congestion and/or systemic venous congestion. Where increases in EDV restore cardiac output in the acute response to cardiac injury, in the chronic state a progressive decline in the functioning of the myocardium requires even higher volumes to maintain cardiac output. As a consequence of working with higher EDVs, with time the heart is left with little or no reserve. As a result, it becomes insensitive to changes in venous return. It is proposed that in CHF the Frank-Starling curve is shifted to the right and becomes flatter (***Figure 1.7***). The physiological consequence of this decline in LV performance is that the heart is unable to match cardiac output to the needs of the body. In cases of severe CHF, the heart may even fail to maintain cardiac output at rest. Furthermore, an inability of the heart to eject all the blood in the left ventricle into the periphery, results in an accumulation of fluid in the pulmonary circulation, which results in pulmonary congestion.

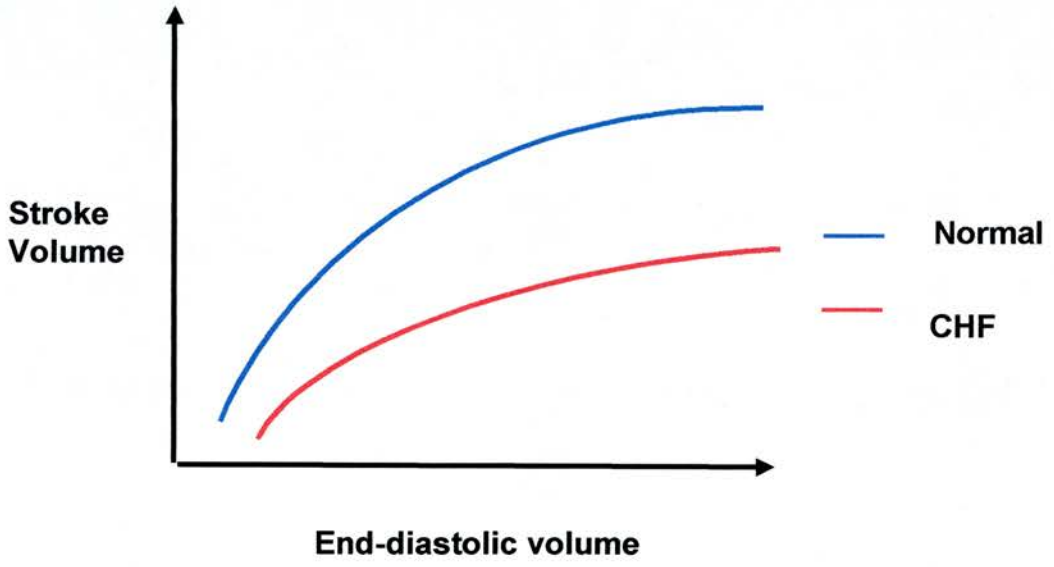

Figure 1.7 *Schematic diagram representing the proposed Frank-Starling relationship in the chronically failing heart (CHF; red line), compared with a normal healthy heart (blue line).*

The precise mechanism responsible for the progressive decline in LV function is not well defined. Research suggests that it is likely to involve a complex interplay of multiple systems including failure of compensatory mechanisms, adverse effects of long-term activation of compensatory mechanisms and the activation of other potentially adverse systems, possibly as a consequence of the disease progression. The role of such mechanisms is discussed in Sections **1.5.5** and **1.5.6**.

1.5.5 Role of compensatory mechanisms in chronic heart failure

1.5.5.1 Cardiac remodelling

During CHF, the left ventricle experiences changes in structure and function that are referred to as remodelling. This process of remodelling is characterised by further hypertrophy, changes in extracellular matrix composition and loss of myocardial cells either by necrosis or apoptosis (Colucci, 1997).

As discussed in Section **1.5.3**, hypertrophy is an important compensatory mechanism; reducing internal stress and helping to restore cardiac output. However, there is a downside to this altered geometry. In the long term, an increase in ventricular size requires the heart to contract even more to expel the blood, as explained by Laplace's Law (Julian & Cowan, 1992). This law states that the tension of the myocardium is proportional to the intraventricular pressure multiplied by the radius of the ventricular chamber. This need for a higher contractile state increases internal stress within the LV, promoting further hypertrophy and ventricular enlargement. Furthermore, numerous neurohumoral factors are believed to play a role in promoting hypertrophy, these include α_1–adrenoceptor agonists (Knowlton *et al.*, 1993), angiotensin-II (Gray *et al.*, 1998) and ET-1 (Mullan *et al.*, 1997). Therefore, although appropriate hypertrophy of the myocardium compensates for myocardial loss in the acute state, excessive hypertrophy is believed to be maladaptive and to be associated with the progressive decline in the functioning of the non-infarcted myocardium (Sakai *et al.*, 1998).

In addition to hypertrophy, CHF often results in changes in the extracellular matrix of the heart. Indeed, the chronically failing human heart is characterised by increased collagen synthesis in the infarcted and noninfarcted myocardium of both right and left ventricles (Beltrami *et al.*, 1994). An accumulation of collagen is believed to increase the stiffness of the failing heart, which may impair the contractility and/or relaxation of the myocardium. In a rat model of CHF, myocardial fibrosis and stiffness impaired the diastolic properties of the heart (Conrad *et al.*, 1995). Numerous factors have been implicated in fibrosis, including angiotensin II (McEwan *et al.*, 1998) inflammatory cytokines (Castagnoli *et al.*, 1993; Bryant *et al.*, 1998; Ono *et al.*, 1998), transforming growth factor-β (TGF-β; Parker *et al.*, 1990) and ET-1 (Mullan *et al.*, 1997).

Narula *et al.* (1996) and Olivetti *et al.* (1997) were the first to demonstrate that apoptosis occurs in the myocardium of patients with end-stage dilated cardiomyopathy. In the study by Olivetti *et al.* (1997), CHF was characterised by an approximate 250-fold increase in the number of apoptotic myocytes. In addition, findings from several *in vitro* studies and animal models suggest that apoptosis can occur in response to a variety of insults, many of which are present within the failing heart including mechanical stretch (Cheng *et al.*, 1995), β-adrenergic stimulation, release of inflammatory cytokines and oxidative stress (Colucci, 1997). Therefore, a progressive loss of myocardial cells by apoptosis may contribute to the myocardial dysfunction associated with CHF. However, the ultimate outcome may depend on its balance with hypertrophy. Therefore, although this evidence is persuasive, the precise role of apoptosis in the LV remodelling associated with the progression of CHF remains to be defined.

1.5.5.2 Sympathetic nervous system

Activation of the sympathetic nervous system improves the inotropic state of the non-infarcted myocardium and also helps redistribute blood flow to pulmonary, coronary and cerebral vascular beds. In addition, vasoconstriction helps maintain PVR and tissue perfusion. Furthermore, it activates the RAAS and stimulates the release of AVP.

However, with time, the heart loses its ability to respond to endogenous catecholamines. This attenuation is thought to occur as a result of changes in the cardiac β-adrenergic pathway, including down-regulation of β_1–receptors, which mediate the inotropic effects of catecholamines, and uncoupling of the receptors from their effector enzyme, adenylate cyclase (Krum, 1997). This impaired response to catecholamines is relatively specific to the heart with the sympathetic innervation of the kidneys and vasculature remaining intact. Indeed, there appears to be an enhanced responsiveness of the peripheral vasculature to α-adrenergic stimulation (Elborn *et al.*, 1989). This effect is enhanced further by a depression in the baroreflex parasympathetic nervous system (Floras, 1993), which normally serves as a physiological antagonist mechanism against the sympathetic nervous system.

Excess catecholamines may have direct pathological effects on the myocardium, but substantial evidence to support this hypothesis is still lacking. Although β_1–receptors are downregulated, β_2 and α_1-receptors become more prominent and may be responsible for mediating adverse effects of catecholamines (Deisher *et al.*, 1995). *In vitro*, norepinephrine stimulates the growth of cardiac myocytes, possibly through both β_2 and α_1-receptors (Knowlton *et al.*, 1993). Furthermore, β-adrenergic stimulation has been shown to cause cardiac myocyte cell death (Mann *et al.*, 1992) and induce DNA and protein synthesis in cardiac fibroblasts *in vitro* (Calderone *et al.*, 1998). Thus, there is convincing evidence that the sympathetic nervous system may play an important role in the LV remodelling associated with CHF.

In conclusion, a decreased inotropic response in combination with enhanced peripheral vasoconstriction increases the cardiac workload, which in turn accentuates the internal stress on the LV. In addition to the effects of increased LV stress, direct effects of catecholamines on the myocardium may also promote LV remodelling.

1.5.5.3 Renin-angiotensin-aldosterone system

In response to a decrease in perfusion or sympathetic stimulation, the juxtaglomerular cells of the kidney secrete renin into the circulation. Renin is a proteolytic enzyme which converts angiotensinogen, a circulating plasma globulin, into angiotensin I. Angiotensin I is then cleaved by angiotension converting enzyme (ACE) to the active peptide angiotensin II (Cockcroft *et al.*, 1995). Angiotensin II mediates its effects through angiotensin receptors, of which two have been cloned and defined: AT_1 and AT_2. The majority of the effects of angiotensin II are mediated via the AT_1 receptor, although recent studies are defining roles for the AT_2 receptor (Matsusaka & Ichikawa, 1997). At normal plasma concentrations the main role of angiotensin II is to stimulate the secretion of the mineralcorticosteroid, aldosterone, from the adrenal glands. The principal and most well characterised action of aldosterone is the reabsorption of sodium and water from the kidney, resulting in an increase in blood volume. At higher concentrations, angiotensin II is a potent vasoconstrictor and is believed to enhance the release of norepinephrine from sympathetic nerve fibres and it can also penetrate the blood-brain barrier to directly stimulate sympathetic activity.

The RAAS plays an important role in maintaining PVR and tissue perfusion in the face of reduced cardiac output after damage to the heart, as well as helping restore cardiac output. However, it is now widely accepted that sustained activation of the RAAS plays a pivotal role in the progression of CHF. Indeed, the degree of activation of the RAAS is often used as prognostic index in patients with CHF (Francis *et al.*, 1990). Furthermore, the importance of the RAAS in the pathogenesis of CHF is emphasised by the success of ACE inhibitors in the treatment of CHF. In large randomised clinical trial, ACE inhibitors have been shown to improve LV function, prolong survival and reduce the need for hospital admissions in patients with CHF (reviewed by Lonn & McKelvie, 2000).

Like the sympathetic nervous system, a sustained increase in blood volume and PVR as a result of persistent activation of the RAAS will accentuate the workload and stress within the heart. Furthermore, this stress will be potentiated by increases in

EDV. Presumably, these mechanical influences will contribute to LV remodelling and the progressive decline in myocardial function. Therefore, in areas where RAAS serves as an important compensatory mechanism in the acute response to cardiac injury, long-term activation may actually be detrimental to the heart. Furthermore, the combination of increased systemic blood volume and reduced cardiac output, results in peripheral oedema.

Studies implicate a tissue-based RAAS within the heart (reviewed by Danser *et al.*, 1999), suggesting that components of the RAAS may be synthesised and act locally within the heart. Furthermore, there is evidence that myocardial expression of ACE is upregulated in experimental CHF and in patients with end-stage CHF (Danser *et al.*, 1999). Like catecholamines, angiotensin II has the potential to have direct effects on the functioning of cardiac cells, independent of its vascular and metabolic effects. Angiotensin II promotes hypertrophy of cultured neonatal rat myocytes (Gray *et al.*, 1998). This effect was shown to be mediated by ET-1 and TGF-β released from fibroblasts. Both ET-1 and TGF-β have been shown to promote hypertrophy of cultured myocytes *in vitro* (Parker *et al.*, 1990; Mullan *et al.*, 1997). In addition, a recent study demonstrated that angiotensin II promoted the proliferation of rat fibroblasts (McEwan *et al.*, 1998) suggesting a role for angiotensin II in cardiac fibrosis.

1.5.5.4 Arginine vasopressin

AVP or anti-diuretic hormone is synthesised by the posterior pituitary gland. Its release is primarily controlled by the hypothalamus, which senses changes in blood osmolarity via osmoreceptors. In addition, afferent signals from baroreceptors in the aortic arch, carotid sinus and LV can also stimulate its release. Recent evidence suggests that AVP is also synthesised in blood vessels and the heart where it may act locally (Simon & Kasson, 1995; Hupf *et al.*, 1999). AVP is considered to be a major hormone in the body responsible for salt and water homeostasis (Phillips *et al.*, 1995). Other effects of AVP include contraction of VSM cells, platelet aggregation, mitogenesis, central regulation of blood pressure and the baroreflex response (Phillips *et al.*, 1995; Sampey *et al.*, 1999).

The release of AVP in response to reduced cardiac output promotes the reabsorption of water from the kidney, which as in the case of the RAAS helps to maintain PVR and restore cardiac output. Acting through vasopressin receptors (V_2) expressed on the collecting duct of the kidney, AVP initiates an intracellular cascade, which leads to the translocation of water channels from cytoplasmic vesicles to the apical surface of the collecting duct (Nielsen *et al.*, 1995). This effectively increases the permeability of the ducts to water.

The precise role of AVP in the progression of CHF is unclear, however, circulating levels of AVP are elevated in CHF (Naitoh *et al.*, 1998). Furthermore, recent studies using novel non-peptide vasopressin receptors support a role for AVP in the pathogenesis of CHF (reviewed by Burrell *et al.*, 2000). Continuous release of AVP will clearly contribute to the effects of the RAAS and sympathetic nervous system on cardiac workload and peripheral oedema. Indeed, Burrell *et al.* (2000) demonstrated that administration of a novel V_2 antagonist to sheep with pacing-induced heart failure, increased water excretion as well as having favourable effects on cardiac output and myocardial contractility. Water retention in excess of sodium retention may occur in CHF and lead to hyponatremia. Indeed, hyponatremia is believed to be a very ominous prognostic indicator in patients with CHF (Lee & Packer, 1986). In patients with CHF and hyponatremia, hypo-osmolarity, which inhibits the release of AVP in healthy humans, is associated with persistently high plasma concentrations of AVP (Szatalowicz *et al.*, 1981), suggesting a pivotal role for AVP in hyponatremia. In addition to its effects on sodium and water homeostasis, AVP may directly increase PVR. Indeed, in dogs with pacing-induced heart failure, a V_1 receptor antagonist decreased systemic vascular resistance and increased cardiac output (Naitoh *et al.*, 1994).

1.5.5.5 Natriuretic peptides

Atrial natriuretic peptide (ANP) and brain natriuretic peptide (BNP) are predominantly synthesised in the atria and ventricles, respectively. ANP and BNP are released into the circulation in response to stretch where they have profound natriuretic, diuretic and vasodilating properties.

Both ANP and BNP are elevated in patients with CHF (Saito *et al.*, 1987; Boland & Abraham, 1998). Increased ANP and BNP secretion from the heart may serve as an important inhibitory pathway for the RAAS, sympathetic nervous system and the effects of AVP. In addition, there is evidence that the natriuretic peptides may directly inhibit fibroblast proliferation and myocardial fibrosis (Itoh *et al.*, 1990; Cao & Gardner, 1995). However, in CHF it is generally accepted that the beneficial effects of these peptides will be overcome by the powerful nature of the RAAS and sympathetic nervous system. Furthermore, patients with CHF appear to be resistant to the natriuretic effects of exogenously administered ANP and BNP (Cody *et al.*, 1986). This resistance may be due to down-regulation of renal natriuretic peptide receptors, increased degradation of natriuretic peptides by neutral endopeptidases in kidney or decreased sodium delivery to the site of action of the peptides (Schrier & Abraham, 1999). Furthermore, there is evidence that the atrial stretch receptors involved in the secretion of ANP may be down-regulated during CHF, as well as there being a reduction in the sensitivity of its vascular receptors (Ferrari & Agnoletti, 1989; Matsumoto *et al.*, 1999).

1.5.6 Other mechanisms

Exciting new observations suggest that there may be other factors that play a role in the progression of CHF. Among the growing list of possibilities are ET-1, inflammatory cytokines, superoxide and NO. The role of NO is pathogenesis of CHF is discussed in Section **1.5.7.**

1.5.6.1 Endothelin-1

The existence of a potent endothelium-derived vasoconstrictor was first demonstrated in 1985 (Hickey *et al.*, 1985), but the peptide responsible was not identified until 1988 (Yanagisawa *et al.*, 1988). ET-1 is a 21 amino acid peptide, which elicits a slow onset and extremely potent contraction of VSM cells. There are at least three different ET-receptors, of which two (ET_A and ET_B) are well characterised. ET_A receptors are expressed exclusively on VSM cells, whereas ET_B receptors are found expressed on both VSM cells and endothelial cells. Stimulation

of ET_A and ET_B on VSM cells results in vasoconstriction, whereas stimulation of endothelial ET_B receptors results in vasodilataion via the release of NO and PGI_2 from the endothelium. Mickley *et al.* (1997) demonstrated the relative role of ET_B - mediated vasoconstriction in rat small mesenteric arteries is greater when the ET_A-mediated effect is blocked, suggesting the presence of a possible 'crosstalk' mechanism existing between the receptors. It is now established that ET-1 and its receptors are also expressed in the heart. Synthesis of ET-1 has been reported in cultured neonatal rat cardiac myocytes (Suzuki *et al.*, 1993b). ET receptors have been detected within the heart in various cells, including myocardial cells, specialised 'conducting' cells (Molenaar *et al.*, 1993), fibroblasts (Katwa *et al.*, 1993) and within the coronary vasculature (Saetrum Opgaard *et al.*, 1996).

The physiological importance of endogenous ET-1 in the maintenance of basal vascular tone and blood pressure in healthy humans has been demonstrated by local and systemic (Haynes *et al.*, 1996) vasodilatation in response to inhibitors of the ET system. More recently, Spratt *et al.* (1999) demonstrated that systemic blockade of the ET_A receptor inhibited the agonist-induced vasoconstriction and decreased PVR, suggesting that ET_A-mediated vascular tone contibutes to the maintenance of basal systemic vascular resistance and blood pressure. The physiological role of ET-1 in the functioning of the heart is less well defined. Studies suggest that ET-1 may have an indirect effect on myocardial function through modulation of coronary tone (Wang *et al.*, 1994). Furthermore, recent studies suggest that ET-1 may act directly on the cardiac myocytes and specialised 'conducting' cells, and may play a role in modulating heart rate, cardiac output and contractility (Kusumoto *et al.*, 1996; Meyer *et al.*, 1996; Spratt *et al.*, 1999; MacCarthy *et al.*, 2000).

Patients with CHF have higher plasma ET-1 concentrations when compared with healthy individuals (McMurray *et al.*, 1992). Furthermore, high concentrations are associated with increased severity and mortality of CHF (Wei *et al.*, 1994). The source of elevated plasma ET-1 concentrations is unclear, but, at least two mechanisms may be responsible. Both angiotensin II and AVP can stimulate the release of ET-1 from the endothelium, and thus may serve as a stimulus in CHF

(Rubanyi & Polokoff, 1994). Another possible explanation is decreased clearance of ET-1 from the circulation (Cavero *et al.*, 1990). In addition to increased plasma concentrations of ET-1, there is some evidence that ET receptor number and sensitivity may also be altered in CHF. In a rat model of CHF, both ET-1 and ET_A receptor subtype expression were increased in the failing heart (Brown *et al.*, 1995). McEwan *et al.* (2001) revealed an upregulation of ET_B receptors in the non-infarcted myocardium of hearts from rats with CHF, 12 weeks after coronary artery ligation. Furthermore, Gray *et al.* (2000) recently reported specific upregulation of ET_B receptor immunoreactivity within the media of small mesenteric arteries from rats with CHF.

The precise role for ET-1 in the pathogenesis of CHF remains to be established. The vasoconstrictor effects of ET-1 may contribute to the increase in PVR associated with CHF. In addition, ET-1 has been shown to have direct effects on the functioning of the myocardium, including promotion of myocardial Ca^{2+} overload, direct toxic effects and an increase in contractility (Sakai *et al.*, 1996a). ET-1 has been shown to induce hypertrophy in cultured neonatal rat cardiac myocytes (Itoh *et al.*, 1990) and ventricular cardiac myocytes from adult rabbits (Mullan *et al.*, 1997), suggesting a role for ET-1 in LV remodelling. Understanding the actions of the ET system during CHF has been aided by the development of compounds that block ET receptors. Sakai *et al* (1996a) found that administration of the ET_A receptor antagonist, BQ-123, to rats for 12 weeks after coronary artery ligation markedly increased the survival of rats, while improving LV function and preventing LV remodelling. Preliminary studies using a mixed ET antagonist called bosentan demonstrated an improvement in LV performance, together with a reduction in mean arterial blood pressure and systemic vascular resistance in patients with severe CHF (Kiowski *et al.*, 1995). Furthermore, recent clinical research in CHF has identified a therapeutic role for ET antagonism during CHF. The REACH-1 trial (reviewed by Mylona & Cleland, 1999) reported improvements in symptoms using bosentan (500 mg BID), though an increase in hepatic transaminases led to a premature halt in the study. However, a follow-up study found that a lower concentration of bosentan (125 mg

BID, Krum *et al.*, 1999) was well tolerated and maintained the clinical improvements observed in REACH-1.

1.5.6.2. Proinflammatory cytokines

Cytokines are a group of low molecular weight proteins secreted primarily by polymorphonuclear cells and are responsible for orchestrating immunological responses to pathogenic infection as well as initiating the repair of tissue after injury. So far, the main cytokines that have been implicated in the pathogenesis of CHF are TNF-α, interleukin 1 (IL-1) and IL-6 (Shan *et al.*, 1997).

Plasma concentrations of TNF-α are increased in patients with CHF, and correlate with severity of symptoms (Levine *et al.*, 1990; Torre-Amione *et al.*, 1996a). Furthermore, TNF-α is found expressed in the failing human myocardium but not in healthy hearts (Torre-Amione *et al.*, 1996a). TNF-α mediates its effects through two membrane bound receptor subtypes, namely Type 1 (TNFR1) and Type 2 (TNFR2), both of which are expressed in the failing human heart (Torre-Amione *et al.*, 1995). After exposure to TNF-α these receptors can be cleaved from the membrane and circulate as soluble receptors, which may bind and neutralise TNF-α (Ferrari *et al.*, 1995). However, there is some evidence that binding of TNF-α to soluble receptors also act to stabilise TNF-α, thereby potentiating its actions (Bozkurt *et al.*, 1996).

TNF-α is known to have negative inotropic effects on isolated cardiomyocytes (Yokoyama *et al.*, 1993; Ferrari *et al.*, 1995; Müller-Werdan *et al.*, 1997). Furthermore, TNF-α has been shown to promote fibrosis of the heart (Castagnoli *et al.*, 1993) as well as apoptosis of cultured cardiac myocytes (Krown *et al.*, 1996). Artificially raising TNF-α activity can mimic many of the hallmarks of CHF. Infusion of TNF-α at levels found in clinical CHF resulted in LV remodelling and dysfunction in normal rats (Bozkurt *et al.*, 1998). Cardiac contractility was depressed within five days of starting the infusion and recovered on cessation. Consistent these findings, transgenic mice overexpressing TNF-α in the heart develop a condition

similar to CHF, characterised by reduced cardiac output, hypertrophy, myocyte apoptosis and fibrosis (Bryant *et al.*, 1998).

Further to its potential role in myocardial dysfunction, TNF-α may have other adverse effects. Patients with severe CHF often develop a wasting condition known as cardiac cachexia. Administration of recombinant TNF-α to healthy rats over a sustained period of time precipitates symptoms analogous to cachexia (Fong *et al.*, 1989). Furthermore, TNF-α levels are markedly increased in cachetic patients with CHF and these levels are found to be the strongest predictors of the degree of weight loss (Anker *et al.*, 1997).

IL-1β is found expressed in the coronary arteries and myocardium of patients with cardiomyopathy, whereas patients with CHF of ischaemic origin appear to express less IL-1β (Francis *et al.*, 1998). In a rat model of CHF, the expression of IL-1β was increased in the non-infarcted myocardium when compared with the myocardium from sham-operated rats (Ono *et al.*, 1998). Furthermore, this expression correlated with LV end-diastolic diameter and collagen deposition in the non-infarcted myocardium, suggesting a role for IL-1β in LV remodelling. In a similar fashion to TNF-α, IL-1β has the potential to reduce contractility of the heart (Balligand *et al.*, 1994).

Elevated levels of IL-6 have been reported in patients with CHF, and are associated with a worsening of NYHA functional class, increased hospital stay, and poorer LV function (Sharma *et al.*, 2000). The precise role of IL-6 in the pathogenesis of CHF remains to be established.

It is unclear if proinflammatory cytokines mediate their effects directly or indirectly. As mentioned in Section **1.3.2,** inflammatory cytokines can induce the expression of iNOS in almost any cell type, including VSM cells and cardiac myocytes. Therefore, NO may well be responsible for mediating the effects of cytokines in CHF. Furthermore, cytokines increase the synthesis of eicosanoids, superoxide, other inflammatory cytokines and they also activate inflammatory cells.

It is clear, therefore, that there is an abundance of evidence to suggest that proinflammatory cytokines may play an important role in the pathogenesis of CHF. Indeed, the emergence of such findings has led to the development of treatments that directly or indirectly reduce their availability within the heart and systemic circulation.

The main stimulus for the immune activation in CHF is not known. In many disease states the activated macrophage is the major source of TNF-α, however, in CHF cardiomyocytes are capable of producing TNF-α (Torre-Amione *et al.*, 1996b; Kapadia *et al.*, 1997). Kapadia *et al.* (1997) demonstrated that mechanical stretch might be the physiological stimuli for the release of TNF-α from the myocardium. In this study, haemodynamic overloading of the isolated perfused feline heart resulted in increased *de novo* synthesis of TNF-α mRNA after only 30 minutes, and *de novo* synthesis of TNF-α protein after 60 minutes. Furthermore, simple passive stretch was a sufficient stimulus for TNF-α biosynthesis in isolated feline papillary muscles (Kapadia *et al.*, 1997).

Oedema of the bowel wall and subsequent bacterial translocation has been postulated as a possible stimulus for immune activation (Anker *et al.*, 1997). Bacterial translocation would result in the release of endotoxin and subsequent immune activation.

1.5.6.3 Superoxide

Plasma malondialdehyde-like activity (MDA), a marker of oxidative stress, is increased in patients with CHF (Belch *et al.*, 1991; Diaz-Velez *et al.*, 1996). Furthermore, levels of oxidative stress appear to correlate with severity and chronicity of symptoms, and inversely with cardiac output and exercise capacity (Diaz-Velez *et al.*, 1996). Moreover, pericardial levels of 8-iso-prostaglandin $F_{2\alpha}$, a specific and quantitative marker of oxidant stress positively correlated with the functional severity of CHF (Mallat *et al.*, 1998).

Although the source of elevated superoxide in CHF is unclear, at least two mechanisms may be responsible. Some studies suggest that a deficiency in antioxidant systems is responsible. Several studies have demonstrated a reduction in antioxidants, such as glutathione peroxidase, vitamin E, catalase and SOD, both in the failing heart (Hill & Singal, 1996; Prasad *et al.*, 1996) and the systemic circulation (Nishiyama *et al.*, 1998; Yucel *et al.*, 1998). In a rat model of CHF, levels of endogenous antioxidant pathways are progressively reduced in the heart between 1 and 16 weeks post MI (Hill & Singal, 1996). The precise reason for a reduced antioxidant reserve is unclear. Other studies suggest that increased synthesis of superoxide is responsible. In cultured VSM cells, angiotensin II stimulates NADH/NADPH oxidase activity (Griendling *et al.*, 1994). As mentioned in Section **1.5.6.2**, TNF-α increases superoxide production from cultured cells (Hennet *et al.*, 1993). Other possible sources include, autoxidation of catecholamines and increased arachidonate metabolism (Givertz & Colucci, 1998).

Increased superoxide production during CHF may have a wide range of effects. superoxide has been shown to induce apoptosis of cardiac myocytes, while stimulating the proliferation of fibroblasts and inducing the expression of TGF-β (Li *et al.*, 1999b). Depressed contractility, impaired energy production and a rise in diastolic tension have all also been demonstrated in various cardiac preparations exposed to superoxide (reviewed by Singal *et al.*, 1998).

1.5.7 Nitric oxide and chronic heart failure

In general, the NO system is assessed by measuring vascular relaxations to the muscarinic receptor agonist, acetylcholine. In rats with CHF following coronary artery ligation (CAL), relaxations of isolated conductance arteries to acetylcholine are impaired when compared with sham-operated control rats (Teerlink *et al.*, 1994; Baggia *et al.*, 1997; Bauersachs *et al.*, 1999). These experimental findings have also been demonstrated in conductance arteries in patients with CHF with varying pathologies (Bank *et al.*, 1994; Ramsey, 1994).

Impaired peripheral vasodilator responses to acetylcholine have also been observed by several laboratories in the forearm and leg resistance vessels of patients with CHF (Drexler *et al.*, 1992; Kubo *et al.*, 1991; Katz *et al.*, 1992; Carville *et al.*, 1998). Furthermore, this impairment appears to correlate with disease severity (Carville *et al.*, 1998). Hindquarter quarter resistance arteries in rats with large infarctions following CAL were less responsive to acetylcholine than control rats (Drexler & Lu, 1992). Furthermore, the reduction in PVR to acetylcholine in the pacing canine model of CHF was shown to be attenuated (Kiuchi *et al.*, 1993).

In a similar manner to agonist-stimulated release of NO, there is evidence that flow-dependent increases in NO-mediated vasodilatation of conductance and resistance arteries are also attenuated in CHF. A recent study demonstration that flow-mediated dilatation skeletal muscle resistance arteries was abolished in rats with CHF following CAL (Varin *et al.*, 1999). Similarly, Hirai *et al.* (1995) found that hyperaemic response of hindquarter resistance arteries was impaired in rats with CHF. Impaired flow-mediated NO-mediated dilatation of conductance and resistance arteries has also been demonstrated in patients with CHF (Hayoz *et al.*, 1993; Katz *et al.*, 1996; Hornig *et al.*, 1996; Mohri *et al.*, 1997; Hornig *et al.*, 1998).

Taken together these experimental and clinical studies provide convincing evidence that the release of NO from the endothelium in resistance and conductance arteries, either in response to agonists or mechanical influences, is impaired in CHF. As discussed, increased blood volume and PVR as a result of activation of neurohormonal mechanisms play an important role in the progression of CHF, contributing to increased internal LV stress and thus LV remodelling. Therefore, impaired release of NO from the vascular endothelium in resistance arteries may contribute to this raised PVR. Dysfunction of the endothelial-NO system in conductance arteries may also have functional consequences. There is evidence that the release of NO from the endothelium serves to increase arterial compliance of conductance arteries (see Section **1.4.1.2**; Bank *et al.*, 1994; Joannides *et al.*, 1997). Therefore, impaired release of NO in CHF may result in a decrease in arterial

compliance, resulting in increased impedence of the failing left ventricle and consequently impairing LV ejection (see Section **1.2.3**).

Somewhat paradoxically, studies have demonstrated that plasma concentrations of nitrate, the stable end product of NO, are elevated or preserved in patients with CHF (Kubo *et al.*, 1994; Winlaw *et al.*, 1994; Carville *et al.*, 1998). Furthermore, there is some functional evidence that basal release of NO from the vasculature is enhanced or preserved in CHF. Drexler *et al.* (1992a) demonstrated that vasoconstrictor responses to L-NMMA in the forearm were exaggerated in patients with CHF when compared with healthy individuals. In the same study group this increase in basal NO release contrasted with impaired dilatory responses to acetylcholine. Habib *et al.* (1994) and Winlaw *et al.* (1994) observed that increases in systemic vascular resistance in response to L-NMMA were enhanced in patients with CHF. Some studies fail to corroborate these findings, however, and instead document a decrease in basal NO release (Baggia *et al.*, 1997). It is clear, therefore, that additional studies are required to elucidate whether basal release of NO is increased in CHF. Furthermore, more research is needed to elucidate why this facet of the vascular NO system remains intact in the face of impaired agonist and/or mechanical induced release of NO. Some investigators have postulated that iNOS might be expressed in the vasculature during CHF (Carville *et al.*, 1998; Drexler & Hornig, 1999), since circulating levels of inflammatory cytokines are elevated in CHF (see Section **1.5.6.2**), and thus may be responsible for the paradoxical increase in basal NO production in CHF. Furthermore, numerous studies have demonstrated that iNOS is expressed in the heart during CHF (de Belder *et al.*, 1993; Haywood *et al.*, 1996). However, the expression of iNOS and its functional significance on vascular function in CHF has not been addressed. Irrespective if basal NO is derived from eNOS or iNOS, one would expect this source of NO to counteract compensatory constrictor mechanisms associated with CHF and thus lower PVR. It is unclear why this counter-regulatory mechanism fails to reduce PVR.

The underlying mechanisms responsible for impaired NO release in CHF may be complex and have not yet been clarified. However, potential mechanisms have been

suggested, these include down regulation of eNOS (Comini *et al.*, 1996; Smith *et al.*, 1996; Wang *et al.*, 1997; Varin *et al.*, 1999), increased release of endothelium-dependent constriction factors (Kaiser *et al.*, 1989; Varin *et al.*, 1999) and impaired endothelial receptor-signal transduction pathways, ie. dysfunctional muscarinic receptor (Hirooka *et al.*, 1992). In other cardiovascular diseases, such as hypercholestrolemia and hypertension, compelling evidence suggests that the endothelial dysfunction results from increased vascular production of superoxide (Ohara *et al.*, 1993; Grunfeld *et al.*, 1995). As discussed in Section **1.5.6.3**, CHF is associated with increased superoxide production. Because superoxide rapidly scavenges NO within the vascular wall, a reduction the bioavailability of NO may be responsible for impaired endothelium-dependent relaxations associated with CHF. Furthermore, this may explain why PVR remains elevated in CHF despite increased basal production of NO. The role of superoxide in modulating the vascular NO system in CHF has not been fully addressed.

1.6 General aims of thesis

As discussed in Section **1.5.7**, evidence suggests that the release of NO from the endothelium in resistance and conductance arteries, either in response to agonists or mechanical influences, is impaired in CHF. However, somewhat paradoxically, there is some evidence that basal release of NO may be preserved or even enhanced. Some investigators have suggested that iNOS may be expressed in the peripheral vasculature, since circulating levels of inflammatory cytokines are elevated in CHF, and may be responsible for the paradoxical increase in basal NO production in CHF. Furthermore, there is substantial evidence that iNOS is expressed in the heart during CHF. The expression of iNOS and the functional significance of this potential source of NO in the peripheral vasculature in CHF have not been addressed.

The localisation of iNOS in the peripheral vasculature would be an intriguing finding itself, but its expression would pose some interesting questions. In particular, why does this potential source of NO fail to counteract compensatory constrictor mechanisms and thus lower PVR? As discussed in Section **1.5.7**, increased scavenging of endothelium-derived NO by superoxide has been implicated in the endothelial dysfunction associated with other cardiovascular diseases. Increased superoxide production has been demonstrated in CHF, however, its role in modulating the bioavailability of NO has not been fully addressed.

Therefore, this thesis set out to investigate following hypothesis:

1. iNOS is expressed in throughout the cardiovascular system in CHF
2. iNOS-derived NO is responsible for increased basal production of NO associated with CHF
3. Increased scavenging of NO by superoxide is responsible for the vascular dysfunction associated with CHF

The primary aim of thesis was therefore to determine whether iNOS was expressed in the cardiovascular system in rats with CHF following CAL and subsequent MI. In

particular, the aim of these experiments was to investigate its expression within the heart, small mesenteric arteries (internal diameters, 300 – 350 μm) and thoracic aortae. After establishing whether iNOS was expressed in small mesenteric arteries and thoracic aortae from rats with CHF, the aim of future experiments was to investigate the functional significance of iNOS on vascular function. The final of aim of this thesis was to examine the role of superoxide in modulating vascular NO bioavailabilty in this model of CHF.

Investigations into the role of iNOS and superoxide in the pathogenesis of cardiovascular diseases have in the past been hampered by the lack of suitable pharmacological tools. The aim of preliminary experiments in this thesis were to investigate the pharmacological properties of the novel iNOS inhibitor, *N*-(3-(Aminomethyl) benzyl) acetamidine dihydrochloride (1400W), and the cell permeable metalloporphyrin superoxide dismutase mimetic, Mn [III] tetrakis [1-methyl-4-pyridyl] porphyrin (MnTMPyP).

Chapter 2

Methods

This chapter describes the experimental techniques used in one or more chapters of this thesis. Specific experimental protocols for each group of experiments are given in the relevant chapters. All experiments using animals were carried out in accordance with the Animals (Scientific Procedures) Act 1986.

2.1 Animal models used

2.1.1 Rat model of septic shock

2.1.1.1 Introduction

Despite extensive research and development of modern therapeutic tools, septic shock remains a complex disease with high mortality. Septic shock results from spread and expansion of an initially localized infection, eg peritonitis, meningitis, into the bloodstream. It is characterised by systemic hypotension, loss of responsiveness to vasoconstrictors, diminished myocardial contractility, activation of the coagulation system and widespread endothelial cell injury (Mitchell & Cotran, 1999). The hypoperfusion resulting from the effects of widespread vasodilatation, myocardial pump failure and disseminated intravascular coagulation results in multiple organ failure. If the underlying infection is not brought under control, septic shock is usually fatal. The pathogenesis of septic shock is complex and not fully understood. However, the most common cause of septic shock is the contamination of the blood with Gram-negative bacilli (Titheradge, 1999). It is now widely accepted that endotoxin, a lipopolysaccharide (LPS) component of the bacteria cell wall, is the major mediator of Gram-negative septic shock (endotoxic shock; Titheradge, 1999). The release of endotoxin induces a cascade of self-perpetuating events. A simplified schematic diagram of this cascade is given in ***Figure 2.1***.

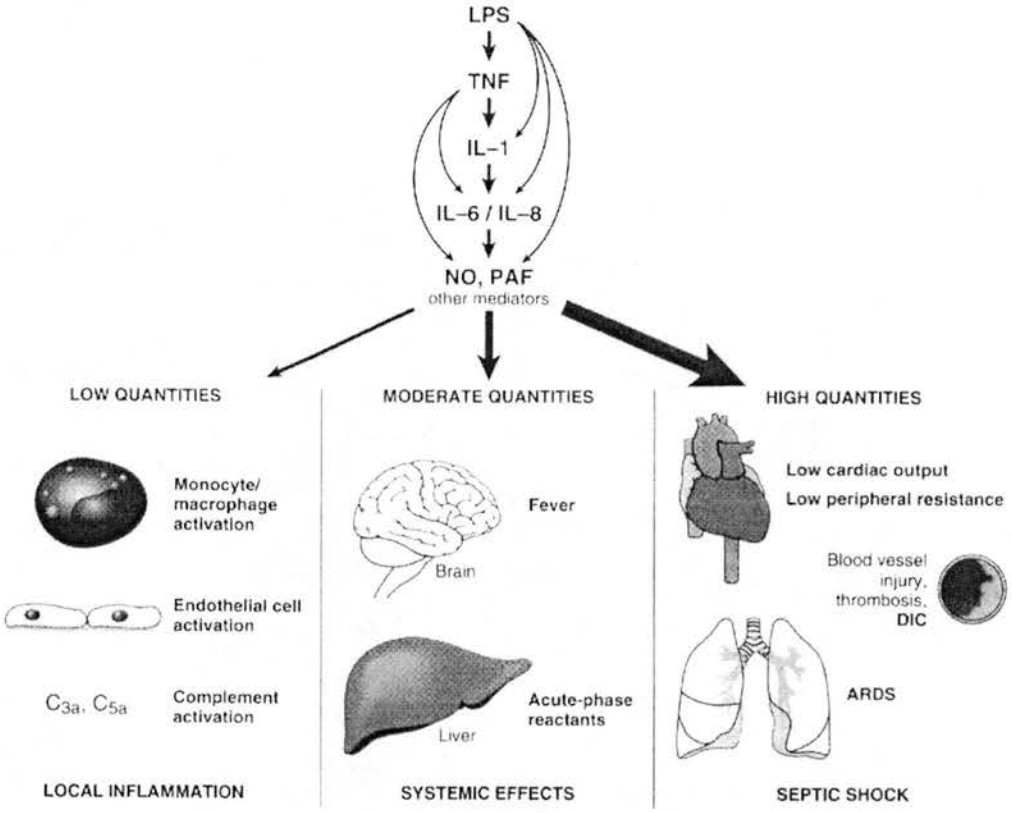

Figure 2.1 *Effects of lipopolysaccharide (**LPS**). **LPS** initiates a cytokine cascade, tumour necrosis factor-α, (**TNF**); interleukin-1, (**IL-1**); interleukin-6, (**IL-6**) and interleukin-8 (**IL-8**). In addition, LPS can directly stimulate down-stream cytokine production and the release of secondary mediators such as nitric oxide (**NO**) and platelet-activating factor (**PAF**). **DIC**, disseminated intravascular coagulation; **ARDS**, adult respiratory distress syndrome. Modified from Abbas et al., (1994), Cellular and Molecular Immunology.*

A number of mediators have been implicated in the pathogenesis of endotoxic shock, including inflammatory cytokines, platelet activating factor (PAF) and nitric oxide (NO) (***Figure 2.1***). LPS and cytokines can induce expression of the inducible isoform of NO synthase (iNOS) in almost any cell type, including vascular endothelial and smooth muscle cells (Schulz *et al.*, 1991; Balligand *et al.*, 1995; Fleming *et al.*, 1991) and cardiac myocytes (Brady *et al.*, 1992; Balligand *et al.*, 1994). In endotoxic shock, the expression of iNOS throughout the cardiovascular

system and the subsequent production of large quantities of NO is thought to play an important role in the cardiovascular dysfunction associated with this disease (for review see Titheradge, 1999).

Animal models have been used extensively to investigate the pathogenesis of endotoxic shock and also in the development of pharmacological agents for both the treatment and investigation of the disease. Administration of LPS to rats reproduces many of the features of endotoxic shock in humans, including hypotension (Gray *et al.*, 1991; Pedoto *et al.*, 1998) and myocardial dysfunction (Schulz *et al.*, 1995; Sun *et al.*, 1997). Endothelium-intact and endothelium-denuded blood vessels from rats treated with LPS, show hyporesponsiveness to a variety of vasoconstrictors (Julou-Schaeffer *et al.*, 1990; Weigert *et al.*, 1995). Furthermore, inhibition of NO synthesis using non-selective inhibitors of NOS reverses this hyporesponsiveness irrespective if the endothelium is intact or not, suggesting that enhanced formation from iNOS accounts for this vascular hyporeactivity. It is not the purpose of this thesis to investigate the pathogenesis of endotoxic shock. However, the expression of iNOS in the vasculature during experimental endotoxic shock provides an ideal model for the establishment of techniques and provides positive controls for the investigation of the expression of iNOS in the cardiovascular system of rats with CHF following coronary artery ligation (CAL). Furthermore, blood vessels isolated from rats treated with LPS should provide an acceptable model to examine the pharmacological selectivity of the novel iNOS inhibitor, *N*-(3-(Aminomethyl)benzyl) acetamidine dihydrochloride (1400W; see **Chapter 3**).

2.1.1.2 Induction of endotoxic shock

Endotoxic shock was induced in male Wistar rats (250 – 350 g, Charles River, U.K.) by injection of LPS. Rats were injected with LPS ($30mgkg^{-1}$, i.p., suspended in 0.1ml saline/100g rat body weight) derived from *Escherichia Coli* (Serotype 055:B5, Sigma, U.K.) and subsequently left for 5 h to develop endotoxic shock.

2.1.1.3 Tissue harvesting and plasma sampling

Where blood samples were required, LPS-treated and control rats were anaesthetised with sodium pentobarbitol (60 $mgkg^{-1}$, i.p. Sagatal). A plastic cannula (2.10mm diameter, Portex Ltd.) was then introduced into the abdominal aorta. Blood was collected (~ 5 ml) into a syringe pre-rinsed with heparin (100 U ml^{-1}, Multiparin, CP Pharmaceuticals, Wrexham, U.K.). Samples were immediately transferred into pre-chilled Eppendorph sample tubes containing 50 µl of 10mmol/l ethylenediaminetetraacetic acid (EDTA; Sigma, U.K.). The blood was fractioned by centrifugation at 2000 revolutions per minute at 4 °C for 20 min. The cell free plasma was collected and stored at – 20°C until use.

Following exsanguination, the thoracic aortae was removed and placed in cold, oxygenated (95% O_2, 5% CO_2), Krebs Henseleit solution (see Appendix) for functional studies (see Section **2.2**). Sections of the thoracic aortae from both LPS-treated and control rats were fixed in 10% neutral buffered formalin (24 h, Sigma) for immunohistochemical staining (see Section **2.3**).

2.1.2 Rat coronary artery ligation model of CHF

2.1.2.1 Introduction

In cardiovascular research, animal models have facilitated the investigation and treatment of cardiovascular disease. An ideal animal model should, for any cardiovascular disease have five characteristics, 1) mimic the human disease, 2) allow studies in chronic, stable disease, 3) produce symptoms which are predictable and controllable, 4) satisfy economic, technical and animal welfare considerations and 5) allow measurement of relevant cardiac, biochemical and haemodynamic parameters (Doggrell & Brown, 1998). Experimental heart failure can be induced by a variety of techniques in a range of species (for reviews see Doggrell & Brown, 1998; Hasenfuss, 1998). It is acknowledged, however, that no single model is able to completely mimic the complex alterations during heart failure in man. The most common model of heart failure, which is used in this thesis, is the rat coronary artery ligation (CAL) model. In the first instance, rat models of heart failure have a clear

advantage over other species with respect to cost, sample size, gestation period and life span (Hasenfuss, 1998). In 1960, Seyle *et al.* were the first to describe the technique of CAL in the rat (Seyle *et al.*, 1960). However, Pfeffer *et al.* were the first to characterise this model (Pfeffer *et al.*, 1979). Occlusion of the coronary artery was found to induce left ventricular (LV) infarctions that were histologically similar to those in man and impairment of LV performance was directly related to the size of the infarct. Furthermore, CAL was associated with LV dilatation, reduced systolic function and increased LV end-diastolic pressures (LVEDP; Pfeffer *et al.*, 1979; Litwin *et al.*, 1994). Further studies have since shown that the progression of myocardial failure after CAL is associated with neurohormonal activation similar to that seen in the human (Hodsman *et al.*, 1988).

Despite the obvious advantages of this model it has disadvantages. Pfeffer *et al.* (1979) acknowledged that CAL in the rat is not analogous to the pathogenesis of coronary artery disease or infarction in humans since surgery is carried out on essentially healthy coronary arteries and myocardium. Furthermore, problems exist with high mortality, variation in infarction size and lack of progression from compensation to end-stage heart failure. Despite these disadvantages, in balance, the rat CAL model of CHF has proven to be a useful and appropriate model in the investigation of CHF. Indeed, the therapeutic potential of angiotensin converting inhibitors (ACE) inhibitors was first realised using this model (Pfeffer & Pfeffer, 1988). It is for this and the aforementioned reasons that the CAL rat model of CHF was used in this thesis.

2.1.2.2 Coronary artery ligation surgery

Myocardial infarction was induced in male Wistar rats (250 – 300 g, Charles River, U.K.) by occlusion of the left anterior descending coronary artery according to the method described by Seyle *et al.* (1960) and modified by Pfeffer *et al.* (1979). Rats were maintained on standard rat chow and tap water *ad libitum* for at least one week prior to surgery. On the day of surgery, rats were weighed before being anaesthetised with sodium pentobarbital (60 $mgkg^{-1}$, i.p. Sagatal, Rhone Merieux Ltd., Essex, U.K.). Prior to surgery, the left side of the chest was shaved and sterilised using 70%

alcohol. Once fully unconscious, rats were placed on a thermostatically controlled heating blanket (37°C) and intubated with a plastic cannula (2.10 mm diameter, Portex Ltd., Kent, U.K.) using a guide wire. Mechanical ventilation (O_2 enriched air) was achieved using a small rodent ventilator (Harvard Apparatus Ltd., Kent, U.K.) at a rate of 60 cycles/minute and a tidal volume of 1 ml/100g body weight.

After a period of stabilisation, an incision (~ 2 cm), parallel to the direction of the ribs, was made into the left side of the chest. Underlying muscle layers were carefully separated and held in position with metal clips to expose the ribs. An incision (~ 1.5 cm) was made in between the 4^{th} and 5^{th} ribs again running parallel with the ribs. Care was taken not to damage the lungs when making this incision. To protect the lungs during exteriorisation of the heart, a piece of sterilised gauze was used to collapse the left lung. The lung was then gently pushed down and away from the heart. Using a pair of blunt scissors, a hole was made in the pericardium, after which the heart was gently and rapidly manipulated out of thoracic cavity. Once the heart was in position, a silk suture (10 mm round bodied, Ethicon Ltd., Edinburgh, U.K.) was positioned around the left descending coronary artery, after which the heart was swiftly returned to the chest. The rat was left for 10 min to allow recovery from exteriorisation before the suture was tied. A plastic cannula (0.75 mm diameter, Portex Ltd.), attached to a 1ml syringe, was then carefully placed in the thoracic cavity and the gauze used to collapse the lung removed. The chest wall was closed using a 16 mm round bodied suture (Ethicon Ltd.). Before tying the last suture, the chest was gently squeezed to remove air from thoracic cavity. The overlying muscles were returned to their original position. Any remaining air within the thoracic cavity was removed by means of the cannula and syringe. The cannula was removed before suturing the skin with a 25 mm round bodied suture (Ethicon Ltd.). Rats were maintained on the ventilator for a further 15 min. After this period rats were taken off the ventilator, placed on a thermostatically controlled heating blanket and left to recovery with 100% oxygen. The tracheal cannula was removed when rats showed signs of recovery from anaesthesia. Rats were returned to their cages when fully recovered from anaesthesia and maintained on standard rat chow and tap water *ad libitum.* All rats were given buprenorphine hydrochloride (0.05 ml, Vetergesic, 0.3

mg/ml; Redcut & Colman, U.K.) subcutaneously upon recovery from anaesthesia and the following morning for analgesia.

For sham-operated control rats, the same procedure was applied except the coronary suture (10 mm round bodied, Ethicon Ltd.) was not tied but pulled under the artery.

2.1.2.3 Haemodynamic measurements

Six weeks after CAL or sham-operation, rats were anaesthetised with sodium pentobarbitol (60 $mgkg^{-1}$, i.p. Sagatal). The right carotid artery was isolated and a fluid-filled (heparin; 100 U ml^{-1}, Multiparin, CP Pharmaceuticals, Wrexham, U.K, diluted in 0.95 saline) cannula (0.75 mm internal diameter, Portex, Ltd.) was introduced into the artery. After a stabilisation period (~ 5 min), arterial blood pressure was analysed using a MacLab (version 3.4/e) data analysis system (AD Instruments, Hastings, U.K.) and recorded on an Apple Mac computer. The catheter was then carefully advanced into the left ventricle for measurement of LVEDP as an index of LV function. A representative trace of arterial blood pressure and LVEDP measured from a CAL rat is shown in ***Figure 2.2***. From ***Figure 2.2*** we can see that as the catheter is advanced into the left ventricle there is an increase in the pressure pulse. The peaks and troughs of this part of the trace represent the LV systolic pressure and LVEDP respectively. LVEDP was measured as an average of ~ 30 troughs of the trace.

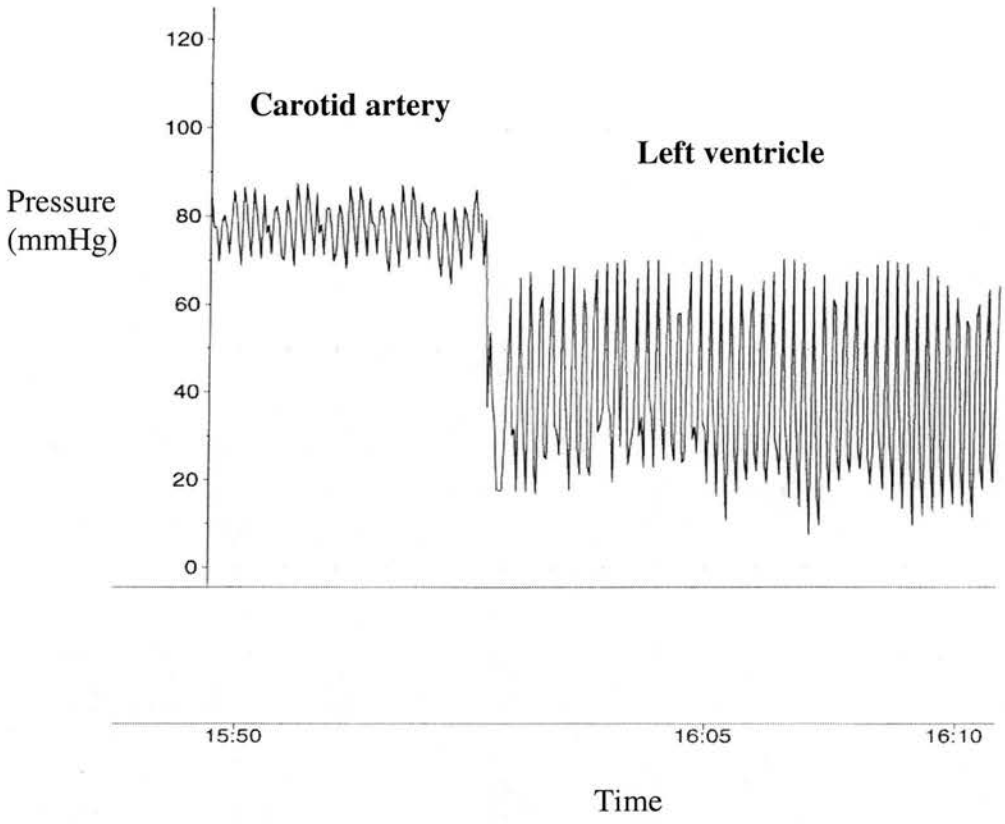

Figure 2.2 *A representative pressure-transducer reading of arterial blood pressures and left ventricular pressures from within the carotid artery and left ventricle, respectively, in a coronary artery ligation rat.*

2.1.2.4 Tissue harvesting

Following exsanguination, the mesenteric bed and thoracic aortae were removed and placed in cold, oxygenated (95% O_2, 5% CO_2), Krebs Henseleit solution for functional studies (see Sections **2.2** and **2.3**). Before storage of mesenteric bed the jejunum was removed and the remaining vascular bed returned to Krebs Henseleit solution. Sections of the mesenteric bed and thoracic aortae from both CAL and sham-operated rats were fixed in 10% neutral buffered formalin (24 h, Sigma.) for immunohistochemical staining (see Section **2.3**). The heart, lungs and kidneys were also removed, washed in saline (0.9%) and weighed. Hearts were bisected from apex to base and placed in formalin as above.

2.1.2.5 Measurement of infarct size

Occlusion of the left coronary artery results in the development of a collagen rich scar in the infarcted zone of the LV (see Section **1.5.2**). Therefore, using a histological stain for collagen, infarct size in relation to the LV free wall can be measured. Formalin fixed hearts from both CAL and sham-operated rats were processed in alcohol (to replace the formalin), infiltrated and embedded in molten paraffin wax. 3 μm sections were taken from cooled blocks and floated on a water bath (45 °C) to remove folds in sections. Sections were then transferred to microscope slides coated with 3-Aminopropyltriethoxy-saline (TESPA, Sigma; see Appendix). Once sections were dry, slides were transferred to an incubator (37 °C) for 24 h to ensure complete adherence of tissues. Sections were de-waxed in xylene (10 min), rehydrated through a descending alcohol series (100, 90 and 70% alcohol; 3 min each) and washed in water (15 min). Sections were then incubated with Celestine Blue (Sigma) for 4 min to stain the nuclei. After washing in water (5 min) sections were treated with van Gieson's collagen stain (see Appendix) for 3 – 5 min and then rinsed with water. Sections were then dehydrated through an ascending alcohol series (70, 90 and 100% alcohol; 3 min each) and xylene (10 min) before mounting in DPX medium (BDH Laboratory Supplies, Poole, U.K.).

Infarct size was measured by a method previously described by Mulder *et al.*, (1998). Briefly sections stained with van Gieson's collagen stain were placed under a CCD video camera module (Sony, U.K.) attached to a microscope with a x20 lens. Images were then electronically transferred to the computer for analysis (***Figure 2.3***).

The endocardial and epicardial circumferences of the infarcted tissue and of the LV free wall were determined with image analysis software (Imaging Associates, U.K.). Infarct size was calculated as a percentage [endocardial + epicardial circumference of the infarcted LV (mm)/ endocardial + epicardial circumference (mm)] of the whole left ventricle.

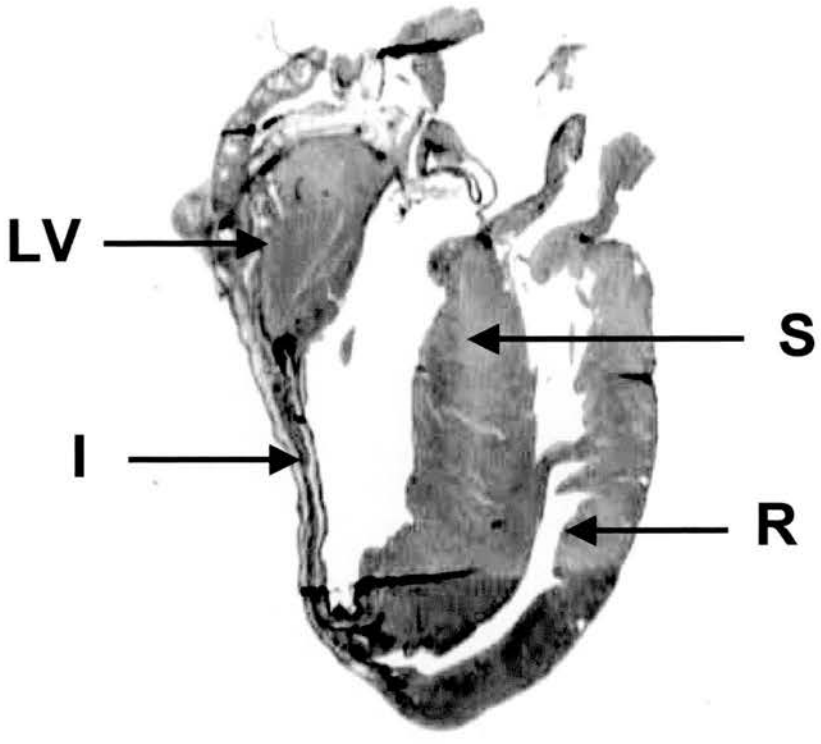

Figure 2.3 *Computer generated image of longitudinal section of a heart from a rat 6 weeks post coronary artery ligation. Images of hearts were used to calculate infarct size in relation to the left ventricular free wall.* ***LV****, left ventricle;* ***I****, infarct;* ***S****, interventricular septum and* ***RV****, right ventricle.*

2.2 Functional pharmacological studies of isolated thoracic aorta

2.2.1 Preparation of aortic rings

The thoracic aorta was pinned out in a silicone-coated (Sylgard, Dow-Corning, U.K.) dissecting dish containing cold Krebs Henseleit solution. Using a blunt pair of scissors, the aorta was carefully cleaned of adhering adipose and connective tissue. The aorta was cut into transverse rings and mounted on two wires in an organ bath (Model 700MO, Danish Myo Technology, Denmark) filled with 10 ml of warm (37 °C), oxygenated (95% O_2, 5% CO_2), Krebs Henseleit solution. To ensure that the same size of segment of aorta was used in each experiment, rings were cut to fit the length of the wires (~ 4 mm). Care was taken not to damage the endothelium during mounting. Isometric tension was measured by a DSC6 strain gauge transducer, linked to a MacLab data analysis system. Aortic rings were placed under 2 g of tension and left for 60 min to equilibrate. During this equilibration period, rings were periodically washed with Krebs Henseleit solution and tension readjusted to 2 g when required.

2.2.2 General protocol

Before commencing experiments, the following protocol was performed on all aortic rings. Rings were exposed to modified Krebs Henseleit solution containing 60 mM potassium chloride (equimolar replacement of NaCl by KCl) to obtain maximal contraction. Once contractions had stabilised (~ 5 min), responses were recorded on an Apple Mac computer and rings washed with Krebs Henseleit solution (~ 10 min) until the tension had returned to 2 g. Rings were exposed once more to modified Krebs Henseleit solution to ensure maximal contraction. After washout with Krebs Henseleit solution (~ 10 min) rings were exposed twice in succession, separated by washout, to a supramaximal concentration of norepinephrine (NE; 10^{-5} M). In all aortic rings the integrity of the endothelium was assessed by measuring acetylcholine (ACh)-induced relaxation of NE-induced tone. A submaximal concentration of NE

(~ EC_{60}) was used to induce arterial tone. Once responses to NE were stable, rings were exposed to a supramaximal concentration of ACh (10^{-5} M). Aortic rings with relaxations greater than 70% of NE-induced tone were classified as having an intact endothelium and used in experiments. Rings failing to reach this criteria were discarded. In some aortic rings the endothelium was removed prior to commencing experiments. This was achieved by gently rubbing the intima of the rings with a pair of fine forceps. As with endothelium-intact aortic rings, ACh-induced relaxation (10^{-5} M) of NE-induced tone (~ EC_{60}) was measured. Denudation of rings was deemed successful in those rings where relaxations to ACh were less than 5% of NE-induced tone. All aortic rings were washed with Krebs Henseleit solution and left to re-equilibrate before commencing experimental protocol.

2.3 Functional pharmacological studies of isolated small mesenteric arteries using perfusion myograph

2.3.1 Introduction to technique

Until the mid-1970s, most of the information concerning the mechanical, morphological and pharmacological properties of blood vessels was attained from *in vitro* studies of large arteries, such as thoracic aorta. Information on smaller arteries was limited to perfusion experiments and histological examination, with size and fragility of smaller vessels discouraging investigators from undertaking mechanical experiments. However, in 1976 wire myography was developed to allow investigators to study blood vessels with internal diameters as small as 100 μm (Mulvany & Halpern, 1976). In this technique segments of small arteries, are mounted between two wires for measurement of isometric force (***Figure 2.4***). This technique has been used extensively in vascular research. In 1991 Halpern & Kelley, were the first to describe an adaptation of the wire myograph called the small vessel arteriograph, or the perfusion myograph. In this technique, vessels are cannulated, in a closed system, at both ends (***Figure 2.4***) and are exposed to a fixed transmural pressure by infusing physiological salt solution into the vessel lumen. Therefore, in contrast to the wire myograph, the perfusion myograph allows the blood vessel to maintain its physiological shape and thus more of their physiological characteristics than those used in the wire myograph. These include the development of myogenic and spontaneous tone (VanBavel *et al.*, 1991), which are rarely seen in the wire myograph. Additionally, equal transmural pressure is achieved across the vessel wall, contrasting with unequal stretch caused by the two wires. This is of paramount importance in studies investigating the role of the endothelium in modulating vascular tone, since transmural pressure within blood vessels *in vivo* is thought to alter the release of endothelium-derived factors (for review see Shore, 1996). Moreover, blood vessels are able to contract and relax as they would *in vivo*. Other practical advantages of the perfusion myograph are given overpage:

1. The endothelium is untouched during mounting and experimentation, in contrast mounting on wires causes local damage to the endothelium.
2. The axial length of the vessel can be altered, thus preventing over stretching during mounting.
3. Drugs can be added both luminally and abluminally.

The perfusion myograph does, however, have disadvantages. In the pressurised system, blood vessels have to be free of holes or branches in order to maintain pressure. This may prove difficult in some vessel types, such as coronary arteries, where holes and branches are impossible to see even at high magnification. Furthermore, although the axial length of vessels can be altered, it is difficult to normalise the length in every vessel. However, because the perfusion myograph is regarded as more a physiologically relevant model than the wire myograph, and for other practical reasons given above, the perfusion myograph was used in this thesis.

a) **Wire Myograph**

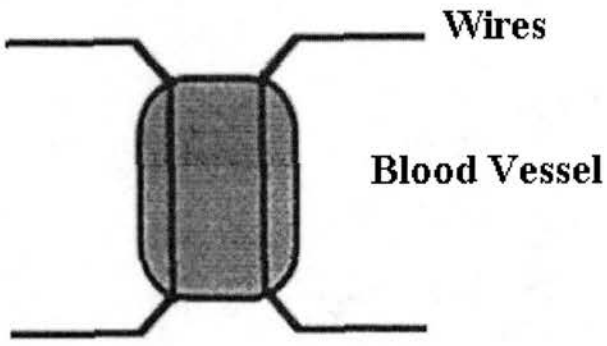

b) **Perfusion Myograph**

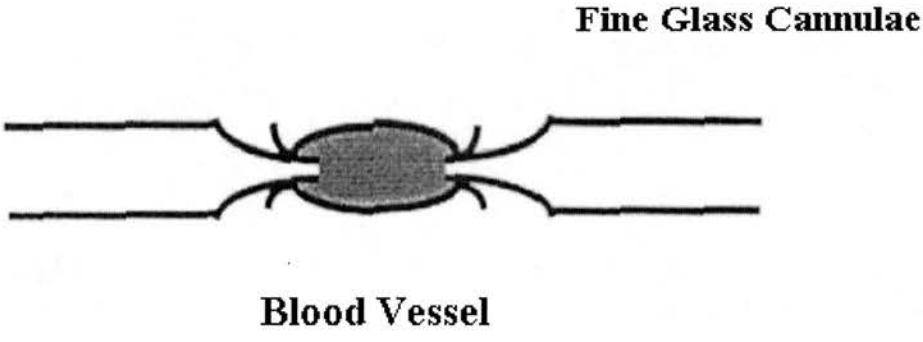

Figure 2.4 *A schematic diagram of wire and perfusion myograph. In the wire myograph (**a**) blood vessels are mounted between two wires and changes in vessel tension measured by isometric force exertion on the wires. In the perfusion myograph (**b**) blood vessels are mounted on two cannulae (with distal cannulae closed) and exposed to a fixed transmural pressure by infusing physiological salt solution into the vessel lumen.*

2.3.2 Preparation of small mesenteric arteries

The mesenteric bed was pinned out on a silicone-coated (Sylgard) dissecting dish containing cold Krebs Henseleit solution. Care was taken not to over stretch the vascular bed during pinning out. Mesenteric arteries with internal diameters of ~ 300 – 350 μm were selected for use in functional studies in this thesis. To achieve this it was necessary to use third order branches of the mesenteric artery (***Figure 2.5***). The artery of choice was selected by counting down the branches from the superior mesenteric artery. The vascular bed is structured such that arteries and veins lie on top of each other covered by adipose tissue. Therefore, with the use of a dissection microscope (Zeiss, U.K.), fine forceps (World Precision Instruments, Inc., Sarasota, U.S.A.) and vannas spring scissors (World Precision Instruments, Inc.), adipose tissue surrounding the artery and vein was carefully removed. This was achieved by gently teasing the adipose tissue away from the vessels and cutting the fine membrane that attaches the adipose tissue to the artery or vein. The artery was distinguished from the vein by examining the junction at the branch of the second and third arteries. As shown in ***Figure 2.5***, arteries have a distinct 'v' shaped junction in comparison with a 'u' shaped junction in veins. Additionally, arteries have thicker, more defined walls than veins. Once the artery was identified, remaining adipose tissue was removed as before. To enable identification of the proximal and distal ends of the artery, and thus mimic blood flow direction when mounting in the myograph, a small area of adipose tissue was left intact on the proximal end of the artery. The artery (~ 4 mm) was cut free from the vascular bed.

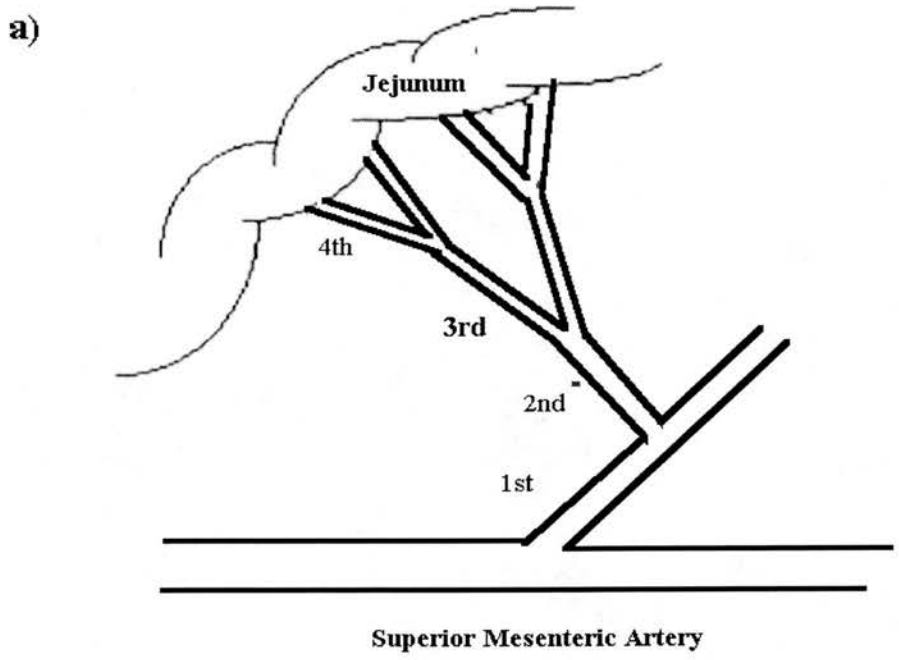

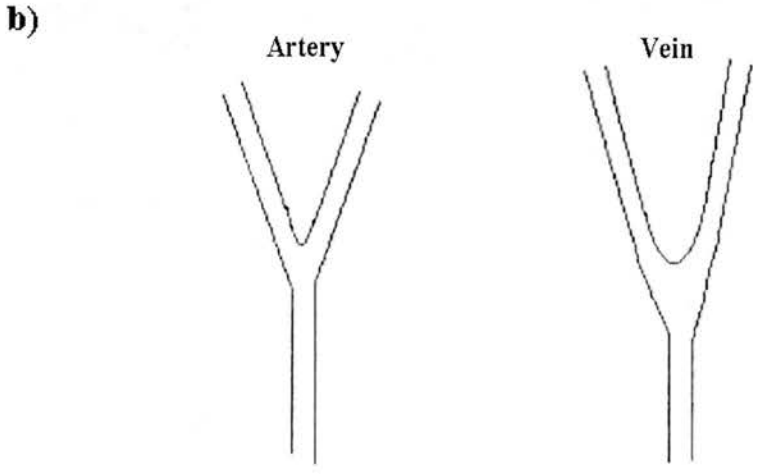

Figure 2.5 *Anatomical selection of 3rd order mesenteric arteries from the rat mesenteric bed, (**a**) localisation of 3rd order arteries counting from the superior mesenteric artery, (**b**) illustrates the differences between arteries and veins at the junctions of branches.*

2.3.3 Mounting of arteries in the myograph

Dissected arteries were transferred to the chamber of the perfusion myograph (Living Systems Instrumentation Inc., Burlington, Vermont, U.S.A.) containing 10 ml of warm (37 °C), oxygenated (95% O_2, 5% CO_2), Krebs Henseleit solution. The artery was then mounted onto fine glass cannulae (~ 100 - 150 μm tip diameter), and secured by single-fibre silk threads. The procedure of mounting mesenteric arteries was as follows: first the proximal end of the artery was gently pulled onto the cannula tip until approximately 200 μm of the tip was inserted into the lumen of the artery. The artery was then secured by two silk threads, which had already been looped onto the cannula. Any blood present in the lumen of the artery was removed by opening the stopcock to the proximal cannula and slowly infusing (1 ml/min) Krebs Henseleit solution through the lumen by means of a miniature peristaltic pump (PS/200, Living Systems Instrumentation Inc., Burlington, Vermont, U.S.A.). Care was taken not to allow the intra-luminal pressure rise above 10 mmHg, in order to prevent damage to the endothelium and vessel wall. After the blood was removed, the stopcock was closed and the distal end of the artery wall tied onto the distal cannula in the same way as described for the proximal end.

An intraluminal pressure of 60 mmHg was attained slowly by introducing Krebs Henseleit solution into the vessel lumen using the miniature peristaltic pump, connected to a pressure servo unit. A pressure of 60 mmHg was chosen because it has been estimated that vessels of this size would experience pressures approximately 50% of mean arterial pressure *in vivo* (Halpern & Kelley, 1991). As the pressure increases, the artery usually developed a bend as a consequence of axial lengthening. These buckles were removed by gently retracting the proximal cannula, using the length transducer, to the original axial length prior to dissection. Care was taken not to introduce any axial stretch. Once a pressure of 60 mmHg was reached the pressure within the artery was maintained and regulated by switching the pressure servo unit from manual to automatic mode. Before and during experimental protocols, arteries were checked for any leaks by changing the pressure servo unit back to manual mode. Under these conditions, any loss in pressure will not be

compensated for by the pressure servo unit, resulting in a rapid drop in pressure. In this case, the artery was discarded and another one mounted.

The myograph was placed on an inverted stage microscope (Nikon TMS-F, Japan) which was connected to a monochrome television camera (Burle, U.S.A.), and the vessel visualised on a television monitor. The lumen diameter and wall thickness were measured using a video dimension analyser (Living Systems Instrumentation Inc., Burlington, Vermont, U.S.A.), calibrated against a stage micrometer (resolution = 1μm). The video dimension analyser senses changes in optical density of the artery at a chosen scan line. The walls have a higher optical density that the rest of the lumen and appear on the television screen as two thick bands. This allows continuous measurement of both wall thickness and lumen diameter. Smaller lumen diameters were measured by hand using a calibrated micrometer since the differences in the optical density at diameters of less than 150 μm were not distinct enough for the optical dimension analyser to detect.

After mounting and pressurisation, the arteries were continuously superfused with warm (37 °C), oxygenated (95% O_2, 5% CO_2), Krebs Henseleit solution. The temperature of the Krebs Henseleit solution was maintained at 37°C by passing it through a glass-jacketed heated coil that was warmed with circulating water from a water bath (Grant Systems, U.K.). The temperature in the chamber of the perfusion myograph was checked regularly.

2.3.4 Protocol for addition of drugs to the perfusion myograph

In traditional organ bath experiments, such as those carried out on isolated aortic rings, cumulative concentration response curves (CRC) are normally performed by addition of increasing concentrations of drugs to the Krebs Henseleit solution bathing the vessel. Unlike conventional organ baths, the chamber of the perfusion myograph is not heated. Instead the temperature within the chamber is maintained by the continuous perfusion of heated Krebs Henseleit solution. Therefore, addition of drugs directly to the chamber itself would require switching off the pump, resulting

in a fall in temperature within the chamber. To overcome this problem a 'reperfusion circuit' was designed, which allowed cumulative CRCs to be performed. The reperfusion circuit consisted of a closed system containing a total volume of 30 ml of Krebs Henseleit solution, which was constantly superfused the artery at a low flow rate (5 ml/min). All drugs used throughout the experiments were applied to this reservoir. The reperfusion circuit was only used during preliminary and experimental protocols; arteries were superfused with Krebs Henseleit solution in an open system at all other times.

2.3.5 General protocol

Small mesenteric arteries were exposed to modified Krebs Henseleit solution containing 60 mM KCl (equimolar replacement of NaCl by KCl) to obtain maximal constriction. Once constrictions had stabilised (~ 5 min), internal diameters of arteries were recorded, and the superfusate replaced with Krebs Henseleit solution. Small mesenteric arteries were exposed once more to modified Krebs Henseleit solution to ensure maximal constriction. After sufficient washout with Krebs Henseleit solution (~ 10 min), arteries were exposed twice in succession, separated by washout, to a supramaximal concentration of phenylephrine (PE; 10^{-5} M). In all arteries the integrity of the endothelium was checked by measuring ACh-induced relaxation (10^{-5} M) of PE-induced tone (10^{-5} M). As with thoracic aortae, mesenteric arteries with relaxations greater than 70% of PE-induced tone were classified as having an intact endothelium and included in experiments. Arteries failing to meet this criteria were discarded.

In some experiments it was necessary to remove the endothelium. In larger arteries, like the thoracic aorta, the endothelium is normally removed by mechanical disruption. Indeed, in this thesis the endothelium of thoracic aortic rings was removed by rubbing the intima of the ring with fine forceps. However, in the case of small mesenteric arteries, mechanical disruption by such a method is not feasible owing to the fragility and size of these arteries. Various methods have been employed in the past to remove the endothelium from small arteries. These include

perfusion of the arteries with detergents such as 3-[(3-cholamidopropyl) dimethylammonio]-1-propane sulphonate (CHAPS) (Hiley *et al.*, 1987; Takase *et al.*, 1995), dissolving the intracellular matrix with enzymes such as collagenase (Carvalho & Furchgott, 1981) or rupturing endothelial cells osmotically with distilled water (Criscione *et al.*, 1984). Although these techniques are successful in removing the endothelium, it is difficult to control the exposure time and shear rate through the vessel lumen and as a result they carry the risk of not only damaging the endothelium but also the underlying vascular smooth muscle (VSM) cells. Consequently, it is difficult to ascertain if any changes in vessel response is due to disruption of the endothelium or simply due to damage to the VSM cells. Mechanical disruption of the endothelium in small arteries can be achieved by two methods. Osol *et al.*, (1989) demonstrated that introduction of a single human hair into the vessel lumen was an effective method of removing the endothelium in small arteries. However, the most commonly method used is that where an air bubble is passed through the vessel lumen (Ralevic *et al.*, 1989; Bjorling *et al.*, 1992; Falloon *et al.*, 1993). Previously studies have demonstrated using confocal, scanning and transmission electron microscopy that the use of an air bubble does not cause damage to the underlying VSM cells (Smith, 1996). It is this method that is employed throughout the experiments described in this thesis.

The method of endothelium denudation was as follows: firstly, the axial length of the artery was noted by recording the setting on the length transducer, thus allowing the vessel to be reset afterwards to its original length. The pressure servo unit was switched to manual and the pressure within the artery slowly decreased. During this decrease in pressure the axial length was decreased to prevent any axial stretch on the artery. The distal stopcock was opened and an air bubble, approximately 2 cm in length, introduced into the proximal tubing. This was achieved by disconnecting the proximal tubing from the proximal stopcock and removing a small amount of Krebs Henseleit solution. The proximal tubing was re-attached and the bubble passed through the vessel lumen, the proximal cannula and artery by slowly increasing the flow of Krebs Henseleit solution. Care was taken to ensure that the pressure within the artery did not exceed 30 mmHg during the passage of the bubble. Once the

bubble had passed through the distal stopcock was left open for a further 10 min to ensure all endothelial cell debris was cleared from the lumen of the artery. After this period the distal stopcock was closed, the flow increased slowly under manual mode as before, and the vessel restored to its original axial length. Once a pressure of 60 mmHg was reached, the pressure servo unit was switched back to automatic mode and the artery allowed time (~ 10 min) to re-equilibrate. As with endothelium-intact mesenteric arteries, ACh-induced relaxation (10^{-5} M) of PE-induced tone (10^{-5} M) was measured. Denudation was deemed successful where relaxations to ACh were less than 5% of maximal PE-constriction.

2.4 Drugs used in functional studies

Drug	Source
Acetylcholine chloride	Sigma (Poole, U.K.)
L-arginine hydrochloride	Sigma
Catalase (bovine liver)	Sigma
Mn [III] tetrakis [1-methyl-4-pyridyl] porphyrin (**MnTMPyP**)	Alexis (Nottingham, U.K.)
N-(3-(Aminomethyl) benzyl acetamidine dihydrochloride (**1400W**)	Calbiochem (Nottingham, U.K.)
N^{ω}-nitro-L-arginine methyl-ester (**L-NAME**)	Sigma
Norepinephrine hydrogentartrate	Sigma
Phenylephrine hydrochloride	Sigma
Pyrogallol	Sigma
Sodium nitroprusside	Sigma
Vitamin C	Sigma

Table 2.1 *List of drugs used in functional studies and their sources.*

2.5 Immunohistochemistry

2.5.1 Introduction

Over a relatively short period of time immunohistochemistry has become an established routine histological technique for the identification of tissue and cellular components. In essence, this technique relies on the interaction of antibodies with antigens on the tissue of interest, with the site of antibody binding identified either by direct labelling of the antibody or by using a secondary labelling method.

Antibodies are produced by terminally differentiated B cells, as part of the humoral immune response to infection, with each antibody having specificity for one antigen. There are five different classes of antibodies, all of which differ in structure and function. The most common antibody found in the blood is called immunoglobulin (Ig) G and is the predominant antibody produced in response to infection. IgG consists of two light and two heavy polypeptide chains, joined by two disulphide bridges. Antibodies are extremely variable in amino acid sequence at the ends of these polypeptide chains. It is within these areas that the antibody gains affinity and avidity for an antigen.

2.5.2 Production of Antibodies for Immunohistochemistry

Two types of antibody are used in immunohistochemistry; polyclonal and monoclonal. Polyclonal antibodies are produced by immunisation of a host animal with the antigen of interest. The introduced antigen mimics an invading pathogen, and thus induces the humoral immune response. In simplified terms, B cells are activated by the antigen resulting in the production and secretion of IgG antibodies specific for that antigen. By purifying the serum, the antibody of interest can be harvested. Although simple and cost effective, the use of polyclonal antibodies does have disadvantages. Immunisation of the host animal with the antigen requires the antigen to be extremely pure and even when pure there is the risk that different B cells will produce antibodies against varying antigenic determinants on the antigen.

Therefore, antibodies produced by this method may be highly variable with respect to antigenic specificity. Moreover, when the serum is harvested it may contain antibodies from the animal itself that are not specific for the antigen. Such antibodies may cross-react with other molecules on the sample tissue and thus reduce the reliability of the procedure.

The use of monoclonal antibodies in immunohistochemistry was made possible in 1975 when Köhler & Milstein described a method for immortalising B cells. As with the production of polyclonal antibodies, the host animal is immunised with the antigen of interest. Normal antibody-producing B cells are then isolated from the host and fused with myeloma B cells, essentially immortalising the B cells. Immortalised B cells that secrete the antibody of desired specificity for the antigen can be isolated and cloned. Besides having an endless supply of antibodies, this technique provides antibodies with absolute specificity for one antigenic determinant on the antigen. Therefore, monoclonal antibodies are regarded as more reliable and are the most commonly used antibodies in immunohistochemistry.

2.5.3 Methods used in Immunohistochemistry

As mentioned in Section **2.5.1** the site of antibody binding on the sample tissue can be identified either by direct labelling of the antibody, or indirectly using a secondary labelling method (***Figure 2.6***). Direct labelling of the antibody is the simplest and shortest method for antigen detection; however, it is considered to be the least sensitive (Robinson *et al.*, 1988). The most common method of secondary labelling is the use of a second antibody, which is specific for the Ig class of the primary antibody. In this technique an unlabelled primary antibody is allowed to bind with its antigen on the sample tissue. A second labelled antibody, raised in another animal host and specific for the animal and Ig class of the primary antibody, is applied to the tissue and allowed to bind to the primary antibody. It is acknowledged that the indirect method for immunohistochemistry is a reliable and relatively sensitive method for antigen detection. The direct and indirect methods are summarised in ***Figure 2.6***.

Enzymes are the most widely used labels for antibodies in immunohistochemistry, and incubation with a substrate chromogen system produces a stable, coloured reaction end product that can be detected by light microscopy. Horseradish peroxidase is the most widely used enzyme and in combination with 3,3'-diaminobenzidinetetrahydrochloride, it produces an insoluble, stable, dark brown coloured end product. The most common alternative to horseradish peroxidase is alkaline phosphatase. Incubation with an alkaline phosphatase substrate and red fuchsin as a chromogen produces a permanent insoluble red product.

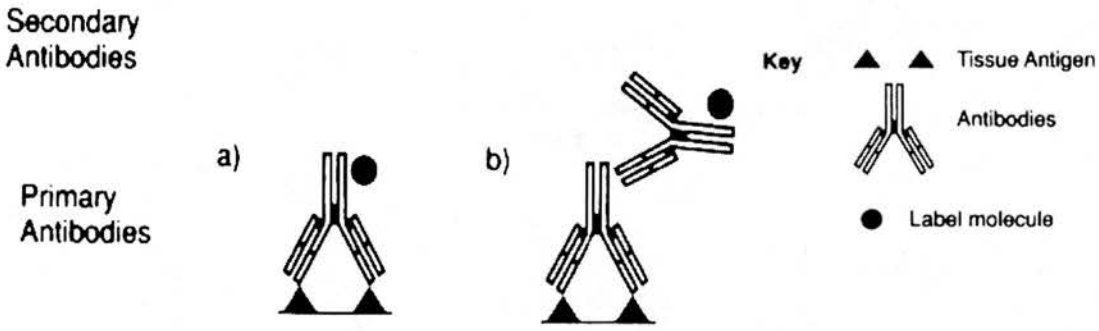

Figure 2.6 *Two methods used in immunohistochemistry, (**a**) direct method where primary antibody is labelled with a marker and (**b**) indirect method where a second labelled antibody is used to identify sites of antigen-antibody binding. Modified from Beltz & Burd: Immunocytochemical Techniques, Blackwell Scientific Publications, 1989.*

2.5.4 Preparation of tissues for Immunohistochemistry

Fixing with formalin is thought to mask antigens within the tissue sample (Huang *et al.*, 1976) and therefore, before staining with antibodies can commence, it is necessary to reverse this process. This is achieved by treating sections of tissues with proteolytic enzymes, such as trypsin or pepsin. Unfortunately there is no universally recommended time or enzyme and much depends on the tissue type and the method

and duration of fixation. Therefore, experimental details given in Section **2.5.5** were those optimised in-lab.

Despite the relative selectivity of antibodies used in immunohistochemistry, non-specific background staining can occur. The main cause of background staining is non-immunological binding of the specific immune sera by hydrophobic and electrostatic forces to certain sites within tissue sections (Kraehenbuhl & Jamieson, 1974). This form of background staining is often recognised as a uniform background colour. To overcome this problem, tissues are treated with non-specific Ig. This Ig will essentially bind to the sites that have non-specific affinity for antibodies, without interfering with the binding of the primary antibody. In general, serum (which will contain non-specific Ig) from the host of the secondary antibody is used.

2.5.5 Protocol for Immunohistochemistry

The method of antibody detection used in this thesis was the indirect method, using a monoclonal primary antibody and a secondary antibody conjugated to alkaline phosphatase. Immunohistochemistry was used to investigate the expression of iNOS in thoracic aortae from rats treated with LPS (see Section **2.1.1**) and in the cardiovascular system of CAL and sham-operated rats 6 weeks post-surgery (see Section **2.1.2**). The concentrations of antibodies used for individual tissues are given in the appropriate chapters. Dilutions of antibodies were made in phosphate buffered saline (PBS, pH 7.6; see Appendix) with 3% Bovine Albumin serum (Sigma). An overview of the protocol used is given below.

Formalin fixed arteries and hearts were processed in alcohol (to replace the formalin), infiltrated and embedded in molten paraffin wax. 3 μm sections were taken from cooled blocks and floated on a water bath (45 °C) to remove folds in the tissues. Sections were then transferred to microscope slides coated with TESPA (Sigma). Once sections were dry slides were transferred to an incubator (37 °C) for 24 h to ensure complete adherence of tissues. Sections were dewaxed in xylene

(10 min), rehydrated through a descending alcohol series (100, 90 and 70% alcohol; 3 min each), washed in water (15 min) and then placed in PBS for 5 min. Sections were then incubated in tris-buffered saline (TBS; pH 7.8; see Appendix) for 15 min at 37 °C before being treated with 0.1% trypsin (made in TBS). Incubation times for trypsin on individual tissues were as follows; mesenteric arteries, 15 min; thoracic aortae, 15 min and hearts, 45 min. After trypsinisation tissues were washed in PBS for 15 min.

Tissues were treated with 1% goat serum (Diagnostics Scotland, Carluke, U.K.), diluted in PBS for 30 min, at room temperature. Excess serum was removed from microscope slides before treating sections with a rabbit anti-iNOS monoclonal antibody (Affiniti Laboratories, Exeter, U.K.) for 24 h at 4 °C. Parallel tissues were treated with an antibody of the same Ig class but not directed against the iNOS epitope (Vector Laboratories, Peterborough, U.K.) again for 24 h at 4 °C. By doing so we can eliminate the possibility that any binding of the anti-iNOS antibody is due to non-specific binding due to the Ig class. After washing for 15 min in PBS, tissues were treated with an alkaline phosphatase-conjugated goat anti-rabbit antibody (Vector Laboratories) for 30 min at room temperature. Tissues were washed in PBS for 15 min. To detect iNOS within the arteries, sections were treated with an alkaline phosphatase substrate and red fuchsin as a chromogen for ~ 20 min (New Fuchsin Substrate System, Dako Corporation, Carpinteria, U.S.A.). Any positive sites of antigen-antibody binding on the tissue were visualised as a crisp, red stain. A summary of this protocol is given in ***Figure 2.7***.

After detection of iNOS, tissues were briefly rinsed with distilled water and treated with Harris' haematoxylin (BDH, Poole, U.K.) to counterstain nuclei of cells. Tissues were rinsed again in distilled water and then mounted in Aquamount mounting medium (Aquamount Improved, BDH).

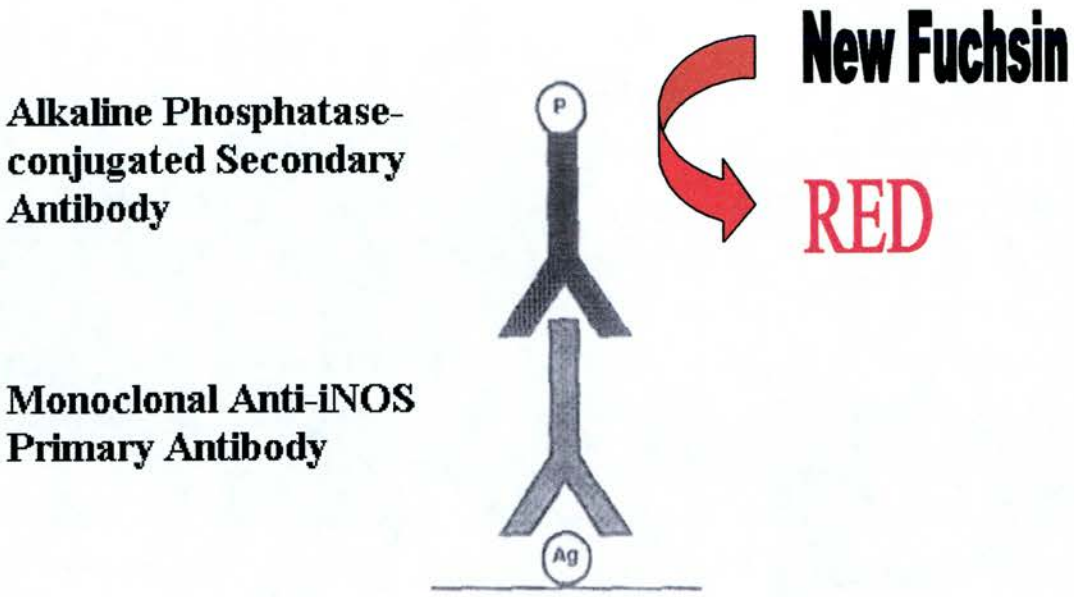

Figure 2.7 *Schematic diagram of immunohistochemistry method used in this thesis.* ***P****; alkaline phosphatase,* ***Ag****; antigen.*

2.6 Measurement of nitric oxide production

2.6.1 Introduction

NO production can be measured by a variety of methods in different types of samples, including urine, plasma and whole cell preparations. The transient and reactive nature of NO makes it unsuitable for most convenient detection methods. However, since NO is rapidly oxidised to nitrite (NO_2^-) and predominantly nitrate (NO_3^-) (collectively termed NO_x) these anions can be quantified and used as an indirect measure of NO production. In cell culture systems NO will rapidly degrade to NO_2^-, however, in the presence of Fe^{2+}haem, for example in the blood, NO_2^- is converted to the more stable product NO_3^-. Therefore, the relative abundance of each anion will depend on the sample type.

The most common and simplest of methods used to measure NO_3^- and NO_2^- is the conversion of NO_3^- to NO_2^- by nitrate reductase followed by the colorimetric detection of NO_2^- as an azo dye product of the Greiss Reaction (Green *et al.*, 1982; Stuehr *et al.*, 1989). Similarly, endogenous NO_2^- within the sample can be measured using the Greiss Reaction, thus allowing both NO_3^- and NO_2^- concentrations to be quantified. Other methods used include measuring NO_2^- by chemiluminescence following reconversion to NO (Knowles *et al.*, 1989; Bush *et al.*, 1992). In this thesis, plasma NO production was quantified by measuring total NO_2^- (after conversion of NO_3^- with nitrate reductase) by means of the Greiss Reaction, using a Nitric Oxide Assay Kit (R&D systems, U.K.). The Greiss Reaction involves the conversion of NO_2^- to a diazonium ion with sulfanilic acid, this ion is then coupled to *N*-(1-napthyl) ethylenediamine to form a chromophoric azo derirative, which absorbs light at 540 nm. This simple assay is summarised in ***Figure 2.8***. Endogenous NO_2^- within plasma samples was not measured because it was presumed that the majority of NO_2^- would have been converted to NO_3^- by Fe^{2+}haem in the blood prior to centrifugation.

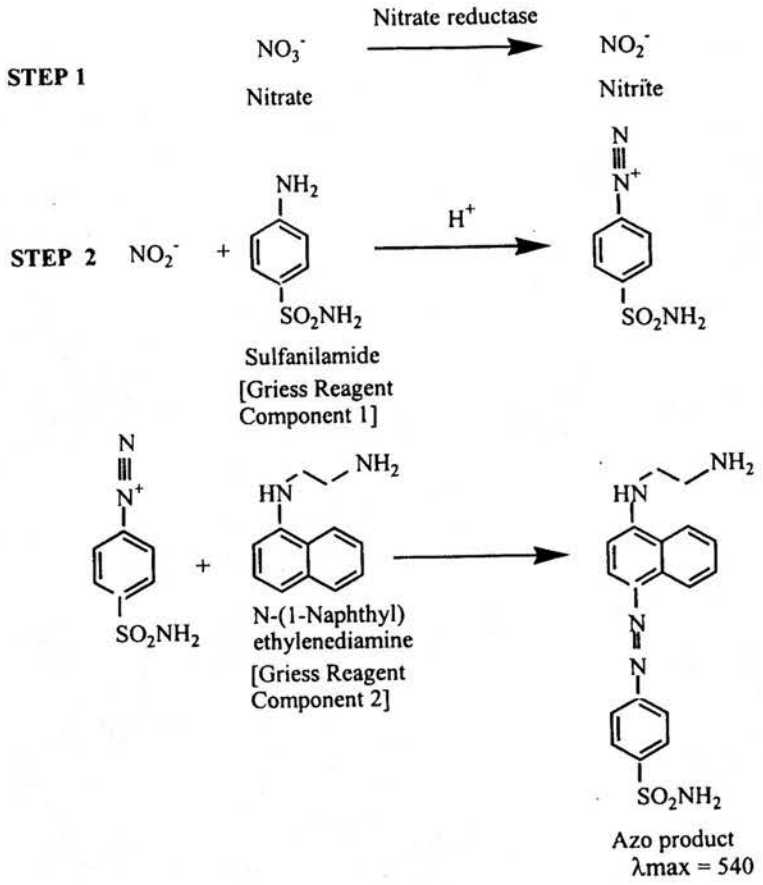

Figure 2.8 *Summary of assay for measurement of nitrite concentrations in plasma samples.* ***Step 1;*** *nitrate is converted to nitrite by nitrate reductase.* ***Step 2****, nitrite is converted to a diazonium ion which is then coupled to N-(1-Naphthyl) ethylenediamine to form an azo product.*

2.6.2. Limitations

Measurement of NO_x is clearly a useful and straight forward index of NO generation, however there are some important limitations of this technique that should be taken into account when interpreting and extrapolating results. NO_x is excreted by the kidney into the urine, therefore, plasma NO_x is not only an indirect index of systemic NO production but also of renal function and plasma volume. In disease states where renal function is impaired, and thus NO_x excretion is decreased, plasma and urine NO_x measurements should be interpreted with caution. Ideally, NO_x measurements should coincide with an independent measurement of renal function. However, difficulty in interpretation arises in those disease states where increased NO production is thought to be responsible for renal dysfunction.

2.6.3 Experimental protocol

Assays were performed with duplicate samples and standards provided with the assay kit.

All assay reagents were brought to room temperature before use. Plasma samples were defrosted at room temperature and diluted 1.5 fold using the reaction buffer provided. To eliminate proteins from the plasma, samples were ultrafiltered through a 10,000 molecular weight filter (14 mm diameter, Amicon, Gloucestershire, U.K.). 50 µl of filtered samples were placed into labelled wells of a microplate. 50 µl of NO_2^- standards were similarly placed in labelled wells, with 50 µl of reaction buffer used as zero standards. To each sample and standard well, 50 µl of reaction buffer was added, followed by 50 µl of Greiss Reagent I and 50 µl of Greiss Reagent II. Wells were mixed by gently tapping the side of the plate. The micropiter plate was covered and left at room temperature for 10 min. The optical density of each well was determined using a microplate reader (source) set at an absorbance of 540 nm.

Values for each duplicate standard and sample were averaged and the optical density for the zero standards subtracted. A standard curve was created using the values from

the standards provided and concentrations of NO_2^- within the samples quantified using this curve. An example of a standard nitrite curve, from which plasma sample concentrations were extrapolated, is given in ***Figure 2.9.*** Plasma samples were originally diluted, therefore, concentrations of NO_2^- were corrected by multiplying by the dilution factor (1.5).

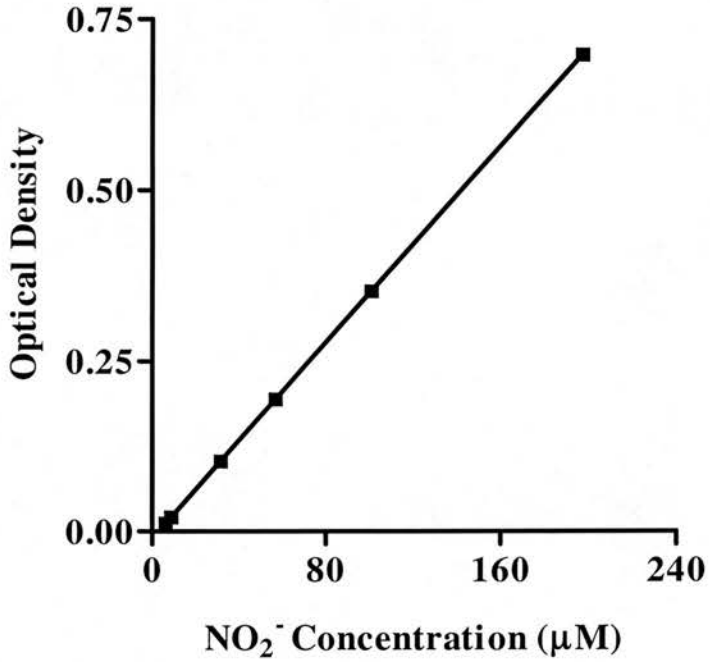

Figure 2.9 *Example of a standard nitrite curve for measurement of plasma nitrite concentrations.*

2.7 Data Analyses

Data analysis for experiments described in this chapter are given in the method sections of relevant chapters.

Chapter 3

Investigation of the pharmacological selectivity of the novel inducible nitric oxide synthase inhibitor 1400W

3.1 Introduction

Nitric oxide (NO) is a unique molecule involved in the regulation of diverse number of physiological processes including vascular smooth muscle (VSM) contractility, platelet reactivity, neurotransmission and the cytotoxic actions of immune cells (see Section **1.3.2**). However, excess production of NO has been linked to the pathogenesis of a number of diseases. This has provided the rationale for designing new therapies that modulate the synthesis of NO.

Expression of the inducible isoform of nitric oxide synthase (iNOS) in macrophages and the subsequent production of large quantities of NO plays an important role in the anti-pathogenic actions of these inflammatory cells (Nathan, 1992). However, it is well established that iNOS can be expressed in almost any cell type including VSM cells (Fleming *et al.*, 1991) and cardiomyocytes (Brady *et al.*, 1992; Balligand *et al.*, 1994) in response to bacterial lipopolysaccharide (LPS) and inflammatory cytokines. The expression of iNOS within the cardiovascular system has been linked to numerous diseases, including myocardial infarction (MI; Wildhirt *et al.*, 1995), chronic heart failure (CHF; Fukuchi *et al.*, 1998; Vejlstrup *et al.*, 1998) and septic shock (Titheradge, 1999). However, due to the ubiquitous nature of endothelial NOS (eNOS)-derived NO within the cardiovascular system and its pivotal role in the regulation of vasomotor tone and arterial blood pressure (Moncada *et al.*, 1991), non-selective inhibition of NO synthesis would be undesirable. It is clear, therefore, that selective inhibitors of NOS may be of considerable therapeutic value. As a result, considerable effort has been made recently to develop novel selective iNOS inhibitors which would be useful pharmacological tools and, more importantly, as possible therapeutic agents in the treatment of such diseases in which iNOS is implicated.

N-(3-(Aminomethyl) benzyl) acetamidine dihydrochloride (1400W) has recently been described as a slow, tight binding inhibitor of human iNOS (Garvey *et al.*, 1997). Using purified NOS, 1400W was shown to be at least 5000-fold more selective for human iNOS than eNOS (Garvey *et al.*, 1997). Furthermore, in a rat

model of endotoxic shock, 1400W prevented the systemic hypotension as well as rises in plasma nitrate levels in rats attributable to LPS-induced iNOS expression (Wray *et al.*, 1998). Despite this evidence, *in vitro* studies directly investigating the effect of 1400W on the synthesis of NO by iNOS and eNOS are still lacking.

Therefore, the aim of experiments in this chapter was to test the hypothesis that 1400W inhibits iNOS *in vitro* without modifying the activity of eNOS.

3.2 Methods

All procedures were carried out as described in **Chapter 2**.

3.2.1 Model of endotoxic shock

As discussed in Section **2.1.1**, administration of LPS to rats reproduces many of the symptoms associated with endotoxic shock in humans, including systemic hypotension (Gray *et al.*, 1991) and lack of responsiveness to vasoconstrictors (Julou-Schaeffer *et al.*, 1990). Induction of iNOS in the vasculature after LPS administration, and the subsequent production of large amounts of NO, has been implicated in the vascular dysfunction observed in rats with endotoxic shock (Julou-Schaeffer *et al.*, 1990; Weigert *et al.*, 1995). Blood vessels isolated from rats treated with LPS should provide an acceptable model to examine the pharmacological selectivity of the novel iNOS inhibitor, 1400W, *in vitro*.

Therefore, preliminary experiments were designed to investigate the expression and functional significance of iNOS in thoracic aortae from rats with endotoxic shock, and to determine the suitability of this model for investigating the pharmacological selectivity of 1400W *in vitro*.

3.2.1.1 Induction of endotoxic shock, plasma sampling and tissue harvesting

Male Wistar rats were weighed (n=8; 250 – 350 g), injected with LPS (30 $mgkg^{-1}$, i.p.) and left for 5 h to develop endotoxic shock. Rats were anaesthetised with sodium pentobarbitol (60 $mgkg^{-1}$, i.p.) and blood collected (~ 5 ml) from the abdominal aortae into a syringe pre-rinsed with heparin (100 U ml^{-1}). Samples were then immediately transferred into pre-chilled Eppendorph sample tubes containing 50 µl of 10mmol/l EDTA. Samples were then immediately centrifuged as described in Section **2.1.1.3**. The cell free plasma was collected and stored at –20 °C prior to nitrate/nitrite analysis (NO_x, see Section **3.2.1.3**).

After exsanguination, thoracic aortae were removed and placed in cold, oxygenated (95% O_2, 5% CO_2) Krebs Henseleit solution. Blood samples and thoracic aortae were also collected from healthy male Wistar rats (n=7, 250 – 350 g). Sections of the thoracic aortae from both LPS-treated and control rats were removed and fixed in 10% neutral buffered formalin for 24 h prior to further processing and wax embedding as described in Section **2.1.1.3**.

3.2.1.2 Localisation of iNOS by immunohistochemistry

3 μm sections were taken from blocks and immunohistochemistry performed using the indirect alkaline phosphatase method, with a rabbit anit-iNOS monoclonal primary antibody (concentration; 1/250) and a goat anti-rabbit alkaline phosphatase-conjugated secondary antibody (concentration; 1/50) as described in Section **2.3.5**. Negative controls were treated with an antibody of the same immunoglobulin (Ig) class but not directed against the iNOS epitope (see Section **2.5.5**). Thoracic aortae were then treated with Harris' haematoxylin to counterstain nuclei.

3.2.1.3 Measurement of nitric oxide production

NO production was quantified by measuring nitrate/nitrite (NO_x) plasma concentrations by means of the Greiss Reaction using a 'Nitric Oxide Assay Kit' (R & D systems, U.K.) as described in Section **2.6.3**.

3.2.1.4 Functional studies in thoracic aortae

Thoracic aortae from both LPS-treated and control rats were cleaned of adhering adipose and connective tissue and then cut into transverse rings. To ensure that same size of aortic ring was used in each experiment, each ring was cut to the length of the wires onto which the aortic ring was to be mounted (~ 4 mm). The endothelium was removed by the method described in Section **2.2.2**. Rings were mounted in a 10 ml organ bath filled with warm (37 °C), oxygenated (95% O_2, 5% CO_2) Krebs Henseleit solution (see Section **2.2.1**), placed under 2 g of tension and left to equilibrate for 60 min. The general protocol (see Section **2.2.2**) was performed on all aortic rings before commencing the experimental protocols described overpage.

To investigate the effect of LPS treatment of rats on responsiveness of thoracic aortae to adrenoceptor stimulation, cumulative concentration response curves (CRC) to norepinephrine (NE; 1 x 10^{-9} to 3 x 10^{-5} M) were constructed in endothelium-denuded rings from both LPS-treated (n=8) and control rats (n=7). On completion of CRCs, rings were repeatedly washed and allowed to re-equilibrate for at least 15 min before further experimentation.

To investigate the role of iNOS in modulating vascular responsiveness in thoracic aortae from LPS-treated rats, endothelium-denuded rings were exposed to the non-selective NOS inhibitor, N^{ω}-nitro-L-arginine methyl-ester (L-NAME; 2 x 10^{-4} M; Rees *et al.*, 1990) for 30 min prior to carrying out cumulative CRCs to NE (1 x 10^{-9} to 3 x 10^{-5} M).

3.2.2 Investigation of the pharmacological selectivity of 1400W

Endotoxic shock was induced in male Wistar rats (n=8, 250 –350 g) as described in Section **3.2.1.1**. Rats were killed by stunning and exsanguination, thoracic aortae removed and placed in cold, oxygenated (95% O_2, 5% CO_2) Krebs Henseleit solution. Thoracic aortae were also collected from healthy male Wistar rats (n=8, 250 – 350 g). Aortic rings (~ 4 mm, see Section **3.1.2.4**) from both LPS-treated and control rats were mounted in a 10 ml organ bath filled with warm (37 °C), oxygenated (95% O_2, 5% CO_2) Krebs Henseleit solution. After a period of equilibration of 60 min, the general protocol (see Section **2.2.2**) was performed on all aortic rings prior to carrying out the experimental protocols described below.

To establish whether 1400W inhibits the synthesis of NO by iNOS, cumulative CRCs (1 x 10^{-9} to 3 x 10^{-5} M, n=8) were constructed in endothelium-intact aortic rings from LPS-treated rats in the presence and absence of *N*-(3-(Aminomethyl) benzyl) acetamidine dihydrochloride (1400W). On the basis of previous studies (Garvey *et al.*, 1997; Wray *et al.*, 1998) and preliminary data (n=4, data not shown) three concentrations of 1400W were used, 10^{-6} M, 10^{-5} M and 10^{-4} M. Rings were treated with 1400W for 30 min prior to commencing CRCs.

Basal production of NO in endothelium-intact isolated rat aortic rings exerts a tonic vasodilatory action, opposing the effects of vasoconstrictors (Martin *et al.*, 1986). Consequently, by measuring vasoconstrictor responses to NE basal production of NO can be indirectly assessed. Therefore, to investigate whether 1400W has any non-selective effects on basal synthesis of NO by eNOS, CRCs to NE (1×10^{-9} to 3×10^{-5} M, n=8) were constructed in endothelium-intact aortic rings from control rats in the presence and absence of 1400W. As before, rings were treated with 1400W (10^{-6} M - 10^{-4} M) for 30 min prior to commencing CRCs.

To investigate whether 1400W has on any non-selective effects on agonist-stimulated synthesis of NO by eNOS, acetylcholine (ACh)-induced relaxations were assessed in the presence and absence of 1400W (10^{-6} M - 10^{-4} M). A submaximal concentration of NE (~ EC_{60}) was used to induce arterial tone. Once constrictions were stable, cumulative CRCs to ACh (1×10^{-9} to 3×10^{-5}M, n>6) were obtained. As before, rings were treated with 1400W (10^{-6} M - 10^{-4} M) for 30 min prior to commencing CRCs.

3.2.3 Preparation of drugs

Norepinephrine hydrogentartrate, acetylcholine chloride and N^{ω}-nitro-L-arginine methyl-ester were diluted in Krebs Henseleit solution to give a stock solution of 10^{-1} M and frozen (-20 °C) in aliquots prior to use. Vitamin C (10^{-6} M) was added to the stock solution of NE to prevent autoxidation. Further dilutions were made in Krebs Henseleit solution. *N*-(3-(Aminomethyl) benzyl acetamidine dihydrochloride (1400W) was diluted in saline (0.9% NaCl) under argon to give a stock solution of 10^{-3} M. Aliquots were then frozen (-20 °C) and stored under argon. Further dilutions were made in Krebs Henseleit solution.

3.2.4 Data Analysis

All results were expressed as means ± s.e.mean. Cumulative CRCs to ACh were measured as percentage relaxations of NE-induced tone. Where maximal values were

obtained for cumulative CRCs to NE and ACh, the negative logarithm of the agonist concentration that results in a half-maximal contraction or relaxation (pD_2) was calculated by nonlinear regression using GraphPad Prism software (Version 3.0). Two-tailed *t*-tests, one-way analysis of variance (ANOVA) with Bonferroni post-test for multiple comparisons and two-way repeated measure ANOVA were used as indicated in the text. $P<0.05$ was considered to be statistically significant.

3.3 Results

3.3.1 Investigation of the expression of iNOS during endotoxic shock

3.3.1.1 Immunohistochemical localisation of iNOS

Immunoreactive iNOS was found in endothelial cells, VSM cells and in the adventitia of thoracic aorate from LPS-treated rats (***Figure 3.1a***). No immunoreactivity was found in thoracic aortae from control rats or in negative controls using IgG antibodies (***Figure 3.1b***, ***c***).

3.3.1.2 Plasma nitrite concentrations

NO_x concentrations in plasma samples from LPS-treated rats were significantly higher than those from control rats (LPS-treated rats, 166.19 ± 5.79 μM; control, 25.61 ± 2.83 μM, $P<0.001$, two-tailed unpaired *t*-test).

3.3.1.3. Effect of lipopolysaccharide administration on vascular responsiveness

Maximal contractions to KCl (60 mM) in endothelium-denuded aortic rings from control rats were significantly greater than those in aortic rings from LPS-treated rats ($P<0.01$, two-tailed unpaired *t*-test, ***Table 3.1***). Interestingly, there were no significant differences between LPS-treated and control rats with respect to contractions to a supramaximal concentration of NE (10^{-5} M, *Table 3.1*). Relaxations to ACh in aortic rings from both LPS-treated and control rats were all but abolished, verifying successful denudation (***Table 3.1***).

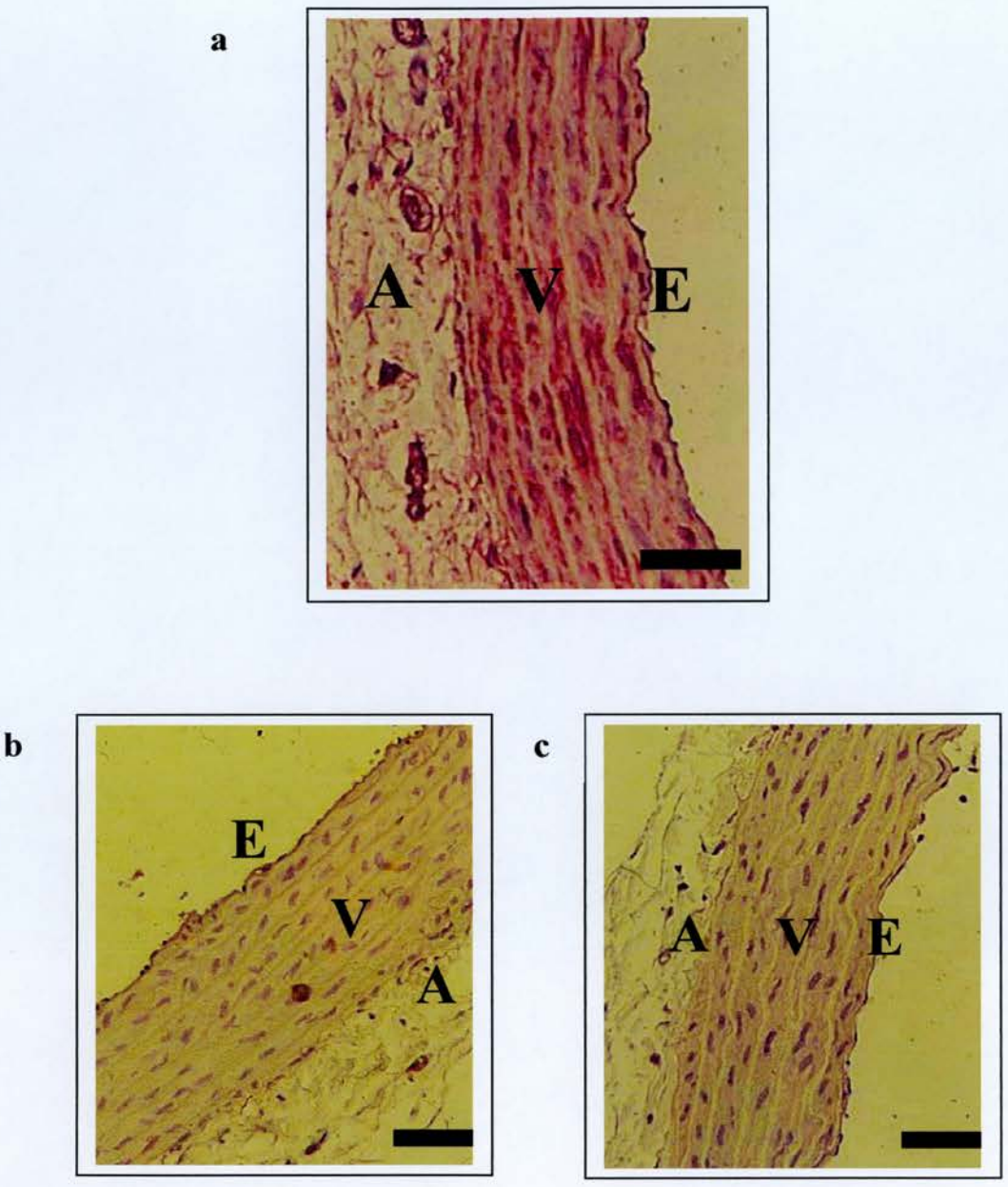

Figure 3.1 *Localisation of iNOS by immunohistochemistry in thoracic aortae isolated from LPS-treated and control rats (n≥7). Immunoreactive iNOS (red staining) was detected in endothelial cells (**E**), vascular smooth muscle cells (**V**) and in the adventitia (**A**) of thoracic aortae from lipopolysaccharide (LPS)-treated rats (Panel **a**) but not in aortae from control rats (Panel **b**). No immunoreactive iNOS was detected in thoracic aortae from LPS-treated rats treated with control IgG antibodies (Panel **c**). Nuclei are counterstained with Harris' Haematoxylin (purple staining). Magnification x200, scale bar = 200 μm.*

	Control (n=7)	*LPS-treated* (n=8)
60 mM **KCl**	2.1±0.2g	1±0.1g*
10^{-5} M **NE**	2.1±0.3g	1.7±0.2g
10^{-5} M **ACh**	0.40±0.2%	0.46±0.1%

Table 3.1 *Maximal contractions of endothelium-denuded thoracic aortic rings from LPS-treated and control rats to* ***KCl*** *and norepinephrine* ***(NE)****. Responses of NE-contracted aortic rings to acetylcholine* ***(ACh)*** *are given as percentages of NE (EC_{50})-induced tone. All values are given as means ± s.e.m. * $P<0.05$ compared with respective responses in aortic rings from control rats (two-tailed unpaired t-test).*

Endothelium-denuded aortic rings from LPS-treated rats were significantly less responsive to NE when compared with responses in endothelium-denuded aortic rings from control rats, as demonstrated by a right and downward shift of NE CRCs ($P<0.01$, two-way ANOVA, ***Figure 3.2***). Indeed, maximal contractions for NE CRCs were significantly lower in aortic rings from LPS-treated rats when compared with those from control rats (LPS-treated, 1.3 ± 0.2; control, 2.7 ± 0.2 gram tension, $P<0.001$, two-tailed unpaired t-test).

Treatment of endothelium-denuded aortic rings from LPS-treated rats with the non-selective NOS inhibitor, L-NAME (2×10^{-4} M), increased responsivenss to NE ($P<0.001$, two-way ANOVA, ***Figure 3.2***). Treatment of aortic rings from control rats with L-NAME had no significant effect on responses to NE (***Figure 3.2***).

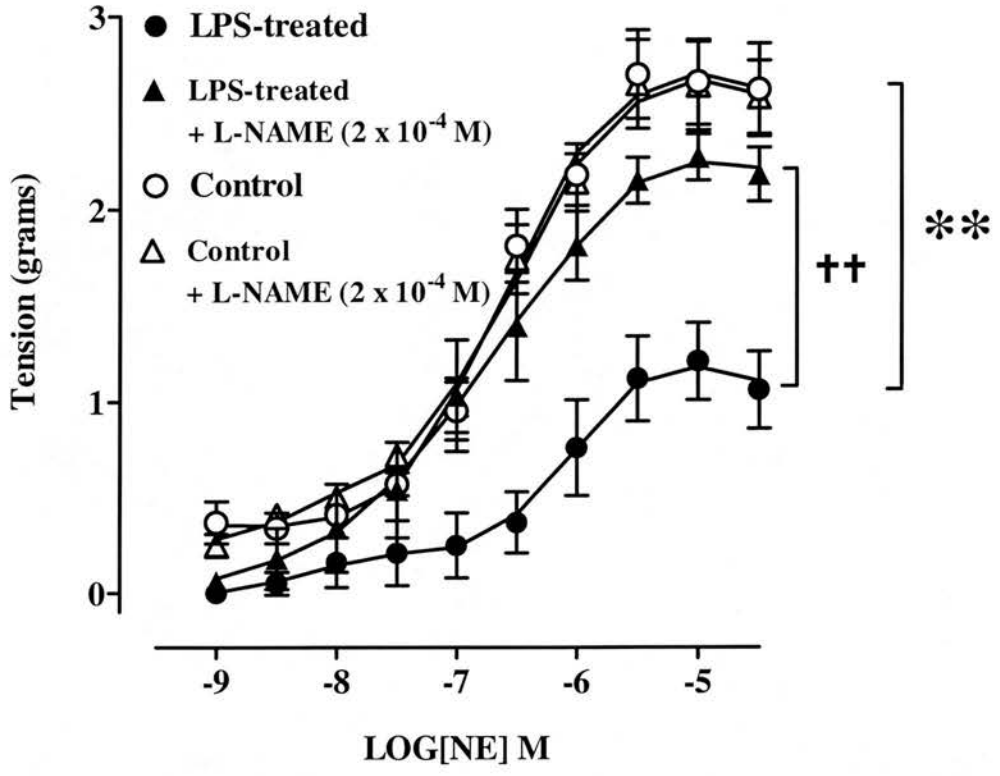

Figure 3.2 *Cumulative concentration response curves (CRC) showing contractile responses to norepinephrine (**NE**; 1 x 10^{-9} to 3 x 10^{-5} M) in endothelium-denuded thoracic aortic rings from LPS-treated (n=8) and control rats (n=7). Also shown are CRCs to NE in the presence of the non-selective nitric oxide synthase inhibitor, L-NAME (2 x 10^{-4} M). Values are given as means ± s.e.m. ** P<0.01 for CRCs in untreated rings from LPS-treated rats compared with CRCs in untreated aortic rings from control rats,* **††** *P<0.01 for CRCs in rings treated with L-NAME compared with untreated aortic rings from LPS-treated rats, (two-way ANOVA).*

3.3.2 Investigation of the pharmacological selectivity of 1400W

3.3.2.1 KCl, norepinephrine maximal constrictions and endothelial integrity

Maximal constrictions to KCl (60 mM) and a supramaximal concentration of NE (10^{-5} M) in endothelium-intact aortic rings from LPS-treated rats were significantly less than those in endothelium-intact rings from control rats ($P<0.05$, two-tailed unpaired *t*-test, ***Table 3.2***). All aortic rings from LPS-treated and control rats had functional endothelium (***Table 3.2***). However, relaxations to ACh were significantly smaller in aortic rings from LPS-treated rats when compared with aortic rings from control rats ($P<0.05$, two-tailed unpaired *t*-test).

	Control (n=8)	***LPS-treated*** (n=8)
60 mM **KCl**	4.6±0.1g	2.7±0.1g*
10^{-5}M **NE**	5.7±0.2g	3.5±0.2g*
10^{-5}M **ACh**	90±2%	74±4%*

Table 3.2 *Maximal contractions (gram tension) of endothelium-intact thoracic aortic rings from lipopolysaccharide (**LPS**)-treated and control rats, to **KCl** and norepinephrine (**NE**). Responses of NE-contracted aortic rings to acetylcholine (**ACh**) are given as percentages of NE (EC_{50})-induced tone. All values are given as means ± s.e.m. * $P<0.05$ as compared with respective responses in aortic rings from control rats (two-tailed unpaired t-test).*

3.3.2.2 Effect of 1400W on vascular responsiveness in aortic rings from LPS-treated rats

There were no significant differences between cumulative CRCs to NE performed in aortic rings treated with 1400W at a concentration of 10^{-6} M when compared with those in aortic rings in the absence of 1400W ($P>0.05$, two-way ANOVA; ***Figure 3.3***, ***Table 3.3***). In contrast, treatment of endothelium-intact aortic rings from LPS-

treated rats with 10^{-5} M or 10^{-4} M 1400W, significantly increased NE responsiveness when compared with responsiveness of aortic rings in the absence of 1400W ($P<0.05$ for both, two-way ANOVA, ***Figure 3.4***, ***3.5***, ***Table 3.3***). pD_2 values and maximal contractions to NE were significantly increased in the presence of 10^{-4} M 1400W when compared with untreated aortic rings ($P<0.05$, one-way ANOVA with Bonferroni post-test, ***Table 3.3***). There was no significant difference between pD_2 values and maximal contractions to NE in aortic rings treated with 10^{-5} M or 10^{-4} M 1400W when compared with those in untreated rings from control rats ($P>0.05$, one-way ANOVA, ***Table 3.3***) indicating that 1400W had effectively restored adrenergic responsiveness to that found in rings from control rats.

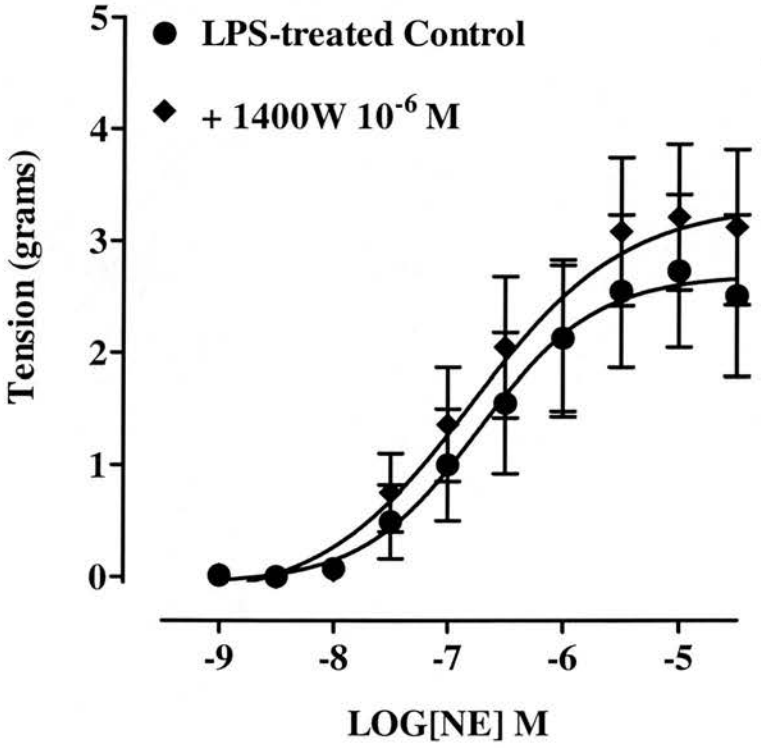

Figure 3.3 *Cumulative concentration response curves (CRC) to norepinephrine (**NE**; 1 x 10^{-9} to 3 x 10^{-5}M) in endothelium-intact aortic rings from lipopolysaccharide (**LPS**)-treated rats (n=8) in the presence of **10^{-6} M** 1400W. Values are given as means ± s.e.mean. P>0.05, two-way ANOVA.*

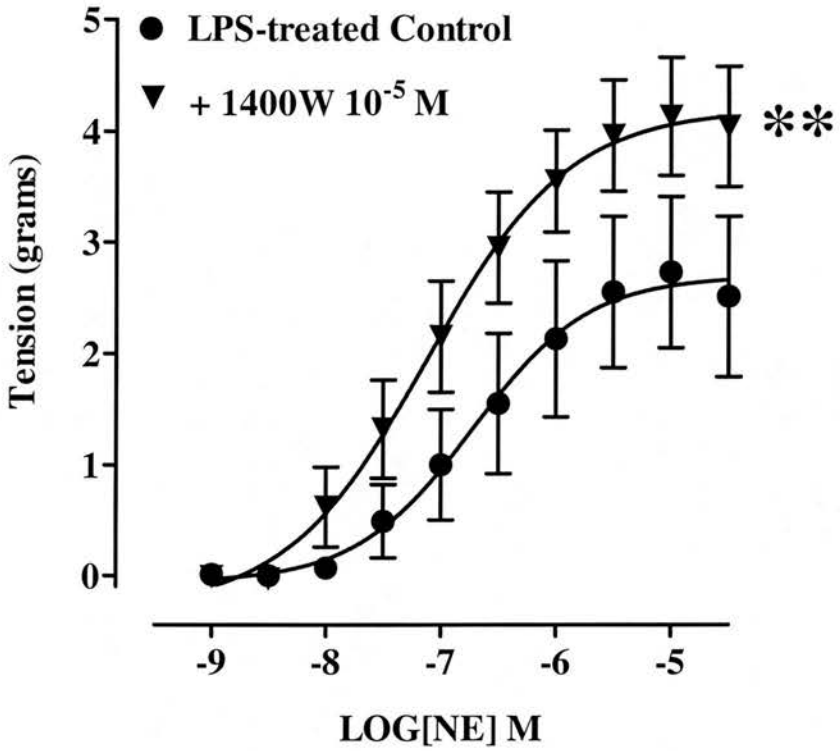

Figure 3.4 *Cumulative concentration response curves (CRC) to norepinephrine (**NE**; 1 x 10^{-9} to 3 x 10^{-5} M) in endothelium-intact aortic rings from lipopolysaccharide (**LPS**)-treated rats (n=8) in the presence of **10^{-5} M** 1400W. Values are given as means ± s.e.mean. ** P<0.01 compared with CRCs in control aortic rings (two-way ANOVA).*

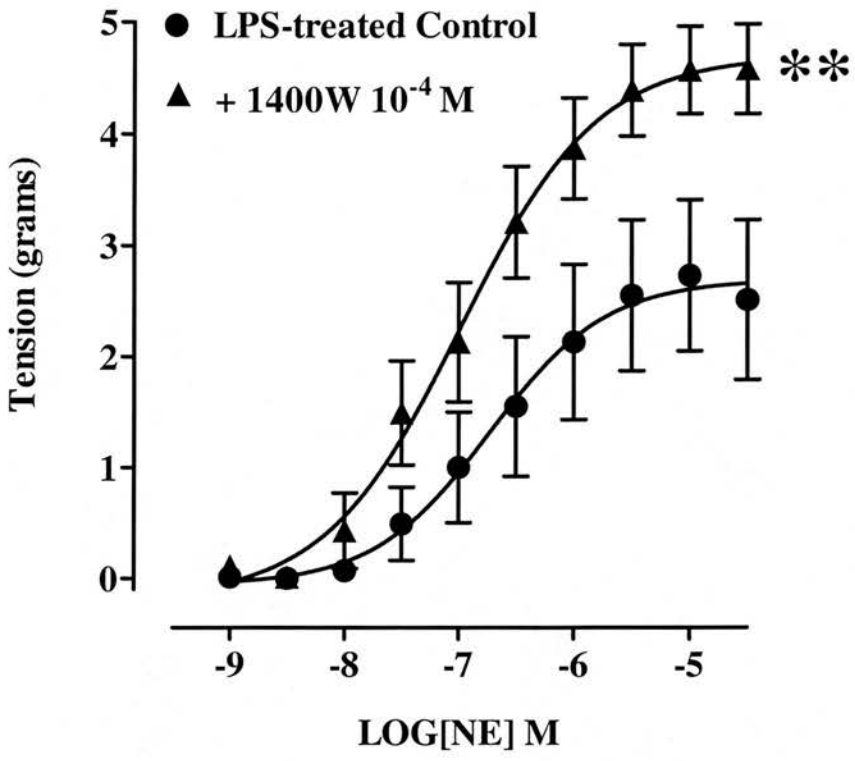

Figure 3.5 *Cumulative concentration response curves (CRC) to norepinephrine (**NE**; 1 x 10^{-9} to 3 x 10^{-5} M) in endothelium-intact aortic rings from lipopolysaccharide (**LPS**)-treated rats (n=8) in the presence of **10^{-4} M** 1400W. Values are given as means ± s.e.mean. ** P<0.01 compared with CRCs in control aortic rings (two-way ANOVA).*

	Control (n=8)		*LPS-treated* (n=8)	
	pD_2	Max (g)	pD_2	Max (g)
Untreated	6.9±0.1	5.4±0.4	6.4±0.2*	2.8±0.7*
1400W 10^{-6} M	7±0.1	6.4±0.6	6.6±0.1	3.3±0.7
1400W 10^{-5} M	7.1±0.1	6.1±0.5	7.0±0.2	4.1±0.5
1400W 10^{-4} M	7.1±0.1	6±0.5	7.2±0.2†	4.6±0.7†

Table 3.3 *pD_2 values and maximal contraction (Max) values to norepinephrine in endothelium-intact aortic rings from LPS-treated and control rats in the presence and absence of 1400W. Values are given as means ± s.e.mean. * $P<0.05$ compared with respective values in untreated aortic rings from control rats (one-way ANOVA with Bonferroni post-test).* † *$P<0.05$ compared with pD_2 values and maximal contractions in untreated aortic rings from LPS-treated rats (one-way ANOVA with Bonferroni post-test).*

3.3.2.3 Effect of 1400W on basal and agonist-stimulated release of nitric oxide from eNOS

No concentration of 1400W (10^{-6} M - 10^{-4} M) had any significant effect on cumulative CRCs to NE in endothelium-intact aortic rings from control rats (***Figure 3.6, Table 3.3***).

Following induction of NE-induced tone (untreated, 58.7 ± 11.1%; 10^{-6} M 1400W, 57.7 ± 7%; 10^{-5} M 1400W, 51.2 ± 6.4%; 10^{-4} M 1400W, 63.5 ± 4.6% of maximal NE contractions, P>0.05, one-way ANOVA) in endothelium-intact aortic rings cumulative additions of ACh (1 x 10^{-9} to 3 x 10^{-5} M) resulted in concentration-dependent relaxations (***Figure 3.7***). No concentration of 1400W (10^{-6} M - 10^{-4} M) had any effect on relaxations to ACh (***Figure 3.7***).

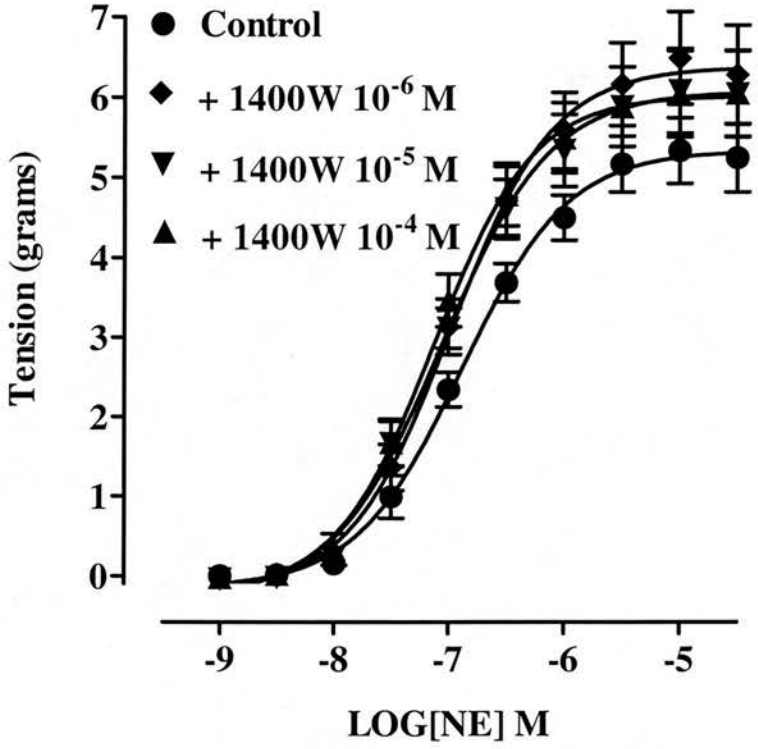

Figure 3.6 *Cumulative concentration response curves to norepinephrine (**NE**; 1 x 10^{-9} to 3 x 10^{-5}M) endothelium-intact aortic rings from control rats (n=8) in the presence of 10^{-6} M 1400W, 10^{-5} M 1400W and 10^{-4} M 1400W. Values are given as means ± s.e.mean. P>0.05 for CRCs in untreated aortic rings compared with CRCs in aortic rings treated with 1400W (two-way ANOVA).*

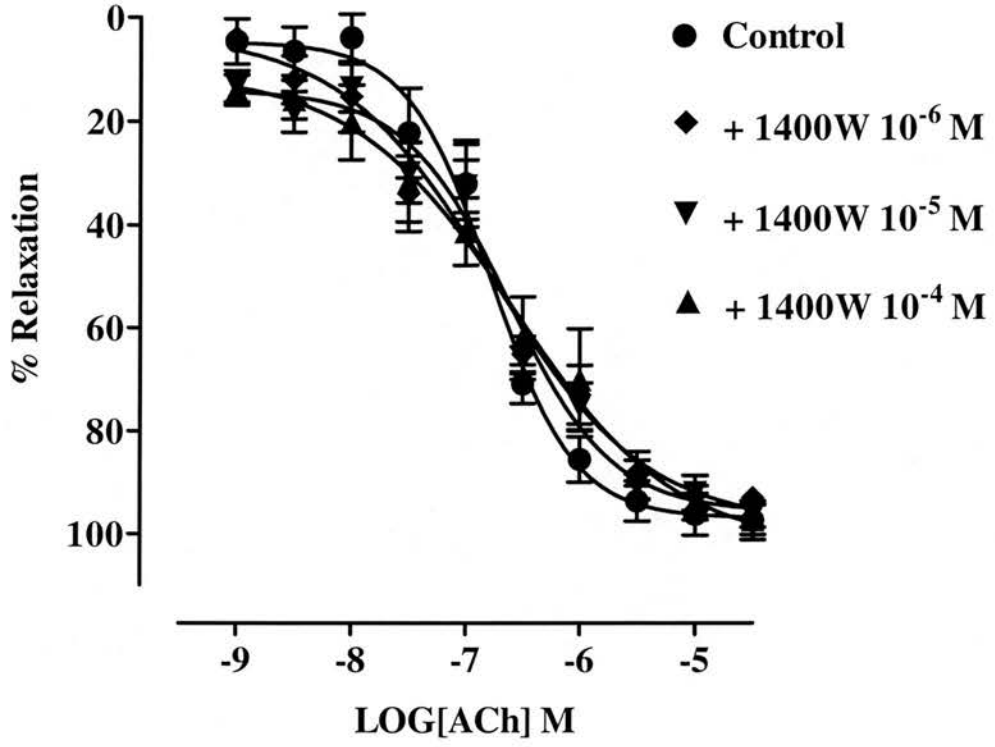

Figure 3.7 *Cumulative concentration response curves to acetylcholine (**ACh**, 1 x 10^{-9} to 3 x 10^{-5} M) in norepinephrine-contracted (~ EC_{60}) endothelium-intact aortic rings from control rats (n=8) in the presence of 10^{-6} M 1400W, 10^{-5} M 1400W and 10^{-4} M 1400W. Values are given as means ± s.e.mean. P>0.05 for CRCs in untreated aortic rings compared with CRCs in aortic rings treated with 1400W (two-way ANOVA).*

3.4 Discussion

Experiments in this chapter demonstrate that the novel iNOS inhibitor, 1400W (10^{-5} M to 10^{-4} M), increased the responsiveness of endothelium-intact rat aortic rings from LPS-treated rats, most likely as a consequence of decreased synthesis of NO by iNOS. Furthermore, in endothelium-intact aortic rings from control rats, 1400W (10^{-6} M to 10^{-4} M) had no significant effect on NE contractions or ACh-mediated relaxations, suggesting that 1400W does not inhibit basal or agonist-stimulated synthesis of NO by eNOS. These results provide convincing evidence that 1400W is a selective iNOS inhibitor *in vitro*.

Numerous studies have demonstrated that endothelium-intact and endothelium-denuded blood vessels isolated from rats treated with LPS are hyporesponsive to a variety of vasoconstrictors (Julou-Schaeffer *et al.*, 1990; Weigert *et al.*, 1995). Furthermore, this hyporesponsiveness is reversed by non-selective inhibitors of NOS irrespective of the presence or absence of the endothelium, implying that enhanced NO formation from iNOS accounts for the hyporeactivity. Indeed, studies have demonstrated that iNOS can be detected within the vasculature from LPS-treated rats (Buttery *et al.*, 1994; Sato *et al.*, 1995). Consistent with these findings, immunohistochemical studies in this chapter demonstrated that iNOS was expressed in endothelial cells, VSM cells and in the adventitia of thoracic aortae from LPS-treated rats but not in thoracic aortae from control rats. Plasma NO_x concentrations were significantly greater in LPS-treated rats when compared with control rats. Therefore, in this model of endotoxic shock, LPS administration results in the expression of iNOS within the thoracic aorta and also a significant increase in the synthesis of NO, probably derived from iNOS. Isolated endothelium-denuded aortic rings from LPS-treated rats were significantly less responsive to NE when compared with responses in endothelium-denuded rings from control rats. Furthermore, treatment of aortic rings with the non-selective NOS inhibitor, L-NAME, reversed this hyperesponsiveness. Therefore, in accordance with the aforementioned studies (Julou-Schaeffer *et al.*, 1990; Weigert *et al.*, 1995), results here indicate that the expression of iNOS in the thoracic aortae as a

consequence of LPS administration results in a profound hyporeactivity to NE. The findings of these experiments are not novel, however, they confirm that this is a reliable *in vitro* model for investigating the pharmacological properties of the novel iNOS inhibitor, 1400W.

Besides its role in the vascular dysfunction associated with the pathogenesis of endotoxic shock, excessive production of NO by iNOS has been linked to the pathogenesis of a wide range of other diseases. These include cerebral ischaemia (Iadecola *et al.*, 1997), chronic inflammation (Moilamen *et al.*, 1999) and neurodegeneration (Okuda *et al.*, 1995). Furthermore, recent studies reveal that iNOS is expressed in the heart in experimental MI (Wildhirt *et al.*, 1995) and in patients with CHF (Fukuchi *et al.*, 1998). However, investigations into the role of iNOS in the pathogenesis of such diseases are limited by the lack of NOS inhibitors that can distinguish between iNOS and eNOS.

Numerous compounds have been developed that are capable of inhibiting the biological activity of NO. These include drugs which prevent the uptake of NOS substrate, L-arginine, into cells (Bogle *et al.*, 1992), agents which reduce the supply of cofactors required for NO synthesis by NOS (Werner-Felmayer *et al.*, 1990), inhibitors of electron flow from nicotanamide adenine dinucleotide phosphate (NADPH) to the flavins in the reductase domain of NOS (Kumagai *et al.*, 1998; Wolff *et al.*, 2000) and drugs which prevent the binding of L-arginine to NOS (reviewed by Hobbs *et al.*, 1999). The most commonly used NOS inhibitors are the L-arginine analogues, for example L-NAME and N^G–monomethyl-L-arginine (L-NMMA), whose main pharmacological action is to compete with L-arginine (Hobbs *et al.*, 1999). However, very little selectivity toward NOS isoforms is achieved with this group of compounds, making them unsuitable for use in studies where selective inhibition of iNOS is essential. There are some compounds available, however, that demonstrate relative selectivity towards iNOS. Guanidines, in particular aminoguanidine has been shown to be equipotent to L-NMMA in inhibiting iNOS *in vitro* but significantly less potent in inhibiting NO synthesis by eNOS (Yen *et al.*, 1995). However, very high doses are required to elicit significant inhibition of iNOS

in vivo (Wu *et al.*, 1995). At such concentrations, aminoguanidine is likely to inhibit eNOS as well as catalase and other iron- and copper-containing enzymes, resulting in the accumulation of superoxide and other free radical species (Ou & Wolff, 1993). The bisisothioureas are also reported to be potent and selective inhibitors of iNOS. For example, the novel bisisothiourea, *S*', *S*'-(1,3-phenylenebis (1,2-ethanediyl))bisisothiourea (PBITU) was found to be 190-fold selective for human purified iNOS compared with eNOS (Garvey *et al.*, 1994). However, their lack of passage across cell membranes and their high toxicity has meant that this group of compounds are unlikely to become useful therapeutic agents (Garvey *et al.*, 1994). Recently, a derivative of PBITU, *N*-(3-(Aminomethyl) benzyl) acetamidine dihydrochloride (1400W), has been described as a selective iNOS inhibitor (Garvey *et al.*, 1997). 1400W is reported to be at least 5000-fold more selective for human iNOS than eNOS and was quoted at its time of discovery to be the most selective inhibitor of human iNOS ever reported (Garvey *et al.*, 1997). Furthermore, in a rat model of endotoxic shock, 1400W has been shown to prevent systemic hypotension as well increased plasma NO_x levels attributable to LPS-induced iNOS expression (Wray *et al.*, 1998). Further to its selectivity for human iNOS, 1400W is active and non-toxic *in vivo* (Garvey *et al.*, 1997; Laszlo & Whittle, 1997; Wray *et al.*, 1998).

Despite the evidence provided by these studies, somewhat surprisingly, *in vitro* studies directly investigating the pharmacological selectivity of 1400W for iNOS over eNOS are still lacking. Therefore, in view of these findings, experiments in this chapter were designed to test the hypothesis that 1400W inhibits the activity of iNOS *in vitro* without modifying the activity of eNOS. In endothelium-intact aortae from rats treated with LPS, 1400W significantly increased responsiveness of endothelium-intact thoracic aortae to NE in a concentration-dependent manner (10^{-5} M - 10^{-4}M). Indeed, in the presence of 1400W there were no significant differences between pD_2 *values* and maximal contractions for NE CRCs in aortae from LPS-treated when compared with responses in control aortic rings, indicating that 1400W had effectively restored responsiveness to NE. To investigate the pharmacological selectivity of 1400W for iNOS over eNOS, both basal and agonist-stimulated synthesis of NO by eNOS were assessed in isolated aortic rings from control rats in

the presence and absence of 1400W. Treatment of rings with 1400W had no significant effect on responses to NE, suggesting that 1400W has no effect on basal production of NO from eNOS. Similarly, 1400W did not modify relaxations to the endothelium-dependent vasodilator ACh, suggesting that 1400W has no effect on the agonist-stimulated synthesis of NO from eNOS. The findings of these experiments provide convincing evidence that 1400W inhibits the activity of iNOS in aortic rings from LPS-treated rats without modifying the activity of eNOS.

From the experiments presented in this chapter the mechanism by which 1400W selectively inhibits the activity of iNOS is not clear. Garvey *et al.* (1997) demonstrate that the binding of 1400W to purified human iNOS could be prevented by pre-treatment with L-arginine, suggesting that 1400W may inhibit iNOS by competiting with L-arginine for the substrate binding site on iNOS. Subsequent experiments demonstrated that once 1400W was bound to the enzyme, L-arginine was unable to reverse its inhibitory effects on NO synthesis. These findings suggest that 1400W is either an irreversible inhibitor of iNOS, or one whose activities are reversed very slowly. Although this data gives some insight into its mechanism of action, it does not explain why 1400W is selective inhibitor of iNOS. Indeed, if it is behaving like an L-arginine analogue one would expect, in a similar manner to other L-arginine analogues, that it would readily inhibit the activity of eNOS. In the study by Garvey *et al.*, further experiments demonstrated that the kinetics of 1400W binding to iNOS were time-dependent, and were described as a two-step mechanism. Furthermore, it was suggested that selectivity of 1400W for iNOS was derived from interactions that developed slowly. Indeed, recent observations have suggested that this slow phase of inhibition involves a conformational change of NOS that is thought to be specific to iNOS (Cooper *et al.*, 2000, unpublished observations by personal communication). In addition to the possible allosteric inhibitory properties of 1400W, Garvey *et al.* (1997) found that the slow phase of its inhibition of iNOS was dependent on the presence of NADPH. Because electrons from NADPH oxidation are essential for the eventual reduction of haem (see Section **1.3.3**), 1400W binding may alter this flow of electrons and thus inactivate iNOS. Again it is not obvious why 1400W would not alter electron flow in other isoforms of NOS. It is

clear from this discussion that further experiments are needed to elucidate the precise mechanism by which 1400W inhibits iNOS, in order to provide further avenues for developing novel iNOS inhibitors with even greater selectivity than 1400W.

In conclusion, experiments in this chapter provide convincing evidence that the recently described iNOS inhibitor, 1400W, inhibits the activity of iNOS *in vitro* without modifying the activity of eNOS. These findings corroborate those of biochemical studies and emphasise its potential as an important investigative and therapeutic tool in diseases associated with the expression of iNOS.

Chapter 4

Investigation of the superoxide dismutase properties of the novel metalloporphyrin MnTMPyP

4.1 Introduction

Endothelium-derived nitric oxide (NO) is rapidly inactivated by the oxygen-derived free radical, superoxide, leading to a loss of its vasodilatory action (Gryglewski *et al.*, 1986). In eukaryotic cells, three isoforms of superoxide dismutase (SOD) exist; an extracellular Cu/Zn-containing form, an intracellular Cu/Zn-containing form, and an Mn-containing form present in the mitochondria (Fridovich, 1983), all of which serve to dismutate endogenous superoxide. Studies involving the use of the copper chelator, diethyldithocarbamate (DETCA), suggest that the Cu/Zn-containing isoforms of SOD are of critical importance in protecting endothelium-derived NO from inactivation by superoxide (Omar *et al.*, 1991; Mian & Martin, 1995; MacKenzie & Martin, 1998).

A loss of NO-mediated vasodilatation as a consequence of increased production or decreased scavenging of superoxide has been linked to the pathogenesis of numerous cardiovascular diseases. For example, atherosclerosis (Ohara *et al.*, 1993), hypertension (Bouloumie *et al.*, 1997) and chronic heart failure (CHF; Belch *et al.*, 1991; Katz *et al.*, 1993) are all associated with increased superoxide and impaired endothelium-dependent relaxations. Elevation of the activity of endogenous SOD might therefore form the basis of a strategy for therapeutic intervention in these cardiovascular diseases. However, it is unlikely that treatment with authentic isoforms of SOD will be of benefit. This is because native isoforms of SOD are large in size and are unlikely to penetrate cellular membranes to protect NO from intracellular superoxide, furthermore, they have a very short half-life and are therefore rapidly cleared from the circulation. To overcome these limitations, an increasing number of low molecular weight, cell permeable compounds that exhibit SOD-like activity have recently been developed. These include simple metal salts (eg. $MnCl_2$; MacKenzie & Martin, 1998), free radical spin traps (eg. 4-hydroxy 2,2,6,6-tetramethylpiperidine, tempol; Mitchell *et al.*, 1990) and metal-based SOD mimetics (eg. metalloporphyrins; Patel & Day, 1999).

The metalloporphyrins have emerged as an important class of novel SOD mimetics, owing to them being stable, active, and non-toxic *in vivo* (Patel & Day, 1999) and also due to their ability to permeate cell membranes (Liochev & Fridovich, 1995). One compound belonging to this group is Mn [III] tetrakis [1-methyl-4-pyridyl] porphyrin (MnTMPyP). MnTMPyP has been shown to facilitate the growth of SOD-deficient *Escherichia Coli.* (Faulkner *et al.*, 1994). Furthermore, MacKenzie & Martin (1998) recently demonstrated that MnTMPyP protects agonist-stimulated activity of NO from inactivation by superoxide in isolated rabbit aortae subjected to intracellular and extracellular oxidative stress. Despite this evidence, recent studies have suggested that MnTMPyP may actually scavenge NO itself by producing superoxide (Gardner *et al.*, 1996; MacKenzie *et al.*, 1999), or it may interfere with the NO/soluble guanylate cyclase (sGC) pathway (Pfeiffer *et al.*, 1998). Furthermore, it has been demonstrated that MnTMPyP may also inhibit the activity of endothelial nitric oxide synthase (eNOS) and inducible NOS (iNOS; Pfeiffer *et al.*, 1998).

In view of these findings, experiments in this chapter were designed to investigate whether MnTMPyP can protect endothelium-derived NO from inactivation by superoxide in an *in vitro* model of oxidative stress (Mian & Martin, 1995), without having any non-selective inhibitory effects on the activity of eNOS or iNOS-derived NO or the enzymes themselves.

4.2 Methods

All procedures were carried out as described in **Chapter 2**.

4.2.1 Tissue harvesting and preparation of aortic rings

Male Wistar rats (n=18, 250 – 350 g) were killed by stunning and exsanguination. Thoracic aortae were removed and placed into cold, oxygenated (95% O_2, 5% CO_2) Krebs Henseleit solution.

For experiments investigating the effect of MnTMPyP on the synthesis of NO by iNOS, male Wistar rats (n=6; 250 – 350 g) were injected with lipopolysaccharide (LPS; 30 $mgkg^{-1}$, i.p.) as described in Section **2.1.1.2** and left for 5 h to develop endotoxic shock. Rats were then killed by stunning and exsanguination, thoracic aortae removed and placed in into cold, oxygenated (95% O_2, 5% CO_2) Krebs Henseleit solution.

Thoracic aortae were cleaned of adhering adipose and connective tissue and cut into transverse rings (~ 4mm). In some aortic rings the endothelium was removed by the method described in Section **2.2.2**. Aortic rings were then mounted in a 10 ml organ bath filled with warm (37 °C), oxygenated (95% O_2, 5% CO_2) Krebs Henseleit solution (see Section **2.2.1**). Aortic rings were placed under 2 gram of tension and left to equilibrate for 60 min. The general protocol (see Section **2.2.2**) was performed on all aortic rings before commencing the experimental protocols described below.

4.2.2 Experimental protocols

4.2.2.1 Model of oxidative stress

Many compounds are capable of producing superoxide, or inducing its production from the tissues themselves, and thus are suitable for inducing oxidative stress within isolated tissues. These compounds include the copper chelator, DETCA (MacKenzie & Martin, 1998), which inhibits Cu/Zn isoforms of SOD, xanthine

oxidase/hypoxanthine (XO/HX), a superoxide generating system, and the superoxide generating compound, pyrogallol (Halliwell & Gutteridge, 1989). Pyrogallol has been used in numerous studies investigating the effects of superoxide on the activity of both endogenous and exogenous NO (Ignarro *et al.*, 1988; Mian & Martin, 1995). Furthermore, pyrogallol has been shown to produce a profound decrease in the magnitude of both basal and agonist-stimulated activity of endothelium-derived NO in isolated rat aortic rings (Ignarro *et al.*, 1988; Mian & Martin, 1995). It was for these reasons that pyrogallol was used in experiments here to induce oxidative stress in isolated rat aortic rings.

Pyrogallol is thought to oxidise spontaneously in solution with simultaneous production of superoxide (Halliwell & Gutteridge, 1989). Hydrogen Peroxide (H_2O_2) is formed whenever superoxide is generated by its rapid one electron reduction and protonation, catalysed by SOD. Additionally superoxide can reduce transition metals such as iron or copper that can, in turn, react with H_2O_2 to generate the highly reactive hydroxyl radical ($OH^{\cdot}$) in the metal catalysed Haber-Weiss reaction (Pal Yu, 1994). Both H_2O_2 and $OH^{\cdot}$ have been shown to damage the endothelium and thus may impair endothelial function (Beckman *et al.*, 1990; Todoki *et al.*, 1992). Furthermore, H_2O_2 increases the liberation of NO (Rubanyi & Vanhoutte, 1986) and there is evidence that it can mediate VSM relaxation directly (Burke & Wolin, 1987; Zembowicz *et al.*, 1993). Indeed, in preliminary experiments, treatment of norepinephrine (NE)-contracted endothelium-intact rat aortic rings with pyrogallol resulted in a delayed but rapid fall in arterial tone (data not shown). Furthermore, this decrease in arterial tone was prevented when rings were pre-treated with catalase (1000 U ml^{-1}), which catalyses the decomposition of H_2O_2 to water and oxygen. Consequently, to remove H_2O_2 and guard against the formation of $OH^{\cdot}$, all experiments described below were carried out in the presence of catalase. Aortic rings were treated with catalase (1000 U ml^{-1}) for 5 min prior to, and throughout, the duration of experiments.

To assess the effects of pyrogallol on the activity of eNOS-derived NO, and thus establish whether this is a reliable model of oxidative stress, both basal and agonist-stimulated activity of NO were assessed in endothelium-intact aortic rings in the absence and presence of pyrogallol.

The activity of basal eNOS-derived NO was assessed indirectly by measuring contractile responses to NE (Martin *et al.*, 1986). To ensure that the amount of superoxide generated throughout the duration of experimental protocols was constant, instead of carrying out cumulative concentration response curves (CRC) to norepinephrine (NE), which can take up to 50 min to complete, a submaximal concentration of NE was chosen and the effect of pyrogallol on this NE-induced tone examined. Therefore, endothelium-intact aortic rings were exposed to a submaximal concentration of NE (~ EC_{60}). Once responses had stabilised, rings were treated with pyrogallol (3×10^{-4} M, n=8). At a concentration of 3×10^{-4} M, pyrogallol has previously been shown to inhibit NO-mediated relaxations in isolated rat aortic rings (Mian & Martin, 1995). Responses were recorded 5 min after addition of pyrogallol.

Agonist-stimulated activity of NO was assessed by measuring ACh-induced relaxations. A submaximal concentration of NE (~ EC_{60}) was used to induce arterial tone. Once contractions were stable, cumulative CRCs to ACh (1×10^{-8} to 3×10^{-5} M, n=6) were obtained. On completion of CRCs, rings were repeatedly washed and allowed to re-equilibrate for at least 15 min before further experimentation. Rings were then treated with pyrogallol (3×10^{-4} M, n=6) for 5 min prior to inducing NE (~ EC_{60}) tone and repeating cumulative CRCs to ACh (1×10^{-8} to 3×10^{-5} M).

4.2.2.2 Effects of MnTMPyP on the activity of eNOS-derived nitric oxide in pyrogallol-treated aortic rings

To investigate whether MnTMPyP can protect NO from destruction by superoxide, experimental protocols described in Section **4.2.2.1** were repeated in the presence of MnTMPyP ($n \geq 6$). On the basis of a previous study, a concentration of 10^{-4} M MnTMPyP was used in these experiments (MacKenzie & Martin, 1998). Rings were exposed to MnTMPyP for 30 min prior to and throughout the duration of the experiments.

4.2.2.3 Effect of MnTMPyP on the synthesis of nitric oxide by eNOS

To determine if MnTMPyP has any non-selective effects on the activity of NO derived from eNOS or the enzyme itself, both basal and agonist-stimulated activity of NO were assessed in endothelium-intact aortic rings in the absence and presence of MnTMPyP.

To assess the effect of MnTMPyP on basal synthesis of NO by eNOS, cumulative CRCs to NE (1×10^{-9} to 3×10^{-5} M, $n=7$) were constructed in endothelium-intact aortic rings. On completion of CRCs rings were repeatedly washed and allowed to re-equilibrate for at least 15 min before further experimentation. Aortic rings were then exposed to MnTMPyP (10^{-4} M, $n=7$) for 30 min prior to repeating cumulative CRCs to NE (1×10^{-9} to 3×10^{-5} M).

To assess the effect of MnTMPyP on agonist-stimulated synthesis of NO by eNOS, cumulative CRCs to ACh (1×10^{-8} to 3×10^{-5} M, $n=8$) were constructed in endothelium-intact aortic rings following induction of NE (~ EC_{60})-induced tone. On completion of CRCs, rings were repeatedly washed and allowed to re-equilibrate for at least 15 min before further experimentation. Aortic rings were then exposed to MnTMPyP (10^{-4} M, $n=8$) for 30 min prior to repeating cumulative CRCs to ACh (1×10^{-8} to 3×10^{-5} M).

4.2.2.4 Effect of MnTMPyP on the synthesis of nitric oxide by iNOS

In **Chapter 3**, experiments demonstrated that administration of LPS to rats resulted in the expression of iNOS in thoracic aortae. Furthermore, as a consequence of iNOS-derived NO, endothelium-intact and endothelium-denuded aortic rings from LPS-treated rats were hyporesponsive to NE when compared with responses in aortic rings from control rats. These findings support the use of thoracic aortae isolated from LPS-treated rats in experiments here, investigating the effect of MnTMPyP on the activity of NO derived from iNOS, and the activity of iNOS itself.

Therefore, to investigate the effect of MnTMPyP on the activity of NO derived from iNOS and the activity of the enzyme itself, cumulative CRCs to NE (1×10^{-9} to 3×10^{-5} M, n=6) were constructed in endothelium-denuded aortic rings from rats treated with LPS. On completion of CRCs, rings were repeatedly washed and allowed to re-equilibrate for at least 15 min before further experimentation. Aortic rings were then exposed to MnTMPyP (10^{-4} M, n=6) for 30 min prior to repeating cumulative CRCs to NE (1×10^{-9} to 3×10^{-5} M). At the end of cumulative CRCs to NE, rings were treated with the NOS substrate, L-arginine (10^{-3} M, n=5) to verify the expression of iNOS within aortic rings (Julou-Schaeffer *et al.*, 1990). A concentration of 10^{-3} M was chosen, since this concentration has been shown to result in a 15-fold increase in the EC_{50} concentration for NE in aortic rings from LPS-treated rats (Schott *et al.*, 1993). Responses were recorded 30 min after addition of L-arginine.

4.2.3 Preparation of drugs

Norepinephrine hydrogentartrate, acetylcholine chloride and L-arginine hydrochlroride were diluted in Krebs Henseleit solution to give a stock solution of 10^{-1} M and frozen (-20 °C) in aliquots until use on day of experiment. Vitamin C (10^{-6} M) was added to the stock solution of NE to prevent autoxidation. Catalase (bovine liver), pyrogallol and Mn [III] tetrakis [1-methyl-4-pyridyl] porphyrin (MnTMPyP) were diluted in Krebs Henseleit solution immediately prior to experimentation.

4.2.4 Data Analysis

All results were expressed as means ± s.e.mean. Cumulative CRCs to ACh and NE were measured as percentage relaxations of NE-induced tone and percentages of maximal contractions to KCl, respectively. The half-maximal relaxation (pD_2) was calculated for ACh CRCs by nonlinear regression using GraphPad Prism software (Version 3.0) where indicated in the text. Two-tailed *t*-tests, one-way analysis of variance (ANOVA) with Bonferroni multiple comparisons post-test and two-way repeated measures ANOVA were used as indicated in the text. $P<0.05$ was considered to be statistically significant.

4.3 Results

4.3.1 Effects of superoxide generation on the activity of eNOS-derived nitric oxide

The endothelium was deemed intact in aortic rings as relaxations to ACh were 86.6 ± 4.4% of NE (~ EC_{60})-induced tone (n=14).

4.3.1.1 Basal activity of nitric oxide

After induction of NE (~ EC_{60}) tone in endothelium-intact aortic rings (1.6 ± 0.3 gram tension), addition of pyrogallol (3 x 10^{-4} M) resulted in a rapid rise in arterial tone (to 2.3 ± 0.3 gram tension, P<0.01, one-way ANOVA with Bonferroni post-test; ***Figure 4.1***, ***Figure 4.2***). Indeed, the tension of aortic rings was increased by 41.2 ± 6.7% in the presence of pyrogallol (***Figure 4.5***).

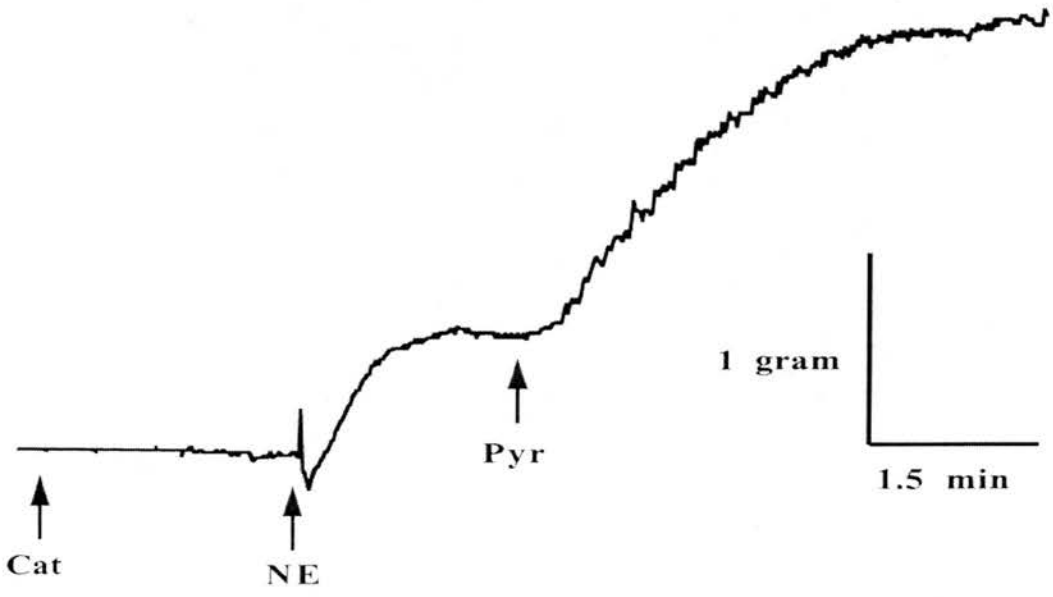

Figure 4.1 *A representative experimental trace showing the effect of pyrogallol (**Pyr**; 3 x 10^{-4} M) on norepinephrine (**NE**; EC_{60})-induced tone in endothelium-intact rat aortic rings (n=8). All experiments were carried out in the presence of catalase (**CAT**; 1000 U ml^{-1}).*

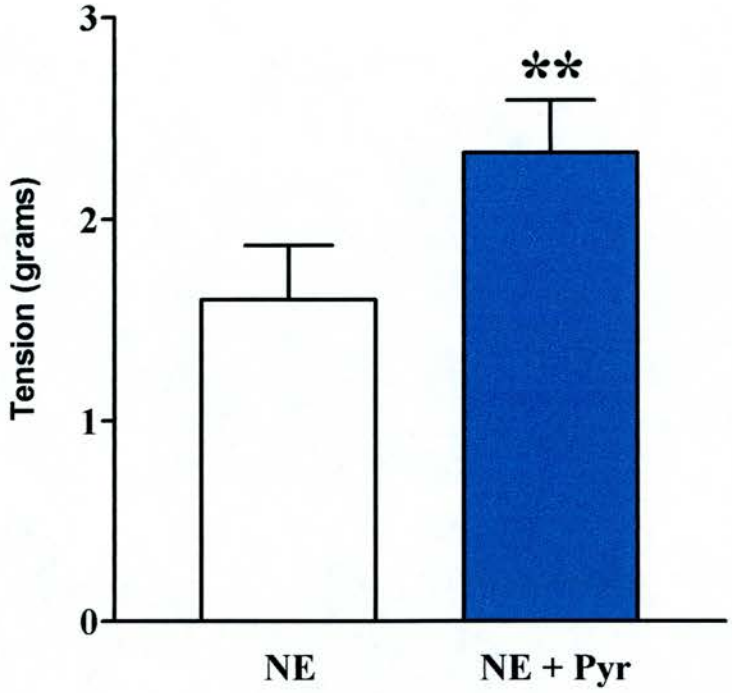

Figure 4.2 *The effect of pyrogallol (**Pyr**; 3 x 10^{-4} M) on norepinephrine (**NE**; EC_{60})-induced tone in endothelium-intact rat aortic rings (n=8). All experiments were carried out in the presence of catalase (1000 U ml^{-1}). Values are given as means ± s.e.mean. ** $P<0.01$ compared with gram tension in untreated aortic rings (one-way ANOVA with Bonferroni post-test).*

4.3.1.2 Agonist-stimulated activity of nitric oxide

Following induction of NE tone (untreated, 65 ± 5.6 %; pyrogallol-treated, 69.3 ± 7.3% of maximal NE contraction) in endothelium-intact aortic rings, cumulative additions of ACh (1 x 10^{-8} to 3 x 10^{-5} M) resulted in concentration dependent relaxations (***Figure 4.3***). Addition of pyrogallol (3 x 10^{-4} M) caused a marked inhibition of ACh relaxations when compared with relaxations in untreated aortic rings ($P<0.001$, two way ANOVA, ***Figure 4.3***). Indeed, maximal % relaxations to ACh were significantly lower in rings treated with pyrogallol when compared with untreated rings (untreated, 93.2 ± 8; pyrogallol-treated, 59.4 ± 5.2% relaxations of NE-induced tone, $P<0.05$, two-tailed paired *t*-test).

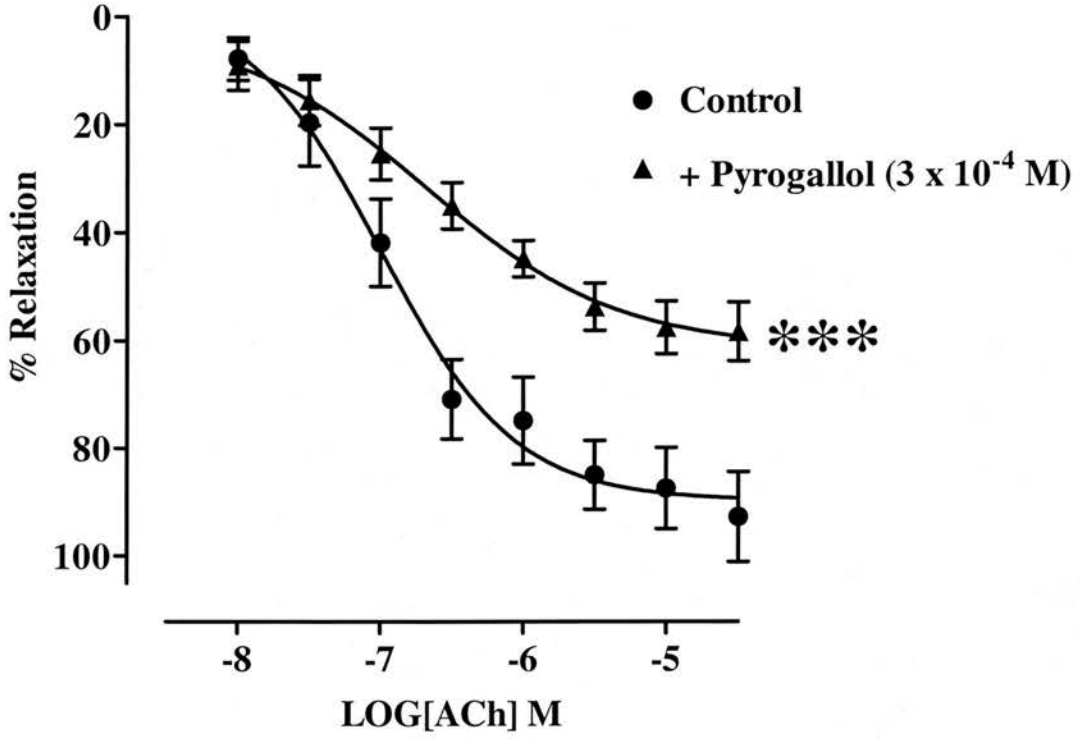

Figure 4.3 *Cumulative concentration response curves (CRC) to acetylcholine (**ACh**; 1 x 10^{-8} to 3 x 10^{-5} M) in norepinephrine (~ EC_{60})-contracted endothelium-intact rat aortic rings (n=6) in the presence and absence of pyrogallol (3 x 10^{-4} M). Values are given as means ± s.e.mean. All experiments were carried out in the presence of catalase (1000 U ml^{-1}). *** P<0.001 compared with cumulative CRCs in untreated aortic rings (two-way ANOVA).*

4.3.2 Effects of MnTMPyP on the activity of eNOS-derived nitric oxide in pyrogallol-treated aortic rings

The endothelium was deemed intact in aortic rings as relaxations to ACh were 81.2 ± 9% of NE (~ EC_{60})-induced tone (n=12).

4.3.2.1 Basal activity of nitric oxide

Arterial tone (~ EC_{60}; 1.9 ± 0.3 gram tension) induced in endothelium-intact aortic rings treated with MnTMPyP (10^{-4} M) did not differ from the tone induced in aortic rings used in Section **4.3.1.1** (P>0.05, one-way ANOVA). Subsequent addition of pyrogallol (3 x 10^{-4} M) to rings had no significant effect on arterial tone (to 2 ± 0.3 gram tension; ***Figure 4.4***) Indeed, the tension of aortic rings was increased by only 8.8 ± 3.6%, contrasting with an increase of 41.2 ± 6.7% in the absence of MnTMPyP (P<0.01, two-tailed unpaired t-test, ***Figure 4.5***).

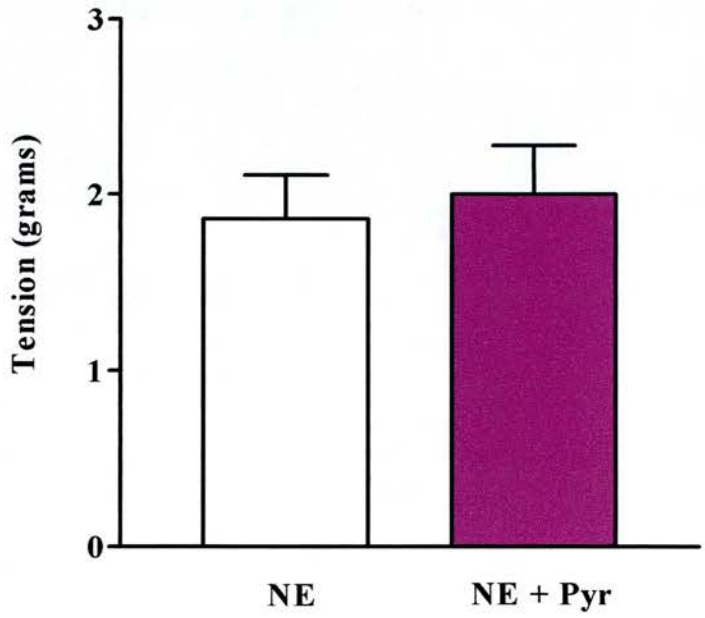

Figure 4.4 *The effect of pyrogallol (**Pyr**; 3 x 10^{-4} M) on norepinephrine (**NE**; EC_{60})-induced tone in endothelium-intact rat aortic rings (n=8) in the presence of MnTMPyP (10^{-4} M). All experiments were carried out in the presence of catalase (1000 U ml^{-1}). Values are given as means ±s.e.mean. P>0.05, one-way ANOVA.*

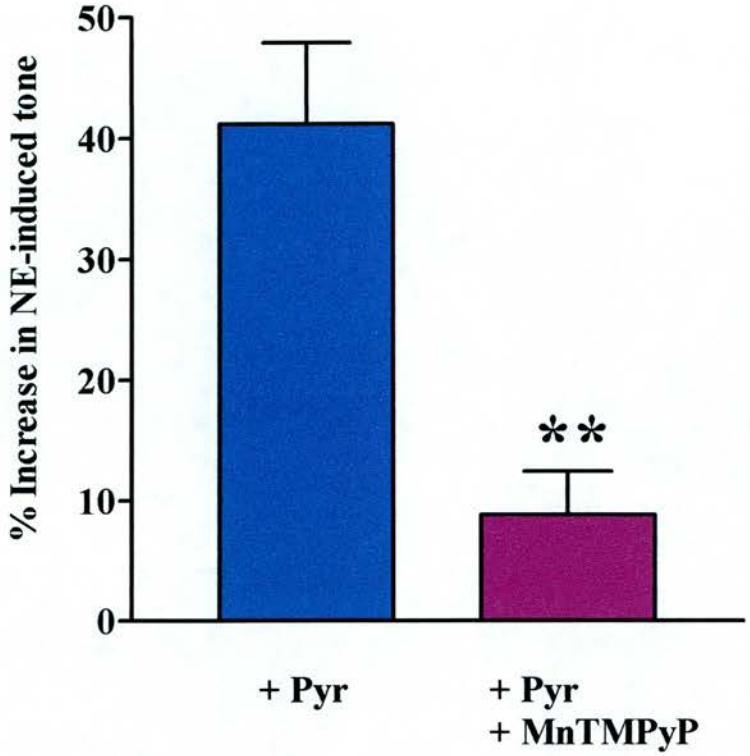

Figure 4.5 *Percentage increases in norepinephrine (**NE**; EC_{60})-induced tone in pyrogallol (**Pyr**; 3 x 10^{-4} M) treated endothelium-intact rat aortic rings (n=16) in the presence and absence of MnTMPyP (10^{-4} M). All experiments were carried out in the presence of catalase (1000 U ml^{-1}). Values are given as means ± s.e.mean. ** P<0.01 compared with percentage increases in arterial tone in rings treated with pyrogallol in the absence of MnTMPyP (two-tailed unpaired t-test).*

4.3.2.2 Agonist-stimulated activity of nitric oxide

In the presence of MnTMPyP, pyrogallol had no significant effect on relaxations to ACh (1 x 10^{-8} to 3 x 10^{-5} M) in NE-contracted (untreated, 61 ± 6%; pyrogallol-treated, 64 ± 9% maximal NE constriction) endothelium-intact aortic rings (***Figure 4.6***).

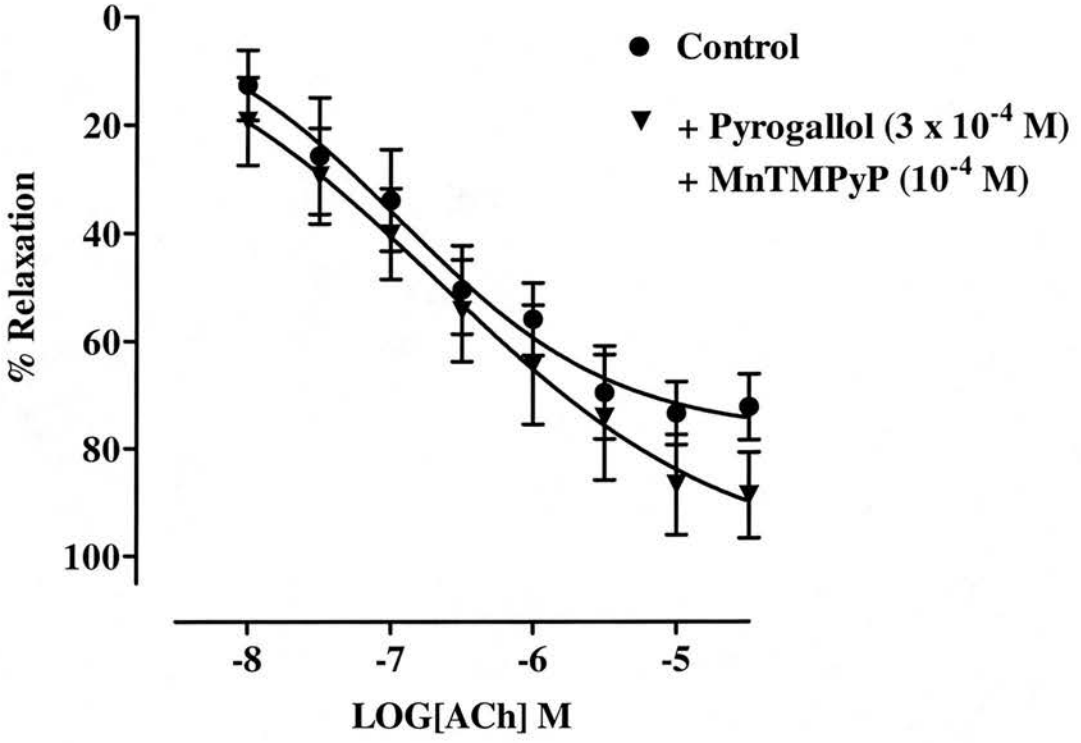

Figure 4.6 *Cumulative concentration response curves to acetylcholine (**ACh**; 1 x 10^{-8} to 3 x 10^{-5} M) in norepinephrine (~ EC_{60})-contracted endothelium-intact rat aortic rings (n=6) in the presence and absence of pyrogallol (3 x 10^{-4} M) and MnTMPyP (10^{-4} M). All experiments were carried out in the presence of catalase (1000 U ml^{-1}). Values are given as means ± s.e.mean. P>0.05, two-way ANOVA.*

4.3.3 Effect of MnTMPyP on eNOS-derived nitric oxide

The endothelium was deemed intact in aortic rings as relaxations to ACh were 74 ± 4.8% of NE (~ EC_{60})-induced tone (n=15).

MnTMPyP (10^{-4} M) had no significant effect on cumulative CRCs to NE (1 x 10^{-9} to 3 x 10^{-5} M) in endothelium-intact aortic rings (***Figure 4.7***). In the presence of MnTMPyP (10^{-4} M) pD_2 values for cumulative CRCs to ACh (1 x 10^{-8} to 3 x 10^{-5} M, ***Figure 4.8***) were significantly increased (pD_2 values; untreated, 6.6 ± 0.1; MnTMPyP-treated, 7.1 ± 0.1, P<0.05, two-tailed paired t-test), indicating an increase in responsiveness to ACh. There were no significant differences between maximal % relaxations to ACh in untreated and MnTMPyP-treated rings (***Figure 4.8***).

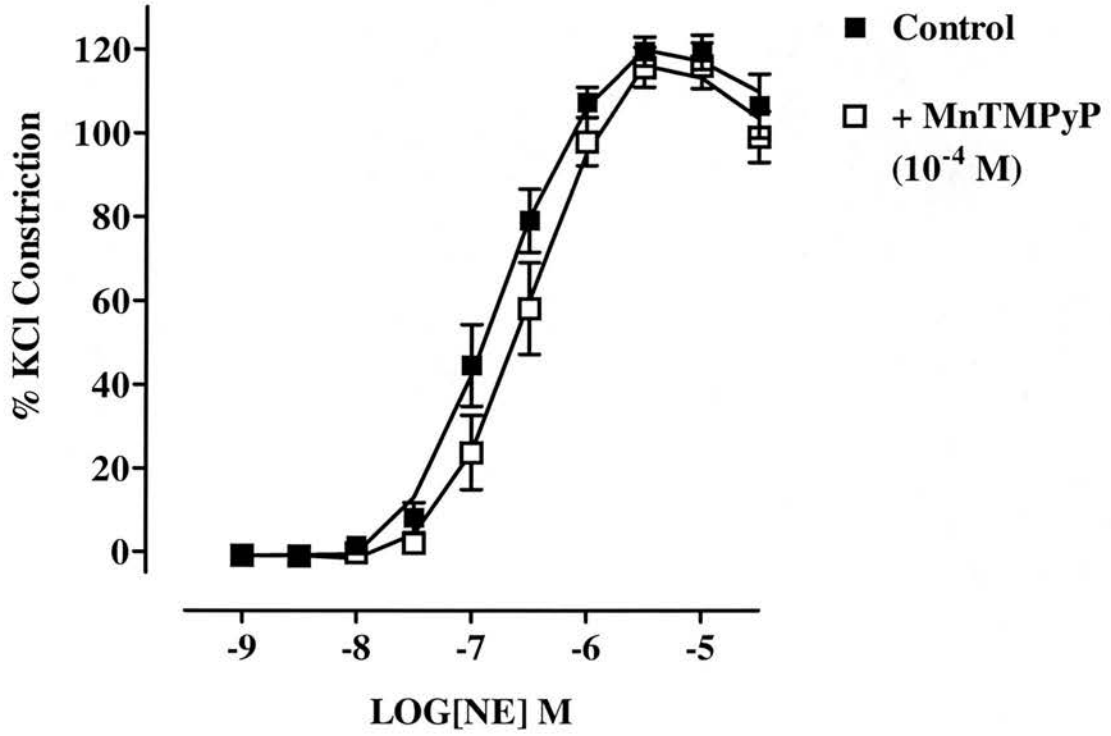

Figure 4.7 *Cumulative concentration response curves to norepinephrine (NE; 1 x 10^{-9} to 3 x 10^{-5} M) in endothelium-intact rat aortic rings (n=7) in the presence and absence of MnTMPyP (10^{-4} M). Values are given as means ± s.e.mean. P>0.05, two-way ANOVA.*

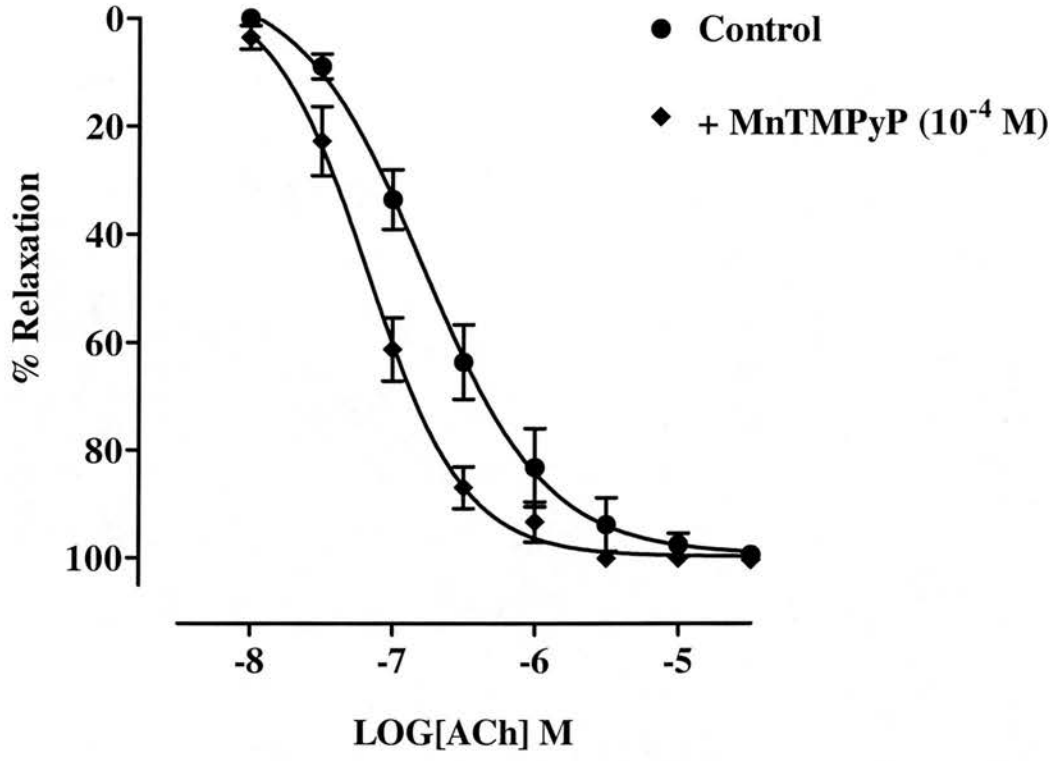

Figure 4.8 *Cumulative concentration response curves to acetylcholine (**ACh**; 1 x 10^{-8} to 3 x 10^{-5} M) in norepinephrine (~ EC_{60})-contracted endothelium-intact rat aortic rings (n=8) in the presence and absence of MnTMPyP (10^{-4} M). Values are given as means ± s.e.mean. P>0.05, two-way ANOVA.*

4.3.4 Effect of MnTMPyP on iNOS-derived nitric oxide

In endothelium-denuded aortic rings from LPS-treated rats, relaxations to ACh (~ EC_{60}) were less than 5% of NE–induced tone (2.3 ± 0.2%, *n*=6) indicating successful denudation.

MnTMPyP (10^{-4} M) had no significant effect on cumulative CRCs to NE (1 x 10^{-9} to 3 x 10^{-5} M) in endothelium-denuded aortic rings from LPS-treated rats (***Figure 4.9***). Treatment of rings with L-arginine (10^{-3} M) at the end of CRCs to NE resulted in a significant decrease in gram tension (without L-arginine, 1.1 ± 0.3 gram

tension; with L-arginine, 0.1 ± 0.1 gram tension, $P<0.05$, two-tailed paired *t*-test), verifying the expression of iNOS in aortic rings (Julou-Schaeffer *et al.*, 1990).

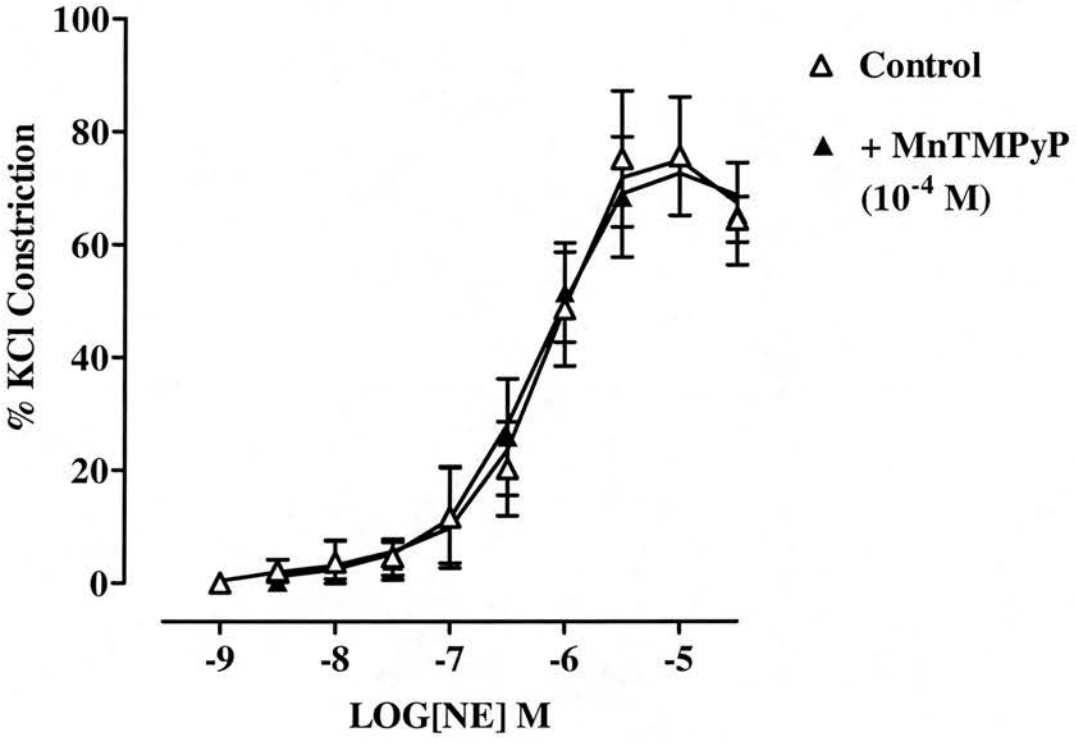

Figure 4.9 *Cumulative concentration response curves to norepinephrine (**NE**; 1 x 10^{-9} to 3 x 10^{-5} M) in endothelium-denuded aortic rings (n=6) from lipopolysaccharide-treated rats in the presence and absence of MnTMPyP (10^{-4} M). Values are given as means ± s.e.mean. P>0.05, two-way ANOVA.*

4.4 Discussion

Experiments in this chapter demonstrate that the novel metalloporphyrin, MnTMPyP (10^{-4} M) prevents both the augmentation of NE-generated arterial tone and the impairment of ACh-mediated relaxations in endothelium-intact rat aortic rings induced by the superoxide-generating compound, pyrogallol (3 x 10^{-4} M). These findings suggest that MnTMPyP can protect both basal and agonist-stimulated endothelium-derived NO from inactivation by superoxide. Under conditions of low oxidative stress, ie. in the absence of pyrogallol, MnTMPyP (10^{-4} M) increased responsiveness of endothelium-intact rat aortic rings to ACh and had no significant effect on NE responsiveness, implying that MnTMPyP (10^{-4} M) does not inhibit basal or agonist-stimulated activity of eNOS-derived NO or the activity of eNOS. Similarly, MnTMPyP appears to have no effect on the activity of NO derived from iNOS or the activity of the enzyme itself, since contractile responses to NE in endothelium-denuded aortic rings from LPS-treated rats were unaffected by MnTMPyP (10^{-4} M).

Endothelium-derived NO is rapidly inactivated by the oxygen-derived free radical, superoxide, leading to a loss of its vasodilatory action (Gryglewski *et al.*, 1986). Treatment of isolated blood vessels with high concentrations of the superoxide-generating compound, pyrogallol, has previously been shown to impair both basal and agonist-stimulated activity of endothelium-derived NO as a consequence of increased inactivation of NO by superoxide (Ignarro *et al.*, 1988; Mian & Martin, 1995). Experiments in this chapter demonstrate that treatment of endothelium-intact rat aortic rings with pyrogallol (3 x 10^{-4} M) augmented NE-induced tone and resulted in a profound decrease in ACh-mediated relaxations. Therefore, in accordance with the aforementioned studies, results here imply that both basal and agonist-stimulated activities of endothelium-derived NO are inhibited by superoxide generated from pyrogallol. These findings confirm that this is a reliable *in vitro* model of oxidative stress, with sufficient quantities of superoxide being produced to impair endothelium-derived NO even when the endothelial-NO pathway is maximally stimulated.

The metalloporphyrins have emerged as a novel class of catalytic antioxidants that scavenge a wide range of reactive oxygen species including superoxide (Patel & Day, 1999). In this chapter, the SOD mimetic properties of one such compound, MnTMPyP, were investigated. As with other compounds belonging to this class of SOD mimetics, MnTMPyP consists of a metal redox active centre embedded in a porphyrin ring (Patel & Day, 1999). Previously, MnTMPyP has been shown to catalyse the dismutation of superoxide in the xanthine-oxidase cytochrome assay with a rate constant of approximately 10^{-7} $M^{-1}s^{-1}$ and in SOD-deficient *E.Coli* with a rate constant of approximately 10^{-9} $M^{-1}s^{-1}$ (Faulkner *et al.*, 1994). Moreover, MnTMPyP protected *E.Coli* against paraquat-induced oxidative stress (Liochev & Fridovich, 1995) and facilitated the growth of SOD-deficient *E.Coli* (Faulkner *et al.*, 1994). The precise mechanism by which this manganese-based metalloporphyrin mediates its SOD-like activity is yet to fully defined, but, it is thought that the manganese moiety functions in the dismutation of superoxide by alternate reduction and oxidation, changing its valence state from Mn(III) to Mn(II) in a similar manner to native Mn-containing SOD (Patel & Day, 1999).

In keeping with its SOD-like properties, experiments in this chapter demonstrate that pre-treatment of endothelium-intact rat aortic rings with MnTMPyP (10^{-4} M) prevents the augmentation of NE arterial tone and the impairment of ACh-mediated relaxations induced by pyrogallol (3×10^{-4} M). These results imply that MnTMPyP can protect both basal and agonist-stimulated endothelium-derived NO under conditions of high oxidative stress by acting as a SOD mimetic. Furthermore, these findings are consistent with recent studies demonstrating that MnTMPyP (10^{-5} M to 6×10^{-4} M) is capable of restoring endothelium-dependent relaxations in isolated rabbit aortic rings subjected to both intracellular and extracellular oxidative stress (MacKenzie & Martin, 1998; Fontana *et al.*, 1999).

Despite the compelling evidence presented here, and from other studies (Faulkner *et al.*, 1994; Liochev & Fridovich, 1995; MacKenzie & Martin, 1998; Fontana *et al.*, 1999), that MnTMPyP is an effective SOD mimetic, recent studies provide evidence that the prevailing redox environment may be of critical importance in determining

its precise pharmacological profile. Interestingly, it has been suggested that in contrast to situations of high oxidative stress, where MnTMPyP preferentially scavenges superoxide, when levels of oxidative stress are low MnTMPyP may participate in other redox reactions resulting in the paradoxical generation of superoxide (Gardner *et al.*, 1996; MacKenzie *et al.*, 1999). In the aforementioned study by MacKenzie *et al.* (1999), MnTMPyP was found to augment phenylephrine (PE)-induced constrictions of endothelium-intact rat aortic rings under conditions of low oxidative stress. Moreover, this augmentation was blocked when the endothelium was removed or when aortic rings were treated with an inhibitor of NOS, suggesting that MnTMPyP was inactivating rather than protecting basal endothelium-NO activity. In subsequent experiments, MacKenzie *et al.* (1999) demonstrated that the effect of MnTMPyP on PE-induced tone was also blocked by pre-treatment of rings with authentic Cu/Zn SOD, implying that this augmentation in constriction arose through inactivation of NO by superoxide derived from MnTMPyP. Interestingly, they also demonstrated that this pharmacological property of MnTMPyP was dependent on its concentration. In particular, increases in PE-induced tone were only seen with concentrations of 10^{-8} M to 3 x 10^{-5} M MnTMPyP, with concentrations greater than 3 x 10^{-5} M failing to increase in contractile responses. From the experiments presented in their study, the mechanism by which MnTMPyP generates superoxide under low levels of oxidative stress was unclear. Furthermore, it is unclear why the concentration of MnTMPyP was so crucial in determining whether it generates superoxide or not.

In addition to its possible pharmacological effect on the bioavailability of eNOS-derived NO, MnTMPyP has also been shown to directly interfere with the NO/sGC pathway in cultured endothelial cells, as well as purified sGC either activated with a NO donor or reconstituted with NOS, under low levels of oxidative stress (Pfeiffer *et al.*, 1998). Specifically, in the presence of reducing agents such as glutathione, MnTMPyP directly inhibited the activity of sGC and decreased the accumulation of NO, as measured by the conversion of L-[^{3}H]arginine to L-[^{3}H]citrulline, as well as the accumulation of cyclic guanosine 3', 5' monophosphate (cGMP). MnTMPyP was also shown to inhibit the activities of recombinant eNOS and iNOS, possibly by

interfering with the flow of electrons from NADPH to the haem moiety of the oxygenase domain (Pfeiffer *et al.*, 1998). In contrast with the findings of MacKenzie *et al.* (1999), experiments in this study found that the inhibitory effects of MnTMPyP on the NO pathway were not dependent on its concentration. Indeed, the inhibitory effects of MnTMPyP were seen over a wide concentration range (10^{-9} M to 5 x 10^{-3} M).

It is clear from the discussion presented here that the use of MnTMPyP in situations of high oxidative stress, may well serve its purpose, protecting endothelium-derived NO from inactivation by superoxide. However, if MnTMPyP is used when levels of superoxide in blood vessels are low, but at a sufficient level to modify NO bioavailability, MnTMPyP may well generate superoxide rather than acting as a scavenger, resulting in a paradoxical increase in vascular tone. Furthermore, it may directly interfere with the NO signalling pathway. It is of paramount importance, therefore, to determine the precise pharmacological properties of MnTMPyP in situations of low oxidative stress. To address this issue, experiments were designed in aortic rings from healthy and LPS-treated rats under conditions of low oxidative stress, ie. in the absence of pyrogallol, to determine whether MnTMPyP, at a concentration of 10^{-4} M, modifies the activity of NO derived from either eNOS or iNOS, or the activities of the enzymes themselves. Findings from these experiments demonstrated that at a concentration of 10^{-4} M, MnTMPyP had no effect on contractile responses of endothelium-intact rat aortic rings to NE and increased responsiveness of rings to ACh. These results imply that at this concentration, MnTMPyP does not inhibit the activity of basal or agonist-stimulated eNOS-derived NO, nor does it inhibit the activity of the enzyme itself. Indeed, the sensitivity of aortic rings to ACh was increased suggesting that MnTMPyP protected agonist-stimulated activity of eNOS-derived NO from low levels of superoxide present in the organ bath. In a similar manner to eNOS, MnTMPyP appears to have no effect on the activity of NO derived from iNOS or the activity of iNOS, since contractile responses to NE in endothelium-intact aortic rings from LPS-treated rats were unaffected by MnTMPyP (10^{-4} M). Therefore, in accordance with the study by MacKenzie *et al.* (1999) findings from these experiments clearly suggest that in

conditions of low oxidative stress and at a concentration of 10^{-4} M, MnTMPyP appears not to generate superoxide. However, these findings contrast with those of Pffefier *et al.* (1998) who show that at this concentration, MnTMPyP interferes with the NO/sGC pathway in cultured endothelial cells and inhibits the activity of purified isoforms of NOS. Differences between cultured cells and tissue preparations may explain these discrepancies. In particular, one may expect levels of oxidative stress to be much lower in cultured endothelial cells than those found in oxygenated organ baths with segments of blood vessels, and thus MnTMPyP may be more prone to participate in other redox reactions and thus interfere with the NO pathway. Indeed, as previously mentioned, responsiveness of aortic rings to ACh were increased in the presence of MnTMPyP, suggesting that superoxide production within the organ baths was at a sufficient level to modify NO bioavailabilty.

In summary, experiments in this chapter clearly demonstrate that at a concentration of 10^{-4} M, MnTMPyP acts as an effective SOD mimetic, protecting endothelium-derived NO from destruction by superoxide. Furthermore, at this concentration MnTMPyP does not inhibit the activity of NO derived from either eNOS or iNOS, or the activity of the enzymes themselves, under conditions of low oxidative stress.

It is clear, however, that for MnTMPyP to emerge as a useful therapeutic tool in the treatment of cardiovascular pathologies, further experiments are required to clarify its precise pharmacological properties. In particular, experiments are required to elucidate how and why it generates superoxide in conditions of low oxidative stress and why its concentration is so crucial in determining this pharmacological property. Furthermore, studies are required to determine if the effects of MnTMPyP on the NO/sGC pathway and the activity of NOS would be a true pharmacological effect *in vivo*, or whether these properties are unique to experiments using cultured endothelial cells and purified enzymes.

Chapter 5

Investigation of the distribution of immunoreactive inducible nitric oxide synthase in the cardiovascular system of rats with chronic heart failure

5.1 Introduction

Although not constitutively expressed within the cardiovascular system, inducible nitric oxide synthase (iNOS) can be induced in most cells, including cardiomyocytes (Brady *et al.*, 1992; Balligand *et al.*, 1994), vascular endothelial and smooth muscle cells (Schulz *et al.*, 1991; Balligand *et al.*, 1995; Fleming *et al.*, 1991) in response to inflammatory cytokines and pathogens. In isolated cardiomyocytes, induction of iNOS by inflammatory cytokines and the subsequent production of large quantities of NO inhibits myocyte contractility (Brady *et al.*, 1992; Brady *et al.*, 1993). Furthermore, the expression of iNOS within the heart during endotoxic shock is associated with depressed cardiac function (Schulz *et al.*, 1995; Sun *et al.*, 1997). Intriguingly, the expression of iNOS in the heart has been linked to chronic heart failure (CHF). Some studies have reported the presence of calcium-independent NOS activity within the myocardium from patients with CHF (de Belder *et al.*, 1993; Drexler *et al.*, 1998). Other investigators have directly detected the presence of iNOS mRNA and protein (Haywood *et al.*, 1996; Fukuchi *et al.*, 1998; Vejlstrup *et al.*, 1998). However, the cellular location of iNOS in the heart during CHF is not well defined. Furthermore, previous studies have at times failed to define its anatomical distribution throughout the heart.

There is abundant evidence demonstrating that endothelium-dependent relaxations in both conductance and resistance arteries are impaired in CHF (Drexler & Lu, 1992; Teerlink *et al.*, 1994; Bauersachs *et al.*, 1999; Bank *et al.*, 1994; Carville *et al.*, 1998). In contrast, data on basal release of NO in CHF is controversial. Some studies suggest that basal release of NO is preserved or may even be enhanced in CHF (Drexler *et al.*, 1992; Habib *et al.*, 1994; Winlaw *et al.*, 1994), while other studies show that it is impaired (Elsner *et al.*, 1991; Teerlink *et al.*, 1994; Hirai *et al.*, 1995; Varin *et al.*, 1999). The expression of iNOS in the peripheral vasculature during CHF has not been directly investigated, but, it has been suggested that iNOS-derived NO is responsible for the dissociation between basal and stimulated release of NO in CHF (Carville *et al.*, 1998; Bauersachs *et al.*, 1999; Varin *et al.*, 1999).

The aims of experiments in this chapter were, therefore, to determine if iNOS is expressed in hearts isolated from rats with CHF following coronary artery ligation (CAL), and if so, investigate its spatial distribution throughout the heart. Furthermore, experiments were carried out to determine if iNOS is expressed in small mesenteric arteries and thoracic aortae from rats with CHF.

5.2 Methods

All procedures were carried out as described in **Chapter 2**.

5.2.1 Rat coronary artery ligation model of chronic heart failure

Myocardial infarction (MI) was induced in 5 week old male Wistar rats (250 –300 g) by ligation of the left anterior descending coronary artery (CAL) as described in Section **2.1.2.2**.

5.2.2 Haemodynamic measurements and tissue harvesting

Six weeks post-surgery, CAL and sham-operated rats were anaesthetised with sodium pentobarbitol (60 $mgkg^{-1}$, i.p.). The right carotid artery was then located, dissected free of extraneous tissue and then cannulated with a fluid filled catheter attached to a pressure transducer, for measurement of mean arterial blood pressure (MAP) and left ventricular end-diastolic pressures (LVEDP; see Section **2.1.2.3**).

Following exsanguination, the mesenteric bed was excised, the gut removed and the remaining vascular bed placed into cold, oxygenated (95% O_2, 5% CO_2), Krebs Henseleit solution for functional studies (see **Chapter 6**). Sections of the mesenteric bed and thoracic aortae from both CAL and sham-operated rats were placed in 10% neutral buffered formalin for 24 h prior to further processing and wax embedding as described in Section **2.1.2.4**. The hearts and lungs were removed, rinsed in ice-cooled saline (0.9%) then individually weighed. Hearts were bisected, fixed and processed as before.

5.2.3 Measurement of infarct size

3 μm sections of hearts were taken from blocks and stained with van Gieson's collagen stain for detection of collagen formation in left ventricular (LV) infarctions

(see Section **2.1.2.5**). Infarct size was then calculated by the method described in Section **2.1.2.5**.

5.2.4 Immunohistochemistry

3 μm sections of small mesenteric arteries, thoracic aortae and hearts were taken from paraffin embedded blocks. Immunohistochemistry was then performed using the indirect alkaline phosphatase method, with a rabbit anti-iNOS monoclonal primary antibody (concentration; mesenteric arteries, 1/250; aortae, 1/250; hearts, 1/300) and a goat anti-rabbit alkaline phosphatase-conjugated secondary antibody (concentration; mesenteric arteries, 1/50; aortae, 1/50; hearts, 1/100) as described in Section **2.5.5**. To verify selectivity of the primary antibody for iNOS, immunohistochemistry was performed on sections of thoracic aortae from lipopolysaccharide (LPS)-treated rats (*E.Coli* LPS, 30 mg kg^{-1} i.p. for 5 h, see **Chapter 3**). Negative controls were treated with an antibody of the same immunoglobulin (Ig) class but not directed against the iNOS epitope (see Section **2.5.5**). Tissues were then treated with Harris' haematoxylin to counterstain nuclei.

5.2.5 Data Analysis

All results were expressed as means ± s.e.mean. Two-tailed unpaired *t*-tests were used as indicated in the text. $P<0.05$ was considered to be statistically significant.

5.3 Results

5.3.1 Effect of left coronary artery ligation

All the animals that survived the first 24 h after CAL surgery (76%) were still alive 6 weeks later. There were no significant differences between rat weights for CAL and sham-operated groups at 6 weeks after surgery (***Table 5.1***). Heart weights (corrected for body weight) for CAL rats were significantly greater than those of sham-operated rats ($P<0.05$, two-tailed unpaired *t*-test, ***Table 5.1***). There were no significant differences between groups with respect to lung weights (corrected for body weight, P=0.1, unpaired *t*-test, *Table 5.1*) and MAPs ($P=0.08$, unpaired *t*-test, ***Table 5.1***). LVEDPs measured from CAL rats were significantly greater than those for sham-operated rats ($P<0.05$, two-tailed unpaired t-test, ***Table 5.1***).

	Sham ($n>8$)	***CAL*** ($n>8$)
Rat Weight (g)	495.7±22.3	473.9±9.7
Heart Weight (g kg^{-1} body weight)	2.7±0.1	3.3±0.2*
Lung Weight (g kg^{-1} body weight)	3.3±0.1	4.3±0.5
LVEDP (mmHg)	6±1.1	15.4±1.5***
Mean arterial pressure (mmHg)	94.8±6.2	78.2±5.7

Table 5.1 *Summary of parameters measured from coronary artery ligation* ***(CAL)*** *and sham-operated* ***(Sham)*** *rats 6 weeks post-surgery. All values are given as means ± s.e.m. * $P<0.05$, *** $P<0.001$ for CAL rats compared with respective values in sham-operated rats (two-tailed unpaired t-test).*

Hearts from CAL rats had LV infarctions which averaged 60 ± 3% of the LV free wall. Treatment of sections with van Gieson's collagen stain, stained LV infarctions pink with a few remaining areas of viable myocytes staining yellow (***Figure 5.1a***). These findings indicate that LV infarctions were principally composed of collagen. In hearts from sham-operated rats, cardiomyocytes and all other cell types were stained yellow, with only the collagenous adventitial layer of blood vessels and interstitial tissue staining pink (***Figure 5.1b***).

a

b

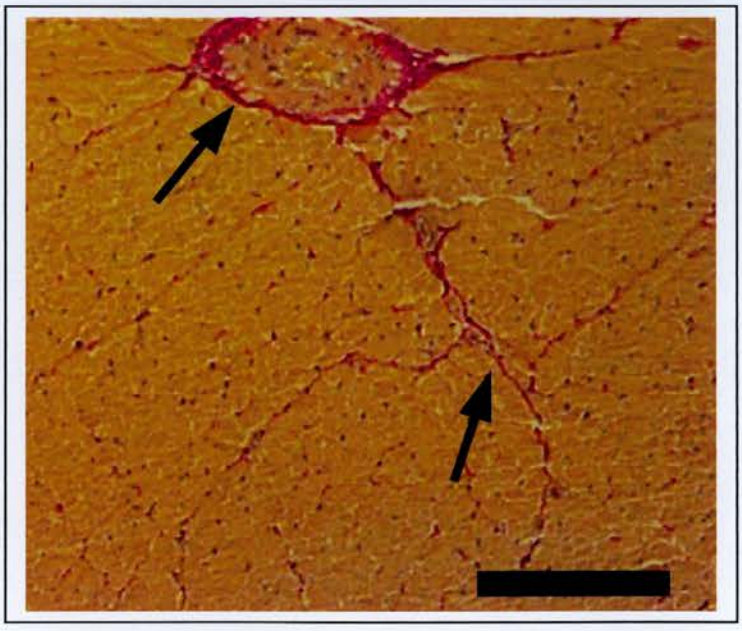

Figure 5.1 *Representative images of heart sections from coronary artery ligation (CAL) and sham-operated rats (n=6) treated with van Gieson's collagen stain. Collagen (pink staining) was detected in left ventricular infarctions of hearts from CAL rats (Panel* ***a****; x100, scale bar = 200 μm). In hearts from sham-operated rats, collagen (pink staining) was detected in the adventitia of blood vessels and interstitial tissue (arrows) of the myocardium (Panel* ***b****; x200, scale bar = 45 μm).*

5.3.2 Localisation of inducible nitric oxide synthase in the heart

iNOS immunoreactivity was found in the cytoplasm of some but not all cardiomyocytes in the interventricular septum in hearts from CAL rats 6 weeks post-ligation (***Figure 5.2a***). Immunoreactive iNOS was found in the cytoplasm of viable cardiomyocytes at the border of the infarct and within the infarct itself (***Figure 5.2b***, ***5.3a***). However, no iNOS immunoreactvity was detected within the infarcted myocardium (***Figure 5.3a***).

In contrast with the LV myocardium, no immunoreactive iNOS was detected in cardiomyocytes within the right ventricular (RV) myocardium of hearts from CAL rats (***Figure 5.3b***).

No immunoreactive iNOS was found in cardiomyocytes of the LV (***Figure 5.4***) and RV myocardium nor in the interventricular septum (data not shown) in hearts from sham-operated rats 6 weeks post-surgery.

Immunoreactive iNOS was found in endothelial cells, vascular smooth muscle (VSM) cells and in the adventitia of thoracic aortae from rats treated with LPS verifying the selectivity of the iNOS antibody (see **Chapter 3**, ***Figure 3.1a***). No immunoreactive staining was found in heart sections from CAL rats using an antibody of the same Ig class but not directed against the iNOS epitope (data not shown).

a

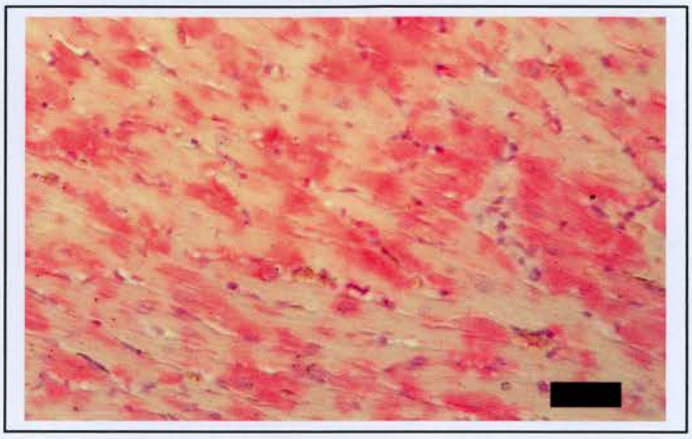

b

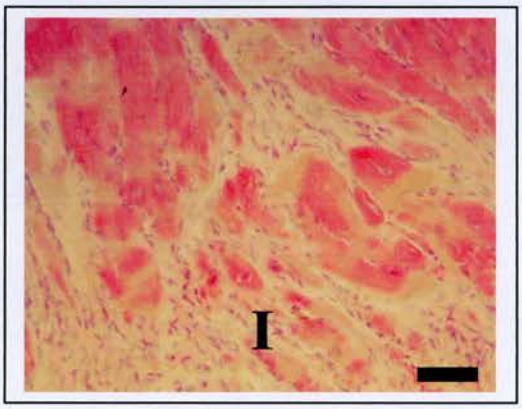

Figure 5.2 *Immunohistochemical localisation of iNOS in representative heart sections from coronary artery ligation rats (n=6) six weeks post-ligation. Immunoreactive iNOS (red staining) was localised to the cytoplasm of viable cardiomyocytes within the interventricular septum (Panel* ***a****) and at the border of the infarct (Panel* ***b****;* ***I*** *= infarcted myocardium). Nuclei are counterstained with Harris' Haematoxylin (purple staining). Magnification x200, scale bar = 40 μm.*

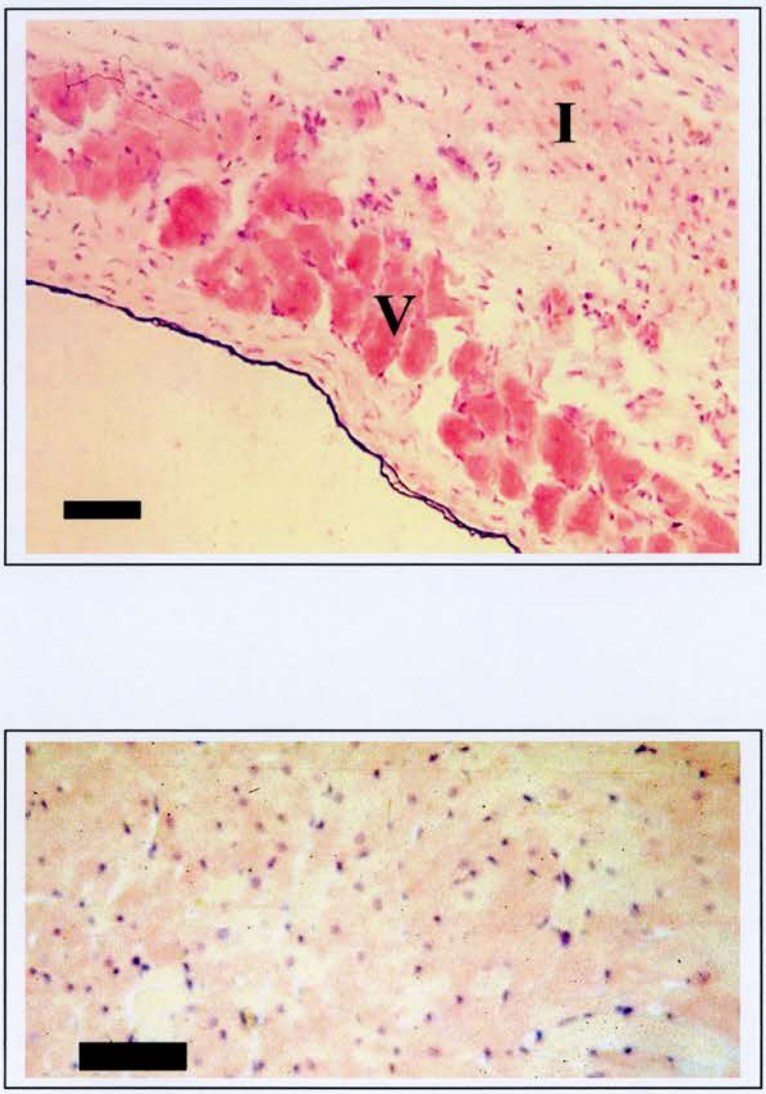

Figure 5.3 *Immunohistochemical localisation of iNOS in representative heart sections from coronary artery ligation rats (n=6) six weeks post-ligation. Immunoreactive iNOS (red staining) was detected in viable cardiomyocytes (**V**) within the infarct (**I**; Panel **a**; scale bar = 30 μm). However, no immunoreactive iNOS was found in cardiomyocytes within the right ventricular myocardium (Panel **b**; scale bar = 40 μm). Nuclei are counterstained with Harris' Haematoxylin (purple staining). Magnification x200.*

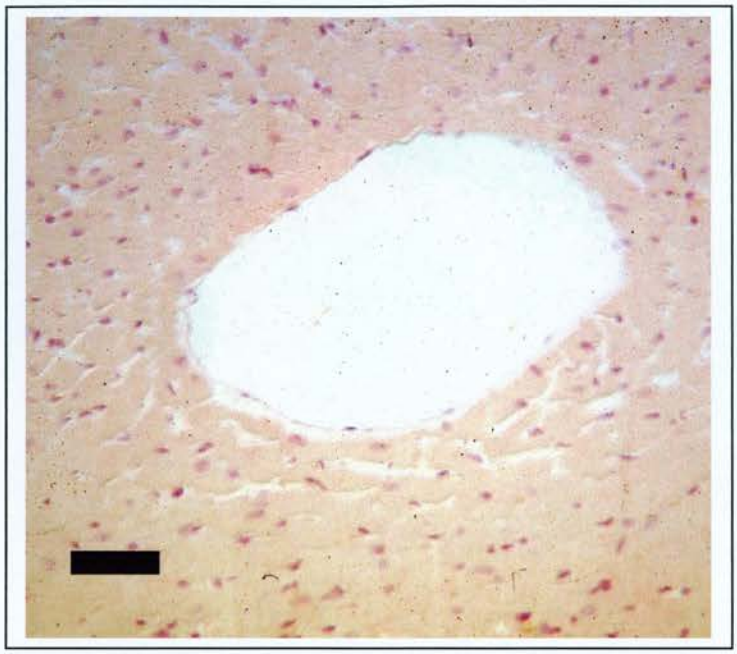

Figure 5.4 *A representative image showing absence of iNOS immunoreactivity in the left ventricular myocardium of hearts from sham-operated rats (n=6) six weeks post-surgery. Nuclei are counterstained with Harris' Haematoxylin (purple staining). Magnification x200, scale bar = 40 μm.*

iNOS immunoreactivity was detected in endothelial cells of intramyocardial blood vessels within the LV myocardium of hearts from CAL rats (***Figure 5.5a***). No immunoreactivity was found, however, in VSM cells or in the adventitia (***Figure 5.5a***). Blood vessels within the RV myocardium of hearts from CAL rats showed no iNOS immunoreactivity (***Figure 5.5b***). Similarly, no iNOS immunoreactivity was found in intramyocardial blood vessels within hearts from sham-operated rats (data not shown).

iNOS immunoreactivity was found in endocardial endothelial cells within the LV myocardium of hearts from CAL rats (***Figure 5.6***).

a

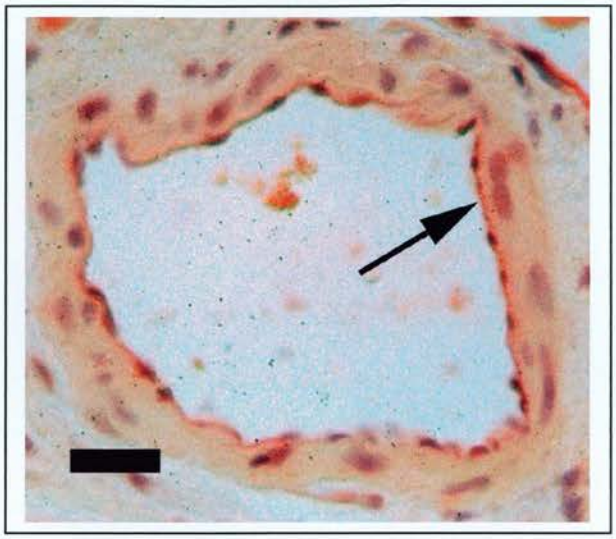

b

Figure 5.5 *Immunohistochemical localisation of iNOS in intramyocardial blood vessels in coronary artery ligation rats (n=6) six weeks post-ligation. Immunoreactive iNOS (red staining) was located to endothelial cells (arrow) of intramyocardial blood vessels within the left ventricular myocardium (Panel* ***a****; scale bar = 20 μm). No iNOS immunoreactivity was detected in intramyocardial blood vessels within the right ventricular myocardium (Panel* ***b****; scale bar = 45 μm). Nuclei are counterstained with Harris' Haematoxylin (purple staining). Magnification x 200.*

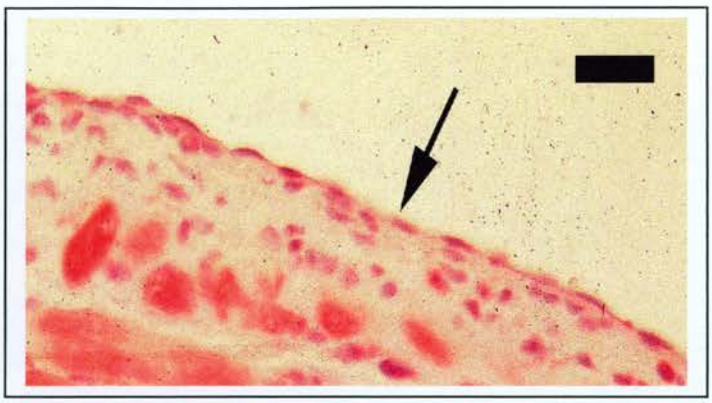

Figure 5.6 *Representative images of heart sections from coronary artery ligation rats (n=6) six weeks post-ligation, showing immunoreactive iNOS (red staining) in endocardial endothelial cells (arrow, x200, scale bar = 25 μm) of the left ventricular myocardium. Nuclei are counterstained with Harris' Haematoxylin (purple staining).*

5.3.3 Localisation of inducible nitric oxide synthase in small mesenteric arteries and thoracic aortae

Immunoreactive iNOS was found in endothelial cells, VSM cells and in the adventitia of small mesenteric arteries from CAL rats (***Figure 5.7a***). No immunoreactivity was found in small mesenteric arteries from sham-operated rats (***Figure 5.7b***) or in negative controls using IgG antibodies (data not shown).

Similarly, immunoreactive iNOS was found in endothelial cells, VSM cells and in the adventitia of thoracic aortae from CAL rats (***Figure 5.8a***). No staining was found in aortae from sham-operated rats (***Figure 5.8b***) or in negative controls using IgG antibodies (data not shown).

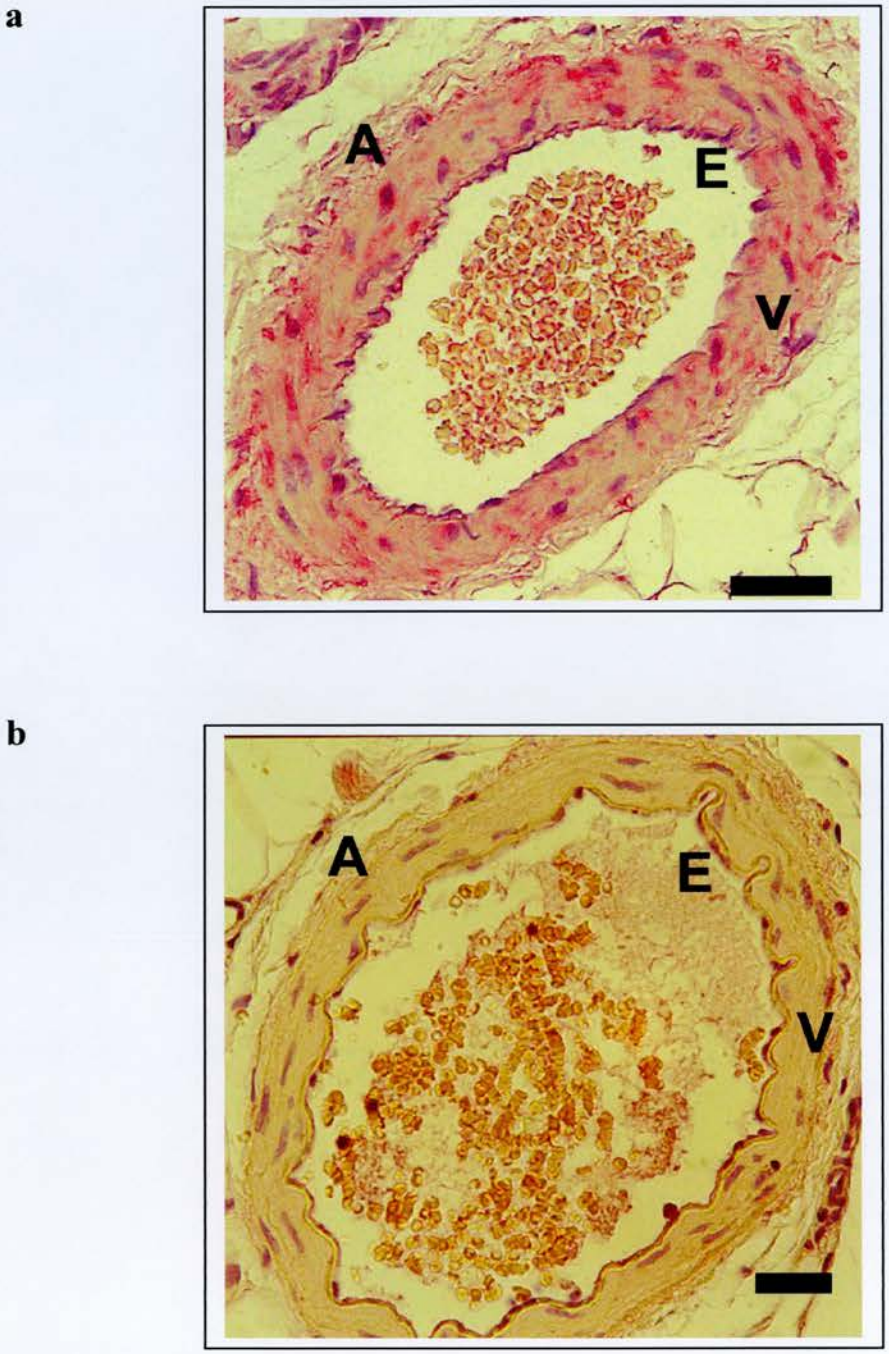

Figure 5.7 *Images of representative sections of small mesenteric arteries from coronary artery ligation (CAL) and sham-operated rats (n=6). Immunoreactive iNOS (red staining) was detected in endothelial cells (**E**), vascular smooth muscle cells (**V**) and in the adventitia (**A**) of arteries from CAL rats (Panel **a**), but not in arteries from sham-operated rats (Panel **b**). Nuclei are counterstained with Harris' Haematoxylin (purple staining). Magnification x400, scale bar = 30 μm.*

a

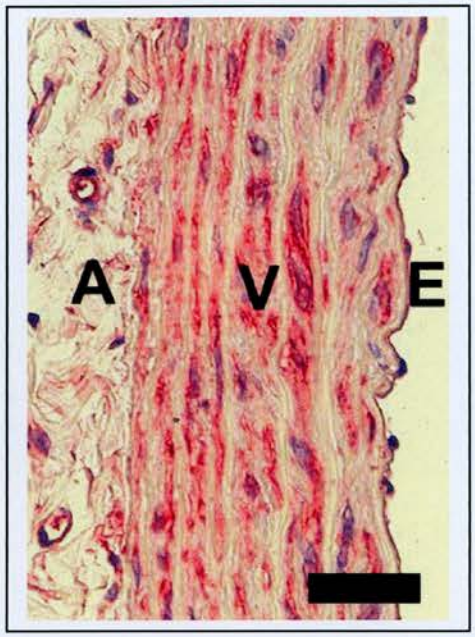

b

Figure 5.8 *Images of representative sections of thoracic aortae from coronary artery ligation (CAL) and sham-operated rats (n=6). Immunoreactive iNOS (red staining) was detected in endothelial cells (**E**), vascular smooth muscle cells (**V**) and in the adventitia (**A**) of aortae from CAL rats (Panel **a**), but not in aortae from sham-operated rats (Panel **b**). Nuclei are counterstained with Harris' Haematoxylin (purple staining). Magnification x400, scale bar = 180 μm.*

5.4 Discussion

The salient finding of experiments described in this chapter is that iNOS is expressed in both the heart and peripheral vasculature in rats with CHF. Using immunohistochemistry, iNOS was found to be located to cardiomyocytes throughout the non-infarcted LV myocardium and also in viable cardiomyocytes within the infarct. Furthermore, iNOS was detected in coronary vascular and endocardial endothelial cells within the LV myocardium. Interestingly, no iNOS was detected within the RV myocardium. In small mesenteric arteries and thoracic aortae from rats with CHF, iNOS was located to endothelial cells, VSM cells and to the adventitia.

LV infarct size is recognised to be a major determinant of the severity of CHF in rats after CAL (Pfeffer *et al.*, 1979). Pfeffer *et al.* (1979) revealed that the degree of myocardial cell death after CAL is directly related to impaired LV function. Furthermore, Pfeffer *et al.* demonstrated that rats with infarctions greater than 46% of the left ventricle resulted in elevated diastolic pressures and reduced cardiac outputs. In this chapter, six weeks after CAL, rats had infarctions averaging 60 % of the LV free wall. Furthermore, LVEDPs were significantly elevated when compared with those in sham-operated rats. Histological examination of hearts using van Gieson's collagen stain revealed that a fibrous scar, composed mainly of collagen, had replaced infarcted areas of hearts from CAL rats. Furthermore, heart weights, corrected for body weight, were significantly greater than those for sham-operated rats, indicating that hearts from CAL rats had undergone compensatory hypertrophy. These results demonstrate that rats had developed CHF as a consequence of CAL. This model resembles those of others who used rats with large infarcts and significantly elevated LVEDPs in the context of severe CHF (Sakai *et al.*, 1996a; Sakai *et al.*, 1996b; Kobayashi *et al.*, 1999).

Experimental studies have demonstrated that iNOS is expressed in the myocardium after CAL and subsequent MI. In rabbits, CAL resulted in a significant increase in NO synthesis within the infarcted myocardium, which persisted for at least 14 days post-MI (Dudek *et al.*, 1995). Furthermore, immunohistochemical studies revealed

that the induction of iNOS in infiltrating macrophages was responsible for this increase in NO synthesis (Dudek *et al.*, 1995; Wildhirt *et al.*, 1995). From these studies it would appear that the expression of iNOS in the heart is transient and associated with injury to the heart and the subsequent inflammatory response. However, there is now evidence that iNOS may be induced in the heart at later stages during CHF (de Belder *et al.*, 1993; Haywood *et al.*, 1996; Fukuchi *et al.*, 1998; Vejlstrup *et al.*, 1998). De Belder *et al.* (1993) reported that iNOS is expressed in heart biopsies from patients with dilated cardiomyopathy and suggested that this was the result of the specific inflammatory etiology of this condition (de Belder *et al.*, 1993b). However, some (Haywood *et al.*, 1996; Fukuchi *et al.*, 1998; Drexler *et al.*, 1998; Vejlstrup *et al.*, 1998) but not all (Stein *et al.*, 1998; Thoenes *et al.*, 1996) investigators have since detected the presence of iNOS mRNA and protein in explanted hearts from patients with ischaemic and non-ischaemic end-stage CHF, suggesting that iNOS expression might be a feature of the CHF condition *per se*.

Since the first report of iNOS induction in CHF, the *in vivo* anatomical distribution of iNOS in the heart has been a matter for debate (Brady, 1993; Shah, 1993). Invariably, iNOS has been located to the LV free wall and intraventricular septum (Haywood *et al.*, 1996; Fukuchi *et al.*, 1998; Vejlstrup *et al.*, 1998), of explanted hearts from patients with ischaemic and non-ischaemic CHF, with only some investigators detecting its presence within the RV myocardium (de Belder *et al.*, 1993; Haywood *et al.*, 1996). Furthermore, the cell types in which iNOS is expressed during CHF are not well defined. It has been suggested that the cardiomyocyte is the predominant source of iNOS in CHF, however, this is not universally accepted. Habib *et al.* (1996) and Haywood *et al.* (1996) reported immunohistochemical evidence for cytoplasmic iNOS protein expression in cardiomyocytes of hearts from patients with end-stage CHF. However, in a study of 22 explanted hearts from patients with end-stage CHF, Vejlstrup *et al.* (1998) reported that iNOS was expressed in cardiomyocytes in only a minority of patients. Furthermore, Fukuchi *et al.* (1998) revealed that increased iNOS activity was intimately associated with infiltrating macrophages and not with cardiomyocytes, in hearts from patients with CHF of varying pathologies. Surprisingly, very little data is available regarding its

expression within the coronary vasculature. Consequently, experiments in this chapter were carried out to determine if iNOS was expressed in the heart in a rat model of CHF, and if so, to investigate its spatial distribution within the heart.

Using immunohistochemistry, experiments in this chapter revealed that iNOS is expressed in hearts from CHF rats but not in hearts from sham-operated rats. In particular, iNOS was located to the LV free wall and interventricular septum. In contrast, no iNOS was detected within the RV myocardium. These results corroborate the findings of some (Haywood *et al.*, 1996; Fukuchi *et al.*, 1998) but not all investigators (de Belder *et al.*, 1993; Vejlstrup *et al.*, 1998), and suggest that the induction of iNOS in the failing heart during CHF might be specific to the LV myocardium.

With respect to its cellular localisation, experiments revealed that in this model of CHF, the cardiomyocyte is the predominant cell type expressing iNOS. In particular, iNOS was localised to viable cardiomyocytes in both the infarcted and non-infarcted myocardium. However, in this model of CHF, the expression of iNOS in the heart is not exclusive to the cardiomyocyte. Indeed, examination of intramyocardial blood vessels within the LV myocardium, revealed that iNOS is also expressed in vascular endothelial cells. Interestingly, iNOS could not be detected in VSM cells or in the adventitia. A recent study by Vejlstrup *et al.* (1998) demonstrated that iNOS was expressed in the coronary vasculature in explanted hearts from patients with end-stage CHF. However, in contrast with the findings in this chapter, Veljstrup *et al.* revealed that iNOS was expressed in both vascular endothelial and smooth muscle cells. In accordance with a recent study by Fukuchi *et al.* (1998), iNOS was detected in endocardial endothelial cells of the interventricular septum, suggesting that iNOS expression might not be exclusive to endothelial cells of the coronary vasculature.

The pathophysiological mechanisms underlying the induction of iNOS in the heart in this model of CHF were not investigated. As discussed in **Chapter 3** of this thesis, inflammatory cytokines, such as TNF-α and interleukin-1 (IL-1) can induce the expression of iNOS in cardiomyocytes (Brady *et al.*, 1992; Balligand *et al.*, 1994),

and vascular endothelial and smooth muscle cells (Schulz *et al.*, 1991; Balligand *et al.*, 1995; Fleming *et al.*, 1991). Interestingly, there is evidence that inflammatory cytokines are expressed in the heart during CHF. Torre-Amione *et al.* (1996b), demonstrated that TNF-α mRNA and protein was expressed in the LV myocardium from patients with both ischaemic and non-ischaemic end-stage CHF. In a more recent study, Francis *et al.* (1998) established that IL-1 mRNA and protein was expressed in cardiomyocytes and vascular endothelial cells within the LV myocardium of explanted hearts from patients with ischaemic CHF. Furthermore, in rats with CHF following CAL, mRNA for TNF-α, IL-1 and IL-6 was detected in the non-infarcted LV myocardium (Ono *et al.*, 1998). Therefore, inflammatory cytokines may well serve a stimulus of iNOS expression in CHF.

Interestingly, a recent study by Kapadia *et al.* (1997), demonstrated that passive mechanical stretch induced the expression of TNF-α in cardiomyocytes and non-cardiomyocytes in the adult feline myocardium. Consequently, the authors of this study suggested that passive mechanical stretch, such as that which occurs during the progressive LV remodelling associated with CHF (see Section **1.5.5.1**), might be a sufficient stimulus to provoke the expression of TNF-α within the failing heart. If this is indeed the case, it is conceivable that the induction of iNOS within the failing heart may be ultimately dependent on the amount of mechanical stretch exerted on the heart. Indeed, the findings from this chapter and from other studies (Haywood *et al.*, 1996; Fukuchi *et al.*, 1998) suggest that iNOS induction in the failing heart might be exclusive to areas of the heart, in particular the non-infarcted LV myocardium, where mechanical stretch is likely to be high. Germane to this discussion is the observation that the expression of TNF-α in the heart in response to other stimuli, besides mechanical stretch, is self-limiting and occurs only in response to the superimposed environmental stimuli (Giroir *et al.*, 1992; Kapadia *et al.*, 1995). Therefore, the expression of TNF-α, and the subsequent induction of iNOS throughout the heart might not be static but instead may vary considerably depending on the levels of mechanical stretch present within the heart. This hypothesis may explain why there is such disparity between studies regarding the cellular and anatomical distribution of iNOS in the heart during CHF. The hypothesis presented

here is provocative, however, it does represent an assumption based on correlations rather than direct evidence. It is clear, therefore, that further studies are required to fully address the relationship between inflammatory cytokines and mechanical stretch in regulating the induction of iNOS in the heart during CHF. As discussed in Section **1.5.5.1**, mechanical stretch is thought to play a important role in the LV remodelling associated with CHF. Studies suggest that mechanical stretch can activate multiple signal transduction pathways, similar to those activated by growth factors (Swynghedauw, 1999). Further to its possible role in the LV hypertrophy associated with remodelling, mechanical stretch has been shown to induce apoptosis of cardiomyocytes (Cheng *et al.*, 1995; see Section **1.5.5.1**). NO has been shown to act as a bifunctional regulator of apoptosis. Physiological relevant levels of NO seem to suppress the apoptotic pathway at multiple levels and by several pathways (Kim *et al.*, 1999; Li *et al.*, 1999a). However, higher concentrations of NO may overwhelm cellular protective mechanisms and exert proapoptotic and cytotoxic effects (Kim *et al.*, 1999). Indeed, cytokine-induced expression of iNOS has been shown to induce cardiomyocyte apoptosis (Ing *et al.*, 1999). Furthermore, the balance between the apoptotic mediators, Bak and BcL-x, which respond specifically to individual cytokines, was shown to modulate the extent of cardiomyocyte apoptosis (Ing *et al.*, 1999). There is some evidence that NO may have an anti-hypertrophic effect on the heart. Ishigai *et al.* (1997), demonstrated in neonatal rat cardiomyocytes that both bradykinin and the angiotensin converting inhibitor, perindoprilat, inhibited phenylephrine-induced increases in protein and DNA content via an NO-dependent mechanism. Furthermore, an anti-hypertrophic effect of NO is also suggested by experimental and clinical studies (reviewed by Shah & MacCarthy, 2000). Taken together these studies suggest an interesting relationship between mechanical stress, inflammatory cytokines, NO and the LV remodelling associated with CHF. However, it is clear that further studies are necessary to exploit this relationship and to investigate further if NO contributes to LV remodelling by inducing apoptosis or if it plays a counter-regulatory role in reducing hypertrophy.

In addition to their upregulation in the heart during CHF, plasma levels of inflammatory cytokines are also elevated in patients with CHF (Levine *et al.*, 1990;

Torre-Amione *et al.*, 1996a; Anker *et al.*, 1997). Furthermore, in contrast with impaired endothelium-dependent relaxations (Drexler *et al.*, 1992; Teerlink *et al.*, 1994b) some studies suggest that basal NO synthesis of NO by the peripheral vasculature may be preserved or even enhanced in CHF (Drexler *et al.*, 1992; Habib *et al.*, 1994; Winlaw *et al.*, 1994). Moreover, some investigators have hypothesised that expression of iNOS is responsible for this dissociation (Carville *et al.*, 1998; Varin *et al.*, 1999). In contrast with the heart, the expression of iNOS within the peripheral vasculature during CHF has not been addressed. Experiments in this chapter reveal that iNOS is expressed in endothelial cells, VSM cells and in the adventitia of small mesenteric arteries and thoracic aortae from rats with CHF, but not in arteries from sham-operated rats. This is the first study to demonstrate iNOS expression in the peripheral vasculature in experimental CHF. These findings are, however, contrast with the findings of a recent study, which failed to detect iNOS in thoracic aortae from rats 8 weeks after CAL (Bauersachs *et al.*, 1999). However, rats used here had larger infarcts than those used in the aforementioned study, perhaps suggesting that the severity of the model influences iNOS expression. The functional significance if iNOS expression in the peripheral vasculature is addressed in **Chapters 6** and **7** of this thesis.

In conclusion, the findings of this chapter reveal for this first time that iNOS is expressed in both the heart and peripheral vasculature in a rat model of CHF. Furthermore, these experiments provide novel insight into its spatial distribution within the failing heart.

Chapter 6

Investigation of the role of inducible nitric oxide synthase and superoxide in modulating vascular function of small arteries from rats with chronic heart failure

6.1 Introduction

Endothelium-derived nitric oxide (NO) plays a vital role in the regulation of vasomotor tone and arterial blood pressure (see Section **1.4.1**). Evidence is accumulating to suggest that impaired NO-mediated vasodilatation of resistance arteries contributes to increased peripheral vascular resistance (PVR) associated with chronic heart failure (CHF). In clinical and experimental CHF, it has been demonstrated that endothelium-dependent relaxations of peripheral resistance arteries in response to acetylcholine are impaired (Drexler & Lu, 1992; Drexler *et al.*, 1992; Katz *et al.*, 1992). In contrast, data on basal release of NO from resistance arteries in CHF is controversial. Some studies suggest that basal release of NO from the peripheral vasculature is preserved or may even be enhanced in CHF (Drexler *et al.*, 1992; Habib *et al.*, 1994; Winlaw *et al.*, 1994). Furthermore, there is evidence that plasma concentrations of nitrate, the stable end product of NO, are increased in patients with CHF (Kubo *et al.*, 1994; Winlaw *et al.*, 1994; Carville *et al.*, 1998). In contrast, other functional studies suggest that basal synthesis of NO is impaired in CHF (Elsner *et al.*, 1991; Hirai *et al.*, 1995; Varin *et al.*, 1999). The aetiology of endothelial dysfunction associated with CHF is unclear and is likely to be complex.

In **Chapter 5**, immunohistochemical studies demonstrated that iNOS is expressed in the hearts from rats with CHF following coronary artery ligation (CAL). Furthermore, experiments revealed that iNOS was also expressed in small mesenteric arteries from rats with CHF following CAL but not in those from sham-operated control rats. It is possible that NO derived from iNOS may be responsible for increased basal production of NO associated with CHF.

Irrespective of its source, increased basal production of NO should counteract compensatory constrictor mechanisms and thus reduce PVR. Increased superoxide is also associated with CHF (Belch *et al.*, 1991; Diaz-Velez *et al.*, 1996). Superoxide scavenges NO (Gryglewski *et al.*, 1986), and a therefore reduction in NO bioavailability might explain why PVR remains elevated in CHF despite a preserved or enhanced basal release of NO. Furthermore, increased scavenging of NO by

superoxide may be responsible for impaired relaxations to endothelium-dependent vasodilators.

The aims of the experiments in this chapter were, therefore, to determine the functional significance of iNOS-derived NO on vascular responsiveness of isolated small mesenteric arteries from rats with CHF following CAL, and to investigate the role that superoxide plays in modulating vascular function in these arteries.

6.2 Methods

All procedures were carried out as described in **Chapter 2**.

6.2.1 Tissue harvesting and preparation of arteries from mesenteric bed

The mesenteric bed was isolated from both CAL and sham-operated rats 6 weeks post-surgery (see **Chapter 5**) and placed in cold, oxygenated (95% O_2, 5% CO_2) Krebs Henseleit solution.

Third order branches of the mesenteric artery (~ 3 mm long; internal diameter, ~ 300 – 350 μm) were dissected free of the mesenteric bed as described in Section **2.3.2**. Arteries were then mounted onto two fine glass microcannulae (~ 100 – 150 μm tip diameter) in a small vessel pressure myograph (see Section **2.3.3**), and were continuously superfused with warm (37 °C), oxygenated (95% O_2, 5% CO_2) Krebs Henseleit solution. Intraluminal pressure of the artery was raised to 60 mmHg and maintained at this level without further intraluminal perfusion. In some arteries the endothelium was removed by the method described in Section **2.3.5**. After an equilibration period of 60 min, the general protocol (see Section **2.3.5**) was performed on all arteries prior to carrying out the experimental protocols described below.

6.2.2 Experimental protocols

6.2.2.1 Vascular responsiveness of arteries from coronary artery ligation and sham-operated rats

To assess vascular responsiveness of small mesenteric arteries from CAL and sham-operated rats to adrenoceptor stimulation, cumulative concentration response curves (CRC) to phenylephrine (PE; 1 x 10^{-9} to 3 x 10^{-5} M) were constructed in endothelium-intact (n=8) and endothelium-denuded (n=6) arteries. Following completion of CRCs, all vessels were repeatedly washed and allowed to re-equilibrate for at least 15 min before further experiments.

6.2.2.2 Effect of inducible nitric oxide synthase inhibition on vascular responsiveness

To investigate the role of iNOS in modulating vascular responsiveness, endothelium-intact mesenteric arteries were exposed to the selective iNOS inhibitor, *N*-(3-(Aminomethyl) benzyl) acetamidine dihydrochloride (1400W; 10^{-6} M, n=8) for 30 min prior to repeating cumulative CRCs to PE (1 x 10^{-9} to 3 x 10^{-5} M). In **Chapter 3**, it was revealed *in vitro* that 1400W inhibits iNOS without modifying the basal or agonist-stimulated activity of eNOS-derived NO. From these experiments, however, concentrations greater than 10^{-6} M were required to achieve significant inhibition of iNOS in thoracic aortae from rats with endotoxic shock. Thoracic aortae are considerably larger in size than the mesenteric arteries used in this chapter. For this reason, 1400W was used at a concentration of 10^{-6} M in experiments here. 1400W was present in the superfusate throughout the cumulative CRC.

6.2.2.3 Effect of superoxide quenching on vascular responsiveness

To investigate the role that superoxide plays in modulating vascular responsiveness, endothelium-intact mesenteric arteries were exposed to the cell permeable metalloporphyrin superoxide dismutase (SOD) mimetic, Mn [III] tetrakis [1-methyl-4-pyridyl] porphyrin (MnTMPyP; 10^{-4} M, *n*=8) for 30 min prior to repeating cumulative CRCs to PE (1 x 10^{-9} to 3 x 10^{-5} M). In **Chapter 4** of this thesis, experiments demonstrate that at a concentration of 10^{-4} M, MnTMPyP protects endothelium–derived NO from inactivation by superoxide in an *in vitro* model of oxidative stress, without having any non-selective effects on the bioavailability of eNOS or iNOS-derived NO, or the activity of the enzymes themselves. These experiments provide convincing evidence that MnTMPyP is an effective SOD mimetic, and support its use in experiments to investigate the role of superoxide in modulating vascular function in small mesenteric arteries from rats following CAL. MnTMPyP (10^{-4} M) was present in the superfusate throughout the cumulative CRC.

6.2.2.4 Effect of combined inducible nitric oxide synthase inhibition and superoxide quenching on vascular responsiveness

To further investigate the role of iNOS and superoxide in modulating vascular responsiveness, endothelium-intact mesenteric arteries were exposed to the iNOS inhibitor, 1400W (10^{-6} M) and the SOD mimetic, MnTMPyP (10^{-4} M) for 30 min prior to repeating cumulative CRC's to PE (1 x 10^{-9} to 3 x 10^{-5} M, n=8). Both drugs were present in the superfusate throughout the CRC.

6.2.2.5 Effect of nitric oxide synthase substrate on vascular responsiveness

To investigate the effect of the NOS substrate, L-arginine, on vascular responsiveness, endothelium-denuded mesenteric arteries were exposed to L-arginine (10^{-3} M, n=6) for 30 min prior to repeating cumulative CRCs to PE (1 x 10^{-9} to 3 x 10^{-5} M). A concentration of 10^{-3} M was chosen, since this concentration has been shown to result in a 15-fold increase in the EC_{50} concentration for norepinephrine in aortic rings from lipopolysaccharide-treated rats (Schott *et al.*, 1993). L-arginine was present in the superfusate throughout the CRC

6.2.2.6 Assessment of endothelium-dependent and endothelium-independent vascular relaxations in arteries from coronary artery ligation and sham-operated rats in the presence and absence of the SOD mimetic, MnTMPyP

To assess endothelium-dependent relaxations, ACh-mediated relaxations were measured in endothelium-intact PE-constricted small mesenteric arteries CAL and sham-operated rats. A submaximal concentration of PE (~ EC_{50}), as determined from PE CRCs, was used to induce arterial tone. Cumulative CRCs to ACh (1 x 10^{-10} to 3 x 10^{-6} M, n=7) were then obtained in the presence and absence of the SOD mimetic MnTMPyP (10^{-4} M, n=6).

To assess endothelium-independent relaxations, sodium nitroprusside (SNP)-mediated relaxations were measured in endothelium-denuded PE-constricted small mesenteric arteries CAL and sham-operated rats. As with ACh relaxations, a

submaximal concentration of PE (~ EC_{50}), as determined from PE CRCs, was used to induce arterial tone. Cumulative CRCs to SNP (1×10^{-9} to 3×10^{-5} M, n=7) were then obtained in the presence and absence of the SOD mimetic MnTMPyP (10^{-4} M, n=7).

Arteries were treated with MnTMPyP for 30 min prior to and throughout the duration of the experiments.

6.2.3 Preparation of drugs

Phenylephrine hydrochloride, acetylcholine chloride, sodium nitroprusside and L-arginine were diluted in Krebs Henseleit solution to give a stock solution of 10^{-1} M and frozen (-20 °C) in aliquots until use on day of experiment. *N*-(3-(Aminomethyl) benzyl acetamidine dihydrochloride (1400W) was diluted in saline (0.9% NaCl) under argon to give a stock solution of 10^{-3} M. Aliquots were then frozen (-20 °C) and stored under argon. Dilutions were made in Krebs Henseleit solution. Mn [III] tetrakis [1-methyl-4-pyridyl] porphyrin (MnTMPyP) and diluted in Krebs Henseleit solution immediately prior to experimentation.

6.2.4 Data Analysis

All results were expressed as means ± s.e.mean. Cumulative CRCs to PE were measured as percentages of maximal constrictions to KCl. ACh and SNP cumulative CRCs were measured as percentage relaxations of PE-induced tone. Where maximal values were obtained for cumulative CRCs, the negative logarithm of the agonist concentration that results in a half-maximal constriction or relaxation (pD_2) was calculated by nonlinear regression using GraphPad Prism software (Version 3.0). Two-tailed t-tests, one-way analysis of variance (ANOVA) with Bonferroni post-test for multiple comparisons and two-way repeated measures ANOVA were used as indicated in the text. $P<0.05$ was considered to be statistically significant.

6.3 Results

6.3.1 Effect of left coronary artery ligation

As discussed in Section **5.3** of **Chapter 5**, CAL rats had significantly greater heart weights than those of sham-operated rats, indicating that hearts from CAL rats had undergone compensatory hypertrophy as a consequence of left ventricular (LV) infarction. Furthermore, LV end-diastolic pressures were significantly elevated when compared with sham-operated rats, which is an indicator of impaired LV function. Infarct sizes for hearts from CAL rats averaged 60 ± 3 % of the LV free wall. Furthermore, there was histological evidence for mature scar formation within the infarcted zone (see **Chapter 5**, ***Figure 5.1a***). These results suggest that rats had developed CHF as a consequence of CAL.

6.3.2 KCl, phenylephrine maximal constrictions and endothelial integrity

There were no significant differences between endothelium-intact and endothelium-denuded small mesenteric arteries from CAL and sham-operated groups with respect to internal diameters at rest and in response to KCl (60 mM, ***Table 6.1***). However, maximal constrictions to PE were significantly greater in endothelium-denuded than in endothelium-intact small mesenteric arteries from both CAL and sham-operated rats ($P<0.05$, one-way ANOVA with Bonferroni post-test, ***Table 6.1***). All endothelium-intact small mesenteric arteries studied had functional endothelium (CAL, 101.3 ± 4%; sham-operated, 95.9 ± 3% ACh relaxation of PE-induced tone) and no significant differences in maximal relaxations were found between CAL and sham-operated groups (***Table 6.1***). Denudation of arteries was deemed successful as relaxations to ACh were all but abolished (CAL, 3.8 ± 2%; sham-operated, 2.7 ± 1% ACh relaxation of PE-induced tone, ***Table 6.1***).

Treatment	*Sham*		*CAL*	
	Internal diameter (μm)		**Internal diameter** (μm)	
	+end	**-end**	**+end**	**-end**
	(*n*=8)	(*n*=8)	(*n*=11)	(*n*=9)
Resting	319±15	310±13	330±9	310±10
60 mM **KCl**	118±15	105±10	125±9	110±10
10^{-5} M **PE**	117±5*	88±10	120±5**	85±5
10^{-5} M **ACh**	305±15	107±20	335±10	95±5

Table 6.1 *Internal diameters (μm) of endothelium-intact (**+end**) and endothelium–denuded (**-end**) small mesenteric arteries from coronary artery ligation (**CAL**) and sham-operated (**Sham**) rats. Internal diameters of arteries at rest, after exposure to **KCl**, phenylephrine (**PE**) and acetylcholine (**ACh**) (arteries pre-contracted with 10^{-5} M PE) are given as mean values ± s.e.mean. * $P<0.05$ compared with respective value in sham-operated endothelium-denuded arteries, ** $P<0.01$ compared with respective values in CAL endothelium-denuded arteries (two-tailed unpaired t-test).*

6.3.3 Assessment of vascular responsiveness to adrenoceptor stimulation in coronary artery ligation and sham-operated rats

In both endothelium-intact and endothelium-denuded small mesenteric arteries from CAL and sham-operated rats, cumulative additions of PE (1×10^{-9} to 3×10^{-5} M) resulted in concentration-dependent constrictions (***Figures 6.1, 6.2***). In endothelium-intact arteries from CAL rats, cumulative CRCs to PE were shifted significantly to the left when compared with responses in sham-operated groups, indicating that arteries from CAL rats were more responsive to PE than those from sham-operated rats ($P<0.05$, two-way ANOVA, ***Figure 6.1***). Indeed, pD_2 values for PE CRCs in arteries from CAL rats were significantly greater than those in sham–operated rats (***Table 6.2***). Furthermore, maximal constrictions to PE were significantly greater in

arteries from CAL rats when compared with constrictions in arteries from sham-operated rats (***Figure 6.1***, ***Table 6.2***). In endothelium-denuded arteries no significant differences were found between CAL and sham-operated rats with respect to PE CRCs (***Figure 6.2***). In addition, there were no significant differences between pD_2 values (***Table 6.2***) and maximal % constrictions (***Figure 6.2***, ***Table 6.2***).

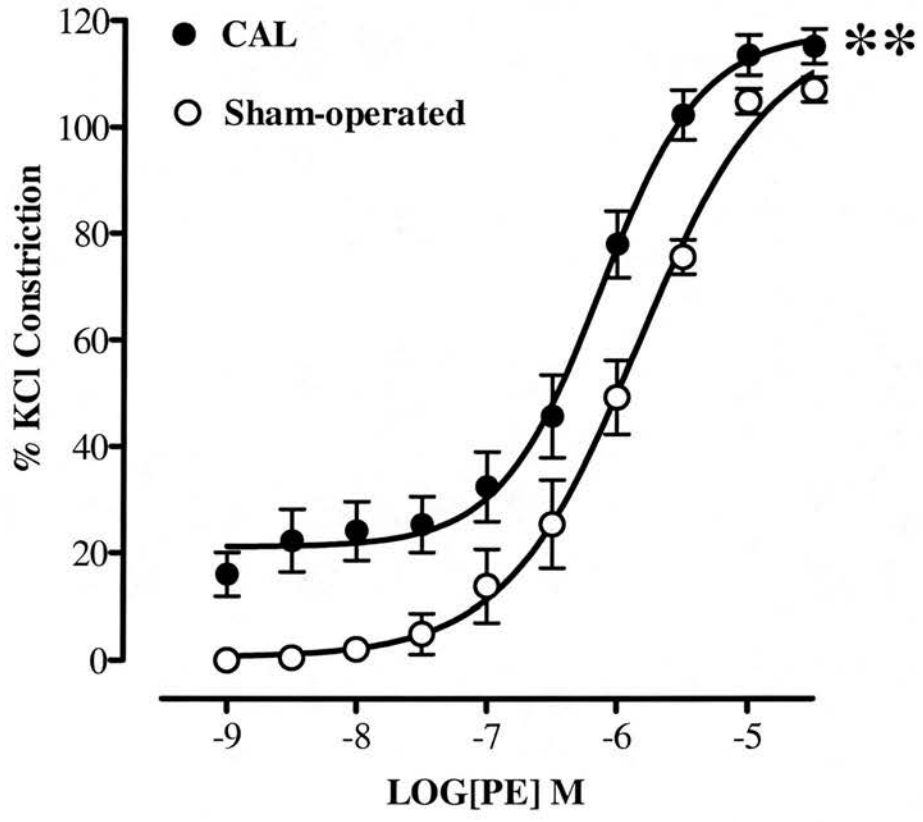

Figure 6.1 *Cumulative concentration response curves (CRC) showing contractile responses to phenylephrine (**PE**; 1 x 10^{-9} to 3 x 10^{-5} M) in endothelium-intact (n=8) small mesenteric arteries from coronary artery ligation (**CAL**) and sham-operated rats (n=8) 6 weeks post-surgery. Values are given as means ± s.e.mean. ** P<0.01 compared with CRCs in sham-operated arteries (two-way ANOVA).*

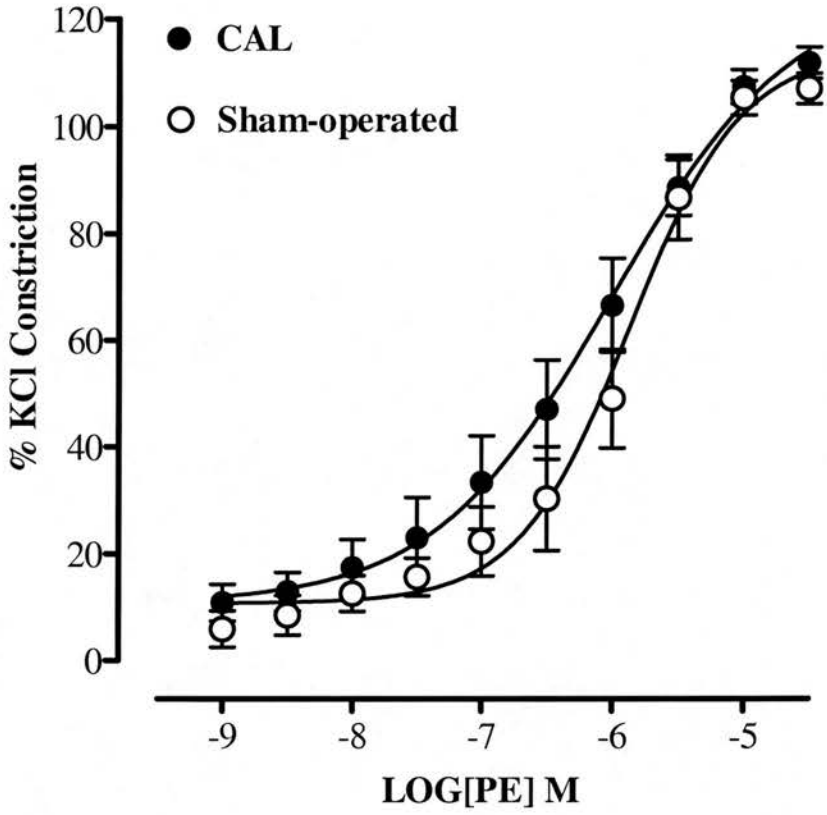

Figure 6.2 *Cumulative concentration response curves showing contractile responses to phenylephrine (**PE**; 1 x 10^{-9} to 3 x 10^{-5} M) in endothelium-denuded (n=6) small mesenteric arteries from coronary artery ligation (**CAL**) and sham-operated rats 6 weeks post-surgery. Values are given as means ± s.e.mean. P>0.05, two-way ANOVA.*

Treatment	*Sham*		*CAL*	
	pD_2 (n>6)	Max (%) (n>6)	pD_2 (n>6)	Max (%) (n>6)
Control ***+end***	5.9±0.1	105±2	6.3±0.1*	115.2±3#
Control ***-end***	5.9±0.2	110±4	6.3±0.3	111.8±4
+ 1400W	5.9±0.1	108.4±3	5.9±0.1✝	108.2±4
+ MnTMPyP	5.7±0.1	112.8±4	5.8±0.1✝	103.3±5
+1400W +MnTMPyP	5.7±0.1	113.7±4	5.7±0.2✝	103.3±3

Table 6.2 *pD_2 values and maximal (**Max**) percentage constrictions for phenylephrine cumulative concentration response curves (CRC) in endothelium-intact (**+end**) and endothelium-denuded (**-end**) small mesenteric arteries from coronary artery ligation (**CAL**) and sham-operated (**Sham**) rats. Also shown are pD_2 values and Max constrictions for PE CRCs in endothelium-intact small mesenteric arteries in presence of 1400W (10^{-6} M) and MnTMPyP (10^{-4} M) either on their own or together. All values are given as mean values ± s.e.mean. * $P<0.05$ compared with pD_2 value in sham endothelium-intact arteries (one-way ANOVA with Bonferroni post-test), # $P<0.05$ compared with max value in control endothelium-intact arteries from sham-operated rats (two-tailed unpaired t-test), ✝ $P<0.05$ as compared with pD_2 values in control endothelium-intact arteries from coronary artery ligation rats (one-way ANOVA with Bonferroni post-test).*

6.3.4 Effect of 1400W and MnTMPyP on vascular responsiveness

Treatment of endothelium-intact arteries from CAL rats with 1400W (10^{-6} M) or MnTMPyP (10^{-4} M) shifted PE CRCs to the right with respect to responses in untreated arteries ($P<0.05$ for both, two-way ANOVA, ***Figure 6.3***), indicating a reduction in responsiveness to PE. Indeed, pD_2 values were significantly decreased in the presence of 1400W or MnTMPyP when compared with untreated arteries (***Table 6.2***). Responses to PE in arteries from CAL rats treated with 1400W or MnTMPyP were not significantly different from those in sham-operated arteries (***Figure 6.3***, ***Table 6.2***). Responses to PE in endothelium-intact arteries from sham-operated rats were unaffected by 1400W (10^{-6} M) or MnTMPyP (10^{-4} M) (***Figure 6.4***, ***Table 6.2***).

In a similar fashion to those arteries treated with 1400W (10^{-6} M) or MnTMPyP (10^{-4} M) alone, combined treatment with both drugs resulted in a significant reduction in responsiveness of arteries from CAL rats to PE ($P<0.01$, two-way ANOVA, ***Figure 6.3***). Indeed, pD_2 values were significantly decreased in the presence of 1400W and MnTMPyP when compared with untreated arteries (***Table 6.2***). However, no differences were found when compared with responses in arteries treated with 1400W alone. In arteries from sham-operated rats, combined treatment had no significant effect on responses to PE (***Figure 6.4***, ***Table 6.2***).

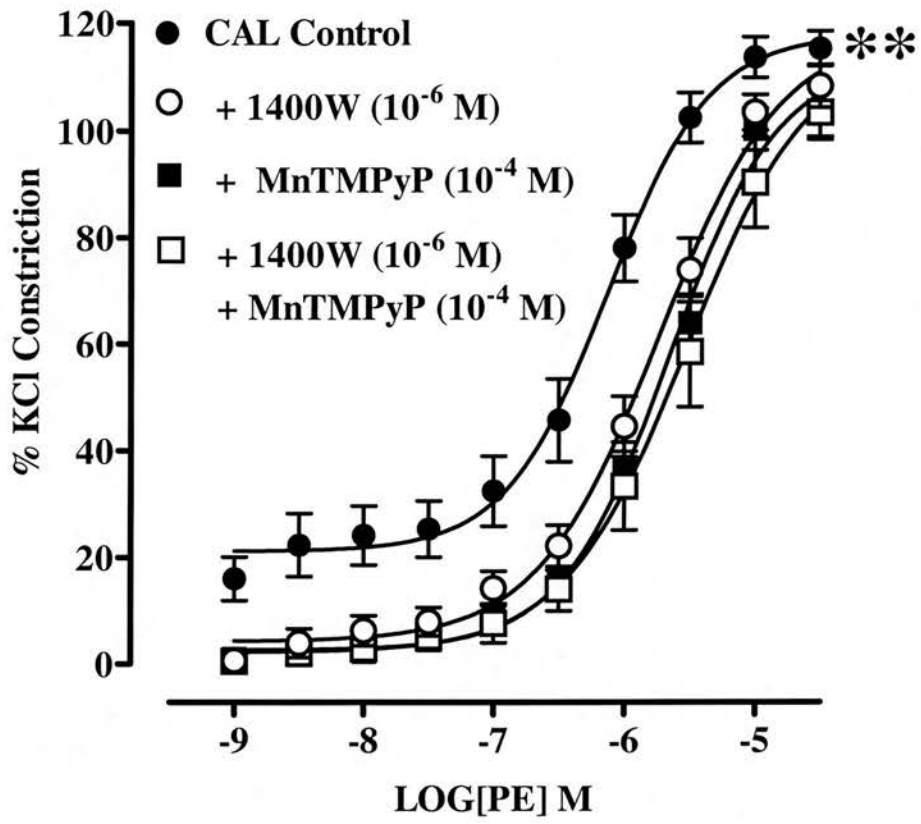

Figure 6.3 *Effect of* ***1400W*** *(10^{-6} M) and* ***MnTMPyP*** *(10^{-4} M), on their own or together on cumulative concentration response curves (CRC) to phenylephrine (**PE**; 1 x 10^{-9} to 3 x 10^{-5} M) in endothelium-intact small mesenteric arteries from coronary artery ligation rats (**CAL**; n=8) 6 weeks post-ligation. Values are given as means ± s.e.mean. ** P<0.01 for CRCs in untreated arteries compared with CRCs in 1400W, MnTMPyP-treated arteries (two-way ANOVA).*

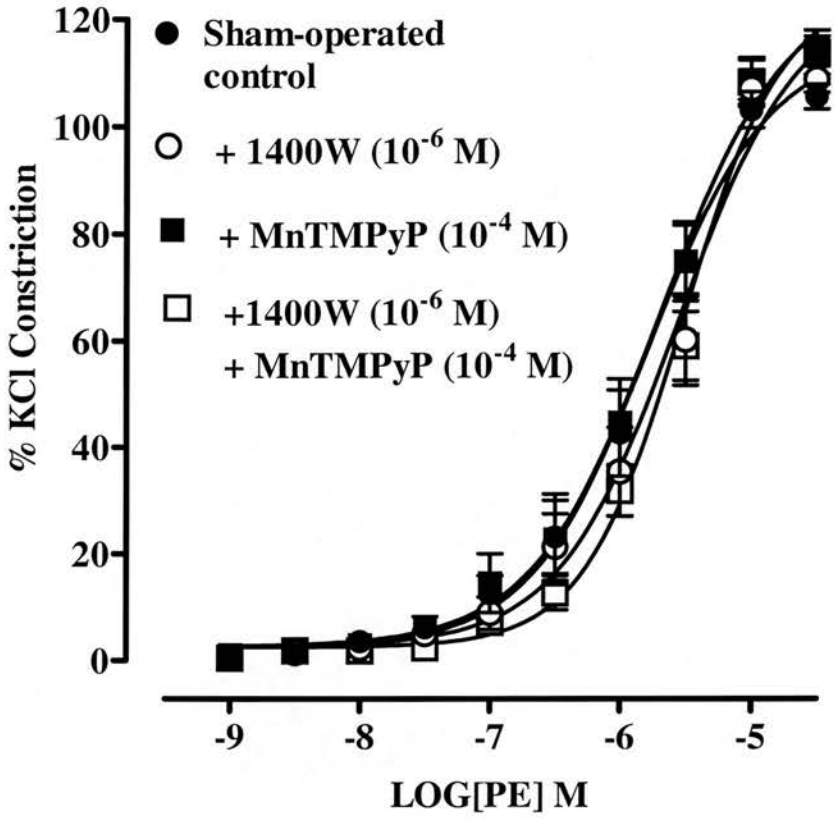

Figure 6.4 *Effect of* ***1400W*** *(10^{-6} M) and* ***MnTMPyP*** *(10^{-4} M), on their own or together on cumulative concentration response curves to phenylephrine (**PE**; 1 x 10^{-9} to 3 x 10^{-5} M) in endothelium-intact small mesenteric arteries from sham-operated rats (n=8) 6 weeks post-surgery. Values are given as means ± s.e.mean.*

6.3.5 Effect of L-arginine on vascular responsiveness

Treatment of endothelium-denuded arteries from CAL rats with the NOS substrate, L-arginine (10^{-3} M), for 30 min shifted PE CRCs to the right with respect to untreated arteries ($P<0.05$, two-way ANOVA, ***Figure 6.5***), indicating that endothelium-denuded arteries are less responsive to PE in the presence of L-arginine. pD_2 values could not be calculated as maximal constrictions were not reached. L-arginine had no significant effect on PE responses in arteries from sham-operated rats (***Figure 6.6***).

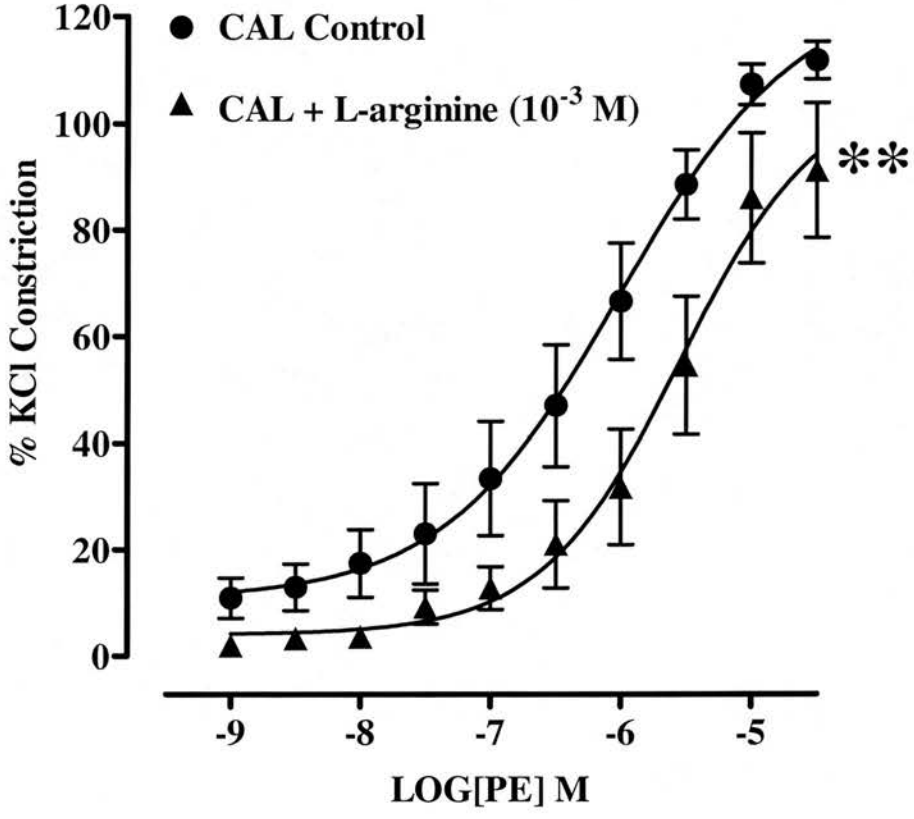

Figure 6.5 *Effect of L-arginine (10^{-3} M) on cumulative concentration response curves (CRC) to phenylephrine (**PE**; 1 x 10^{-9} to 3 x 10^{-5} M) in endothelium-denuded small mesenteric arteries from coronary artery ligation rats (**CAL**; n=6) 6 weeks post-ligation. Values are given as means ± s.e.mean. ** P<0.01 compared with CRCs in untreated arteries (two-way ANOVA).*

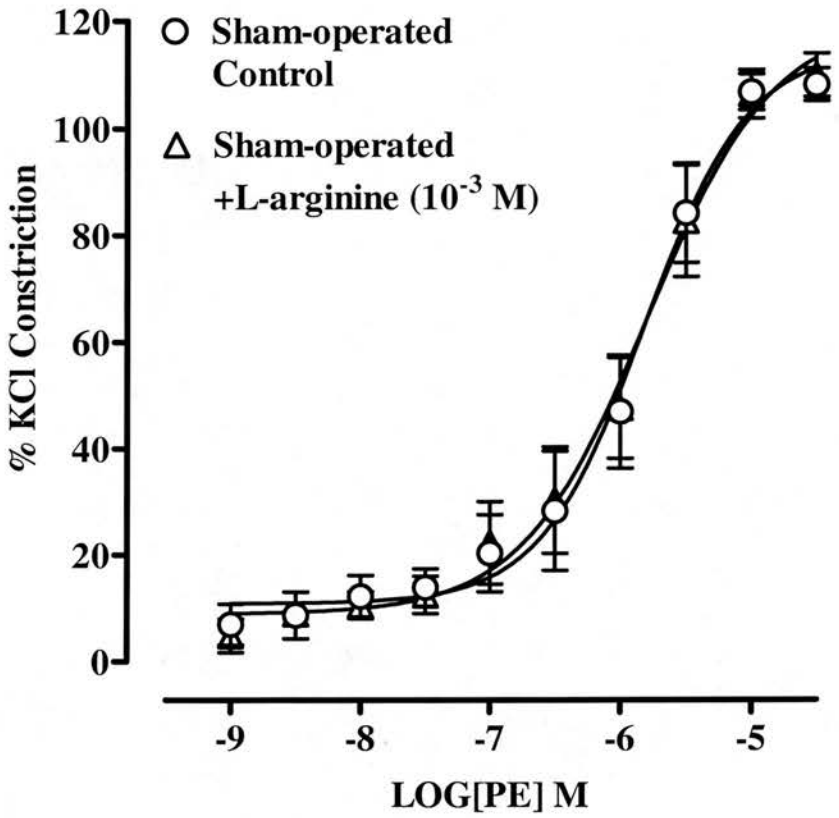

Figure 6.6 *Effect of L-arginine (10^{-3} M) on cumulative concentration response curves to phenylephrine (**PE**; 1 x 10^{-9} to 3 x 10^{-5} M) in endothelium-denuded small mesenteric arteries from sham-operated rats (n=6) 6 weeks post-surgery. Values are given as means ± s.e.mean. P>0.05, two-way ANOVA.*

6.3.6 Assessment of endothelium-dependent and endothelium–independent vascular relaxations in coronary artery ligation and sham-operated rats. Effect of superoxide quenching

Following induction of PE (~ EC_{50})-induced tone (CAL, 49.1 ± 2.3%; sham-operated, 52.6 ± 2.4% of maximal PE constriction) in endothelium-intact arteries from CAL and sham-operated rats, cumulative additions of ACh (1×10^{-10} to 3×10^{-6} M) resulted in concentration-dependent relaxations (***Figure 6.7***). pD_2 values for cumulative CRCs in arteries from CAL rats were significantly lower than those in sham–operated rats, indicating that endothelium-dependent relaxations were blunted in small mesenteric arteries from CAL rats (***Table 6.3***). Maximum relaxations to ACh were achieved in most arteries at a concentration of 3×10^{-6} M and no significant differences were found between CAL and sham-operated groups (***Table 6.3***).

Treatment of PE-constricted (57.5 ± 3.2% of maximal PE constriction) endothelium-intact arteries from CAL rats with MnTMPyP (10^{-4} M) significantly increased pD_2 values for ACh CRCs when compared with values in untreated arteries, indicating an increase in responsiveness to ACh (***Figure 6.8, Table 6.3***). Treatment of PE-contracted (53.9 ± 3.5% of maximal PE constriction) endothelium-intact arteries from sham-operated rats with MnTMPyP had no significant effect on ACh CRCs (***Figure 6.9, Table 6.3***).

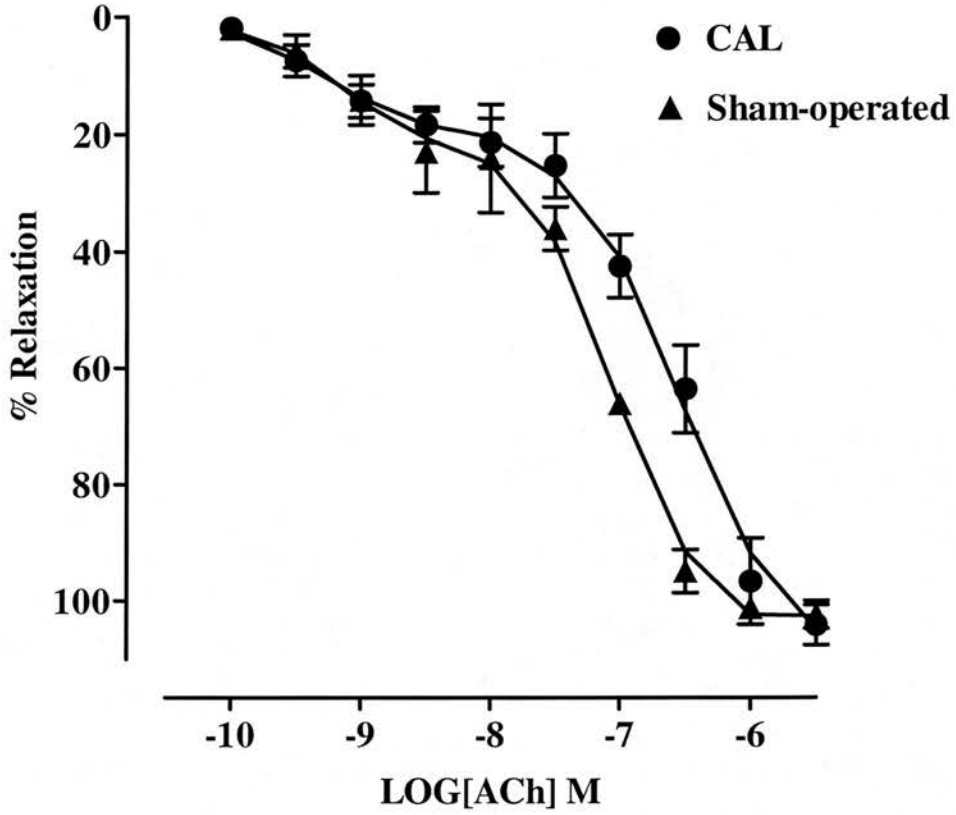

Figure 6.7 *Cumulative concentration response curves showing endothelium-dependent relaxations to acetylcholine (**ACh**; 1 x 10^{-10} to 3 x 10^{-6} M) in phenylephrine (~ EC_{50})-constricted endothelium-intact small mesenteric arteries from coronary artery ligation (**CAL**) and sham-operated rats (n=7) 6 weeks post-surgery. Values are given as means ± s.e.mean. P>0.05, two-way ANOVA.*

Treatment	*Sham*		*CAL*	
	pD_2 (n>6)	Max (%) (n>6)	pD_2 (n>6)	Max (%) (n>6)
ACh Control	7.9±0.1	102.3±2.2	7.4±0.1*	104.1±3.5
ACh +MnTMPyP	-	94.5±8.3	7.9±0.1✝	102.9±1.7
SNP Control	-	97.1±1	7.3±0.2	104.9±1.4
SNP +MnTMPyP	-	98.9±1	7.4±3	102.8±3

Table 6.3 ***pD_2*** *values and maximal* ***(Max)*** *percentage relaxations for acetylcholine* ***(ACh)*** *and sodium nitroprusside* ***(SNP)*** *cumulative concentration response curves (CRC) in phenylephrine (~ EC_{50})-constricted endothelium-intact and endothelium-denuded small mesenteric arteries, respectively, from coronary artery ligation* ***(CAL)*** *and sham-operated* ***(Sham)*** *rats, in the presence and absence of MnTMPyP (10^{-4} M). pD_2 values could not be calculated for CRCs to ACh in the presence of MnTMPyP or for SNP CRCs in the absence and presence of MnTMPyP, because maximal values were not reached. All values are given as mean values ± s.e.mean. * $P<0.05$ compared with pD_2 values for ACh CRCs in control endothelium-intact arteries from sham-operated rats, ✝ $P<0.05$ compared with pD_2 values for ACh CRCs in control endothelium-intact arteries from CAL rats (one-way ANOVA with Bonferroni post-test).*

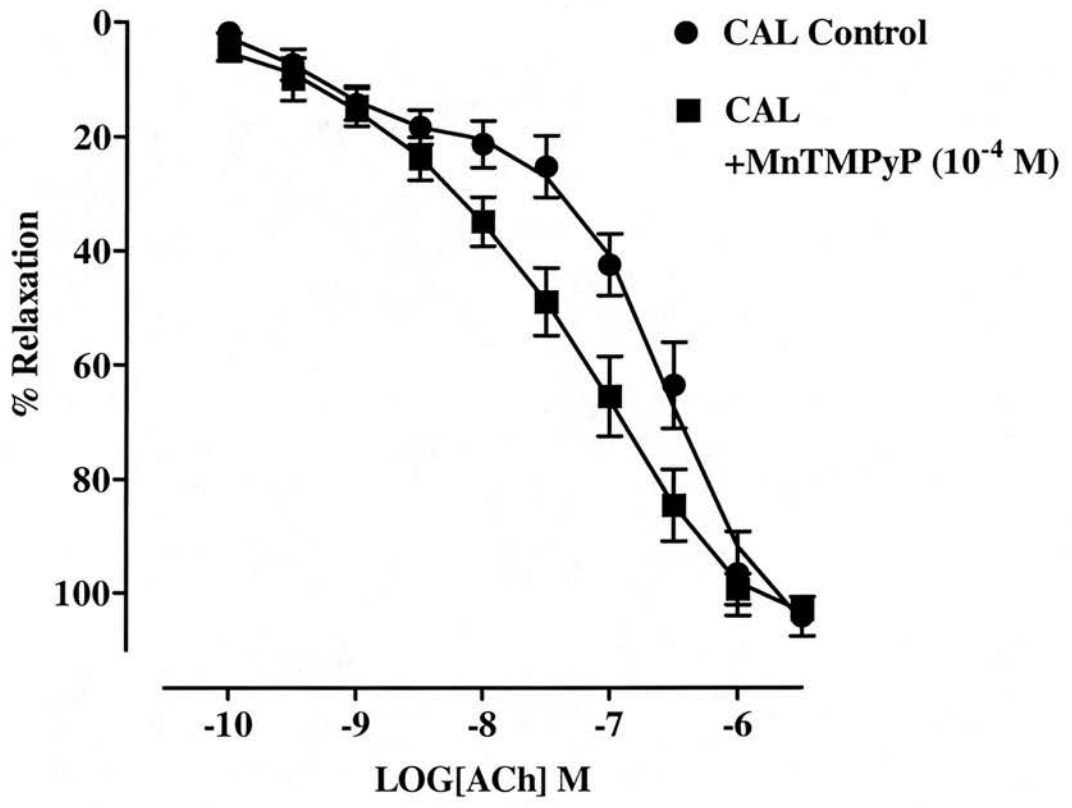

Figure 6.8 *Cumulative concentration response curves showing endothelium-dependent relaxations to acetylcholine (**ACh**; 1 x 10^{-10} to 3 x 10^{-6} M) in phenylephrine (~ EC_{50})-constricted endothelium-intact small mesenteric arteries from coronary artery ligation rats (**CAL**; n≥6) 6 weeks post-surgery, in the presence and absence of MnTMPyP (10^{-4} M). Values are given as means ± s.e.mean*

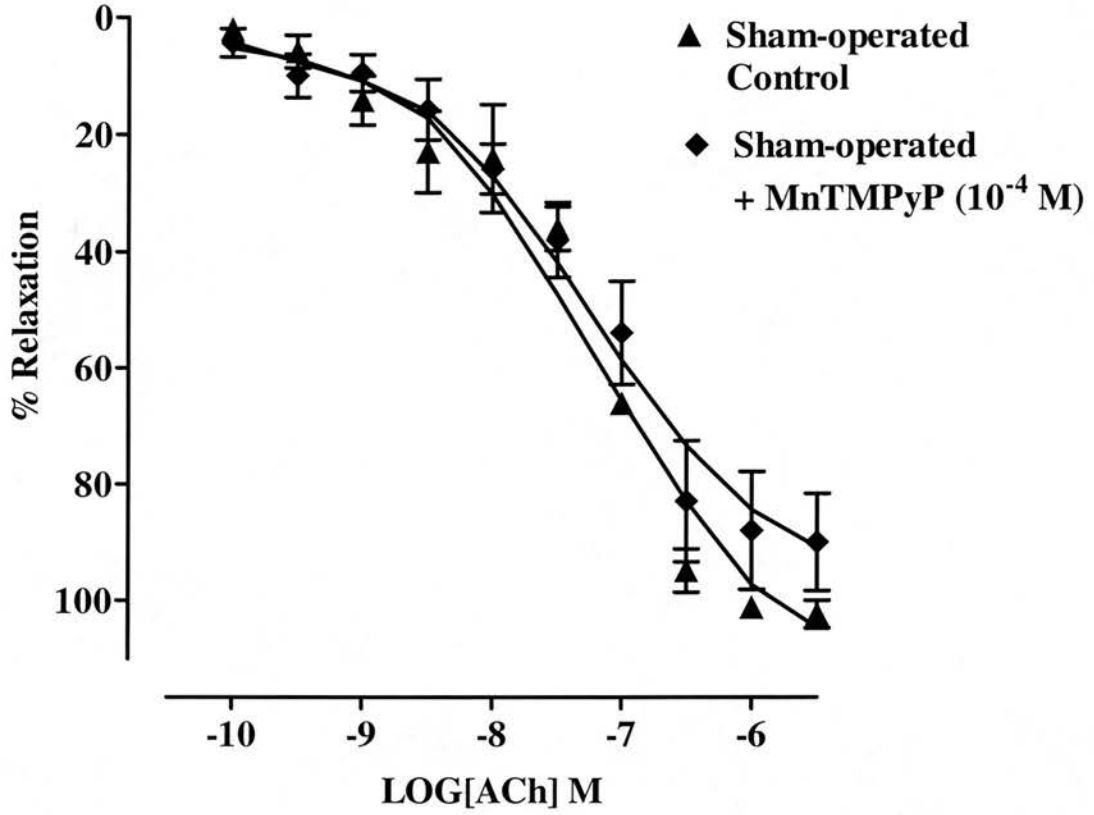

Figure 6.9 *Cumulative concentration response curves showing endothelium-dependent relaxations to acetylcholine (**ACh**; 1 x 10^{-10} to 3 x 10^{-6} M) in phenylephrine (~ EC_{50})-constricted endothelium-intact small mesenteric arteries from sham-operated rats (n≥6) 6 weeks post-surgery, in the presence and absence of MnTMPyP (10^{-4} M). Values are given as means ± s.e.mean. P>0.05, two-way ANOVA.*

Following induction of PE (~ EC_{60})-induced tone (CAL, 57.3 ± 6.5%; sham-operated, 53.8 ± 4.6% of maximal PE constriction) in endothelium-denuded arteries from CAL and sham-operated rats, cumulative additions of SNP (1 x 10^{-9} to 3 x 10^{-6} M) resulted in concentration-dependent relaxations (***Figure 6.10***, ***Table 6.3***). There were no significant differences between SNP CRCs in CAL and sham-operated rats

(***Figure 6.10***). MnTMPyP had no significant effect on SNP cumulative CRCs in PE-constricted (CAL, 53.4 ± 5.4%; sham-operated, 56.7 ± 5% of maximal PE constriction) arteries from either CAL or sham-operated rats (***Table 6.3***).

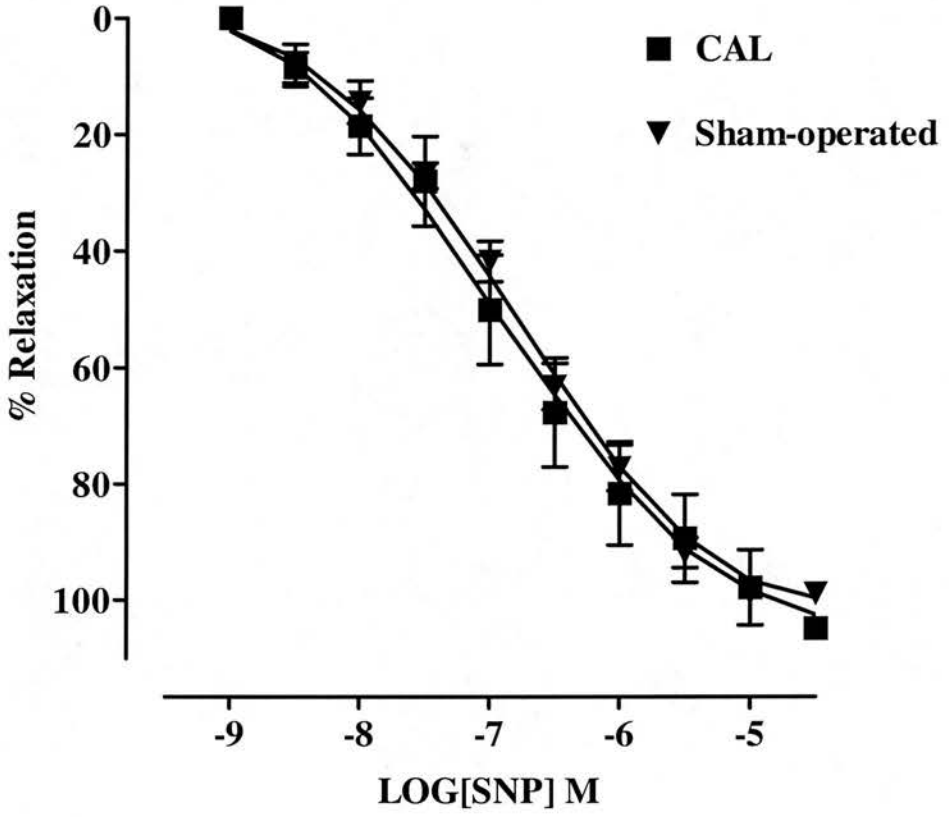

Figure 6.10 *Cumulative concentration response curves showing endothelium-independent relaxations to sodium nitroprusside (**SNP**; 1 x 10^{-9} to 3 x 10^{-5} M) in phenylephrine (~ EC_{50})-constricted endothelium-intact small mesenteric arteries from coronary artery ligation (**CAL**) and sham-operated rats (n=7) 6 weeks post-surgery. Values are given as means ± s.e.mean. P>0.05, two-way ANOVA.*

6.4 Discussion

In the previous chapter, immunohistochemical studies demonstrated that iNOS was expressed in endothelial cells, VSM cells, and in the adventitia of small mesenteric arteries from rats with CHF, but not in arteries from sham-operated rats. However, despite the presence of iNOS, functional studies in the present chapter demonstrate that endothelium-intact small mesenteric arteries from CHF rats were more responsive to PE than those from sham-operated rats. Hyperesponsiveness of endothelium-intact arteries from CHF rats was reversed by the selective iNOS inhibitor, 1400W and by the cell permeable metalloporphyrin SOD mimetic, MnTMPyP. Furthermore, supplementation of endothelium-denuded arteries from CHF rats with the NOS substrate, L-arginine, resulted in a significant reduction in responsivness to PE when compared with untreated arteries. Endothelium-dependent, but not endothelium-independent relaxations, were impaired in arteries from CHF rats when compared with relaxations in arteries from sham-operated rats. Furthermore, MnTMPyP restored endothelium-dependent relaxations. These results suggest that substrate deficient, iNOS-derived superoxide may be responsible for the vascular dysfunction associated with this model of CHF.

During endotoxemia, expression of iNOS in the vasculature, and the subsequent production of NO, plays an important role in the vascular hyporeactivity to vasoconstrictors (see **Chapter 3**). Therefore, in this model of CHF, increased production of NO from iNOS would be expected to reduce vascular responsiveness to PE. Somewhat paradoxically, endothelium-intact small mesenteric arteries from CHF rats were more responsive to PE than arteries from sham-operated rats. There were no significant differences between responses to PE in endothelium-denuded arteries from CHF or sham-operated rats, demonstrating that this vascular dysfunction is dependent on the presence of the endothelium. Basal NO from eNOS serves to dampen the effects of vasoconstrictors. One could speculate, therefore, that decreased basal release of NO is responsible for the hyperesponsivness to PE. Indeed, there is some evidence that basal release of NO from the endothelium may be impaired in CHF. A recent study demonstrated that flow-mediated dilatation was

abolished in peripheral resistance arteries in rats with CHF, suggesting that basal release of NO was impaired (Varin *et al.*, 1999). Similarly, Hirari *et al.* (1995) found that the hyperaemic response of hindquarter resistance arteries were impaired in rats with CHF.

To investigate the role that iNOS plays in modulating vascular function in this model of CHF the selective iNOS inhibitor, 1400W, and the NOS substrate, L-arginine were used. Garvey *et al.* (1997) demonstrated that 1400W is an irreversible inhibitor of iNOS that is at least 5000-fold more selective for purified human iNOS than eNOS. Furthermore, experiments in **Chapter 3** demonstrated that 1400W inhibited the activity of iNOS in isolated thoracic aortae from rats with endotoxic shock, without modifying the activity of eNOS, providing convincing evidence that 1400W is a selective inhibitor of iNOS. Experiments in this chapter show, somewhat surprisingly, that inhibition of iNOS with 1400W reversed rather than potentiated the hyperresponsiveness of small mesenteric arteries from CHF rats. These results suggest that induction of iNOS does not result in the expected increase in NO generation. Instead, expression of the enzyme appears to be a major contributory factor in the hyperresponsive nature of endothelium-intact CHF arteries. In experimental endotoxic shock, addition of the NOS substrate, L-arginine, to isolated blood vessels increases NO production from iNOS and potentiates hyporesponsiveness to vasoconstrictors (Julou-Schaeffer *et al.*, 1990). Experiments here demonstrate that supplementation of endothelium-denuded small mesenteric arteries from CHF rats, but not sham-operated rats, with a supramaximal concentration of L-arginine results in a reduction in responsiveness to PE, likely through production of NO from iNOS. These results suggest that although iNOS is present in small mesenteric arteries from CHF rats, it is unable to synthesise NO because there is insufficient substrate. As discussed in Section **1.3.3**, the synthesis of NO by NOS requires a tightly coupled electron transfer from the flavin domain of NOS to haem in the oxygenase domain, which in turn is tightly coupled with the reduction of oxygen and subsequent oxidation of L-arginine. Uncoupled electron transfer occurs in most oxygenase enzymes and refers to a diversion or loss of electrons that would be otherwise used to generate a product from a substrate

(Griffith & Stuehr, 1995). Oxygen is the usual acceptor of the stray electrons, giving rise to superoxide. Therefore, with respect to NOS, the main product will certainly be NO, however, some electrons may become uncoupled from its domains resulting in the formation of superoxide. It has been demonstrated, however, that in the presence of low concentrations of L-arginine or in its absence, nNOS catalyses the uncoupled reduction of oxygen, leading to the production of large quantities of superoxide (Klatt *et al.*, 1993a). It has since been shown that iNOS can also produce superoxide when deficient in L-arginine (Xia *et al.*, 1998a). With no substrate to accept the electrons from oxygen, the production of superoxide from NOS is self-explanatory. Therefore, in this model of CHF, it is possible that a deficiency in L-arginine will not only prevent iNOS from generating NO but will also result in the enzyme producing superoxide. Increased scavenging of NO by superoxide would result in a reduction in the bioavailability of basal endothelium-derived NO, which may explain the marked increase in responsiveness of endothelium-intact arteries from CHF rats to PE.

Plasma malondialdehyde, a marker of oxidative stress, is increased in patients with CHF (Belch *et al.*, 1991; Diaz-Velez *et al.*, 1996; Bauersachs *et al.*, 1999). To determine if increased superoxide production plays a role in modulating vascular function in this model of CHF, the cell permeable metalloporphyrin SOD mimetic, MnTMPyP (see **Chapter 4**), was used. In a similar fashion to 1400W, MnTMPyP reversed the hyperesponsiveness of endothelium-intact small mesenteric arteries from CHF rats. This implies that mesenteric arteries from CHF rats are indeed generating increased amounts of superoxide, which is responsible for the marked elevation in responsiveness to PE. These findings are consistent with recent studies demonstrating increased superoxide production by the peripheral vasculature from rats with CHF following CAL (Bauersachs *et al.*, 1999; Varin *et al.*, 1999). Despite evidence demonstrating increased levels of superoxide in CHF, the precise source is unclear. Some studies suggest that a deficiency in antioxidant systems is responsible. Several studies have demonstrated a reduction in antioxidants, such as glutathione peroxidase, vitamin E, catalase and SOD, both in the failing heart (Hill & Singal, 1996; Prasad *et al.*, 1996) and the systemic circulation (Nishiyama *et al.*, 1998; Yucel *et al.*, 1998). Other studies suggest that increased synthesis of superoxide is

responsible. In rats with CHF following CAL, thoracic aortae were shown to produce increased amounts of superoxide that was probably derived from NADH/NADPH oxidases (Bauersachs *et al.*, 1999). Furthermore, autoxidation of catecholamines, increased arachidonate metabolism and inflammatory cytokines have all been suggested as possible sources of superoxide in CHF (Givertz & Colucci, 1998). In the present study, however, both inhibition of iNOS and superoxide quenching reverses the hyperesponsiveness to PE suggesting that iNOS is the source of superoxide in these arteries. Indeed, there were no significant differences between responses to PE in arteries treated with 1400W alone and those treated with both 1400W and MnTMPyP.

There is evidence that agonist-stimulated release of NO from the endothelium of the peripheral vasculature is impaired in clinical and experimental CHF. In rats with CHF following CAL, relaxations of isolated conductance arteries to ACh were impaired when compared with sham-operated control (Ontkean *et al.*, 1991; Teerlink *et al.*, 1994; Baggia *et al.*, 1997; Bauersachs *et al.*, 1999). In contrast, relaxations to ACh in resistance arteries during experimental CHF appear to be normal (Baggia *et al.*, 1997; Prior *et al.*, 1998). These studies suggest that NO-mediated relaxations may not be universally impaired throughout the arterial circulation. However, Drexler & Lu, (1992) demonstrated that hindquarter resistance arteries in rats with large infarctions following CAL were less responsive to ACh than control rats. Furthermore, impaired peripheral vasodilator responses to muscarinic agonists have been observed extensively in the forearm resistance vessels of patients with CHF of varying pathologies (Drexler *et al.*, 1992; Kubo *et al.*, 1991; Katz *et al.*, 1992; Nakamura *et al.*, 1996; Carville *et al.*, 1998). Consistent with these studies, experiments in this chapter reveal that small mesenteric arteries from rats with CHF are less responsive to ACh when compared with responses in arteries from sham-operated rats, suggesting that agonist-stimulated activity of NO is impaired in these arteries.

The underlying mechanisms responsible for impaired agonist-stimulated activity of NO in CHF may be complex and have not yet been clarified. Some (Zelis *et al.*,

1970; Nasa *et al.*, 1996; Nakamura *et al.*, 1996; Carville *et al.*, 1998) but not all studies (Drexler *et al.*, 1992; Baggia *et al.*, 1997; Bauersachs *et al.*, 1999) have demonstrated that endothelium-independent relaxations may also be impaired in CHF, suggesting that abnormalities of the VSM may be responsible for impaired relaxations to ACh. In this chapter, however, experiments reveal that endothelium-independent relaxations to the NO donor, SNP, are not attenuated in small mesenteric arteries from CHF rats, implying that endothelium-dependent relaxations are selectively impaired in these arteries. Other potential mechanisms for impaired agonist-stimulated activity of NO include down regulation of eNOS (Comini *et al.*, 1996; Smith *et al.*, 1996; Wang *et al.*, 1997; Varin *et al.*, 1999), increased release of endothelium-dependent constriction factors (Kaiser *et al.*, 1989; Varin *et al.*, 1999) and impaired endothelial receptor-signal transduction pathways, ie. dysfunctional muscarinic receptor (Hirooka *et al.*, 1992). As discussed earlier, CHF is associated with increased levels of superoxide. Furthermore, earlier experiments in this chapter demonstrated that increased superoxide production might account for the marked increase in vascular responsiveness of small mesenteric arteries, possibly as a consequence of increased scavenging of basal endothelium-derived NO. Therefore, increased scavenging of NO by superoxide may also account for impaired responses to ACh. Indeed, subsequent experiments demonstrate that the SOD mimetic, MnTMPyP restored responsiveness of small mesenteric arteries to ACh, suggesting that increased superoxide is indeed responsible for impaired endothelium-dependent relaxations.

In **Chapter 4**, the pharmacological properties of MnTMPyP were investigated. As discussed in this chapter, recent studies have suggested that MnTMPyP may actually scavenge NO itself and directly inhibit the activity of both iNOS and eNOS (Pfeiffer *et al.*, 1998, MacKenzie *et al.*, 1999). However, experiments in **Chapter 4** provided convincing evidence that at a concentration of 10^{-4} M, MnTMPyP acts a SOD mimetic without modifying the activity of NO derived from iNOS or eNOS, or the enzymes themselves. Consistent with these findings, experiments in the present study demonstrate that MnTMPyP reduced responsiveness to PE in endothelium-intact small mesenteric arteries from CHF rats and had no significant effect on responses in

arteries from sham-operated rats. Furthermore, MnTMPyP increased responsiveness of endothelium-intact small mesenteric arteries from CHF rats to ACh and had no significant effect on responses in arteries from sham-operated rats. The findings of the experiments in this chapter and those from **Chapter 4** provide convincing evidence that the effects of MnTMPyP in the present study are a direct consequence of its SOD mimetic properties.

The findings of this chapter present an interesting new facet to the impact of iNOS in CHF. In this model of CHF, instead of generating large quantities of NO, iNOS appears to be generating superoxide, perhaps because of a deficiency in its substrate, L-arginine. Moreover, this increase in superoxide production is responsible for the hyperresponsive nature of endothelium-intact small mesenteric arteries from rats with CHF. The precise mechanism and time course by which superoxide results in arteries being hyperresponsive is unclear from these experiments alone. However, the fact that the hypereactivity is dependent on the endothelium suggests that increased scavenging of basal, eNOS-derived, NO by superoxide is responsible. In addition to impaired basal release of NO, experiments also show that ACh-mediated endothelium-dependent relaxations are impaired in arteries from rats with CHF. Moreover, MnTMPyP increased responsiveness to ACh suggesting that increased scavenging of agonist-stimulated NO by superoxide was responsible for this dysfunction. While it remains to be established if this study mirrors clinical CHF, these findings may represent an important mechanism for the endothelial dysfunction and raised PVR associated with CHF.

Chapter 7

Investigation of the role of inducible nitric oxide synthase and superoxide in modulating vascular function of conductance arteries from rats with chronic heart failure

7.1 Introduction

The elastic properties of conductance arteries are important in minimising both the load on the left ventricle and the rise in arterial pressure during systole (see Section **1.2.3**). Therefore, although conductance arteries play a minimal role in modulating peripheral vascular resistance, they play an important role in the overall mechanical efficiency of the cardiovascular system.

Vascular smooth muscle (VSM) tone plays a role in modulating the elastic properties of conductance arteries (Dobrin & Rovick, 1969; Wilson *et al.*, 1995; Bank, 1997, Joannides *et al.*, 1997). Furthermore, there is evidence that the release of endothelium-derived nitric oxide (NO) increases arterial compliance (Ramsey, 1994; Joannides *et al.*, 1997). Therefore, endothelium-derived NO may play an important role in reducing cardiac workload relative to peripheral needs by altering the mechanical properties of conductance arteries.

Decreased compliance of conductance arteries has been demonstrated in many cardiovascular diseases, including hypertension (Bella *et al.*, 1999), atherosclerosis (Hodes *et al.*, 1995) and chronic heart failure (CHF; Arnold *et al.*, 1991; Giannattasio *et al.*, 1995; Duprez *et al.*, 1998). Maruyama *et al.* (1993) demonstrated using a canine model of CHF that decreased arterial compliance results in a further decline in left ventricular (LV) ejection. Furthermore, investigators have demonstrated that the decreased arterial compliance associated with hypertension correlates with cardiac hypertrophy (Girerd *et al.*, 1991; Ohtsuka *et al.*, 1996).

Numerous clinical and experimental studies have demonstrated that endothelium-dependent relaxations to acetylcholine in conductance arteries are impaired in CHF (Teerlink *et al.*, 1994; Bank *et al.*, 1994; Baggia *et al.*, 1997; Bauersachs *et al.*, 1999). Furthermore, there is evidence that NO-mediated (Joannides *et al.*, 1995) flow-dependent dilatation is also impaired (Hornig *et al.*, 1996; Mohri *et al.*, 1997; Hornig *et al.*, 1998). Teerlink *et al.* (1994) showed increased adrenergic responsiveness of endothelium-intact but not endothelium-denuded thoracic aortic

rings from rats with CHF. These studies suggest that agonist-stimulated and basal release of NO from the endothelium in conductance arteries is impaired during CHF. Experiments in **Chapter 6** demonstrated that substrate deficient, inducible nitric oxide synthase (iNOS)-derived superoxide was responsible for impaired relaxations to acetylcholine in small mesenteric arteries from rats with CHF. Furthermore, it was revealed that iNOS-derived superoxide plays a major role in the vascular hyperesponsiveness to phenylephrine, possibly as a consequence of increased scavenging of basal endothelium-derived NO. Immunohistochemical studies in Chapter **5** revealed that iNOS is also expressed in thoracic aortae from rats with CHF. Therefore, it is possible that iNOS-derived superoxide is responsible for the vascular dysfunction of conductance arteries associated with CHF.

The aims of the experiments in this chapter were, therefore, to investigate the functional significance of iNOS and superoxide in isolated thoracic aortae from rats with CHF following coronary artery ligation (CAL), and to determine whether substrate deficient iNOS-derived superoxide plays a role in the vascular dysfunction associated with these arteries.

7.2 Methods

All procedures were carried out as described in **Chapter 2**.

7.2.1 Rat coronary artery ligation model of chronic heart failure

Myocardial infarction was induced in 5 week old male Wistar rats (250 –300 g) by ligation of the left anterior descending coronary artery as described in Section **2.1.2.2**.

7.2.2 Haemodynamic measurements and tissue harvesting

Six weeks post-surgery, CAL and sham-operated rats were anaesthetised with sodium pentobarbitol (60 $mgkg^{-1}$, i.p.) and the right carotid artery located, dissected free of extraneous tissue and cannulated with a fluid filled catheter attached to a pressure transducer, for measurement of mean arterial blood pressure (MAP) and LV end-diastolic pressures (LVEDP; see Section **2.1.2.3**).

Following exsanguination, thoracic aortae were removed and placed into cold, oxygenated (95% O_2, 5% CO_2), Krebs Henseleit solution. The hearts and lungs were removed, rinsed in ice-cooled saline (0.9%) then individually weighed. Hearts were then bisected, placed in 10% neutral buffered formalin for 24 h prior to further processing and wax embedding as described in Section **2.3.5**.

7.2.3 Measurement of infarct size

3 μm sections of hearts were taken from blocks and stained with van Gieson's collagen stain for detection of collagen formation in LV infarctions (see Section **2.1.2.4**). Infarct size was then calculated by the method described in Section **2.1.2.5**.

7.2.4 Preparation of aortic rings

Thoracic aortae from both CAL and sham-operated rats were cleaned of adhering adipose and connective tissue and cut into transverse rings (~ 4mm). In some aortic rings the endothelium was removed by the method described in Section **2.2.2**. Aortic rings were then mounted in a 10 ml organ bath filled with warm (37 °C), oxygenated (95% O_2, 5% CO_2) Krebs Henseleit solution (see Section **2.2.1**). Aortic rings were placed under 2 gram of tension and left to equilibrate for 60 min. The general protocol (see Section **2.2.2**) was performed on all aortic rings before commencing the experimental protocols described below.

7.2.5 Experimental protocols

7.2.5.1 Vascular responsiveness of aortic rings from coronary artery ligation and sham-operated rats

To assess vascular responsiveness of aortic rings from CAL and sham-operated rats to adrenoceptor stimulation, cumulative concentration response curves (CRC) to norepinephrine (NE; 1 x 10^{-9} to 3 x 10^{-5} M) were constructed in endothelium-intact (CAL, n=5; Sham-operated, n=8) and endothelium-denuded (CAL, n=5; sham-operated, n=6) aortic rings. Following completion of CRCs, all rings were repeatedly washed and allowed to re-equilibrate for at least 15 min before further experiments.

7.2.5.2 Effect of inducible nitric oxide synthase inhibition on vascular responsiveness

To investigate the role of iNOS in modulating vascular responsiveness, endothelium-intact aortic rings were exposed to the selective iNOS inhibitor, *N*-(3-(Aminomethyl) benzyl) acetamidine dihydrochloride (1400W; 10^{-5} M; CAL, n=5; sham-operated, n=8) for 30 min prior to repeating cumulative CRCs to NE (1 x 10^{-9} to 3 x 10^{-5} M). In **Chapter 3**, experiments demonstrated that at a concentration of 10^{-5} M, 1400W inhibits iNOS without modifying the activity of either basal or agonist-stimulated activity of eNOS. 1400W was present in the superfusate throughout the cumulative CRC.

7.2.5.3 Effect of superoxide quenching on vascular responsiveness

To investigate the role that superoxide plays in modulating vascular responsiveness, aortic rings were exposed to the superoxide dismutase (SOD) mimetic, Mn [III] tetrakis [1-methyl-4-pyridyl] porphyrin (MnTMPyP; 10^{-4} M, CAL, n=5; sham-operated, n=7) for 30 min prior to repeating cumulative CRCs to NE (1 x 10^{-9} to 3 x 10^{-5} M). In **Chapter 4** of this thesis, experiments demonstrated that at a concentration of 10^{-4} M, MnTMPyP protected endothelium–derived NO from inactivation by superoxide in an *in vitro* model of oxidative stress, without having any non-selective effects on the activity of eNOS or iNOS-derived NO, or the enzymes themselves. MnTMPyP (10^{-4} M) was present in the superfusate throughout the cumulative CRC.

7.2.5.4 Effect of combined inducible nitric oxide synthase inhibition and superoxide quenching on vascular responsiveness

To further investigate the role of iNOS and superoxide in modulating vascular responsiveness, endothelium-intact aortic rings were exposed to the iNOS inhibitor, 1400W (10^{-5} M) and the SOD mimetic, MnTMPyP (10^{-4} M) for 30 min prior to repeating cumulative CRC's to NE (1 x 10^{-9} to 3 x 10^{-5} M; CAL, n=5; sham-operated, n=7). Both drugs were present in the superfusate throughout the CRC.

7.2.5.5 Effect of nitric oxide synthase substrate on vascular responsiveness

To investigate the effect of the NOS substrate, L-arginine, on vascular responsiveness, endothelium-denuded aortic rings were exposed to a supramaximal concentration (Schott *et al.*, 1993) of L-arginine (10^{-3} M, CAL, n=5; sham-operated, n=6) for 30 min prior to repeating cumulative CRCs to NE (1 x 10^{-9} to 3 x 10^{-5} M). L-arginine was present in the superfusate throughout the CRC

7.2.5.6 Assessment of endothelium-dependent vascular relaxations in aortic rings from coronary artery ligation and sham-operated rats in the presence and absence of the SOD mimetic, MnTMPyP

To assess endothelium-dependent relaxations in aortic rings from CAL and sham-operated rats, ACh-mediated relaxations were measured in endothelium-intact NE-contracted aortic rings. A submaximal concentration of NE (~ EC_{60}), as determined from NE CRCs, was used to induce arterial tone. Cumulative CRCs to ACh (1×10^{-9} to 3×10^{-5} M, CAL, n=6; sham-operated, n=8) were then obtained in presence and absence of the SOD mimetic MnTMPyP (10^{-4} M). Aortic rings were treated with MnTMPyP for 30 min prior to and throughout the duration of the experiments.

7.2.6 Preparation of drugs

Norepinephrine hydrogentartrate, acetylcholine chloride and L-arginine were diluted in Krebs Henseleit solution to give a stock solution of 10^{-1} M and frozen (-20 °C) in aliquots until use on day of experiment. Vitamin C (10^{-6} M) was added to the stock solution of NE to prevent autoxidation. *N*-(3-(Aminomethyl) benzyl acetamidine dihydrochloride (1400W) was diluted in saline (0.9% NaCl) under argon to give a stock solution of 10^{-3} M. Aliquots were then frozen (-20 °C) and stored under argon. Dilutions were made in Krebs Henseleit solution. MnTMPyP (Mn [III] tetrakis [1-methyl-4-pyridyl] porphyrin) and diluted in Krebs Henseleit solution immediately prior to experimentation.

7.2.7 Data Analysis

All results were expressed as means ± s.e.mean. ACh and SNP cumulative CRCs were measured as percentage relaxations of NE-induced tone. Where maximal values were obtained for cumulative CRCs, the negative logarithm of the agonist concentration that results in a half-maximal contraction or relaxation (pD_2) was calculated by nonlinear regression using GraphPad Prism software (Version 3.0). Two-tailed t-tests, one-way analysis of variance (ANOVA) with Bonferroni post-test

for multiple comparisons and two-way repeated measure ANOVA were used as indicated in the text. $P<0.05$ was considered to be statistically significant.

7.3 Results

7.3.1 Effect of left coronary artery ligation

Survival rate during the first 24 h after CAL surgery was 60%. Two additional CAL rats died before the six-week study period was completed. There were no significant differences between rat weights for CAL and sham-operated groups 6 weeks post-surgery (***Table 7.1***). Heart weights (corrected for body weight) for CAL rats were significantly greater than those of sham-operated rats ($P<0.05$, two-tailed unpaired *t*-test, ***Table 7.1***). There were no significant differences between groups with respect to lung weights (corrected for body weight) and mean arterial blood pressures (***Table 7.1***). LVEDPs measured from CAL rats were significantly greater than those for sham-operated rats ($P<0.05$, two-tailed unpaired *t*-test, ***Table 7.1***). Hearts from CAL rats had visible infarctions, which averaged 45 ± 3 % of the LV free wall. Furthermore, there was evidence for mature collagen deposition within infarctions (data not shown).

	Sham (n=8)	***CAL*** (n=6)
Rat Weight (g)	489.6±18	514±21.9
Heart Weight (g kg^{-1} body weight)	3.2±0.1	3.7±0.1**
Lung Weight (g kg^{-1} body weight)	3.6±0.1	3.9±0.1
LVEDP (mmHg)	5.9±0.4	13±0.6***
Mean arterial pressure (mmHg)	99.6±9	99.6±5.4

Table 7.1 *Summary of parameters measured from coronary artery ligation* ***(CAL)*** *and sham-operated* ***(Sham)*** *rats 6 weeks post-surgery. All values are given as means ± s.e.m. ** $P<0.01$, *** $P<0.001$ for CAL rats compared with respective values in sham-operated rats (two-tailed unpaired t-test).*

7.3.2 KCl, norepinephrine maximal constrictions and endothelial integrity

Maximal constrictions to KCl were significantly lower in endothelium-intact aortic rings from CAL rats when compared with sham-operated rats ($P<0.01$, two-tailed unpaired t-test; ***Table 7.2***). There were no significant differences between endothelium-intact and endothelium-denuded aortic rings from CAL and sham-operated groups with respect to maximal constrictions to a supramaximal concentration of NE (***Table 7.2***). All endothelium-intact aortic rings studied had functional endothelium and no significant differences in maximal relaxations were found between CAL and sham-operated groups (***Table 7.2***). Denudation of aortic rings was deemed successful as relaxations to ACh were all but abolished (***Table 7.2***).

Treatment	Sham		*CAL*	
	+end (n=8)	**-end** (n=8)	**+end** (n=6)	**-end** (n=6)
60 mM **KCl**	4.3±0.4g	4.5±0.4g	3.5±0.2g**	3.8±0.5g
10^{-5} M **NE**	4.1±0.3g	4.9±0.4g	3.7±0.3g	4.1±0.6g
10^{-5} M **ACh**	83.1±1.9%	1±5.3%	79.8±6.2%	1.8±0.8%

Table 7.2 *Maximal contractions of endothelium-intact (**+end**) and endothelium–denuded (**-end**) arteries from coronary artery ligation (**CAL**) and sham-operated (**Sham**) rats to **KCl** and norepinephrine (**NE**). Responses of NE-contracted aortic rings to acetylcholine (**ACh**) are given as percentages of NE (EC_{50})-induced tone. All values are given as mean ± s.e.mean. ** $P<0.01$ compared with KCl responses in sham-operated endothelium-intact aortic rings (two-tailed unpaired t-test).*

7.3.3 Assessment of vascular responsiveness to adrenoceptor stimulation in coronary artery ligation and sham-operated rats

In both endothelium-intact and endothelium-denuded aortic rings from CAL and sham-operated rats, cumulative additions of NE (1 x 10^{-9} to 3 x 10^{-5} M) resulted in concentration-dependent contractions (***Figures 7.1***). In endothelium-intact aortic rings from CAL rats, pD_2 values and maximal contractions for NE CRCs were significantly lower when compared with values in endothelium-intact aortic rings from sham-operated rats ($P<0.05$, two-tailed unpaired *t*-test, ***Table 7.3***), suggesting that endothelium-intact aortic rings from CAL rats were less responsive to NE than aortae from sham-operated rats. In endothelium-denuded aortic rings from CAL rats there was a significant increase in responsiveness to NE ($P<0.05$, two-way ANOVA, ***Figure 7.1***). Indeed, pD_2 values and maximal contractions for NE CRCs when compared with responses in endothelium-intact aortic rings ($P<0.05$, one-way ANOVA with Bonferroni post-test, ***Table 7.3***). In contrast, there were no significant differences between NE CRCs in endothelium-intact and –denuded aortic rings from sham-operated rats (***Figure 7.1***).

Treatment	*Sham*		*CAL*	
	pD_2 ($n\geq6$)	Max (g) ($n\geq6$)	pD_2 (n=5)	Max (g) (n=5)
Control ***+end***	6.3±0.2	5±0.3	5.8±0.2*	3.8±0.4*
Control ***-end***	6.5±0.2	5.5±0.2	6.8±0.4#	4.6±0.6#
+ 1400W	6.3±0.2	5.1±0.4	6.1±0.3	4.2±0.7
+ MnTMPyP	5.9±0.1✝	3.7±0.6✝	6.1±0.2	3.7±0.5
+1400W +MnTMPyP	6.1±0.3	3.9±0.5✝	6.0±0.2	4.4±0.4

Table 7.3 pD_2 *values and maximal (**Max**) contractions (gram tension) for norepinephrine cumulative concentration response curves (CRC) in endothelium-intact (**+end**) and endothelium-denuded (**-end**) aortic rings from coronary artery ligation (**CAL**) and sham-operated (**Sham**) rats. Also shown are pD_2 values and Max contractions for NE CRCs in endothelium-intact aortic rings in presence of 1400W (10^{-6} M) and MnTMPyP (10^{-4} M) either on their own or together. All values are given as mean values ± s.e.mean. * $P<0.05$ compared with respective values in control endothelium-intact aortic rings from sham-operated rats, # $P<0.05$ compared with respective values in control endothelium-intact aortic rings from CAL rats, ✝ $P<0.05$ compared with respective values in control endothelium-intact aortic rings from sham-operated rats (one-way ANOVA with Bonferroni post-test).*

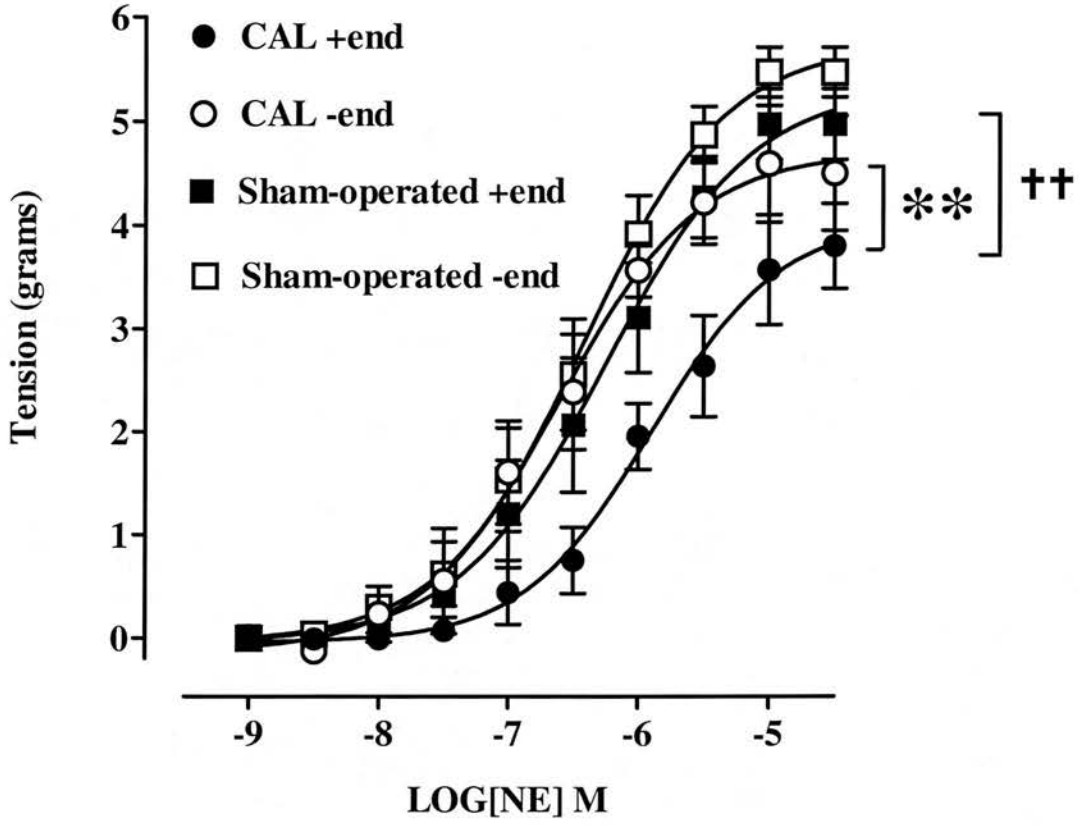

Figure 7.1 *Cumulative concentration response curves (CRC) showing contractile responses to norepinephrine (NE; 1 x 10^{-9} to 3 x 10^{-5} M) in endothelium-intact (+end) and endothelium-denuded (-end) aortic rings from coronary artery ligation (CAL; n=5) and sham-operated rats (n=6) 6 weeks post-surgery. Values are given as means ± s.e.mean. ** P<0.01 compared with CRCs in -end aortic rings from CAL rats,* **††** *P<0.01 compared with CRCs in +end aortic rings from sham-operated rats, (two-way ANOVA).*

7.3.4 Effect of 1400W and MnTMPyP on vascular responsiveness

Treatment of endothelium-intact aortic rings from CAL rats with 1400W (10^{-5} M) or MnTMPyP (10^{-4} M), on their own or together had no significant effect on contractile responses to NE (***Figure 7.2***, ***Figure 7.3, Table 7.3***). Contractile responses to NE in endothelium-intact aortic rings from sham-operated rats were unaffected by 1400W (***Figure 7.4***, ***Table 7.3***). However, treatment with MnTMPyP on its own or in combination with 1400W resulted in a significant decrease in reponsiveness to NE ($P<0.05$, two-way ANOVA, ***Figure 7.5***) Indeed, there was a significant decrease in pD_2 and maximal contractions for NE CRCs when compared responses in untreated aortic rings ($P<0.05$, one-way ANOVA with Bonferroni post-test, ***Table 7.3***).

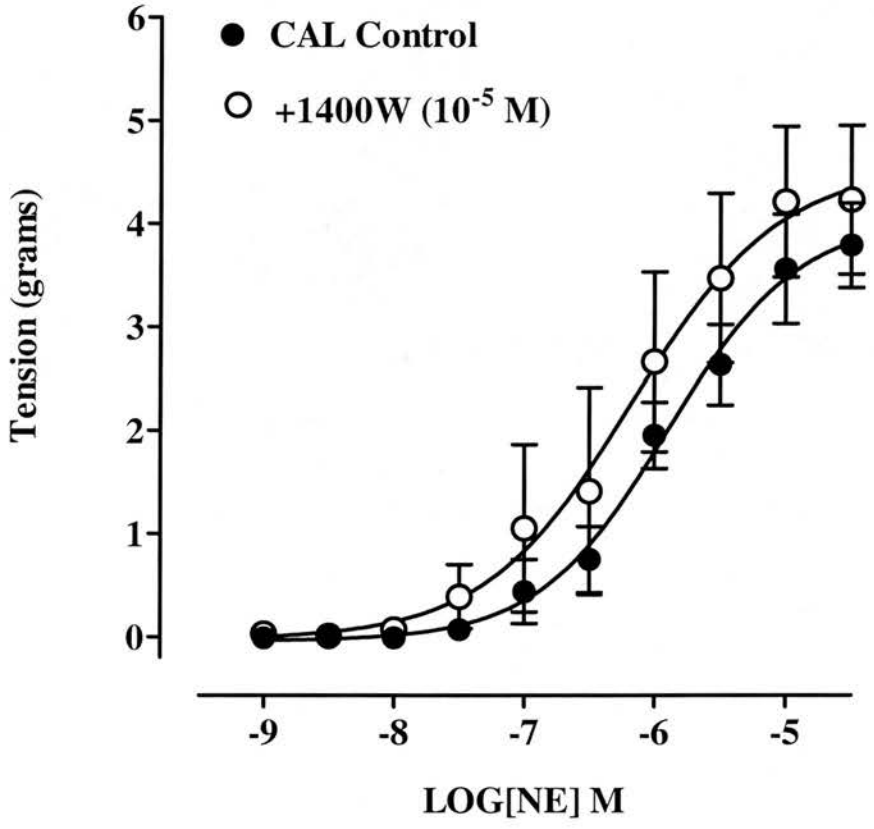

Figure 7.2 *Effect of 1400W (10^{-5} M) on cumulative concentration response curves to norepinephrine (NE; 1 x 10^{-9} to 3 x 10^{-5} M) in endothelium-intact aortic rings from coronary artery ligation rats (CAL; n=5) 6 weeks post-ligation. Values are given as means ± s.e.mean. P>0.05, two-way ANOVA.*

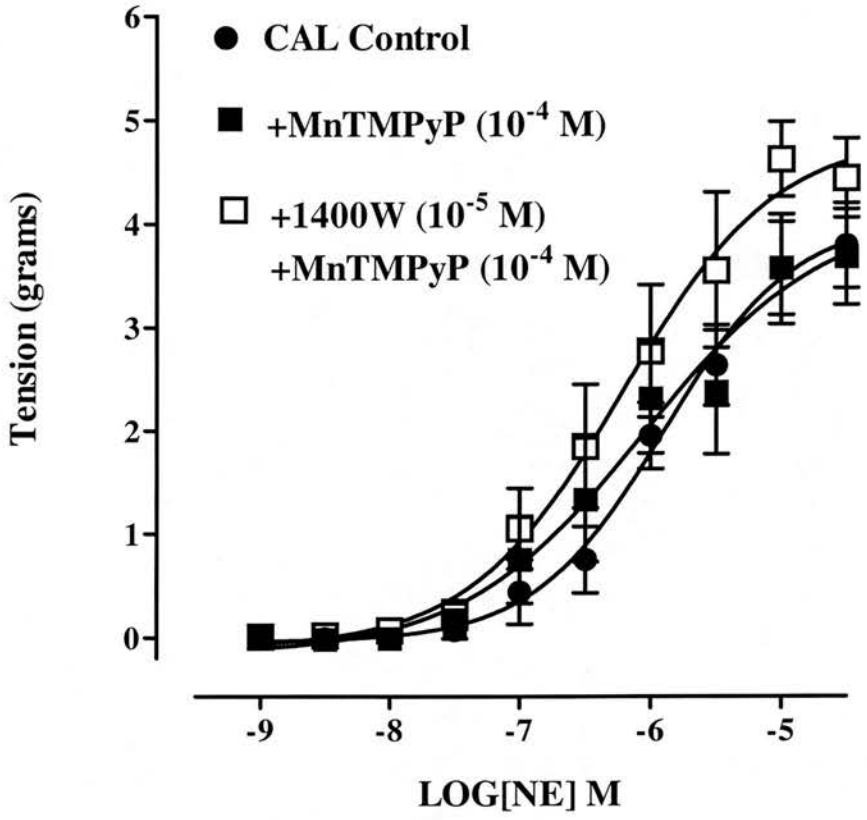

Figure 7.3 *Effect of* ***MnTMPyP*** *(10^{-4} M) on its own or in combination with* ***1400W*** *(10^{-5} M) on cumulative concentration response curves to norepinephrine (**NE**; 1 x 10^{-9} to 3 x 10^{-5} M) in endothelium-intact aortic rings from coronary artery ligation rats (**CAL**; n=5) 6 weeks post-ligation. Values are given as means ± s.e.mean. P>0.05, for CRCs in untreated aortic rings compared with CRCs in 1400W, MnTMPyP as treated aortic rings (two-way ANOVA).*

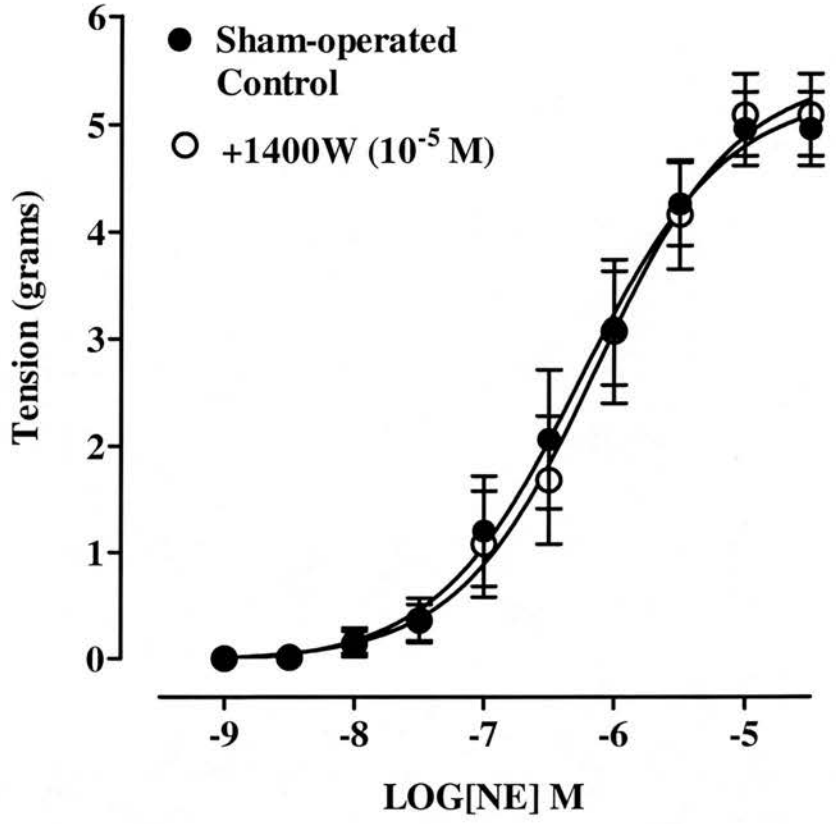

Figure 7.4 *Effect of* ***1400W*** *(10^{-5} M) on cumulative concentration response curves to norepinephrine (**NE**; 1 x 10^{-9} to 3 x 10^{-5} M) in endothelium-intact aortic rings from sham-operated rats (n=8) 6 weeks post-surgery. Values are given as means ± s.e.mean. P>0.05, two-way ANOVA.*

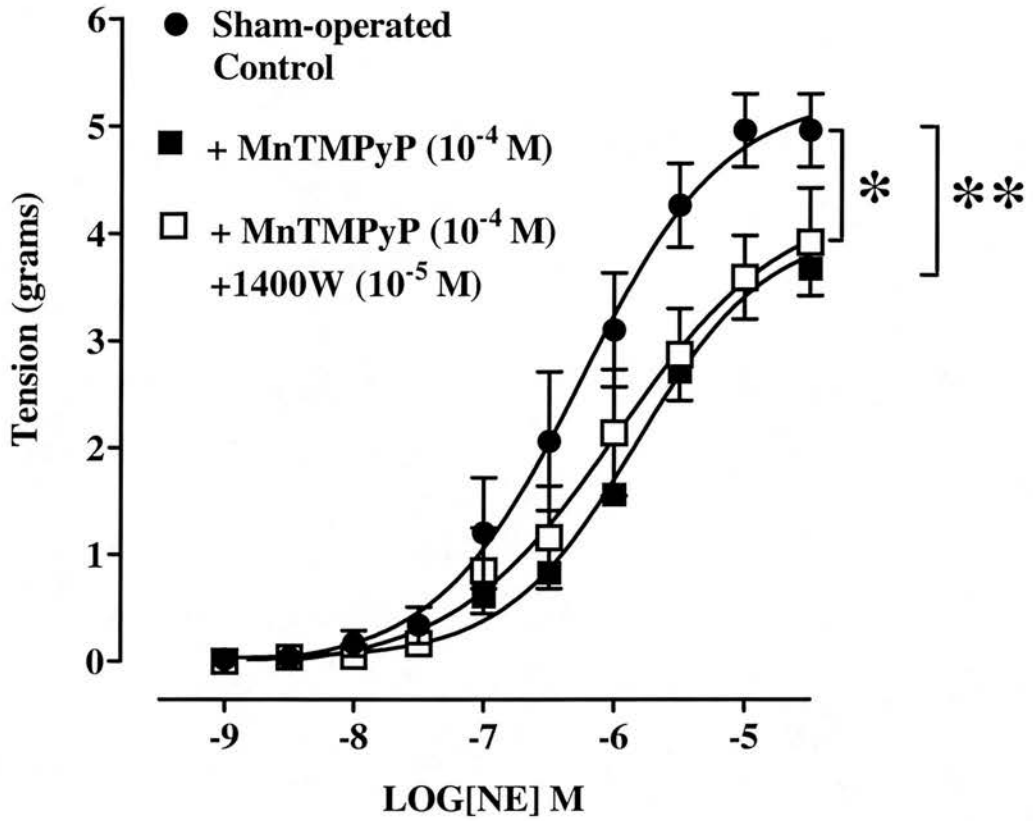

Figure 7.5 *Effect of MnTMPyP (10^{-4} M) on its own or in combination with 1400W (10^{-5} M) on cumulative concentration response curves to norepinephrine (NE; 1 x 10^{-9} to 3 x 10^{-5} M) in endothelium-intact aortic rings from sham-operated rats (n=7) 6 weeks post-surgery. Values are given as means ± s.e.mean. * P<0.05 for CRCs in untreated rings compared with CRCs in MnTMPyP and 1400W-treated rings, ** P<0.01 for CRCs in untreated rings compared with CRCs in MnTMPyP-treated rings (two-way ANOVA).*

7.3.5 Effect of L-arginine on vascular responsiveness

Treatment of endothelium-denuded aortic rings from CAL rats with the NOS substrate, L-arginine (10^{-3} M), resulted in a significant decrease in pD_2 values for NE CRCs (untreated; 6.8 ± 0.4; L-arginine-treated, 6.1 ± 0.1, $P<0.05$, two-tailed paired *t*-test, ***Figure 7.6***), indicating that in the presence of L-arginine arteries are less responsive to NE. There were no significant differences between maximal constrictions to NE in untreated and L-arginine-treated aortic rings (***Figure 7.6***). L-arginine had no significant effect on NE responses in aortic rings from sham-operated rats (***Figure 7.7***).

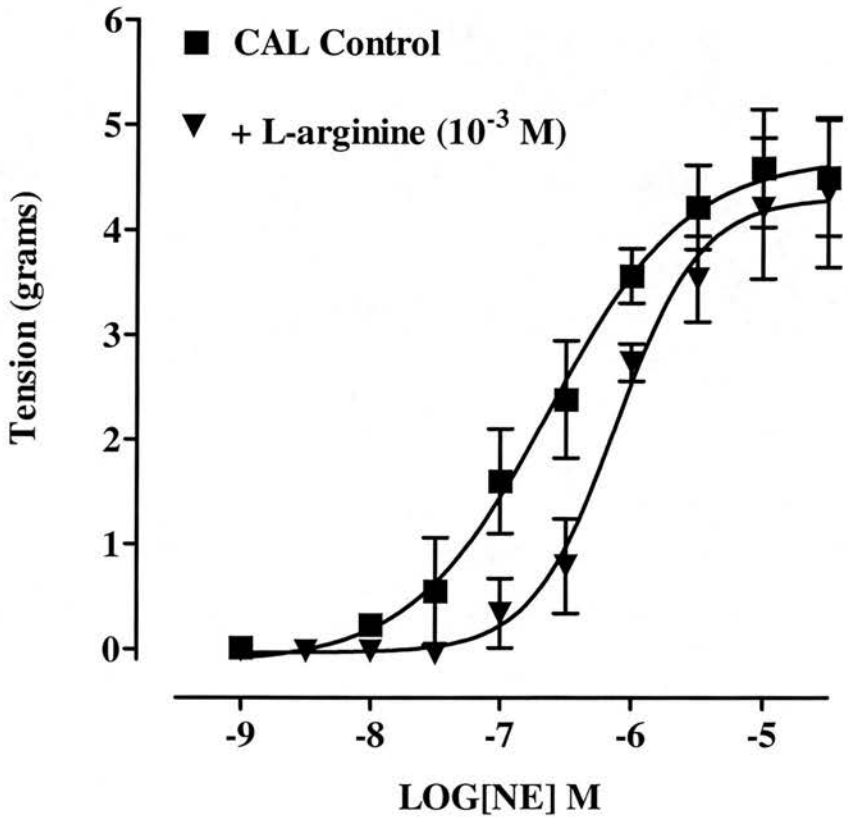

Figure 7.6 *Effect of L-arginine (10^{-3} M) on cumulative concentration response curves (CRC) to norepinephrine (**NE**; 1 x 10^{-9} to 3 x 10^{-5} M) in endothelium-denuded aortic rings from coronary artery ligation (**CAL**) rats (n=5) 6 weeks post-ligation. Values are given as means ± s.e.mean. P>0.05, two-way ANOVA.*

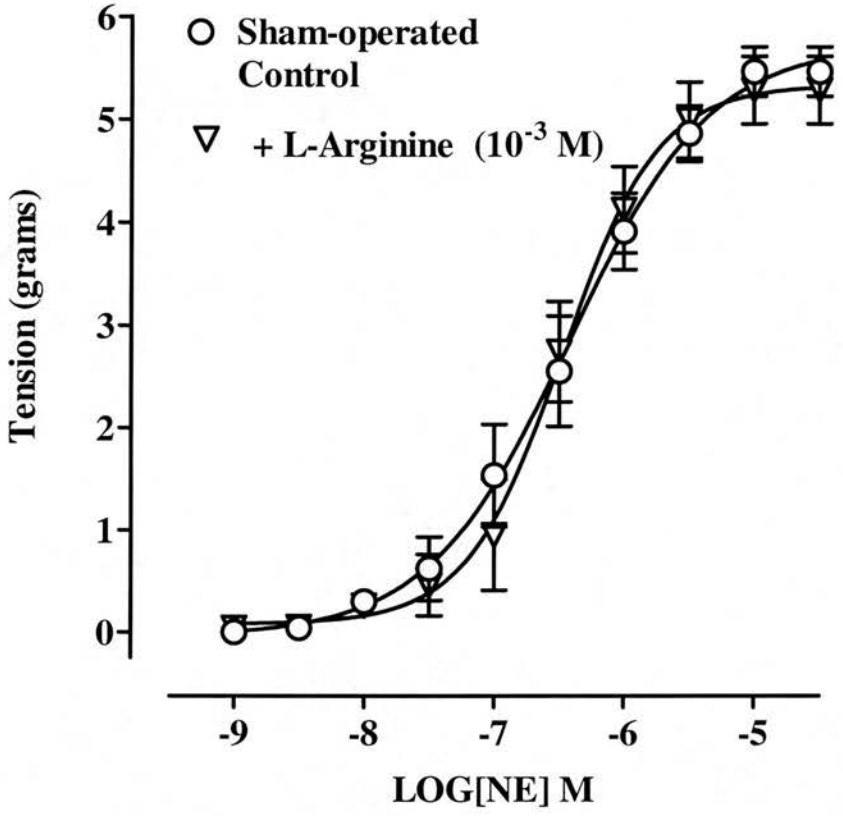

***Figure** 7.7 Effect of L-arginine (10^{-3} M) on cumulative concentration response curves to norepinephrine (**NE**; 1 x 10^{-9} to 3 x 10^{-5} M) in endothelium-denuded aortic rings from sham-operated rats (n=6) 6 weeks post-surgery. Values are given as means ± s.e.mean. P>0.05, two-way ANOVA.*

7.3.6 Assessment of endothelium-dependent vascular relaxations in coronary artery ligation and sham-operated rats. Effect of superoxide quenching

Following induction of NE (EC_{60})-induced tone (CAL, 62.5 ± 4.8%; sham-operated; 60.3 ± 5.6% of maximal NE contractions) in endothelium-intact aortic rings from CAL and sham-operated rats, cumulative additions of ACh (1×10^{-9} to 3×10^{-5} M) resulted in concentration-dependent relaxations (***Figure 7.8***). Relaxations to ACh were significantly greater in aortic rings from CAL rats when compared with sham-operated rats ($P<0.01$, two-way ANOVA; ***Figure 7.8***).

Treatment of NE-contracted (62.6 ± 8.9% of maximal NE contracted) endothelium-intact aortic rings from CAL rats with MnTMPyP (10^{-4} M) tended to shift CRCs to the left suggesting an increase in responsiveness to ACh in the presence of MnTMPyP. However, these differences failed to reach statistical significance ($P>0.05$, one-way ANOVA, ***Figure 7.9***), furthermore, pD_2 values for ACh CRCs could not be calculated as maximal relaxations were not achieved. In contrast, treatment of NE-constricted (65.1 ± 6.6% of maximal NE contracted) endothelium-intact aortic rings from sham-operated rats with MnTMPyP (10^{-4} M) significantly increased responsiveness of aortic rings to ACh, as demonstrated by a leftward shift of ACh CRCs ($P<0.05$, two-way ANOVA, ***Figure 7.10***). pD_2 values for ACh CRCs could not be calculated as maximal relaxations were not achieved.

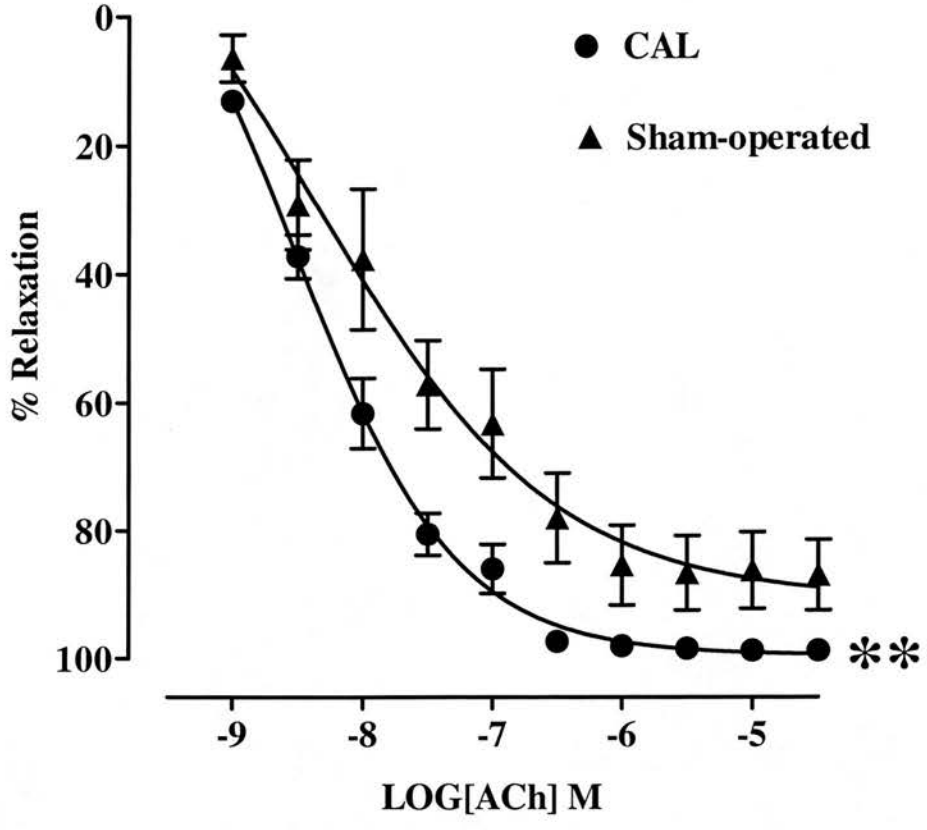

Figure 7.8 *Cumulative concentration response curves (CRC) showing endothelium-dependent relaxations to acetylcholine (**ACh**; 1 x 10^{-9} to 3 x 10^{-5} M) in endothelium-intact aortic rings from coronary artery ligation (**CAL**; n=6) and sham-operated (n=8) rats 6 weeks post-surgery. Values are given as means ± s.e.mean. ** P<0.01 as compared with CRCs in sham operated aortic rings (two-way ANOVA).*

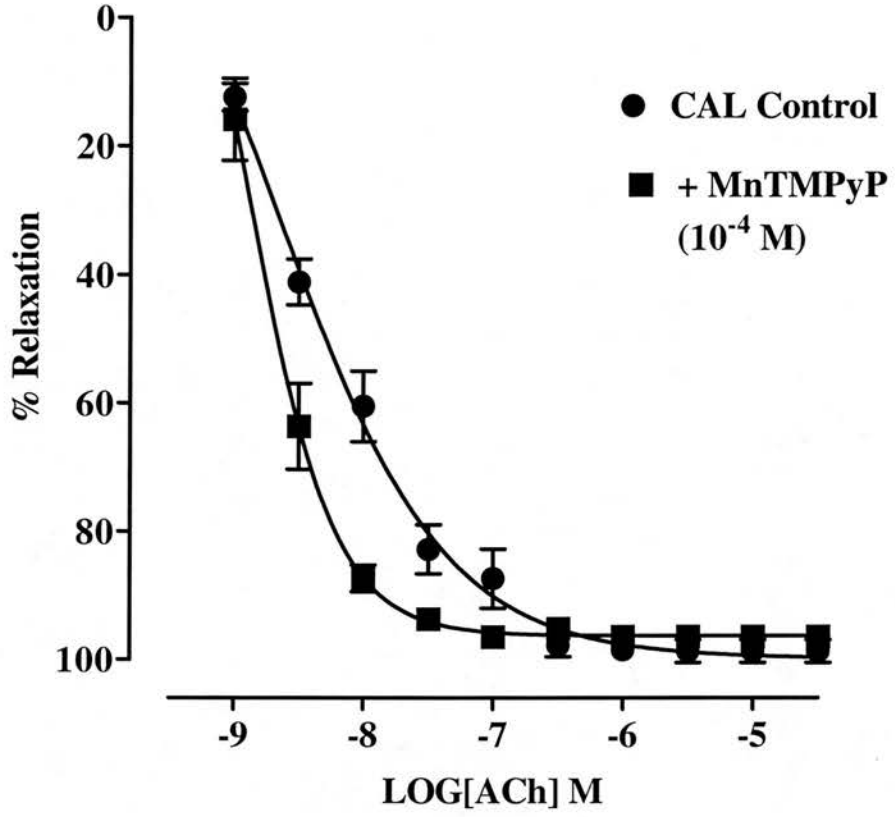

Figure 7.9 *Cumulative concentration response curves (CRC) showing endothelium-dependent relaxations to acetylcholine (**ACh**; 1 x 10^{-9} to 3 x 10^{-5} M) in endothelium-intact aortic rings from coronary artery ligation (**CAL**) rats (n=6) 6 weeks post-surgery, in the presence and absence of MnTMPyP (10^{-4} M). Values are given as means ± s.e.mean. P>0.05, two-way ANOVA.*

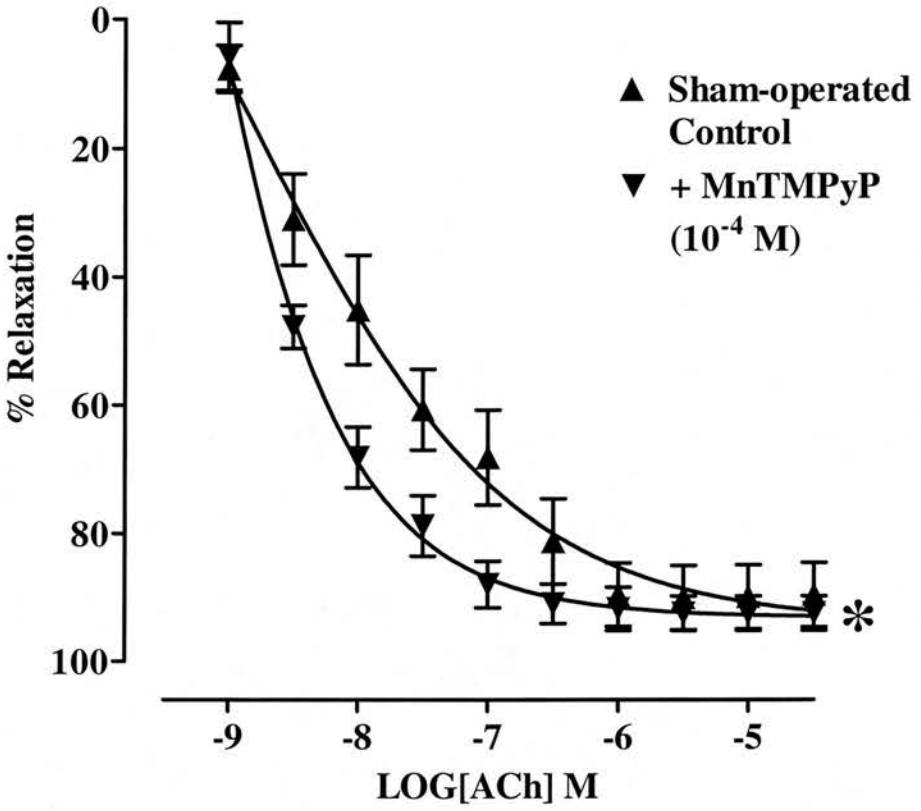

Figure 7.10 *Cumulative concentration response curves (CRC) showing endothelium-dependent relaxations to acetylcholine (**ACh**; 1 x 10^{-9} to 3 x 10^{-5} M) in endothelium-intact aortic rings from and sham-operated (n=8) rats 6 weeks post-surgery, in the presence and absence of MnTMPyP (10^{-4} M). Values are given as means ± s.e.mean. * P<0.05 as compared with CRCs in untreated aortic rings (two-way ANOVA.).*

7.4 Discussion

In **Chapter 6** of this thesis, experiments revealed that substrate deficient, iNOS-derived superoxide plays a major role in the vascular hyperesponsiveness of small mesenteric arteries from CHF rats. Furthermore, it was suggested that this is probably as a result of increased inactivation of endothelium-derived NO. Immunohistochemical studies in **Chapter 5** revealed that, in addition to its expression in small mesenteric arteries, iNOS is also expressed in thoracic aortae from rats with CHF. Therefore, in view of these findings, experiments in the present chapter were designed to investigate the functional significance of iNOS and superoxide in these conductance arteries from rats with CHF. The main findings of experiments in this chapter were that the selective iNOS inhibitor, 1400W, had no significant effect on the vascular responsiveness of endothelium-intact aortic rings from CHF rats. Supplementation of endothelium-denuded aortic rings from CHF but not sham-operated rats with the NOS substrate, L-arginine, resulted in a significant reduction in responsiveness to NE. However, the metalloporphyrin SOD mimetic, had no significant effect on contractile responses in endothelium-intact aortic rings from CHF rats. These results suggest that superoxide deficient iNOS plays no role in modulating vascular responsiveness in conductance arteries in this model of CHF.

Six weeks after CAL, rats had infarctions averaging 45% of the LV free wall. Furthermore, LVEDPs were significantly elevated when compared with those in sham-operated rats. Histological examination of hearts using van Gieson's stain revealed that a fibrous scar, composed mainly of collagen, had replaced infarcted areas of hearts from CAL rats. Furthermore, heart weights were significantly greater than those for sham-operated rats, indicating that hearts had undergone compensatory hypertrophy as a consequence of LV infarction. These results demonstrate that rats had developed CHF as a consequence of CAL. However, in contrast with the model used in **Chapters 5** and **6** of this thesis, this model resembled a more moderate form of CHF (Fraccarollo *et al.*, 1997; Mulder *et al.*, 1998), as evidenced by smaller infarct sizes and lower LVEDPs.

In contrast with small mesenteric arteries (see **Chapter 6**), endothelium-intact aortic rings from rats with CHF were less responsive to NE when compared with responses in endothelium-intact aortic rings from sham-operated rats. This hyporeactivity would suggest that, in contrast with small mesenteric arteries, where iNOS-derived superoxide was responsible for the hyperresponsive nature of these arteries, the expression of iNOS in thoracic aortae results in the expected increase in NO generation. Immunohistochemical studies in **Chapter 5** revealed that iNOS was located to all cell types in thoracic aortae from CHF rats, therefore, one might expect endothelium-denuded aortic rings to also be hyporesponsive to NE. However, somewhat surprisingly, there were no significant differences between responses to NE in endothelium-denuded aortic rings from CHF and sham-operated rats. These results suggest that this vascular hyporeactivity is dependent on the presence of the endothelium. Furthermore, they suggest that iNOS-derived NO might not play an active role in modulating vascular function in these arteries.

As discussed in previous chapters, basal production of NO in endothelium-intact isolated rat aortic rings exerts a tonic vasodilatory action, opposing the effects of vasoconstrictors (Martin *et al.*, 1986). Indeed, in the present chapter, denudation of aortic rings from CHF rats resulted in a significant increase in responsiveness to NE, implying that endothelium-derived relaxing factors, including NO play an active role in modulating vascular responsiveness in these arteries. In contrast, however, denudation of aortic rings from sham-operated rats had no significant effect on responsiveness to NE. It is unclear from these experiments alone why this disparity between CHF and sham-operated rats exists. What is clear from this finding, however, is that the observed hyporeactivity of endothelium-intact aortic rings from CHF rats should be interpretated with caution. Indeed, it is possible that endothelium-intact aortic rings from CHF rats appear hyporeactive when compared with aortae from sham-operated rats simply because in aortic rings from sham-operated rats endothelium-derived NO is playing no tonic vasodilatory role in modulating vascular responsiveness. Consistent with this hypothesis, endothelium-intact aortic rings from sham-operated rats were significantly less responsive to ACh than aortic rings from CHF rats. Taken together these results would suggest that the

release of NO from the endothelium in aortic rings from sham-operated rats is impaired. While it remains to be established if this is indeed the case, it is clear that comparisons between CHF and sham-operated rats should be approached with caution.

To establish if iNOS plays a role in modulating vascular responsiveness in thoracic aortae from rats with CHF, the selective iNOS inhibitor, 1400W (see **Chapter 3**), and the NOS substrate, L-arginine were used. 1400W had no significant effect on the responsiveness of endothelium-intact aortic rings from CHF or sham-operated rats to NE. Therefore, as proposed earlier, these results suggest that the induction of iNOS in thoracic aortae does not play an active role in modulating vascular responsiveness in these arteries. In experimental endotoxic shock, addition of the NOS substrate, L-arginine, to isolated blood vessels increases NO production from iNOS and potentiates hyporesponsiveness to vasoconstrictors (Julou-Schaeffer *et al.*, 1990). Experiments here demonstrate that supplementation of endothelium-denuded aortic rings from CHF rats, but not sham-operated rats, with a supramaximal concentration of L-arginine resulted in a significant reduction in responsiveness to NE. These results confirm the presence of iNOS within thoracic aortae from CHF rats. Furthermore, they suggest that, in a similar fashion to small mesenteric arteries (see **Chapter 6**), iNOS may be unable to synthesize NO because there is insufficient substrate.

In **Chapter 6** of this thesis, experiments suggested that a deficiency in L-arginine not only prevented iNOS from generating NO, but also resulted in the enzyme producing superoxide. Moreover, as previously mentioned, this source of superoxide was deemed responsible for the hyperresponsive nature of endothelium-intact small mesenteric arteries, possibly as a consequence of increased scavenging of eNOS-derived NO. Experiments here suggest that in aortic rings from CHF rats, iNOS may also be deficient in L-arginine. However, as discussed, the endothelium appears to play an active tonic vasodilatory role in modulating vascular responsiveness in these arteries. Therefore, if iNOS is generating superoxide it is unlikely that this source of superoxide has a significant effect on the bioavailability of endothelium-derived NO.

Consistent with this hypothesis, treatment of endothelium-intact aortic rings from CHF rats with the cell permeable metalloporphyrin, MnTMPyP (see **Chapter 4**), on its own or in combination with 1400W had no significant effect on responsiveness to NE. Furthermore, MnTMPyP had no significant effect on relaxations to ACh in endothelium-intact aortic rings from CHF rats. Therefore, these findings suggest that either iNOS is not generating superoxide or the superoxide generated by iNOS has no effect on the bioavailability of endothelium-derived NO and hence vascular function in these arteries from CHF rats.

Interestingly, in contrast with aortic rings from CHF rats, treatment of endothelium-intact aortic rings from sham-operated rats with MnTMPyP resulted in a significant reduction in responsiveness to NE when compared with responses in untreated rings. In **Chapter 4**, MnTMPyP was shown to increase responsiveness of endothelium-intact aortic rings to ACh by protecting endothelium-derived NO from inactivation by low levels of endogenous or exogenous superoxide generated within the organ bath. Therefore, in sham-operated aortic rings treated with MnTMPyP, an increase in the bioavailability of endothelium-derived NO is probably responsible for the marked decrease in responsiveness to NE. As discussed, earlier experiments suggested that basal release of NO from the endothelium in aortic rings from sham-operated rats was impaired. Increased inactivation of endothelium-derived NO by superoxide generated within the organ bath may well explain this finding. Indeed, MnTMPyP, significantly increased the responsiveness of endothelium-intact aortic rings to ACh. More importantly, however, these findings highlight important differences between endothelium-intact aortic rings from CHF and sham-operated rats with respect to the susceptibility of basal endothelium-derived NO to inactivation by superoxide. In particular, these results suggest that in aortic rings from CHF rats, endothelium-derived NO is less prone to inactivation by superoxide than in aortic rings from sham-operated rats. This hypothesis is provocative, however, it is based on correlations rather than direct evidence. However, if this hypothesis is proven, it may explain why earlier studies using MnTMPyP suggest that, despite being substrate deficient, iNOS expressed in aortic rings from CHF rats is not generating superoxide. Indeed, it may be that iNOS is generating superoxide,

however, because these arteries from CHF rats are less susceptible to inactivation by superoxide, it has no significant effect on the bioavailability of endothelium-derived NO, and thus vascular responsivenss.

It is clear from this discussion that the experiments in this chapter present a complex story regarding the role of iNOS and superoxide in modulating vascular function in conductance arteries from rats with CHF. In particular, interpretation of the results presented in this chapter are complicated by the finding that in aortic rings from sham-operated but not CHF rats, the release of endothelium-derived NO is impaired, probably as a consequence of increased scavenging by superoxide. However, there are some important conclusions that can be drawn from this study. In a particular, experiments provide convincing evidence that iNOS plays no role in modulating vascular responsiveness of thoracic aortae from CHF rats. Experiments also suggest that, as in small mesenteric arteries from CHF rats (see **Chapter 6**), iNOS expressed in thoracic aortae might be substrate deficient. However from the data presented here it is unclear if iNOS is generating superoxide or not. In conclusion, therefore, this study presents some interesting differences between small mesenteric arteries and thoracic aortae from CHF rats with respect to the role of iNOS and superoxide in modulating vascular function. However, it is clear that further studies are required to elucidate why these differences exist.

Chapter 8

General Discussion

8.1 Summary

Chronic heart failure (CHF) is a major cause of cardiovascular mortality and morbidity, accounting for 5% of acute hospital admissions in the UK (Sutton *et al.*, 1997). In CHF, a complex interplay of haemodynamic and neurohormonal mechanisms are activated to maintain arterial blood pressure in the face of reduced cardiac output. Increased peripheral vascular resistance (PVR), as a consequence of these compensatory mechanisms plays an important role in the progression of CHF, contributing to increased internal left ventricular (LV) stress and LV remodelling (see Section **1.5.5**).

Resistance arteries are know to be the most important blood vessels in the body in determining PVR (see Section **1.2.3**). There is evidence to suggest that impaired nitric oxide (NO)-mediated vasodilatation of resistance arteries contributes to the increased PVR associated with CHF. However, there is some evidence that basal synthesis of NO may be preserved or even enhanced in CHF, perhaps due to the expression of inducible NO synthase (iNOS). Increased superoxide production has been demonstrated in CHF and, since superoxide inactivates NO, a reduction in NO bioavailability may be responsible for impaired NO-mediated relaxations and may also explain why PVR remains elevated despite increased NO production. Increased basal production of NO, contrasting with impaired NO-mediated vasodilatation, has also been demonstrated in conductance arteries during CHF. Although conductance arteries play a minimal role in modulating PVR, they do play an important role in the overall mechanical efficiency of the cardiovascular system (see Section **1.2.3**). At the onset of this thesis, the expression of iNOS in the cardiovascular system in CHF and its role in modulating vascular function had not been investigated. Furthermore, the role of superoxide in modulating the bioavailability of the vascular NO system in CHF had not been fully addressed.

The ultimate goal of this thesis was to investigate the role of iNOS and superoxide in modulating vascular function in rats with CHF following coronary artery ligation (CAL) and subsequent myocardial infarction (MI). Therefore, the primary aim of

experiments was to determine whether iNOS was expressed in the cardiovascular system in this model of CHF. In particular, its expression within the heart, small mesenteric arteries (internal diameters, 300 – 350 μm) and thoracic aortae was investigated. After establishing whether iNOS was expressed in small mesenteric arteries and thoracic aortae from rats with CHF, the aim of future experiments was to investigate the functional significance of iNOS on vascular function. The final aim of this thesis was to examine the role of superoxide in modulating vascular NO bioavailabiltiy in this model of CHF. In summary, therefore, experiments in this thesis set out to attain a more comprehensive understanding of the role of the NO system in modulating vascular function during CHF, with the ultimate goal of evaluating its potential as a viable target for future drug therapy.

To investigate the role of iNOS and superoxide in modulating vascular function in this model of CHF, the pharmacological properties of the novel iNOS inhibitor, *N*-(3-(Aminomethyl) benzyl) acetamidine dihydrochloride (1400W), and the cell permeable superoxide dismutase mimetic, Mn [III] tetrakis [1-methyl-4-pyridyl] porphyrin (MnTMPyP) were investigated. Experiments in **Chapter 3** provided convincing evidence that 1400W inhibits the activity of iNOS *in vitro* without modifying the activity of eNOS and thus supported its use in furture experiments to investigate the role of iNOS in modulating vascular function of arteries from CHF rats. In **Chapter 4**, experiments provided convincing evidence that MnTMPyP was an effective SOD mimetic and thus was suitable for use in future experiments investigating the role of superoxide in modulating NO bioavailability in the peripheral vasculature from CHF rats.

The primary finding of this thesis was that iNOS was detected in both the heart and peripheral vasculature in rats with CHF six weeks post-ligation. Furthermore, no iNOS was detected within the heart and peripheral vasculature in sham-operated rats, providing convincing evidence that the expression of iNOS in the cardiovascular system was specific to the induction of CHF *per se*. iNOS immunoreactivity was detected in all cell types of both small mesenteric arteries and thoracic aortae from rats with CHF. Previous functional studies have suggested that iNOS-derived NO is

responsible for the increased basal NO production associated with CHF (Drexler *et al.*, 1992; Habib *et al.*, 1994; Winlaw *et al.*, 1994). However, this is the first time iNOS has been detected in the peripheral vasculature in CHF. Therefore, these findings complement and extend functional studies in suggesting that iNOS-derived NO may be responsible for the increased basal NO production associated with CHF. In contrast with the peripheral vasculature, previous clinical studies have detected iNOS mRNA and protein in hearts from patients with CHF, providing convincing evidence that CHF is associated with iNOS expression in the heart. However, as discussed in **Chapter 5**, the spatial distribution of iNOS in the human failing heart remains a matter for debate. In the model of CHF used in this thesis, immunohistochemical studies revealed that iNOS was exclusively expressed within the LV free wall and interventricular septum. These results corroborate the findings of some (Haywood *et al.*, 1996; Fukuchi *et al.*, 1998) but not all investigators (de Belder et al., 1993; Vejlstrup *et al.*, 1998), and suggest that the induction of iNOS in the heart during CHF might be specific to the LV myocardium. With respect to its cellular localisation, iNOS could be detected in viable cardiomyocytes, coronary vascular and endocardial endothelial cells. Therefore, besides complementing previous clinical studies, the findings from these experiments extend these studies by providing some novel information regarding the possible spatial distribution of iNOS within the failing heart.

Experiments in **Chapter 6** were designed to investigate the functional significance of iNOS and superoxide in isolated small mesenteric arteries (300 – 350 μm) from rats with CHF. Despite the presence of iNOS in these arteries, *in vitro* studies in this chapter revealed that endothelium-intact but not endothelium-denuded small mesenteric arteries from CHF rats were more responsive to phenylephrine (PE) than those from sham-operated rats. The hypereponsiveness of endothelium-intact arteries from CHF rats was reversed by the selective iNOS inhibitor, 1400W and by the metalloporphyrin SOD mimetic, MnTMPyP. Supplementation of endothelium-denuded arteries from CHF but not sham-operated rats with the NOS substrate, L-arginine, resulted in a significant reduction in responsivness to PE when compared with untreated arteries. Endothelium-dependent, but not endothelium-independent

relaxations, were impaired in arteries from CHF rats when compared with relaxations in arteries from sham-operated rats. Furthermore, MnTMPyP restored endothelium-dependent relaxations.

The findings of this chapter may present an interesting new facet to the impact of iNOS in modulating vascular function of resistance arteries in CHF. iNOS expression in blood vessels is normally associated with the production of large quantities of NO and a subsequent decrease in vascular responsiveness (see **Chapter 3**). However, in this model of CHF, instead of generating large quantities of NO, iNOS appears to be generating superoxide, perhaps because of a deficiency in its substrate, L-arginine. Furthermore, results suggested that this source of superoxide was responsible for the hyperresponsive nature of these arteries, possibly as a consequence of increased scavenging of eNOS-derived NO. Moreover, iNOS-derived superoxide was deemed responsible for impaired endothelium-dependent relaxations. All three isoforms of NOS have been shown to generate superoxide rather than NO when deficient in substrate and/or cofactors (Klatt *et al.*, 1993b; Xia *et al.*, 1998a; Xia *et al.*, 1998b). Furthermore, there is evidence to suggest that tetrahydrobiopterin deficient eNOS-derived superoxide may contribute to the endothelial dysfunction associated with atherosclerosis (reviewed by Wever *et al.* 1998). Therefore, the concept of NOS generating superoxide under conditions of low substrate and/or cofactor is not novel. However, the findings of this thesis are the first to implicate a pathophysiological role for substrate deficient iNOS-derived superoxide. While the clinical significance of this finding remains to be established, they may represent an important mechanism for the endothelial dysfunction and raised PVR associated with CHF.

The next finding in this thesis indicated that, in contrast to small mesenteric arteries, substrate deficient iNOS played no role in modulating function of thoracic aortae from rats with CHF. Initial experiments suggested that endothelium-intact aortic rings from CHF rats were less responsive to norepinephrine (NE) when compared with responses in aortic rings from sham-operated rats. This hyporeactivity would suggest that iNOS is generating NO in these arteries from CHF rats. However, as

discussed in **Chapter 7**, subsequent experiments in endothelium-denuded aortic rings revealed that this apparent hyporeactivity was probably because the release of NO from the endothelium in aortic rings from sham-operated rats was impaired. Despite being unable to make comparisons between responses in aortic rings from CHF and sham-operated rats, there are some important conclusions that can be drawn from the experiments in this chapter. In particular, inhibition of iNOS and/or scavenging of superoxide in endothelium-intact aortic rings from CHF rats had no significant effect on NE responsiveness, providing convincing evidence that iNOS and superoxide play no role in modulating vascular function of these arteries. Subsequent experiments using L-arginine, however, revealed that in a similar manner to small mesenteric arteries, there might be insufficient substrate available for iNOS in thoracic aortae to generate NO. The experiments in this thesis fail to provide a comprehensive explanation for why in these arteries substrate deficient iNOS is not generating superoxide. In the discussion of **Chapter 7**, it was suggested that iNOS might be generating superoxide, but because endothelium-derived NO in these arteries was less prone to destruction by superoxide then this source of superoxide had no significant effect on vascular responsiveness. This hypothesis was based on the finding that in endothelium-intact aortic rings from sham-operated but not CHF rats endothelium-derived NO was destroyed by endogenous or exogenous superoxide production within organ bath.

8.2 Future studies

Having considered the results, there are now additional studies that should be carried out to exploit the findings of this thesis and to further enhance the understanding of the role of iNOS and superoxide in the cardiovascular system in CHF. The crucial finding here is that in small mesenteric arteries from rats with CHF, iNOS generates superoxide rather NO, perhaps because of a deficiency in its substrate. These conclusions are based on pharmacological observations and are substantiated by previous biochemical studies showing that iNOS generates superoxide when deficient in L-arginine (Xia *et al.*, 1998a). Despite this compelling evidence, direct measurement of superoxide generation by iNOS in the presence and absence of

1400W and L-arginine would clearly enhance the impact of this hypothesis. Similarly, experiments directly measuring L-arginine levels within these arteries could strengthen this hypothesis. The most obvious progression from this thesis would be to establish if the findings presented in this thesis using a rat model of CHF are mirrored in clinical CHF. One viable option would be to isolate resistance arteries from gluteal biopsies from patients with CHF and perform functional experiments using the perfusion myograph.

As discussed, this thesis presents some important differences between small mesenteric arteries and thoracic aortae in this model of CHF with respect to the roles of iNOS and superoxide in modulating vascular function. Additional studies are warranted to substantiate these differences. In particular, experiments are required to elucidate why substrate deficient iNOS is generating superoxide in small mesenteric arteries but not in thoracic aortae. Furthermore, future studies are necessary to investigate and substantiate the finding that endothelium-derived NO in thoracic aortae from CHF rats appears to be less susceptible to destruction by superoxide than thoracic aortae from sham-operated rats.

In this model of CHF, it is unclear why iNOS is substrate deficient. A recent study observed a 76% reduction in mRNA expression for the cationic amino acid transporter responsible for the transportation of L-arginine into cells, in peripheral mononuclear cells from patients with CHF (Kaye *et al.*, 2000). This finding suggests that the uptake of L-arginine into cells may be impaired in CHF. In contrast, however, a more recent study demonstrated that L-arginine uptake into thoracic aortae was enhanced in rats with CHF when compared with sham-operated rats (Stathopulos *et al.*, 2001). Future experiments should encompass measuring the uptake of L-arginine into the vasculature in this model of CHF and/or measuring mRNA or protein levels of the membrane transporter.

The pathophysiological mechanisms underlying the induction of iNOS in the peripheral vasculature in this model of CHF were not investigated. As discussed in **Chapter 5**, plasma levels of inflammatory cytokines are elevated in patients with

CHF, and thus may serve as a stimulus for iNOS in the vasculature. To determine if indeed, cytokines are responsible for the expression of iNOS in this model of CHF, future studies should include measuring plasma levels of inflammatory cytokines.

As discussed in Section **1.3.6.3**, under conditions where NO and superoxide are generated, a diffusion-limited, essentially irreversible reaction between equimolar amounts of NO and superoxide results in the formation of peroxynitrite ($ONOO^-$; Beckman & Koppenol, 1996). Low levels of $ONOO^-$ can have beneficial effects on vascular function, mediated via stimulation of guanylate cyclase and generation of cyclic guanosine monophosphate (cGMP; Nossuli *et al.*, 1997). However, at high concentrations $ONOO^-$ is cytotoxic (Crow & Beckman, 1995), causing lipid peroxidation and DNA damage. Moreover, $ONOO^-$ induces apoptosis in cultured cells (Lin *et al.*, 1998) and has been implicated vascular injury associated with endotoxic shock (Szabo *et al.*, 1996) and atherosclerosis (Stroes *et al.*, 1998). In this model of CHF, increased scavenging of endothelium-derived NO by superoxide was deemed responsible for vascular dysfunction, therefore, it is possible that $ONOO^-$ is being formed in these arteries and thus may result in vascular injury. To substantiate this hypothesis, future studies should investigate whether $ONOO^-$ levels are increased in the peripheral vasculature in this model of CHF. This could be achieved by detecting nitrated tyrosine residues, which is widely accepted as a marker for $ONOO^-$ formation, within isolated arteries.

The main bulk of this thesis concentrated on investigating the role of iNOS and superoxide in modulating vascular function in rats with CHF. However, experiments in **Chapter 5** provided some additional information regarding the distribution of iNOS in the heart in this model of CHF. The findings of these experiments provide the impetus for a wealth of future studies, which would hopefully expand the understanding of the role of iNOS and superoxide in modulating the cardiovascular system in CHF. As discussed, immunohistochemical studies in **Chapter 5** revealed that iNOS was exclusively expressed within the LV myocardium in this model of CHF. In the discussion of this chapter, it was hypothesised that mechanical stretch, such as that which occurs during the progressive LV remodelling associated with

CHF, might be a sufficient stimulus to provoke the gene expression of the inflammatory cytokine, tumour necrosis factor-α (TNF-α) within the failing heart. Inflammatory cytokines can induce the expression of iNOS, and therefore it was suggested that mechanical stretch might be the ultimate regulatory factor in inducing iNOS expression within the failing heart. Though provocative this hypothesis requires confirmation. It is clear, therefore, that further studies are required to fully address the relationship between inflammatory cytokines and mechanical stretch in regulating the induction of iNOS in the heart during CHF. By doing so these studies may explain why iNOS expression in the heart is not uniform throughout the heart.

Another important aim of future experiments would be to investigate the functional significance of iNOS expression in the failing heart. As discussed in Section **1.4.2**, the physiological significance of NO on the functioning of the heart is not fully understood. In isolated cardiomyocytes, induction of iNOS by inflammatory cytokines and the subsequent production of large quantities of NO inhibits myocyte contractility (Brady *et al.*, 1992; Brady *et al.*, 1993). Furthermore, the expression of iNOS within the heart during endotoxic shock is associated with depressed cardiac function (Schulz *et al.*, 1995; Sun *et al.*, 1997). There is some evidence that NO may inhibit the positive inotropic response to β-adrenergic stimulation (Balligand *et al.*, 1993). Furthermore, increased NO production by iNOS has been implicated in the hyporesponsiveness of the myocardium to β-adrenergic stimulation in patients with LV dysfunction (Hare *et al.*, 1998). Taken together these results may suggest, therefore, that iNOS expression in the failing heart may play a pathological role in modulating cardiac function. However, it has been demonstrated that endogenous eNOS-derived NO released during diastole results in a faster onset of LV relaxation. Indeed, as discussed in Section **1.4.2.4** it has been postulated that the release of NO during diastole serves to increase diastolic distensibility during the cardiac cycle. On the basis of this hypothesis, therefore, increased NO production in the failing heart may play a beneficial role in LV dysfunction associated with CHF by maintaining the Frank-Starling mechanism. Indeed, a recent study revealed that in patients with CHF, an increase in iNOS gene expression augmented LV stroke volume and LV stroke work because of a NO-mediated rightward shift of the diastolic LV pressure-

volume relation and a concomitant increase in LV preload reserve (Heymes *et al.*, 1999). This hypothesis remains an intriguing possibilty, however, experiments presented in this thesis should not be ignored when evaluating whether iNOS plays an overall beneficial or detrimental role in modulating cardiac function in CHF. In particular, it may be that as with the peripheral vasculature, iNOS expressed in the failing heart is substrate deficient. If so, then, iNOS expression in the heart may be associated with increased generation of superoxide. This could in turn reduce the bioavailability of eNOS-derived NO and result in a worsening of LV function. It is clear, therefore, that extensive studies are necessary to address the role of iNOS and superoxide in modulating cardiac function.

8.3 Clinical Implications

The findings of this thesis present evidence that iNOS may play an important role in the endothelial dysfunction and raised PVR associated with CHF. Although further studies are necessary to determine if these experimental findings are mirrored in clinical CHF, the findings reported here suggest that dysfunctional iNOS may be a viable target for future drug therapies in CHF.

Inhibition of iNOS may be a viable therapeutic option, particular so, with the emergence of an increasing amount of compounds that offer selectivity for iNOS over eNOS (Garvey *et al.*, 1997; McMillan *et al.*, 2000). Another option may be to increase the amount of substrate available to iNOS. Increasing the availability of L-arginine may prevent the production of superoxide by iNOS in resistance arteries and thus increase the bioavailability of eNOS-derived NO. Furthermore, L-arginine supplementation may facilitate the synthesis of NO by iNOS, which may in turn reduce PVR further. In addition to its potential benefits in lowering PVR, increasing the generation of NO from iNOS in conductance arteries may increase the elasticity of these arteries. This may in turn, have beneficial effects on the overall mechanical efficiency of the cardiovascular system. Recent studies investigating therapeutic options to restore endothelial function in CHF revealed that L-arginine supplementation may be beneficial. In clinical CHF, intravenous infusion of

L-arginine increased cardiac output (Goumas *et al.*, 2001) and increased NO-mediated relaxations to acetylcholine (Prior *et al.*, 2000). Furthermore, chronic administration of L-arginine increased forearm blood flow during exercise, improved functional status and arterial compliance (Rector *et al.*, 1996). Larger clinical studies are required to substantiate the findings of these clinical studies and to further evaluate the benefit of L-arginine supplementation in the treatment of CHF.

As discussed, the underlying mechanisms responsible for the induction of iNOS in the cardiovascular system in this model of CHF were not investigated. However, compelling evidence suggests that inflammatory cytokines, such as TNF-α, may be responsible. Therapies directed against this cytokine may represent a novel approach to CHF management, particular so since TNF-α has been implicated in a number of other pathophysiological processes that are thought important to the progression of CHF (see Section **1.5.6.2**). Anti-TNF-α strategies may target the mechanisms of immune activation, the intracellular pathways regulating TNF-α production or the fate of TNF-α once released into the circulation (Torre-Amione *et al.*, 2000). A recent study demonstrated that treatment of transgenic mice overexpressing TNF-α with an adenoviral vector expressing soluble TNF-α receptor type 1 preserved myocardial function (Li *et al.*, 2000). Furthermore, Deswal *et al.* (1997) reported preliminary results from a phase I study of a recombinant human TNF-receptor-fusion protein, which binds to TNF-α and inactivates it, in patients with functional class III CHF. In this study, circulating concentrations of TNF-α were reduced on the first day of therapy and remained low for 2 weeks. Moreover, the treatment was well tolerated and was associated with an improvement in symptoms. These encouraging results have led to phase II placebo-controlled studies, which are underway and are expected to be complete in the next two years (Torre-Amione *et al.*, 2000).

The findings presented here and from other studies suggest a role for increased superoxide production in the pathogenesis of CHF (see Section **1.5.6.3**). Raising endogenous levels of superoxide dismutase may therefore prove beneficial in the treatment of CHF. There have been some studies evaluating the potential of conenzyme Q10 (CQ10), a natural cofactor in mitochondrial respiration and

superoxide scavenger. Anecdotal reports and uncontrolled studies (Langsjoen & Folkers, 1990) have shown beneficial effects of CQ10 in patients with CHF. However, there have been only limited controlled studies. A recent study, however, demonstrated that CQ10 had no effect on ejection fraction or exercise capacity in patients with class III CHF (Khatta *et al.*, 2000). Similar studies have been carried out to evaluate the benefit of Vitamin C and E in the treatment of CHF. Eilis *et al.* (2000) revealed that both chronic and acute administration of Vitamin C reduced oxidative stress and increased flow-dependent vasodilation in patients with CHF. A recent clinical study, revealed that supplementation of Vitamin E did not result in any significant improvement in prognostic or functional indexes of CHF or in the quality of life of patients with CHF (Keith *et al.*, 2001). Notably, however, some drugs that have been found to be effective in the treatment of CHF may have important antioxidant properties. For example, the β-adrenergic antagonist carvediol and one of its metabolites exert potent antioxidant properties *in vitro* that may be realised at therapeutic concentrations in patients with CHF (Yue *et al.*, 1992). Furthermore, there is evidence that carvediol can reduce oxidative stress in patients with CHF. Angiotensin-converting inhibitors have also been shown to scavenge free radicals *in vitro* (Suzuki *et al.*, 1993a). From this discussion, it is clear that further studies are warranted to further evaluate the benefit of antioxidant therapy in the management of CHF.

8.4 Conclusion

In conclusion, this thesis presents an interesting new facet to the role of iNOS in modulating vascular function in CHF. In particular, findings of this thesis reveal that substrate deficient iNOS-derived superoxide may play an important role in the endothelial dysfunction and raised PVR associated with CHF. Although further research is required at both an experimental and clinical level to substantiate these findings, this thesis suggests that targeting the NO system, in particular the activity of iNOS, may prove beneficial in lowering PVR and ultimately slowing the progression of CHF.

Appendix

Buffers

All salts were purchased from BDH, U.K.

Krebs Henseleit solution

Composition in mM:
sodium chloride, 118; potassium chloride, 4.7; calcium chloride, 2.5, magnesium sulphate, 1.2, potassium di-hydrogen orthophosphate, 1.2; sodium carbonate, 25 and glucose 5.5

Phosphate Buffered Saline (PBS) pH 7.6

1. Dissolve 12.7g di-sodium hydrogen orthophosphate in 80 ml deionised H_2O. Microwave for 30 seconds.
2. In a separate container, dissolve 1.7g of sodium di-hydrogen orthophosphate in 80 ml deionised H_2O.
3. Add both solutions to 800 ml deionised H_2O and pH to 7.6 with concentrated HCl.

Make up final volume to 1L with deionised H_2O.

Tris-Buffered Saline (TBS) pH 7.8

1. Dissolve 6.04g of tris in 80 ml deionised H_2O. Add 2.77 ml of concentrated HCl.
2. In a separate container, dissolve 8.1 g of sodium chloride in 900 ml deionised H_2O.

Mix the 2 solutions, adjust to pH 7.8 using concentrated HCl and make up to 1L

Aminopropylethoxysaline (TESPA) slide coating

Bathe slides for 10 seconds in each of the following:

1. 10% HCl in 70% ethanol
2. deionised H_2O
3. 100% acetone

Air dry the slides, then 10 seconds in each of the following:

4. 2% TESPA in acetone
5. 100% acetone
6. 100% acetone

Slides are air dried again, can be stored for one month in airtight containers

Stains

van Gieson's collagen stain

To 50 ml of deionised H_2O, add:

1. 50 ml of saturated aqueous picric acid solution (BDH, U.K)
2. 9 ml of 1% aqueous acid fuschin solution (BDH, U.K.)

References

ABU-SOUD, H.M., FELDMAN, P.L., CLARK, P. & STUEHR, D.J. (1994). Electron Transfer in the Nitric-Oxide Synthases. Characterization of L-Arginine Analogs That Block Heme Iron Reduction. *J Biol Chem*, **269**, 32318-26.

ANKER, S.D., CHUA, T.P., PONIKOWSKI, P., HARRINGTON, D., SWAN, J.W., KOX, W.J., POOLE-WILSON, P.A. & COATS, A.J. (1997). Hormonal Changes and Catabolic/Anabolic Imbalance in Chronic Heart Failure and Their Importance for Cardiac Cachexia. *Circulation*, **96**, 526-34.

ARNOLD, J.M., MARCHIORI, G.E., IMRIE, J.R., BURTON, G.L., PFLUGFELDER, P.W. & KOSTUK, W.J. (1991). Large Artery Function in Patients with Chronic Heart Failure. Studies of Brachial Artery Diameter and Hemodynamics. *Circulation*, **84**, 2418-25.

AYAJIKI, K., KINDERMANN, M., HECKER, M., FLEMING, I. & BUSSE, R. (1996). Intracellular pH and Tyrosine Phosphorylation but Not Calcium Determine Shear Stress-Induced Nitric Oxide Production in Native Endothelial Cells. *Circ Res*, **78**, 750-8.

BAEK, K.J., THIEL, B.A., LUCAS, S. & STUEHR, D.J. (1993). Macrophage Nitric Oxide Synthase Subunits. Purification, Characterization, and Role of Prosthetic Groups and Substrate in Regulating Their Association into a Dimeric Enzyme. *J Biol Chem*, **268**, 21120-9.

BAGGIA, S., PERKINS, K. & GREENBERG, B. (1997). Endothelium-Dependent Relaxation is Not Uniformly Impaired in Chronic Heart Failure. *J Cardiovasc Pharmacol*, **29**, 389-96.

BALLIGAND, J.L., KELLY, R.A., MARSDEN, P.A., SMITH, T.W. & MICHEL, T. (1993). Control of Cardiac Muscle Cell Function by an Endogenous Nitric Oxide Signaling System. *Proc Natl Acad Sci U S A*, **90**, 347-51.

BALLIGAND, J.L., UNGUREANU-LONGROIS, D., SIMMONS, W.W., PIMENTAL, D., MALINSKI, T.A., KAPTURCZAK, M., TAHA, Z., LOWENSTEIN, C.J., DAVIDOFF, A.J., KELLY, R.A. & ET AL. (1994). Cytokine-Inducible Nitric Oxide Synthase (iNOS) Expression in Cardiac Myocytes. Characterization and Regulation of iNOS Expression and Detection of iNOS Activity in Single Cardiac Myocytes in Vitro. *J Biol Chem*, **269**, 27580-8.

BALLIGAND, J.L., UNGUREANU-LONGROIS, D., SIMMONS, W.W., KOBZIK, L., LOWENSTEIN, C.J., LAMAS, S., KELLY, R.A., SMITH, T.W. & MICHEL, T. (1995). Induction of No Synthase in Rat Cardiac Microvascular Endothelial Cells by Il-1 Beta and IFN-δ. *Am J Physiol*, **268**, H1293-303.

BANK, A.J., RECTOR, T.S., TSCHUMPERLIN, L.K., KRAEMER, M.D., LETOURNEAU, J.G. & KUBO, S.H. (1994). Endothelium-Dependent Vasodilation of Peripheral Conduit Arteries in Patients with Heart Failure. *J Card Fail*, **1**, 35-43.

BANK, A.J. (1997). Physiologic Aspects of Drug Therapy and Large Artery Elastic Properties. *Vasc Med*, **2**, 44-50.

BARTUNEK, J., SHAH, A.M., VANDERHEYDEN, M. & PAULUS, W.J. (1997). Dobutamine Enhances Cardiodepressant Effects of Receptor-Mediated Coronary Endothelial Stimulation. *Circulation*, **95**, 90-6.

BAUERSACHS, J., BOULOUMIE, A., FRACCAROLLO, D., HU, K., BUSSE, R. & ERTL, G. (1999). Endothelial Dysfunction in Chronic Myocardial Infarction Despite Increased Vascular Endothelial Nitric Oxide Synthase and Soluble Guanylate Cyclase Expression: Role of Enhanced Vascular Superoxide Production. *Circulation*, **100**, 292-8.

BECKMAN, J.S., BECKMAN, T.W., CHEN, J., MARSHALL, P.A. & FREEMAN, B.A. (1990). Apparent Hydroxyl Radical Production by Peroxynitrite: Implications for Endothelial Injury from Nitric Oxide and Superoxide. *Proc Natl Acad Sci U S A*, **87**, 1620-4.

BECKMAN, J.S. & KOPPENOL, W.H. (1996). Nitric Oxide, Superoxide, and Peroxynitrite: The Good, the Bad, and Ugly. *Am J Physiol*, **271**, C1424-37.

BELCH, J.J., BRIDGES, A.B., SCOTT, N. & CHOPRA, M. (1991). Oxygen Free Radicals and Congestive Heart Failure. *British Heart Journal*, **65**, 245-8.

BELLA, J.N., ROMAN, M.J., PINI, R., SCHWARTZ, J.E., PICKERING, T.G. & DEVEREUX, R.B. (1999). Assessment of Arterial Compliance by Carotid Midwall Strain-Stress Relation in Hypertension. *Hypertension*, **33**, 793-9.

BELTRAMI, C.A., FINATO, N., ROCCO, M., FERUGLIO, G.A., PURICELLI, C., CIGOLA, E., QUAINI, F., SONNENBLICK, E.H., OLIVETTI, G. & ANVERSA, P. (1994). Structural Basis of End-Stage Failure in Ischemic Cardiomyopathy in Humans. *Circulation*, **89**, 151-63.

BJORLING, D.E., SABAN, R., TENGOWSKI, M.W., GRUEL, S.M. & RAO, V.K. (1992). Removal of Venous Endothelium with Air. *J Pharmacol Toxicol Methods*, **28**, 149-57.

BOGLE, R.G., MONCADA, S., PEARSON, J.D. & MANN, G.E. (1992). Identification of Inhibitors of Nitric Oxide Synthase That Do Not Interact with the Endothelial Cell L-Arginine Transporter. *Br J Pharmacol*, **105**, 768-70.

BOLOTINA, V.M., NAJIBI, S., PALACINO, J.J., PAGANO, P.J. & COHEN, R.A. (1994). Nitric Oxide Directly Activates Calcium-Dependent Potassium Channels in Vascular Smooth Muscle. *Nature*, **368**, 850-3.

BOULOUMIE, A., BAUERSACHS, J., LINZ, W., SCHOLKENS, B.A., WIEMER, G., FLEMING, I. & BUSSE, R. (1997). Endothelial Dysfunction Coincides with an Enhanced Nitric Oxide Synthase Expression and Superoxide Anion Production. *Hypertension*, **30**, 934-41.

BOZKURT, B., KRIBBS, S.B., CLUBB, F.J., JR., MICHAEL, L.H., DIDENKO, V.V., HORNSBY, P.J., SETA, Y., ORAL, H., SPINALE, F.G. & MANN, D.L. (1998). Pathophysiologically Relevant Concentrations of Tumor Necrosis Factor-α Promote Progressive Left Ventricular Dysfunction and Remodeling in Rats. *Circulation*, **97**, 1382-91.

BRADY, A.J., POOLE-WILSON, P.A., HARDING, S.E. & WARREN, J.B. (1992). Nitric Oxide Production within Cardiac Myocytes Reduces Their Contractility in Endotoxemia. *Am J Physiol*, **263**, H1963-6.

BRADY, A.J. (1993). Nitric Oxide Synthase Activities in Human Myocardium. *Lancet*, **341**, 448.

BRADY, A.J., WARREN, J.B., POOLE-WILSON, P.A., WILLIAMS, T.J. & HARDING, S.E. (1993). Nitric Oxide Attenuates Cardiac Myocyte Contraction. *Am J Physiol*, **265**, H176-82.

BREDT, D.S. & SNYDER, S.H. (1990). Isolation of Nitric Oxide Synthetase, a Calmodulin-Requiring Enzyme. *Proc Natl Acad Sci U S A*, **87**, 682-5.

BREDT, D.S., HWANG, P.M., GLATT, C.E., LOWENSTEIN, C., REED, R.R. & SNYDER, S.H. (1991). Cloned and Expressed Nitric Oxide Synthase Structurally Resembles Cytochrome P-450 Reductase. *Nature*, **351**, 714-8.

BREDT, D.S., FERRIS, C.D. & SNYDER, S.H. (1992). Nitric Oxide Synthase Regulatory Sites. Phosphorylation by Cyclic AMP-Dependent Protein Kinase, Protein Kinase C, and Calcium/Calmodulin Protein Kinase; Identification of Flavin and Calmodulin Binding Sites. *J Biol Chem*, **267**, 10976-81.

BROWN, G.C. (1995). Nitric Oxide Regulates Mitochondrial Respiration and Cell Functions by Inhibiting Cytochrome Oxidase. *FEBS Lett*, **369**, 136-9.

BROWN, L.A., NUNEZ, D.J., BROOKES, C.I. & WILKINS, M.R. (1995). Selective Increase in Endothelin-1 and Endothelin A Receptor Subtype in the Hypertrophied Myocardium of the Aorto-Venacaval Fistula Rat. *Cardiovasc Res*, **29**, 768-74.

BRYANT, D., BECKER, L., RICHARDSON, J., SHELTON, J., FRANCO, F., PESHOCK, R., THOMPSON, M. & GIROIR, B. (1998). Cardiac Failure in Transgenic Mice with Myocardial Expression of Tumor Necrosis Factor-α. *Circulation*, **97**, 1375-81.

BUGA, G.M., GRISCAVAGE, J.M., ROGERS, N.E. & IGNARRO, L.J. (1993). Negative Feedback Regulation of Endothelial Cell Function by Nitric Oxide. *Circ Res*, **73**, 808-12.

BURKE, T.M. & WOLIN, M.S. (1987). Hydrogen Peroxide Elicits Pulmonary Arterial Relaxation and Guanylate Cyclase Activation. *Am J Physiol*, **252**, H721-32.

BURRELL, L.M., RISVANIS, J., JOHNSTON, C.I., NAITOH, M. & BALDING, L.C. (2000). Vasopressin Receptor Antagonism-α Therapeutic Option in Heart Failure and Hypertension. *Exp Physiol*, **85**, 259S-265S.

BUSH, P.A., GONZALEZ, N.E. & IGNARRO, L.J. (1992). Biosynthesis of Nitric Oxide and Citrulline from L-Arginine by Constitutive Nitric Oxide Synthase Present in Rabbit Corpus Cavernosum. *Biochem Biophys Res Commun*, **186**, 308-14.

BUTT, E., BERNHARDT, M., SMOLENSKI, A., KOTSONIS, P., FROHLICH, L.G., SICKMANN, A., MEYER, H.E., LOHMANN, S.M. & SCHMIDT, H.H. (2000). Endothelial Nitric-Oxide Synthase (Type III) Is Activated and Becomes Calcium Independent Upon Phosphorylation by Cyclic Nucleotide-Dependent Protein Kinases. *J Biol Chem*, **275**, 5179-87.

BUTTERY, L.D., EVANS, T.J., SPRINGALL, D.R., CARPENTER, A., COHEN, J. & POLAK, J.M. (1994). Immunochemical Localization of Inducible Nitric Oxide Synthase in Endotoxin-Treated Rats. *Lab Invest*, **71**, 755-64.

CALDERONE, A., THAIK, C.M., TAKAHASHI, N., CHANG, D.L.F. & COLUCCI, W.S. (1998). Nitric Oxide, Atrial Natriuretic Peptide, and Cyclic GMP Inhibit the Growth-Promoting Effects of Norepinephrine in Cardiac Myocytes and Fibroblasts. *J Clin Invest*, **101**, 812-8.

CAO, L. & GARDNER, D.G. (1995). Natriuretic Peptides Inhibit DNA Synthesis in Cardiac Fibroblasts. *Hypertension*, **25**, 227-34.

CARVALHO, M.H.C & FURCHGOTT, R.F. (1981). Vasodilatation of the rabbit mesenteric vascular bed by acetylcholine and A23187. *Pharmacologist*, **23**, 223.

CARVAJAL, J.A., GERMAIN, A.M., HUIDOBRO-TORO, J.P. & WEINER, C.P. (2000). Molecular Mechanism of cGMP-Mediated Smooth Muscle Relaxation. *J Cell Physiol*, **184**, 409-20.

CARVILLE, C., ADNOT, S., SEDIAME, S., BENACERRAF, S., CASTAIGNE, A., CALVO, F., DE CREMOU, P. & DUBOIS-RANDE, J.L. (1998). Relation between Impairment in Nitric Oxide Pathway and Clinical Status in Patients with Congestive Heart Failure. *J Cardiovasc Pharmacol*, **32**, 562-70.

CASTAGNOLI, C., STELLA, M., BERTHOD, C., MAGLIACANI, G. & RICHIARDI, P.M. (1993). TNF Production and Hypertrophic Scarring. *Cell Immunol*, **147**, 51-63.

CAVERO, P.G., MILLER, W.L., HEUBLEIN, D.M., MARGULIES, K.B. & BURNETT, J.C., JR. (1990). Endothelin in Experimental Congestive Heart Failure in the Anesthetized Dog. *Am J Physiol*, **259**, F312-7.

CEDERQVIST, B., WIKLUND, N.P., PERSSON, M.G. & GUSTAFSSON, L.E. (1991). Modulation of Neuroeffector Transmission in the Guinea Pig Pulmonary Artery by Endogenous Nitric Oxide. *Neurosci Lett*, **127**, 67-9.

CHENG, W., LI, B., KAJSTURA, J., LI, P., WOLIN, M.S., SONNENBLICK, E.H., HINTZE, T.H., OLIVETTI, G. & ANVERSA, P. (1995). Stretch-Induced Programmed Myocyte Cell Death. *J Clin Invest*, **96**, 2247-59.

CHO, H.J., XIE, Q.W., CALAYCAY, J., MUMFORD, R.A., SWIDEREK, K.M., LEE, T.D. & NATHAN, C. (1992). Calmodulin is a Subunit of Nitric Oxide Synthase from Macrophages. *J Exp Med*, **176**, 599-604.

CLEMENTI, E., BROWN, G.C., FEELISCH, M. & MONCADA, S. (1998). Persistent Inhibition of Cell Respiration by Nitric Oxide: Crucial Role of S-Nitrosylation of Mitochondrial Complex I and Protective Action of Glutathione. *Proc Natl Acad Sci U S A*, **95**, 7631-6.

COCKCROFT, J.R., O'KANE, K.P. & WEBB, D.J. (1995). Tissue Angiotensin Generation and Regulation of Vascular Tone. *Pharmacol Ther*, **65**, 193-213.

CODY, R.J., ATLAS, S.A., LARAGH, J.H., KUBO, S.H., COVIT, A.B., RYMAN, K.S., SHAKNOVICH, A., PONDOLFINO, K., CLARK, M., CAMARGO, M.J. & ET AL. (1986). Atrial Natriuretic Factor in Normal Subjects and Heart Failure Patients. Plasma Levels and Renal, Hormonal, and Hemodynamic Responses to Peptide Infusion. *J Clin Invest*, **78**, 1362-74.

COLUCCI, W.S. (1997). Molecular and Cellular Mechanisms of Myocardial Failure. *Am J Cardiol*, **80**, 15L-25L.

COMINI, L., BACHETTI, T., GAIA, G., PASINI, E., AGNOLETTI, L., PEPI, P., CECONI, C., CURELLO, S. & FERRARI, R. (1996). Aorta and Skeletal Muscle NO Synthase Expression in Experimental Heart Failure. *J Mol Cell Cardiol*, **28**, 2241-8.

CONRAD, C.H., BROOKS, W.W., HAYES, J.A., SEN, S., ROBINSON, K.G. & BING, O.H. (1995). Myocardial Fibrosis and Stiffness with Hypertrophy and Heart Failure in the Spontaneously Hypertensive Rat. *Circulation*, **91**, 161-70.

CORNWELL, T.L., PRYZWANSKY, K.B., WYATT, T.A. & LINCOLN, T.M. (1991). Regulation of Sarcoplasmic Reticulum Protein Phosphorylation by Localized Cyclic GMP-Dependent Protein Kinase in Vascular Smooth Muscle Cells. *Mol Pharmacol*, **40**, 923-31.

COWIE, M.R., MOSTERD, A., WOOD, D.A., DECKERS, J.W., POOLE-WILSON, P.A., SUTTON, G.C. & GROBBEE, D.E. (1997). The Epidemiology of Heart Failure. *Eur Heart J*, **18**, 208-25.

CRAVEN, P.A. & DERUBERTIS, F.R. (1978). Restoration of the Responsiveness of Purified Guanylate Cyclase to Nitrosoguanidine, Nitric Oxide, and Related Activators by Heme and Hemeproteins. Evidence for Involvement of the Paramagnetic Nitrosyl-Heme Complex in Enzyme Activation. *J Biol Chem*, **253**, 8433-43.

CRISCIONE, L., MULLER, K. & FORNEY PRESCOTT, M. (1984). Endothelial Cell Loss Enhances the Pressor Response in Resistance Vessels. *J Hypertens Suppl*, **2**, S441-4.

CROFT, J.B., GILES, W.H., POLLARD, R.A., KEENAN, N.L., CASPER, M.L. & ANDA, R.F. (1999). Heart Failure Survival among Older Adults in the United States: A Poor Prognosis for an Emerging Epidemic in the Medicare Population. *Arch Intern Med*, **159**, 505-10.

CROW, J.P. & BECKMAN, J.S. (1995). The Role of Peroxynitrite in Nitric Oxide-Mediated Toxicity. *Curr Top Microbiol Immunol*, **196**, 57-73.

DANSER, A.H., SARIS, J.J., SCHUIJT, M.P. & VAN KATS, J.P. (1999). Is There a Local Renin-Angiotensin System in the Heart? *Cardiovasc Res*, **44**, 252-65.

DE BELDER, A.J., RADOMSKI, M.W., WHY, H.J., RICHARDSON, P.J., BUCKNALL, C.A., SALAS, E., MARTIN, J.F. & MONCADA, S. (1993). Nitric Oxide Synthase Activities in Human Myocardium. *Lancet*, **341**, 84-5.

DESWAL, A., SETA, Y., BLOSCH, C.M., MANN, D.L. (1997). A phase I trial of tumour necrosis factor receptor (p75) fusion protein (TNFR:Fc) in patients with advanced heart failure. *Circulation*, **96**, I-323

DEISHER, T.A., GINSBURG, R., FOWLER, M.B., BILLINGHAM, M.E. & BRISTOW, M.R. (1995). Spontaneous Reversibility of Catecholamine-Induced Cardiotoxicity in Rats. *Am J Cardiovasc Pathol*, **5**, 79-88.

DIAZ-VELEZ, C.R., GARCIA-CASTINEIRAS, S., MENDOZA-RAMOS, E. & HERNANDEZ-LOPEZ, E. (1996). Increased Malondialdehyde in Peripheral Blood of Patients with Congestive Heart Failure. *American Heart Journal*, **131**, 146-52.

DOBRIN, P.B. & ROVICK, A.A. (1969). Influence of Vascular Smooth Muscle on Contractile Mechanics and Elasticity of Arteries. *Am J Physiol*, **217**, 1644-51.

DOGGRELL, S.A. & BROWN, L. (1998). Rat Models of Hypertension, Cardiac Hypertrophy and Failure. *Cardiovasc Res*, **39**, 89-105.

DREXLER, H., HAYOZ, D., MUNZEL, T., HORNIG, B., JUST, H., BRUNNER, H.R. & ZELIS, R. (1992). Endothelial Function in Chronic Congestive Heart Failure. *American Journal of Cardiology*, **69**, 1596-601.

DREXLER, H. & LU, W. (1992). Endothelial Dysfunction of Hindquarter Resistance Vessels in Experimental Heart Failure. *Am J Physiol*, **262**, H1640-5.

DREXLER, H., KASTNER, S., STROBEL, A., STUDER, R., BRODDE, O.E. & HASENFUSS, G. (1998). Expression, Activity and Functional Significance of Inducible Nitric Oxide Synthase in the Failing Human Heart. *J Am Coll Cardiol*, **32**, 955-63.

DREXLER, H. & HORNIG, B. (1999). Endothelial Dysfunction in Human Disease. *J Mol Cell Cardiol*, **31**, 51-60.

DUDEK, R.R., WILDHIRT, S., CONFORTO, A., PINTO, V., SUZUKI, H., WINDER, S. & BING, R.J. (1995). Immunohistochemistry in the Identification of Nitric Oxide Synthase Isoenzymes in Myocardial Infarction. *Cardiovascular Research*, **29**, 526-31.

DUPREZ, D.A., DE BUYZERE, M.L., RIETZSCHEL, E.R., TAES, Y., CLEMENT, D.L., MORGAN, D. & COHN, J.N. (1998). Inverse Relationship between Aldosterone and Large Artery Compliance in Chronically Treated Heart Failure Patients. *Eur Heart J*, **19**, 1371-6.

EBIHARA, Y. & KARMAZYN, M. (1996). Inhibition of β- but Not α_1-Mediated Adrenergic Responses in Isolated Hearts and Cardiomyocytes by Nitric Oxide and 8-Bromo Cyclic GMP. *Cardiovasc Res*, **32**, 622-9.

ELBORN, J.S., STANFORD, C.F. & NICHOLLS, D.P. (1989). Effect of Flosequinan on Exercise Capacity and Symptoms in Severe Heart Failure. *Br Heart J*, **61**, 331-5.

ELLIS, G.R., ANDERSON, R.A., LANG, D., BLACKMAN, D.J., MORRIS, R.H., MORRIS-THURGOOD, J., MCDOWELL, I.F., JACKSON, S.K., LEWIS, M.J. & FRENNEAUX, M.P. (2000). Neutrophil Superoxide Anion--Generating Capacity, Endothelial Function and Oxidative Stress in Chronic Heart Failure: Effects of Short- and Long-Term Vitamin C Therapy. *J Am Coll Cardiol*, **36**, 1474-82.

ELSNER, D., MUNTZE, A., KROMER, E.P. & RIEGGER, G.A. (1991). Systemic Vasoconstriction Induced by Inhibition of Nitric Oxide Synthesis Is Attenuated in Conscious Dogs with Heart Failure. *Cardiovascular Research*, **25**, 438-40.

ENTMAN, M.L., MICHAEL, L., ROSSEN, R.D., DREYER, W.J., ANDERSON, D.C., TAYLOR, A.A. & SMITH, C.W. (1991). Inflammation in the Course of Early Myocardial Ischemia. *Faseb J*, **5**, 2529-37.

FALK, E. & SHAH, P.K. (1996). Pathology of acute ischaemia syndromes. In: *Acute myocardial infarction and other acute ischaemic syndromes*. Ch. 3, Edition 8, ed. Calliff, R.M., Mosby.

FALLOON, B.J., BUND, S.J., TULIP, J.R. & HEAGERTY, A.M. (1993). *In vitro* Perfusion Studies of Resistance Artery Function in Genetic Hypertension. *Hypertension*, **22**, 486-95.

FAULKNER, K.M., LIOCHEV, S.I. & FRIDOVICH, I. (1994). Stable Mn(III) Porphyrins Mimic Superoxide Dismutase *in vitro* and Substitute for it *in vivo*. *J Biol Chem*, **269**, 23471-6.

FERON, O., SALDANA, F., MICHEL, J.B. & MICHEL, T. (1998). The Endothelial Nitric-Oxide Synthase-Caveolin Regulatory Cycle. *J Biol Chem*, **273**, 3125-8.

FERRARI, R. & AGNOLETTI, G. (1989). Atrial Natriuretic Peptide: Its Mechanism of Release from the Atrium. *Int J Cardiol*, **24**, 137-49.

FERRARI, R., BACHETTI, T., CONFORTINI, R., OPASICH, C., FEBO, O., CORTI, A., CASSANI, G. & VISIOLI, O. (1995). Tumor Necrosis Factor Soluble Receptors in Patients with Various Degrees of Congestive Heart Failure. *Circulation*, **92**, 1479-86.

FISSLTHALER, B., DIMMELER, S., HERMANN, C., BUSSE, R. & FLEMING, I. (2000). Phosphorylation and Activation of the Endothelial Nitric Oxide Synthase by Fluid Shear Stress. *Acta Physiol Scand*, **168**, 81-8.

FLEMING, I., GRAY, G.A., SCHOTT, C. & STOCLET, J.C. (1991). Inducible but not Constitutive Production of Nitric Oxide by Vascular Smooth Muscle Cells. *Eur J Pharmacol*, **200**, 375-6.

FLEMING, I., BAUERSACHS, J., SCHAFER, A., SCHOLZ, D., ALDERSHVILE, J. & BUSSE, R. (1999). Isometric Contraction Induces the Ca^{2+}-Independent Activation of the Endothelial Nitric Oxide Synthase. *Proc Natl Acad Sci U S A*, **96**, 1123-8.

FLORAS, J.S. (1993). Clinical Aspects of Sympathetic Activation and Parasympathetic Withdrawal in Heart Failure. *J Am Coll Cardiol*, **22**, 72A-84A.

FONG, Y., MOLDAWER, L.L., MARANO, M., WEI, H., BARBER, A., MANOGUE, K., TRACEY, K.J., KUO, G., FISCHMAN, D.A., CERAMI, A. & ET AL. (1989). Cachectin/TNF or Il-1 α Induces Cachexia with Redistribution of Body Proteins. *Am J Physiol*, **256**, R659-65.

FONTANA, L., MCNEILL, K.L., RITTER, J.M. & CHOWIENCZYK, P.J. (1999). Effects of Vitamin C and of a Cell Permeable Superoxide Dismutase Mimetic on Acute Lipoprotein Induced Endothelial Dysfunction in Rabbit Aortic Rings. *Br J Pharmacol*, **126**, 730-4.

FÖRSTERMANN, U., CLOSS, E.I., POLLOCK, J.S., NAKANE, M., SCHWARZ, P., GATH, I. & KLEINERT, H. (1994). Nitric Oxide Synthase Isozymes. Characterization, Purification, Molecular Cloning, and Functions. *Hypertension*, **23**, 1121-31.

FRACCAROLLO, D., HU, K., GALUPPO, P., GAUDRON, P. & ERTL, G. (1997). Chronic Endothelin Receptor Blockade Attenuates Progressive Ventricular Dilation and Improves Cardiac Function in Rats with Myocardial Infarction: Possible Involvement of Myocardial Endothelin System in Ventricular Remodeling. *Circulation*, **96**, 3963-73.

FRANCIS, G.S., BENEDICT, C., JOHNSTONE, D.E., KIRLIN, P.C., NICKLAS, J., LIANG, C.S., KUBO, S.H., RUDIN-TORETSKY, E. & YUSUF, S. (1990). Comparison of Neuroendocrine Activation in Patients with Left Ventricular Dysfunction with and without Congestive Heart Failure. A Substudy of the Studies of Left Ventricular Dysfunction (SOLVD). *Circulation*, **82**, 1724-9.

FRANCIS, S.E., HOLDEN, H., HOLT, C.M. & DUFF, G.W. (1998). Interleukin-1 in Myocardium and Coronary Arteries of Patients with Dilated Cardiomyopathy. *J Mol Cell Cardiol*, **30**, 215-23.

FRIDOVICH, I. (1983). Superoxide Radical: An Endogenous Toxicant. *Annu Rev Pharmacol Toxicol*, **23**, 239-57.

FUKUCHI, M., HUSSAIN, S.N. & GIAID, A. (1998). Heterogeneous Expression and Activity of Endothelial and Inducible Nitric Oxide Synthases in End-Stage Human Heart Failure: Their Relation to Lesion Site and β-Adrenergic Receptor Therapy. *Circulation*, **98**, 132-9.

FURCHGOTT, R.F. & ZAWADZKI, J.V. (1980). The Obligatory Role of Endothelial Cells in the Relaxation of Arterial Smooth Muscle by Acetylcholine. *Nature*, **288**, 373-6.

FURUKAWA, K., TAWADA, Y. & SHIGEKAWA, M. (1988). Regulation of the Plasma Membrane Ca^{2+} Pump by Cyclic Nucleotides in Cultured Vascular Smooth Muscle Cells. *J Biol Chem*, **263**, 8058-65.

GABRIEL, A., KUDDUS, R.H., RAO, A.S. & GANDHI, C.R. (1999). Down-Regulation of Endothelin Receptors by Transforming Growth Factor β_1 in Hepatic Stellate Cells. *J Hepatol*, **30**, 440-50.

GACHHUI, R., PRESTA, A., BENTLEY, D.F., ABU-SOUD, H.M., MCARTHUR, R., BRUDVIG, G., GHOSH, D.K. & STUEHR, D.J. (1996). Characterization of the Reductase Domain of Rat Neuronal Nitric Oxide Synthase Generated in the Methylotrophic Yeast Pichia Pastoris. Calmodulin Response is Complete within the Reductase Domain Itself. *J Biol Chem*, **271**, 20594-602.

GARDNER, P.R., NGUYEN, D.D. & WHITE, C.W. (1996). Superoxide Scavenging by Mn(II/III) Tetrakis (1-Methyl-4-Pyridyl) Porphyrin in Mammalian Cells. *Arch Biochem Biophys*, **325**, 20-8.

GARVEY, E.P., OPLINGER, J.A., TANOURY, G.J., SHERMAN, P.A., FOWLER, M., MARSHALL, S., HARMON, M.F., PAITH, J.E. & FURFINE, E.S. (1994). Potent and Selective Inhibition of Human Nitric Oxide Synthases. Inhibition by non-Amino Acid Isothioureas. *J Biol Chem*, **269**, 26669-76.

GARVEY, E.P., OPLINGER, J.A., FURFINE, E.S., KIFF, R.J., LASZLO, F., WHITTLE, B.J. & KNOWLES, R.G. (1997). 1400W is a Slow, Tight Binding, and Highly Selective Inhibitor of Inducible Nitric-Oxide Synthase *in vitro* and *in vivo*. *J Biol Chem*, **272**, 4959-63.

GASTON, B. (1999). Nitric Oxide and Thiol Groups. *Biochim Biophys Acta*, **1411**, 323-33.

GHOSH, D.K. & STUEHR, D.J. (1995). Macrophage NO Synthase: Characterization of Isolated Oxygenase and Reductase Domains Reveals a Head-to-Head Subunit Interaction. *Biochemistry*, **34**, 801-7.

GHOSH, S., GACHHUI, R., CROOKS, C., WU, C., LISANTI, M.P. & STUEHR, D.J. (1998). Interaction between Caveolin-1 and the Reductase Domain of Endothelial Nitric-Oxide Synthase. Consequences for Catalysis. *J Biol Chem*, **273**, 22267-71.

GIANNATTASIO, C., FAILLA, M., STELLA, M.L., MANGONI, A.A., CARUGO, S., POZZI, M., GRASSI, G. & MANCIA, G. (1995). Alterations of Radial Artery Compliance in Patients with Congestive Heart Failure. *Am J Cardiol*, **76**, 381-5.

GIRERD, X., LAURENT, S., PANNIER, B., ASMAR, R. & SAFAR, M. (1991). Arterial Distensibility and Left Ventricular Hypertrophy in Patients with Sustained Essential Hypertension. *Am Heart J*, **122**, 1210-4.

GIROIR, B.P., JOHNSON, J.H., BROWN, T., ALLEN, G.L. & BEUTLER, B. (1992). The Tissue Distribution of Tumor Necrosis Factor Biosynthesis During Endotoxemia. *J Clin Invest*, **90**, 693-8.

GIULIVI, C. (1998). Functional Implications of Nitric Oxide Produced by Mitochondria in Mitochondrial Metabolism. *Biochem J*, **332**, 673-9.

GIVERTZ, M.M. & COLUCCI, W.S. (1998). New Targets for Heart-Failure Therapy: Endothelin, Inflammatory Cytokines, and Oxidative Stress. *Lancet*, **352**.

GOPALAKRISHNA, R., CHEN, Z.H. & GUNDIMEDA, U. (1993). Nitric Oxide and Nitric Oxide-Generating Agents Induce a Reversible Inactivation of Protein Kinase C Activity and Phorbol Ester Binding. *J Biol Chem*, **268**, 27180-5.

GOUMAS, G., TENTOLOURIS, C., TOUSOULIS, D., STEFANADIS, C. & TOUTOUZAS, P. (2001). Therapeutic Modification of the L-Arginine-eNOS Pathway in Cardiovascular Diseases. *Atherosclerosis*, **154**, 255-67.

GRAY, G.A., SCHOTT, C., JULOU-SCHAEFFER, G., FLEMING, I., PARRATT, J.R. & STOCLET, J.C. (1991). The Effect of Inhibitors of the L-Arginine/Nitric Oxide Pathway on Endotoxin-Induced Loss of Vascular Responsiveness in Anaesthetized Rats. *Br J Pharmacol*, **103**, 1218-24.

GRAY, G.A., MICKLEY, E.J., WEBB, D.J. & MCEWAN, P.E. (2000). Localization and Function of ET-1 and ET Receptors in Small Arteries Post-Myocardial Infarction: Upregulation of Smooth Muscle ET(B) Receptors That Modulate Contraction. *Br J Pharmacol*, **130**, 1735-44.

GRAY, M.O., LONG, C.S., KALINYAK, J.E., LI, H.T. & KARLINER, J.S. (1998). Angiotensin II Stimulates Cardiac Myocyte Hypertrophy Via Paracrine Release of TGF-β_1 and Endothelin-1 from Fibroblasts. *Cardiovasc Res*, **40**, 352-63.

GREEN, L.C., WAGNER, D.A., GLOGOWSKI, J., SKIPPER, P.L., WISHNOK, J.S. & TANNENBAUM, S.R. (1982). Analysis of Nitrate, Nitrite, and [15^n]Nitrate in Biological Fluids. *Anal Biochem*, **126**, 131-8.

GRIENDLING, K.K., MINIERI, C.A., OLLERENSHAW, J.D. & ALEXANDER, R.W. (1994). Angiotensin II Stimulates NADH and NADPH Oxidase Activity in Cultured Vascular Smooth Muscle Cells. *Circ Res*, **74**, 1141-8.

GRIFFITH, O.W. & STUEHR, D.J. (1995). Nitric Oxide Synthases: Properties and Catalytic Mechanism. *Annu Rev Physiol*, **57**, 707-36.

GRUNFELD, S., HAMILTON, C.A., MESAROS, S., MCCLAIN, S.W., DOMINICZAK, A.F., BOHR, D.F. & MALINSKI, T. (1995). Role of Superoxide in the Depressed Nitric Oxide Production by the Endothelium of Genetically Hypertensive Rats. *Hypertension*, **26**, 854-7.

GRYGLEWSKI, R.J., PALMER, R.M. & MONCADA, S. (1986). Superoxide Anion is Involved in the Breakdown of Endothelium-Derived Vascular Relaxing Factor. *Nature*, **320**, 454-6.

GUPTA, S., MCARTHUR, C., GRADY, C. & RUDERMAN, N.B. (1994). Stimulation of Vascular Na^+-K^+-ATPase Activity by Nitric Oxide: A cGMP-Independent Effect. *Am J Physiol*, **266**, H2146-51.

GUTTERMAN, D.D. (1999). Adventitia-Dependent Influences on Vascular Function. *Am J Physiol*, **277**, H1265-72.

HABIB, F., DUTKA, D., CROSSMAN, D., OAKLEY, C.M. & CLELAND, J.G. (1994). Enhanced Basal Nitric Oxide Production in Heart Failure: Another Failed Counter-Regulatory Vasodilator Mechanism? *Lancet*, **344**, 371-3.

HABIB, F.M., SPRINGALL, D.R., DAVIES, G.J., OAKLEY, C.M., YACOUB, M.H. & POLAK, J.M. (1996). Tumour Necrosis Factor and Inducible Nitric Oxide Synthase in Dilated Cardiomyopathy. *Lancet*, **347**, 1151-5.

HALLIWELL, B. & GUTTERIDGE M.C. (1989). *Free Radicals in biology and medicine*, Edition 2, Oxford, Clarendon Press.

HALPERN, W. & KELLEY, M. (1991). *In vitro* Methodology for Resistance Arteries. *Blood Vessels*, **28**, 245-51.

HAN, X., KOBZIK, L., BALLIGAND, J.L., KELLY, R.A. & SMITH, T.W. (1996). Nitric Oxide Synthase (NOS3)-Mediated Cholinergic Modulation of Ca^{2+} Current in Adult Rabbit Atrioventricular Nodal Cells. *Circ Res*, **78**, 998-1008.

HARE, J.M., GIVERTZ, M.M., CREAGER, M.A. & COLUCCI, W.S. (1998). Increased Sensitivity to Nitric Oxide Synthase Inhibition in Patients with Heart Failure: Potentiation of β-Adrenergic Inotropic Responsiveness. *Circulation*, **97**, 161-6.

HASENFUSS, G. (1998). Animal Models of Human Cardiovascular Disease, Heart Failure and Hypertrophy. *Cardiovasc Res*, **39**, 60-76.

HAYNES, W.G., NOON, J.P., WALKER, B.R. & WEBB, D.J. (1993). L-NMMA Increases Blood Pressure in Man. *Lancet*, **342**, 931-2.

HAYNES, W.G., FERRO, C.J., O'KANE, K.P., SOMERVILLE, D., LOMAX, C.C. & WEBB, D.J. (1996). Systemic Endothelin Receptor Blockade Decreases Peripheral Vascular Resistance and Blood Pressure in Humans. *Circulation*, **93**, 1860-70.

HAYOZ, D., DREXLER, H., MÜNZEL, T., HORNIG, B., ZEIHER, A., JUST H., BRUNNER, H.R. & ZELIA, R. (1993). Flow-mediated arteriolar dilation is abnormal in congestive heart failure. *Circulation*, **87** (suppl VII), VII-92 – VII-96.

HAYWOOD, G.A., TSAO, P.S., VON DER LEYEN, H.E., MANN, M.J., KEELING, P.J., TRINDADE, P.T., LEWIS, N.P., BYRNE, C.D., RICKENBACHER, P.R., BISHOPRIC, N.H., COOKE, J.P., MCKENNA, W.J. & FOWLER, M.B. (1996). Expression of Inducible Nitric Oxide Synthase in Human Heart Failure. *Circulation*, **93**, 1087-94.

HELLERMANN, G.R. & SOLOMONSON, L.P. (1997). Calmodulin Promotes Dimerization of the Oxygenase Domain of Human Endothelial Nitric-Oxide Synthase. *J Biol Chem*, **272**, 12030-4.

HENNET, T., RICHTER, C. & PETERHANS, E. (1993). Tumour Necrosis Factor-α Induces Superoxide Anion Generation in Mitochondria of L929 Cells. *Biochem J*, **289**, 587-92.

HEYMES, C., VANDERHEYDEN, M., BRONZWAER, J.G., SHAH, A.M. & PAULUS, W.J. (1999). Endomyocardial Nitric Oxide Synthase and Left Ventricular Preload Reserve in Dilated Cardiomyopathy. *Circulation*, **99**, 3009-16.

HICKEY, K.A., RUBANYI, G., PAUL, R.J. & HIGHSMITH, R.F. (1985). Characterization of a Coronary Vasoconstrictor Produced by Cultured Endothelial Cells. *Am J Physiol*, **248**, C550-6.

HILEY, C.R., PHOON, C.K.L. & THOMAS, G.R. (1987). Acetylcholine vasorelaxation in superior mesenteric arterial bed of the rat is endothelium-dependent and sensitive to antioxidants. *Br J Pharmacol*, **91**, 378P.

HILL, M.F. & SINGAL, P.K. (1996). Antioxidant and Oxidative Stress Changes During Heart Failure Subsequent to Myocardial Infarction in Rats. *American Journal of Pathology*, **148**, 291-300.

HIRAI, T., ZELIS, R. & MUSCH, T.I. (1995). Effects of Nitric Oxide Synthase Inhibition on the Muscle Blood Flow Response to Exercise in Rats with Heart Failure. *Cardiovasc Res*, **30**, 469-76.

HIROOKA, Y., IMAIZUMI, T., HARADA, S., MASAKI, H., MOMOHARA, M., TAGAWA, T. & TAKESHITA, A. (1992). Endothelium-Dependent Forearm Vasodilation to Acetylcholine but Not to Substance P Is Impaired in Patients with Heart Failure. *J Cardiovasc Pharmacol*, **20** (Suppl 12), S221-5.

HOBBS, A.J., HIGGS, A. & MONCADA, S. (1999). Inhibition of Nitric Oxide Synthase as a Potential Therapeutic Target. *Annu Rev Pharmacol Toxicol*, **39**, 191-220.

HODES, R.J., LAKATTA, E.G. & MCNEIL, C.T. (1995). Another Modifiable Risk Factor for Cardiovascular Disease? Some Evidence Points to Arterial Stiffness. *J Am Geriatr Soc*, **43**, 581-2.

HODSMAN, G.P., KOHZUKI, M., HOWES, L.G., SUMITHRAN, E., TSUNODA, K. & JOHNSTON, C.I. (1988). Neurohumoral Responses to Chronic Myocardial Infarction in Rats. *Circulation*, **78**, 376-81.

HOMER, K.L. & WANSTALL, J.C. (2000). Cyclic GMP-Independent Relaxation of Rat Pulmonary Artery by Spermine NONOate, a Diazeniumdiolate Nitric Oxide Donor. *Br J Pharmacol*, **131**, 673-82.

HORNIG, B., MAIER, V. & DREXLER, H. (1996). Physical Training Improves Endothelial Function in Patients with Chronic Heart Failure. *Circulation*, **93**, 210-4.

HORNIG, B., ARAKAWA, N., KOHLER, C. & DREXLER, H. (1998). Vitamin C Improves Endothelial Function of Conduit Arteries in Patients with Chronic Heart Failure. *Circulation*, **97**, 363-8.

HUANG, P.L., HUANG, Z., MASHIMO, H., BLOCH, K.D., MOSKOWITZ, M.A., BEVAN, J.A. & FISHMAN, M.C. (1995). Hypertension in Mice Lacking the Gene for Endothelial Nitric Oxide Synthase. *Nature*, **377**, 239-42.

HUANG, S.N., MINASSIAN, H. & MORE, J.D. (1976). Application of Immunofluorescent Staining on Paraffin Sections Improved by Trypsin Digestion. *Lab Invest*, **35**, 383-90.

HUPF, H., GRIMM, D., RIEGGER, G.A. & SCHUNKERT, H. (1999). Evidence for a Vasopressin System in the Rat Heart. *Circ Res*, **84**, 365-70.

HUTCHESON, I.R. & GRIFFITH, T.M. (1991). Release of Endothelium-Derived Relaxing Factor Is Modulated Both by Frequency and Amplitude of Pulsatile Flow. *Am J Physiol*, **261**, H257-62.

IGNARRO, L.J., LIPPTON, H., EDWARDS, J.C., BARICOS, W.H., HYMAN, A.L., KADOWITZ, P.J. & GRUETTER, C.A. (1981). Mechanism of Vascular Smooth Muscle Relaxation by Organic Nitrates, Nitrites, Nitroprusside and Nitric Oxide: Evidence for the Involvement of S-Nitrosothiols as Active Intermediates. *J Pharmacol Exp Ther*, **218**, 739-49.

IGNARRO, L.J., BUGA, G.M., WOOD, K.S., BYRNS, R.E. & CHAUDHURI, G. (1987). Endothelium-Derived Relaxing Factor Produced and Released from Artery and Vein Is Nitric Oxide. *Proc Natl Acad Sci U S A*, **84**, 9265-9.

IGNARRO, L.J., BYRNS, R.E., BUGA, G.M., WOOD, K.S. & CHAUDHURI, G. (1988). Pharmacological Evidence That Endothelium-Derived Relaxing Factor Is Nitric Oxide: Use of Pyrogallol and Superoxide Dismutase to Study Endothelium-Dependent and Nitric Oxide-Elicited Vascular Smooth Muscle Relaxation. *J Pharmacol Exp Ther*, **244**, 181-9.

ING, D.J., ZANG, J., DZAU, V.J., WEBSTER, K.A. & BISHOPRIC, N.H. (1999). Modulation of Cytokine-Induced Cardiac Myocyte Apoptosis by Nitric Oxide, Bak, and Bcl-X. *Circ Res*, **84**, 21-33.

INGBER, D.E. (1997). Tensegrity: The Architectural Basis of Cellular Mechanotransduction. *Annu Rev Physiol*, **59**, 575-99.

ISCHIROPOULOS, H. & AL-MEHDI, A.B. (1995). Peroxynitrite-Mediated Oxidative Protein Modifications. *FEBS Lett*, **364**, 279-82.

ISHIGAI, Y., MORI, T., IKEDA, T., FUKUZAWA, A. & SHIBANO, T. (1997). Role of Bradykinin-NO Pathway in Prevention of Cardiac Hypertrophy by ACE Inhibitor in Rat Cardiomyocytes. *Am J Physiol*, **273**, H2659-63.

ITOH, H., PRATT, R.E. & DZAU, V.J. (1990). Atrial Natriuretic Polypeptide Inhibits Hypertrophy of Vascular Smooth Muscle Cells. *J Clin Invest*, **86**, 1690-7.

JOANNIDES, R., HAEFELI, W.E., LINDER, L., RICHARD, V., BAKKALI, E.H., THUILLEZ, C. & LUSCHER, T.F. (1995). Nitric Oxide Is Responsible for Flow-Dependent Dilatation of Human Peripheral Conduit Arteries *in vivo*. *Circulation*, **91**, 1314-9.

JOANNIDES, R., RICHARD, V., HAEFELI, W.E., BENOIST, A., LINDER, L., LUSCHER, T.F. & THUILLEZ, C. (1997). Role of Nitric Oxide in the Regulation of the Mechanical Properties of Peripheral Conduit Arteries in Humans. *Hypertension*, **30**, 1465-70.

JULIAN, D.G. & COWAN, J.C. (1992). *Cardiology*, Bailliere Tindall, W.B. Saunders Publishing.

JULOU-SCHAEFFER, G., GRAY, G.A., FLEMING, I., SCHOTT, C., PARRATT, J.R. & STOCLET, J.C. (1990). Loss of Vascular Responsiveness Induced by Endotoxin Involves L-Arginine Pathway. *Am J Physiol*, **259**, H1038-43.

KAISER, L., SPICKARD, R.C. & OLIVIER, N.B. (1989). Heart Failure Depresses Endothelium-Dependent Responses in Canine Femoral Artery. *Am J Physiol*, **256**, H962-7.

KAJSTURA, J., CHENG, W., REISS, K., CLARK, W.A., SONNENBLICK, E.H., KRAJEWSKI, S., REED, J.C., OLIVETTI, G. & ANVERSA, P. (1996). Apoptotic and Necrotic Myocyte Cell Deaths Are Independent Contributing Variables of Infarct Size in Rats. *Lab Invest*, **74**, 86-107.

KAPADIA, S., LEE, J., TORRE-AMIONE, G., BIRDSALL, H.H., MA, T.S. & MANN, D.L. (1995). Tumor Necrosis Factor- α Gene and Protein Expression in Adult Feline Myocardium after Endotoxin Administration. *J Clin Invest*, **96**, 1042-52.

KAPADIA, S.R., ORAL, H., LEE, J., NAKANO, M., TAFFET, G.E. & MANN, D.L. (1997). Hemodynamic Regulation of Tumor Necrosis Factor-α Gene and Protein Expression in Adult Feline Myocardium. *Circ Res*, **81**, 187-95.

KATWA, L.C., GUARDA, E. & WEBER, K.T. (1993). Endothelin Receptors in Cultured Adult Rat Cardiac Fibroblasts. *Cardiovasc Res*, **27**, 2125-9.

KATZ, S.D., BIASUCCI, L., SABBA, C., STROM, J.A., JONDEAU, G., GALVAO, M., SOLOMON, S., NIKOLIC, S.D., FORMAN, R. & LEJEMTEL, T.H. (1992). Impaired Endothelium-Mediated Vasodilation in the Peripheral Vasculature of Patients with Congestive Heart Failure. *Journal of the American College of Cardiology*, **19**, 918-25.

KATZ, S.D., SCHWARZ, M., YUEN, J. & LEJEMTEL, T.H. (1993). Impaired Acetylcholine-Mediated Vasodilation in Patients with Congestive Heart Failure. Role of Endothelium-Derived Vasodilating and Vasoconstricting Factors. *Circulation*, **88**, 55-61.

KATZ, S.D., KRUM, H., KHAN, T. & KNECHT, M. (1996). Exercise-Induced Vasodilation in Forearm Circulation of Normal Subjects and Patients with Congestive Heart Failure: Role of Endothelium-Derived Nitric Oxide. *J Am Coll Cardiol*, **28**, 585-90.

KAYE, D.M., AHLERS, B.A., AUTELITANO, D.J. & CHIN-DUSTING, J.P. (2000). *In vivo* and *in vitro* Evidence for Impaired Arginine Transport in Human Heart Failure. *Circulation*, **102**, 2707-12.

KEITH, M.E., JEEJEEBHOY, K.N., LANGER, A., KURIAN, R., BARR, A., O'KELLY, B. & SOLE, M.J. (2001). A Controlled Clinical Trial of Vitamin E Supplementation in Patients with Congestive Heart Failure. *Am J Clin Nutr*, **73**, 219-24.

KHATTA, M., ALEXANDER, B.S., KRICHTEN, C.M., FISHER, M.L., FREUDENBERGER, R., ROBINSON, S.W. & GOTTLIEB, S.S. (2000). The Effect of Coenzyme Q10 in Patients with Congestive Heart Failure. *Ann Intern Med*, **132**, 636-40.

KIM, Y.M., BOMBECK, C.A. & BILLIAR, T.R. (1999). Nitric Oxide as a Bifunctional Regulator of Apoptosis. *Circ Res*, **84**, 253-6.

KIOWSKI, W., SUTSCH, G., HUNZIKER, P., MULLER, P., KIM, J., OECHSLIN, E., SCHMITT, R., JONES, R. & BERTEL, O. (1995). Evidence for Endothelin-1-Mediated Vasoconstriction in Severe Chronic Heart Failure. *Lancet*, **346**, 732-6.

KIRSTEIN, M., RIVET-BASTIDE, M., HATEM, S., BENARDEAU, A., MERCADIER, J.J. & FISCHMEISTER, R. (1995). Nitric Oxide Regulates the Calcium Current in Isolated Human Atrial Myocytes. *J Clin Invest*, **95**, 794-802.

KIUCHI, K., SATO, N., SHANNON, R.P., VATNER, D.E., MORGAN, K. & VATNER, S.F. (1993). Depressed β-Adrenergic Receptor- and Endothelium-Mediated Vasodilation in Conscious Dogs with Heart Failure. *Circ Res*, **73**, 1013-23.

KLABUNDE, R.E., RITGER, R.C. & HELGREN, M.C. (1991). Cardiovascular Actions of Inhibitors of Endothelium-Derived Relaxing Factor (Nitric Oxide) Formation/Release in Anesthetized Dogs. *Eur J Pharmacol*, **199**, 51-9.

KLATT, P., SCHMIDT, K., URAY, G. & MAYER, B. (1993a). Multiple Catalytic Functions of Brain Nitric Oxide Synthase. Biochemical Characterization, Cofactor-Requirement, and the Role of N^{ϖ}-Hydroxy-L-Arginine as an Intermediate. *J Biol Chem*, **268**, 14781-7.

KLATT, P., SCHMIDT, K., URAY, G. & MAYER, B. (1993b). Multiple Catalytic Functions of Brain Nitric Oxide Synthase. *Journal of Biological Chemistry*, **268**, 14781-7.

KLATT, P., SCHMID, M., LEOPOLD, E., SCHMIDT, K., WERNER, E.R. & MAYER, B. (1994). The Pteridine Binding Site of Brain Nitric Oxide Synthase. Tetrahydrobiopterin Binding Kinetics, Specificity, and Allosteric Interaction with the Substrate Domain. *J Biol Chem*, **269**, 13861-6.

KLATT, P., SCHMIDT, K., LEHNER, D., GLATTER, O., BACHINGER, H.P. & MAYER, B. (1995). Structural Analysis of Porcine Brain Nitric Oxide Synthase Reveals a Role for Tetrahydrobiopterin and L-Arginine in the Formation of an Sds-Resistant Dimer. *Embo J*, **14**, 3687-95.

KNOWLES, R.G., PALACIOS, M., PALMER, R.M. & MONCADA, S. (1989). Formation of Nitric Oxide from L-Arginine in the Central Nervous System: A Transduction Mechanism for Stimulation of the Soluble Guanylate Cyclase. *Proc Natl Acad Sci U S A*, **86**, 5159-62.

KNOWLES, R.G. & MONCADA, S. (1994). Nitric Oxide Synthases in Mammals. *Biochem J*, **298**, 249-58.

KNOWLTON, K.U., MICHEL, M.C., ITANI, M., SHUBEITA, H.E., ISHIHARA, K., BROWN, J.H. & CHIEN, K.R. (1993). The α_{1a}-Adrenergic Receptor Subtype Mediates Biochemical, Molecular, and Morphologic Features of Cultured Myocardial Cell Hypertrophy. *J Biol Chem*, **268**, 15374-80.

KOBAYASHI, T., MIYAUCHI, T., SAKAI, S., KOBAYASHI, M., YAMAGUCHI, I., GOTO, K. & SUGISHITA, Y. (1999). Expression of Endothelin-1, ET_A and ET_B Receptors, and ECE and Distribution of Endothelin-1 in Failing Rat Heart. *Am J Physiol*, **276**, H1197-206.

KÖHLER, G. & MILSTEIN, C. (1975). Continuous cultures of fused cells secreting antibody of predefined specificity. *Nature*, **256**, 495 – 497.

KOJDA, G., KOTTENBERG, K., NIX, P., SCHLUTER, K.D., PIPER, H.M. & NOACK, E. (1996). Low Increase in cGMP Induced by Organic Nitrates and Nitrovasodilators Improves Contractile Response of Rat Ventricular Myocytes. *Circ Res*, **78**, 91-101.

KOMALAVILAS, P. & LINCOLN, T.M. (1996). Phosphorylation of the Inositol 1,4,5-Trisphosphate Receptor. Cyclic GMP-Dependent Protein Kinase Mediates cAMP and cGMP Dependent Phosphorylation in the Intact Rat Aorta. *J Biol Chem*, **271**, 21933-8.

KRAEHENBUHL, J.P. & JAMIESON, J.D. (1974). Localization of Intracellular Antigens by Immunoelectron Microscopy. *Int Rev Exp Pathol*, **13**, 1-53.

KROWN, K.A., PAGE, M.T., NGUYEN, C., ZECHNER, D., GUTIERREZ, V., COMSTOCK, K.L., GLEMBOTSKI, C.C., QUINTANA, P.J. & SABBADINI, R.A. (1996). Tumor Necrosis Factor α-Induced Apoptosis in Cardiac Myocytes. Involvement of the Sphingolipid Signaling Cascade in Cardiac Cell Death. *J Clin Invest*, **98**, 2854-65.

KRUM, H. (1997). β-Adrenoceptor Blockers in Chronic Heart Failure-a Review. *Br J Clin Pharmacol*, **44**, 111-8.

KRUM H., CHARLON, V., WILDMANN, T. & PACKER M. (1999). Long-term open-label experience with an endothelin receptor antagonist, bosentan, in patients with severe chronic heart failure. *Circulation*, **100**, A3408.

KUBO, S.H., RECTOR, T.S., BANK, A.J., WILLIAMS, R.E. & HEIFETZ, S.M. (1991). Endothelium-Dependent Vasodilation Is Attenuated in Patients with Heart Failure. *Circulation*, **84**, 1589-96.

KUBO, S.H., RECTOR, T.S., BANK, A.J., RAIJ, L., KRAEMER, M.D., TADROS, P., BEARDSLEE, M. & GARR, M.D. (1994). Lack of Contribution of Nitric Oxide to Basal Vasomotor Tone in Heart Failure. *Am J Cardiol*, **74**, 1133-6.

KUMAGAI, Y., MIDORIKAWA, K., NAKAI, Y., YOSHIKAWA, T., KUSHIDA, K., HOMMA-TAKEDA, S. & SHIMOJO, N. (1998). Inhibition of Nitric Oxide Formation and Superoxide Generation During Reduction of Ly83583 by Neuronal Nitric Oxide Synthase. *Eur J Pharmacol*, **360**, 213-8.

KUMAR, R., CARTLEDGE, W.A., LINCOLN, T.M. & PANDEY, K.N. (1997). Expression of Guanylyl Cyclase-α/Atrial Natriuretic Peptide Receptor Blocks the Activation of Protein Kinase C in Vascular Smooth Muscle Cells. Role of cGMP and cGMP-Dependent Protein Kinase. *Hypertension*, **29**, 414-21.

KUSUMOTO, K., FUJIWARA, A., IKEDA, S., WATANABE, T. & FUJINO, M. (1996). Pharmacological Characterization of Cardiovascular Responses Induced by Endothelin-1 in the Perfused Rat Heart. *Eur J Pharmacol*, **296**, 65-74.

LANDER, H.M., SEHAJPAL, P.K. & NOVOGRODSKY, A. (1993). Nitric Oxide Signaling: A Possible Role for G Proteins. *J Immunol*, **151**, 7182-7.

LANGSJOEN, P.H. & FOLKERS, K. (1990). Long-Term Efficacy and Safety of Coenzyme Q10 Therapy for Idiopathic Dilated Cardiomyopathy. *Am J Cardiol*, **65**, 521-3.

LASZLO, F. & WHITTLE, B.J. (1997). Actions of Isoform-Selective and Non-Selective Nitric Oxide Synthase Inhibitors on Endotoxin-Induced Vascular Leakage in Rat Colon. *Eur J Pharmacol*, **334**, 99-102.

LEE, M.R., LI, L. & KITAZAWA, T. (1997). Cyclic GMP Causes Ca^{2+} Desensitization in Vascular Smooth Muscle by Activating the Myosin Light Chain Phosphatase. *J Biol Chem*, **272**, 5063-8.

LEE, W.H. & PACKER, M. (1986). Prognostic Importance of Serum Sodium Concentration and Its Modification by Converting-Enzyme Inhibition in Patients with Severe Chronic Heart Failure. *Circulation*, **73**, 257-67.

LEFROY, D.C., CRAKE, T., UREN, N.G., DAVIES, G.J. & MASERI, A. (1993). Effect of Inhibition of Nitric Oxide Synthesis on Epicardial Coronary Artery Caliber and Coronary Blood Flow in Humans. *Circulation*, **88**, 43-54.

LENFANT, C. (1994). Report of the Task Force on Research in Heart Failure. *Circulation*, **90**, 1118-23.

LEVINE, B., KALMAN, J., MAYER, L., FILLIT, H.M. & PACKER, M. (1990). Elevated Circulating Levels of Tumor Necrosis Factor in Severe Chronic Heart Failure. *N Engl J Med*, **323**, 236-41.

LI, J., BOMBECK, C.A., YANG, S., KIM, Y.M. & BILLIAR, T.R. (1999a). Nitric Oxide Suppresses Apoptosis Via Interrupting Caspase Activation and Mitochondrial Dysfunction in Cultured Hepatocytes. *J Biol Chem*, **274**, 17325-33.

LI, P.F., DIETZ, R. & VON HARSDORF, R. (1999b). Superoxide Induces Apoptosis in Cardiomyocytes, but Proliferation and Expression of Transforming Growth Factor-β_1 in Cardiac Fibroblasts. *FEBS Lett*, **448**, 206-10.

LI, Y.Y., FENG, Y.Q., KADOKAMI, T., MCTIERNAN, C.F., DRAVIAM, R., WATKINS, S.C. & FELDMAN, A.M. (2000). Myocardial Extracellular Matrix Remodeling in Transgenic Mice Overexpressing Tumor Necrosis Factor α Can Be Modulated by Anti-Tumor Necrosis Factor α Therapy. *Proc Natl Acad Sci U S A*, **97**, 12746-51.

LIN, K.T., XUE, J.Y., LIN, M.C., SPOKAS, E.G., SUN, F.F. & WONG, P.Y. (1998). Peroxynitrite Induces Apoptosis of Hl-60 Cells by Activation of a Caspase-3 Family Protease. *American Journal of Physiology*, **274**, C855-60.

LINCOLN, T.M. & CORNWELL, T.L. (1993). Intracellular Cyclic GMP Receptor Proteins. *Faseb J*, **7**, 328-38.

LIOCHEV, S.I. & FRIDOVICH, I. (1995). A Cationic Manganic Porphyrin Inhibits Uptake of Paraquat by *Escherichia Coli*. *Arch Biochem Biophys*, **321**, 271-5.

LIPTON, S.A., CHOI, Y.B., PAN, Z.H., LEI, S.Z., CHEN, H.S., SUCHER, N.J., LOSCALZO, J., SINGEL, D.J. & STAMLER, J.S. (1993). A Redox-Based Mechanism for the Neuroprotective and Neurodestructive Effects of Nitric Oxide and Related Nitroso-Compounds. *Nature*, **364**, 626-32.

LITWIN, S.E., KATZ, S.E., MORGAN, J.P. & DOUGLAS, P.S. (1994). Serial Echocardiographic Assessment of Left Ventricular Geometry and Function after Large Myocardial Infarction in the Rat. *Circulation*, **89**, 345-54.

LONDON, G.M. & GUERIN, A.P. (1999). Influence of Arterial Pulse and Reflected Waves on Blood Pressure and Cardiac Function. *Am Heart J*, **138**, 220-4.

LONN, E. & MCKELVIE, R. (2000). Drug Treatment in Heart Failure. *BMJ*, **320**, 1188-92.

LOWENSTEIN, C.J., GLATT, C.S., BREDT, D.S. & SNYDER, S.H. (1992). Cloned and Expressed Macrophage Nitric Oxide Synthase Contrasts with the Brain Enzyme. *Proc Natl Acad Sci U S A*, **89**, 6711-5.

MACCARTHY, P.A., GROCOTT-MASON, R., PRENDERGAST, B.D. & SHAH, A.M. (2000). Contrasting Inotropic Effects of Endogenous Endothelin in the Normal and Failing Human Heart: Studies with an Intracoronary ET_A Receptor Antagonist. *Circulation*, **101**, 142-7.

MACKENZIE, A. & MARTIN, W. (1998). Loss of Endothelium-Derived Nitric Oxide in Rabbit Aorta by Oxidant Stress: Restoration by Superoxide Dismutase Mimetics. *Br J Pharmacol*, **124**, 719-28.

MACKENZIE, A., FILIPPINI, S. & MARTIN, W. (1999). Effects of Superoxide Dismutase Mimetics on the Activity of Nitric Oxide in Rat Aorta. *Br J Pharmacol*, **127**, 1159-64.

MALLAT, Z., PHILIP, I., LEBRET, M., CHATEL, D., MACLOUF, J. & TEDGUI, A. (1998). Elevated Levels of 8-Iso-Prostaglandin F2α in Pericardial Fluid of Patients with Heart Failure: A Potential Role for *in vivo* Oxidant Stress in Ventricular Dilatation and Progression to Heart Failure. *Circulation*, **97**, 1536-9.

MANN, D.L., KENT, R.L., PARSONS, B. & COOPER, G.T. (1992). Adrenergic Effects on the Biology of the Adult Mammalian Cardiocyte. *Circulation*, **85**, 790-804.

MAROKO, P.R., KJEKSHUS, J.K., SOBEL, B.E., WATANABE, T., COVELL, J.W., ROSS, J., JR. & BRAUNWALD, E. (1971). Factors Influencing Infarct Size Following Experimental Coronary Artery Occlusions. *Circulation*, **43**, 67-82.

MARSDEN, P.A., HENG, H.H., SCHERER, S.W., STEWART, R.J., HALL, A.V., SHI, X.M., TSUI, L.C. & SCHAPPERT, K.T. (1993). Structure and Chromosomal Localization of the Human Constitutive Endothelial Nitric Oxide Synthase Gene. *J Biol Chem*, **268**, 17478-88.

MARTIN, W., FURCHGOTT, R.F., VILLANI, G.M. & JOTHIANANDAN, D. (1986). Depression of Contractile Responses in Rat Aorta by Spontaneously Released Endothelium-Derived Relaxing Factor. *J Pharmacol Exp Ther*, **237**, 529-38.

MARUYAMA, Y., NISHIOKA, O., NOZAKI, E., KINOSHITA, H., KYONO, H., KOIWA, Y. & TAKISHIMA, T. (1993). Effects of Arterial Distensibility on Left Ventricular Ejection in the Depressed Contractile State. *Cardiovasc Res*, **27**, 182-7.

MATSUMOTO, T., WADA, A., TSUTAMOTO, T., OMURA, T., YOKOHAMA, H., OHNISHI, M., NAKAE, I., TAKAHASHI, M. & KINOSHITA, M. (1999). Vasorelaxing Effects of Atrial and Brain Natriuretic Peptides on Coronary Circulation in Heart Failure. *Am J Physiol*, **276**, H1935-42.

MATSUSAKA, T. & ICHIKAWA, I. (1997). Biological Functions of Angiotensin and Its Receptors. *Annu Rev Physiol*, **59**, 395-412.

MAYER, B., JOHN, M. & BOHME, E. (1990). Purification of a Ca^{2+}/Calmodulin-Dependent Nitric Oxide Synthase from Porcine Cerebellum. Cofactor-Role of Tetrahydrobiopterin. *FEBS Lett*, **277**, 215-9.

MAYER, B., PFEIFFER, S., SCHRAMMEL, A., KOESLING, D., SCHMIDT, K. & BRUNNER, F. (1998). A New Pathway of Nitric Oxide/Cyclic GMP Signaling Involving S-Nitrosoglutathione. *J Biol Chem*, **273**, 3264-70.

MCEWAN, P.E., GRAY, G.A. SHERRY, L., WEBB, D.J. & KENYON, C.J. (1998). Differential Effect of Angiotensin II on Cardiac Cell Proliferation and Intramyocardial Perivascular Fibrosis *in vivo*. *Circulation*, **98**, 2765-73.

MCEWAN P.E., SHERRY L., PATRIZIO, M., WEBB, D.J. & GRAY G.A. (2001). Endothelin B receptors are upregulated post myocardial infarction in the rat and co-localise with early growth genes in the hypertrophied non-infarcted left ventricle, *submitted for publication.*

MCKAY, R.G., PFEFFER, M.A., PASTERNAK, R.C., MARKIS, J.E., COME, P.C., NAKAO, S., ALDERMAN, J.D., FERGUSON, J.J., SAFIAN, R.D. & GROSSMAN, W. (1986). Left Ventricular Remodeling after Myocardial Infarction: A Corollary to Infarct Expansion. *Circulation*, **74**, 693-702.

MCMILLAN, K. & MASTERS, B.S. (1993). Optical Difference Spectrophotometry as a Probe of Rat Brain Nitric Oxide Synthase Heme-Substrate Interaction. *Biochemistry*, **32**, 9875-80.

MCMILLAN, K. & MASTERS, B.S. (1995). Prokaryotic Expression of the Heme- and Flavin-Binding Domains of Rat Neuronal Nitric Oxide Synthase as Distinct Polypeptides: Identification of the Heme-Binding Proximal Thiolate Ligand as Cysteine-415. *Biochemistry*, **34**, 3686-93.

MCMILLAN, K., ADLER, M., AULD, D.S., BALDWIN, J.J., BLASKO, E., BROWNE, L.J., CHELSKY, D., DAVEY, D., DOLLE, R.E., EAGEN, K.A., ERICKSON, S., FELDMAN, R.I., GLASER, C.B., MALLARI, C., MORRISSEY, M.M., OHLMEYER, M.H., PAN, G., PARKINSON, J.F., PHILLIPS, G.B., POLOKOFF, M.A., SIGAL, N.H., VERGONA, R., WHITLOW, M., YOUNG, T.A. & DEVLIN, J.J. (2000). Allosteric Inhibitors of Inducible Nitric Oxide Synthase Dimerization Discovered Via Combinatorial Chemistry. *Proc Natl Acad Sci U S A*, **97**, 1506-11.

MCMURRAY, J.J., RAY, S.G., ABDULLAH, I., DARGIE, H.J. & MORTON, J.J. (1992). Plasma Endothelin in Chronic Heart Failure. *Circulation*, **85**, 1374-9.

MELLION, B.T., IGNARRO, L.J., MYERS, C.B., OHLSTEIN, E.H., BALLOT, B.A., HYMAN, A.L. & KADOWITZ, P.J. (1983). Inhibition of Human Platelet Aggregation by S-Nitrosothiols. Heme-Dependent Activation of Soluble Guanylate Cyclase and Stimulation of Cyclic GMP Accumulation. *Mol Pharmacol*, **23**, 653-64.

MEYER, M., LEHNART, S., PIESKE, B., SCHLOTTAUER, K., MUNK, S., HOLUBARSCH, C., JUST, H. & HASENFUSS, G. (1996). Influence of Endothelin 1 on Human Atrial Myocardium-Myocardial Function and Subcellular Pathways. *Basic Res Cardiol*, **91**, 86-93.

MIAN, K.B. & MARTIN, W. (1995). Differential Sensitivity of Basal and Acetylcholine-Stimulated Activity of Nitric Oxide to Destruction by Superoxide Anion in Rat Aorta. *Br J Pharmacol*, **115**, 993-1000.

MICHEL, J.B., FERON, O., SASE, K., PRABHAKAR, P. & MICHEL, T. (1997). Caveolin Versus Calmodulin. Counterbalancing Allosteric Modulators of Endothelial Nitric Oxide Synthase. *J Biol Chem*, **272**, 25907-12.

MICKLEY, E.J., GRAY, G.A. & WEBB, D.J. (1997). Activation of Endothelin Eta Receptors Masks the Constrictor Role of Endothelin ET_B Receptors in Rat Isolated Small Mesenteric Arteries. *Br J Pharmacol*, **120**, 1376-82.

MIKAWA, K., KUME, H. & TAKAGI, K. (1998). Effects of Atrial Natriuretic Peptide and 8-Brom Cyclic Guanosine Monophosphate on Human Tracheal Smooth Muscle. *Arzneimittelforschung*, **48**, 914-8.

MILLER, V.M. & VANHOUTTE, P.M. (1988). Enhanced Release of Endothelium-Derived Factor(s) by Chronic Increases in Blood Flow. *Am J Physiol*, **255**, H446-51.

MISTRY, D.K. & GARLAND, C.J. (1998). Nitric Oxide (NO)-Induced Activation of Large Conductance Ca^{2+}-Dependent K^+ Channels (Bk(Ca)) in Smooth Muscle Cells Isolated from the Rat Mesenteric Artery. *Br J Pharmacol*, **124**, 1131-40.

MITCHELL, R.N. & COTRAN, R.S. (1999). Hemodynamic disorders, thrombosis and shock. In: *Pathological Basis of Disease*, Ch 5, Edition 6, ed. Cotran, R.S., Kumar, V. & Collins, T., W.B. Saunders Company.

MITCHELL, J.B., SAMUNI, A., KRISHNA, M.C., DEGRAFF, W.G., AHN, M.S., SAMUNI, U. & RUSSO, A. (1990). Biologically Active Metal-Independent Superoxide Dismutase Mimics. *Biochemistry*, **29**, 2802-7.

MIYAMOTO, Y., SAITO, Y., KAJIYAMA, N., YOSHIMURA, M., SHIMASAKI, Y., NAKAYAMA, M., KAMITANI, S., HARADA, M., ISHIKAWA, M., KUWAHARA, K., OGAWA, E., HAMANAKA, I., TAKAHASHI, N., KANESHIGE, T., TERAOKA, H., AKAMIZU, T., AZUMA, N., YOSHIMASA, Y., YOSHIMASA, T., ITOH, H., MASUDA, I., YASUE, H. & NAKAO, K. (1998). Endothelial Nitric Oxide Synthase Gene Is Positively Associated with Essential Hypertension. *Hypertension*, **32**, 3-8.

MO, M., ESKIN, S.G. & SCHILLING, W.P. (1991). Flow-Induced Changes in Ca^{2+} Signaling of Vascular Endothelial Cells: Effect of Shear Stress and ATP. *Am J Physiol*, **260**, H1698-707.

MOHAN, P., BRUTSAERT, D.L., PAULUS, W.J. & SYS, S.U. (1996). Myocardial Contractile Response to Nitric Oxide and cGMP. *Circulation*, **93**, 1223-9.

MOHRI, M., EGASHIRA, K., TAGAWA, T., KUGA, T., TAGAWA, H., HARASAWA, Y., SHIMOKAWA, H. & TAKESHITA, A. (1997). Basal Release of Nitric Oxide Is Decreased in the Coronary Circulation in Patients with Heart Failure. *Hypertension*, **30**, 50-6.

MOLENAAR, P., O'REILLY, G., SHARKEY, A., KUC, R.E., HARDING, D.P., PLUMPTON, C., GRESHAM, G.A. & DAVENPORT, A.P. (1993). Characterization and Localization of Endothelin Receptor Subtypes in the Human Atrioventricular Conducting System and Myocardium. *Circ Res*, **72**, 526-38.

MONCADA, S., PALMER, R.M. & HIGGS, E.A. (1991). Nitric Oxide: Physiology, Pathophysiology, and Pharmacology. *Pharmacological Reviews*, **43**, 109-42.

MULDER, P., RICHARD, V., BOUCHART, F., DERUMEAUX, G., MUNTER, K. & THUILLEZ, C. (1998). Selective ET_A Receptor Blockade Prevents Left Ventricular Remodeling and Deterioration of Cardiac Function in Experimental Heart Failure. *Cardiovasc Res*, **39**, 600-8.

MULLAN, D.M., BELL, D., KELSO, E.J. & MCDERMOTT, B.J. (1997). Involvement of Endothelin ET_A and ET_B Receptors in the Hypertrophic Effects of ET-1 in Rabbit Ventricular Cardiomyocytes. *J Cardiovasc Pharmacol*, **29**, 350-9.

MULLER-WERDAN, U., SCHUMANN, H., FUCHS, R., REITHMANN, C., LOPPNOW, H., KOCH, S., ZIMNY-ARNDT, U., HE, C., DARMER, D., JUNGBLUT, P., STADLER, J., HOLTZ, J. & WERDAN, K. (1997). Tumor Necrosis Factor Alpha (TNF-α) Is Cardiodepressant in Pathophysiologically Relevant Concentrations without Inducing Inducible Nitric Oxide-(NO)-Synthase (iNOS) or Triggering Serious Cytotoxicity. *J Mol Cell Cardiol*, **29**, 2915-23.

MÜLSCH, A., BASSENGE, E. & BUSSE, R. (1989). Nitric Oxide Synthesis in Endothelial Cytosol: Evidence for a Calcium-Dependent and a Calcium-Independent Mechanism. *Naunyn Schmiedebergs Arch Pharmacol*, **340**, 767-70.

MULVANY, M.J. & HALPERN, W. (1976). Mechanical Properties of Vascular Smooth Muscle Cells in Situ. *Nature*, **260**, 617-9.

MYERS, P.R., MINOR, R.L., GUERRA, R., BATES, J.N. & HARRISON, D.G. (1990). Vasorelaxant Properties of the Endothelium-Derived Relaxing Factor More Closely Resemble S-Nitrosocysteine Than Nitric Oxide. *Nature*, **345**, 161-3.

MYLONA, P. & CLELAND, J.G. (1999). Update of REACH-1 and MERIT-HF Clinical Trials in Heart Failure. Cardio.Net Editorial Team. *Eur J Heart Fail*, **1**, 197-200.

NAITOH, M., SUZUKI, H., MURAKAMI, M., MATSUMOTO, A., ARAKAWA, K., ICHIHARA, A., NAKAMOTO, H., OKA, K., YAMAMURA, Y. & SARUTA, T. (1994). Effects of Oral AVP Receptor Antagonists Opc-21268 and Opc-31260 on Congestive Heart Failure in Conscious Dogs. *Am J Physiol*, **267**, H2245-54.

NAITOH, M., POWER, J., PHILLIPS, P.A., RISVANIS, J., JOHNSTON, C.I. & BURRELL, L.M. (1998). Effects of Chronic AVP V_{2r} Blockade in Congestive Heart Failure in Sheep. Comparison with Chronic ACE Inhibition. *Adv Exp Med Biol*, **449**, 445-6.

NAKAMURA, M., YOSHIDA, H., ARAKAWA, N., MIZUNUMA, Y., MAKITA, S. & HIRAMORI, K. (1996). Endothelium-Dependent Vasodilatation Is Not Selectively Impaired in Patients with Chronic Heart Failure Secondary to Valvular Heart Disease and Congenital Heart Disease. *Eur Heart J*, **17**, 1875-81.

NAKANO, T., TOMINAGA, R., NAGANO, I., OKABE, H. & YASUI, H. (2000). Pulsatile Flow Enhances Endothelium-Derived Nitric Oxide Release in the Peripheral Vasculature. *Am J Physiol Heart Circ Physiol*, **278**, H1098-104.

NARULA, J., HAIDER, N., VIRMANI, R., DISALVO, T.G., KOLODGIE, F.D., HAJJAR, R.J., SCHMIDT, U., SEMIGRAN, M.J., DEC, G.W. & KHAW, B.A. (1996). Apoptosis in Myocytes in End-Stage Heart Failure. *N Engl J Med*, **335**, 1182-9.

NASA, Y., TOYOSHIMA, H., OHAKU, H., HASHIZUME, Y., SANBE, A. & TAKEO, S. (1996). Impairment of cGMP- and cAMP-Mediated Vasorelaxations in Rats with Chronic Heart Failure. *Am J Physiol*, **271**, H2228-37.

NATHAN, C. (1992). Nitric Oxide as a Secretory Product of Mammalian Cells. *Faseb J*, **6**, 3051-64.

NATHAN, C. & XIE, Q.W. (1994). Nitric Oxide Synthases: Roles, Tolls, and Controls. *Cell*, **78**, 915-8.

NIELSEN, S., CHOU, C.L., MARPLES, D., CHRISTENSEN, E.I., KISHORE, B.K. & KNEPPER, M.A. (1995). Vasopressin Increases Water Permeability of Kidney Collecting Duct by Inducing Translocation of Aquaporin-CD Water Channels to Plasma Membrane. *Proc Natl Acad Sci U S A*, **92**, 1013-7.

NISHIDA, K., HARRISON, D.G., NAVAS, J.P., FISHER, A.A., DOCKERY, S.P., UEMATSU, M., NEREM, R.M., ALEXANDER, R.W. & MURPHY, T.J. (1992). Molecular Cloning and Characterization of the Constitutive Bovine Aortic Endothelial Cell Nitric Oxide Synthase. *J Clin Invest*, **90**, 2092-6.

NISHIYAMA, Y., IKEDA, H., HARAMAKI, N., YOSHIDA, N. & IMAIZUMI, T. (1998). Oxidative Stress Is Related to Exercise Intolerance in Patients with Heart Failure. *American Heart Journal*, **135**, 115-20.

NOSSULI, T.O., HAYWARD, R., SCALIA, R. & LEFER, A.M. (1997). Peroxynitrite Reduces Myocardial Infarct Size and Preserves Coronary Endothelium after Ischemia and Reperfusion in Cats. *Circulation*, **96**, 2317-24.

OHARA, Y., PETERSON, T.E. & HARRISON, D.G. (1993). Hypercholesterolemia Increases Endothelial Superoxide Anion Production. *J Clin Invest*, **91**, 2546-51.

OHTSUKA, S., KAKIHANA, M., WATANABE, H., ENOMOTO, T., AJISAKA, R. & SUGISHITA, Y. (1996). Alterations in Left Ventricular Wall Stress and Coronary Circulation in Patients with Isolated Systolic Hypertension. *J Hypertens*, **14**, 1349-55.

OLIVETTI, G., ABBI, R., QUAINI, F., KAJSTURA, J., CHENG, W., NITAHARA, J.A., QUAINI, E., DI LORETO, C., BELTRAMI, C.A., KRAJEWSKI, S., REED, J.C. & ANVERSA, P. (1997). Apoptosis in the Failing Human Heart. *N Engl J Med*, **336**, 1131-41.

OMAR, H.A., CHERRY, P.D., MORTELLITI, M.P., BURKE-WOLIN, T. & WOLIN, M.S. (1991). Inhibition of Coronary Artery Superoxide Dismutase Attenuates Endothelium-Dependent and -Independent Nitrovasodilator Relaxation. *Circ Res*, **69**, 601-8.

ONO, K., MATSUMORI, A., SHIOI, T., FURUKAWA, Y. & SASAYAMA, S. (1998). Cytokine Gene Expression after Myocardial Infarction in Rat Hearts: Possible Implication in Left Ventricular Remodeling. *Circulation*, **98**, 149-56.

ONTKEAN, M., GAY, R. & GREENBERG, B. (1991). Diminished Endothelium-Derived Relaxing Factor Activity in an Experimental Model of Chronic Heart Failure. *Circulation Research*, **69**, 1088-96.

OSOL, G., CIPOLLA, M. & KNUTSON, S. (1989). A New Method for Mechanically Denuding the Endothelium of Small (50-150 μM) Arteries with a Human Hair. *Blood Vessels*, **26**, 320-4.

OU, P. & WOLFF, S.P. (1993). Aminoguanidine: A Drug Proposed for Prophylaxis in Diabetes Inhibits Catalase and Generates Hydrogen Peroxide in Vitro. *Biochem Pharmacol*, **46**, 1139-44.

PACKER, M. (1992). Pathophysiology of Chronic Heart Failure. *Lancet*, **340**, 88-92.

PALMER, R.M., FERRIGE, A.G. & MONCADA, S. (1987). Nitric Oxide Release Accounts for the Biological Activity of Endothelium-Derived Relaxing Factor. *Nature*, **327**, 524-6.

PARKER, T.G., PACKER, S.E. & SCHNEIDER, M.D. (1990). Peptide Growth Factors Can Provoke & Fetal Contractile Protein Gene Expression in Rat Cardiac Myocytes. *J Clin Invest*, **85**, 507-14.

PATEL, M. & DAY, B.J. (1999). Metalloporphyrin Class of Therapeutic Catalytic Antioxidants. *Trends Pharmacol Sci*, **20**, 359-64.

PAULUS, W.J., VANTRIMPONT, P.J. & SHAH, A.M. (1994). Acute Effects of Nitric Oxide on Left Ventricular Relaxation and Diastolic Distensibility in Humans. Assessment by Bicoronary Sodium Nitroprusside Infusion. *Circulation*, **89**, 2070-8.

PAULUS, W.J., VANTRIMPONT, P.J. & SHAH, A.M. (1995). Paracrine coronary endothelial control of left ventricular function in humans. *Circulation*, **92**, 2119 - 2126

PEDOTO, A., TASSIOPOULOS, A.K., OLER, A., MCGRAW, D.J., HOFFMANN, S.P., CAMPORESI, E.M. & HAKIM, T.S. (1998). Treatment of Septic Shock in Rats with Nitric Oxide Synthase Inhibitors and Inhaled Nitric Oxide. *Crit Care Med*, **26**, 2021-8.

PFEFFER, J.M. & PFEFFER, M.A. (1988). Angiotensin Converting Enzyme Inhibition and Ventricular Remodeling in Heart Failure. *Am J Med*, **84**, 37-44.

PFEFFER, M.A., PFEFFER, J.M., FISHBEIN, M.C., FLETCHER, P.J., SPADARO, J., KLONER, R.A. & BRAUNWALD, E. (1979). Myocardial Infarct Size and Ventricular Function in Rats. *Circ Res*, **44**, 503-12.

PFEIFFER, S., SCHRAMMEL, A., KOESLING, D., SCHMIDT, K. & MAYER, B. (1998). Molecular Actions of a Mn(III)Porphyrin Superoxide Dismutase Mimetic and Peroxynitrite Scavenger: Reaction with Nitric Oxide and Direct Inhibition of NO Synthase and Soluble Guanylyl Cyclase. *Mol Pharmacol*, **53**, 795-800.

PHILLIPS, P.A., BURRELL, L.M., GOW, C.B., JOHNSTON, C.I., GRANT, S., RISVANIS, J. & ALDRED, K. (1995). Vasopressin antagonism: physiological and pharmacological roles. In: *Neurohypophysis: Recent Progress of Vasopressin and Oxyctocin Research*, pp. 643-58, Edition 1, ed. Saito, T., Kurokawa, K & Yoshida, S., Elsevier Science, Amsterdam.

PINTO, A., ABRAHAM, N.G. & MULLANE, K.M. (1986). Cytochrome P-450-Dependent Monooxygenase Activity and Endothelial-Dependent Relaxations Induced by Arachidonic Acid. *J Pharmacol Exp Ther*, **236**, 445-51.

POOLE-WILSON, P.A. (1989). Chronic heart failure. Causes, pathophysiology, prognosis, clinical manifestations, investigations.

PRASAD, K., GUPTA, J.B., KALRA, J., LEE, P., MANTHA, S.V. & BHARADWAJ, B. (1996). Oxidative Stress as a Mechanism of Cardiac Failure in Chronic Volume Overload in Canine Model. *Journal of Molecular & Cellular Cardiology*, **28**, 375-85.

PRESTA, A., SIDDHANTA, U., WU, C., SENNEQUIER, N., HUANG, L., ABU-SOUD, H.M., ERZURUM, S. & STUEHR, D.J. (1998). Comparative Functioning of Dihydro- and Tetrahydropterins in Supporting Electron Transfer, Catalysis, and Subunit Dimerization in Inducible Nitric Oxide Synthase. *Biochemistry*, **37**, 298-310.

PRIOR, D.L., JENNINGS, G.L., ARNOLD, P., DU, X.J. & CHIN-DUSTING, J.P. (1998). Impaired Endothelium-Dependent Relaxation in Large, but Not Small Arteries in Rats after Coronary Ligation. *Eur J Pharmacol*, **355**, 167-74.

PRIOR, D.L., JENNINGS, G.L.R. & CHIN-DUSTING, J.P. (2000). Transient Improvement of Acetylcholine Responses after Short-Term Oral L-Arginine in Forearms of Human Heart Failure. *J Cardiovasc Pharmacol*, **36**, 31-7.

RALEVIC, V., KRISTEK, F., HUDLICKA, O. & BURNSTOCK, G. (1989). A New Protocol for Removal of the Endothelium from the Perfused Rat Hind-Limb Preparation. *Circ Res*, **64**, 1190-6.

RAMSEY, J.C.J. (1994). Large Arteries Are More Than Passive Conduits. *Br Heart J.*, **72**, 3-4.

RASHATWAR, S.S., CORNWELL, T.L. & LINCOLN, T.M. (1987). Effects of 8-Bromo-Cgmp on Ca^{2+} Levels in Vascular Smooth Muscle Cells: Possible Regulation of Ca^{2+}-ATPase by cGMP-Dependent Protein Kinase. *Proc Natl Acad Sci U S A*, **84**, 5685-9.

RECTOR, T.S., BANK, A.J., MULLEN, K.A., TSCHUMPERLIN, L.K., SIH, R., PILLAI, K. & KUBO, S.H. (1996). Randomized, Double-Blind, Placebo-Controlled Study of Supplemental Oral L-Arginine in Patients with Heart Failure. *Circulation*, **93**, 2135-41.

REES, D.D., PALMER, R.M., SCHULZ, R., HODSON, H.F. & MONCADA, S. (1990). Characterization of Three Inhibitors of Endothelial Nitric Oxide Synthase in Vitro and in Vivo. *Br J Pharmacol*, **101**, 746-52.

RHODIN, J.A.G. (1980). Architecture of the vessel wall. In: *Handbook of Physiology, The Cardiovascular System*; Volume II, Ch.1, ed. Bohr, D.F., Somlylo, A.P. & Sparks, H.V., Bethesda.

ROBINSON, G., EILLIS, I.O. & MACLELLAN, K.A. (1988). Immunocytochemistry. In: *The Theory and Practise of Histological Techniques*, Ch 20

RODRIGUEZ-CRESPO, I., GERBER, N.C. & ORTIZ DE MONTELLANO, P.R. (1996). Endothelial Nitric-Oxide Synthase. Expression in *Escherichia Coli*, Spectroscopic Characterization, and Role of Tetrahydrobiopterin in Dimer Formation. *J Biol Chem*, **271**, 11462-7.

RUBANYI, G.M. & VANHOUTTE, P.M. (1986). Oxygen-Derived Free Radicals, Endothelium, and Responsiveness of Vascular Smooth Muscle. *Am J Physiol*, **250**, H815-21.

RUBANYI, G.M., JOHNS, A., WILCOX, D., BATES, F.N. & HARRISON, D. (1991). Evidence that a S-nitrosothiol, but not nitric oxide, may be identical with endothelium-derived relaxing factor. *Journal of Cardiovascular Pharmacology*, **17** (suppl 3), S41 – 5

RUBANYI, G.M. & POLOKOFF, M.A. (1994). Endothelins: Molecular Biology, Biochemistry, Pharmacology, Physiology, and Pathophysiology. *Pharmacol Rev*, **46**, 325-415.

RUMBERGER, J.A. (1994). Ventricular Dilatation and Remodeling after Myocardial Infarction. *Mayo Clin Proc*, **69**, 664-74.

SADOSHIMA, J., JAHN, L., TAKAHASHI, T., KULIK, T.J. & IZUMO, S. (1992). Molecular Characterization of the Stretch-Induced Adaptation of Cultured Cardiac Cells. An *in vitro* Model of Load-Induced Cardiac Hypertrophy. *J Biol Chem*, **267**, 10551-60.

SAETRUM OPGAARD, O., CANTERA, L., ADNER, M. & EDVINSSON, L. (1996). Endothelin-A and -B Receptors in Human Coronary Arteries and Veins. *Regul Pept*, **63**, 149-56.

SAITO, Y., NAKAO, K., ARAI, H., SUGAWARA, A., MORII, N., YAMADA, T., ITOH, H., SHIONO, S., MUKOYAMA, M., OBATA, K. & ET AL. (1987). Atrial Natriuretic Polypeptide (ANP) in Human Ventricle. Increased Gene Expression of ANP in Dilated Cardiomyopathy. *Biochem Biophys Res Commun*, **148**, 211-7.

SAKAI, S., MIYAUCHI, T., KOBAYASHI, M., YAMAGUCHI, I., GOTO, K. & SUGISHITA, Y. (1996a). Inhibition of Myocardial Endothelin Pathway Improves Long-Term Survival in Heart Failure. *Nature*, **384**, 353-5.

SAKAI, S., MIYAUCHI, T., SAKURAI, T., KASUYA, Y., IHARA, M., YAMAGUCHI, I., GOTO, K. & SUGISHITA, Y. (1996b). Endogenous Endothelin-1 Participates in the Maintenance of Cardiac Function in Rats with Congestive Heart Failure. Marked Increase in Endothelin-1 Production in the Failing Heart. *Circulation*, **93**, 1214-22.

SAKAI, S., MIYAUCHI, T., KOBAYASHI, T., YAMAGUCHI, I., GOTO, K. & SUGISHITA, Y. (1998). Altered Expression of Isoforms of Myosin Heavy Chain mRNA in the Failing Rat Heart Is Ameliorated by Chronic Treatment with an Endothelin Receptor Antagonist. *J Cardiovasc Pharmacol*, **31**, S302-5.

SALERNO, J.C., MARTASEK, P., ROMAN, L.J. & MASTERS, B.S. (1996). Electron Paramagnetic Resonance Spectroscopy of the Heme Domain of Inducible Nitric Oxide Synthase: Binding of Ligands at the Arginine Site Induces Changes in the Heme Ligation Geometry. *Biochemistry*, **35**, 7626-30.

SAMPEY, D.B., BURRELL, L.M. & WIDDOP, R.E. (1999). Vasopressin V_2 Receptor Enhances Gain of Baroreflex in Conscious Spontaneously Hypertensive Rats. *Am J Physiol*, **276**, R872-9.

SARASTE, A., PULKKI, K., KALLAJOKI, M., HENRIKSEN, K., PARVINEN, M. & VOIPIO-PULKKI, L.M. (1997). Apoptosis in Human Acute Myocardial Infarction. *Circulation*, **95**, 320-3.

SATO, K., MIYAKAWA, K., TAKEYA, M., HATTORI, R., YUI, Y., SUNAMOTO, M., ICHIMORI, Y., USHIO, Y. & TAKAHASHI, K. (1995). Immunohistochemical Expression of Inducible Nitric Oxide Synthase (iNOS) in Reversible Endotoxic Shock Studied by a Novel Monoclonal Antibody against Rat Inos. *J Leukoc Biol*, **57**, 36-44.

SCHAPER, W. & PASYK, S. (1976). Influence of Collateral Flow on the Ischemic Tolerance of the Heart Following Acute and Subacute Coronary Occlusion. *Circulation*, **53**, I57-62.

SCHOTT, C.A., GRAY, G.A. & STOCLET, J.C. (1993). Dependence of Endotoxin-Induced Vascular Hyporeactivity on Extracellular L-Arginine. *Br J Pharmacol*, **108**, 38-43.

SCHRIER, R.W. & ABRAHAM, W.T. (1999). Hormones and Hemodynamics in Heart Failure. *N Engl J Med*, **341**, 577-85.

SCHULZ, R., SMITH, J.A., LEWIS, M.J. & MONCADA, S. (1991). Nitric Oxide Synthase in Cultured Endocardial Cells of the Pig. *Br J Pharmacol*, **104**, 21-4.

SCHULZ, R., PANAS, D.L., CATENA, R., MONCADA, S., OLLEY, P.M. & LOPASCHUK, G.D. (1995). The Role of Nitric Oxide in Cardiac Depression Induced by Interleukin-1 β and Tumour Necrosis Factor-α. *Br J Pharmacol*, **114**, 27-34.

SCHUMAN, E.M. & MADISON, D.V. (1991). A Requirement for the Intercellular Messenger Nitric Oxide in Long-Term Potentiation. *Science*, **254**, 1503-6.

SEKI, T., HAGIWARA, H., NARUSE, K., KADOWAKI, M., KASHIWAGI, M., DEMURA, H., HIROSE, S. & NARUSE, M. (1996). *In Situ* Identification of Messenger RNA of Endothelial Type Nitric Oxide Synthase in Rat Cardiac Myocytes. *Biochem Biophys Res Commun*, **218**, 601-5.

SEYLE, H., BAJUSZ, E., GRASSO, S. & MENDELL, P. (1960). Simple technique for the surgical occlusion of coronary vessels in rats. *Angiology*, **11**, 398 – 407.

SHAH, A.M. (1993). Nitric Oxide Synthase Activities in Human Myocardium. *Lancet*, **341**, 448.

SHAH, A.M., SPURGEON, H.A., SOLLOTT, S.J., TALO, A. & LAKATTA, E.G. (1994). 8-Bromo cGMP Reduces the Myofilament Response to Ca^{2+} in Intact Cardiac Myocytes. *Circ Res*, **74**, 970-8.

SHAH, A.M. & MACCARTHY, P.A. (2000). Paracrine and Autocrine Effects of Nitric Oxide on Myocardial Function. *Pharmacol Ther*, **86**, 49-86.

SHAN, K., KURRELMEYER, K., SETA, Y., WANG, F., DIBBS, Z., DESWAL, A., LEE-JACKSON, D. & MANN, D.L. (1997). The Role of Cytokines in Disease Progression in Heart Failure. *Curr Opin Cardiol*, **12**, 218-23.

SHARMA, R., RAUCHHAUS, M., PONIKOWSKI, P.P., VARNEY, S., POOLE-WILSON, P.A., MANN, D.L., COATS, A.J. & ANKER, S.D. (2000). The Relationship of the Erythrocyte Sedimentation Rate to Inflammatory Cytokines and Survival in Patients with Chronic Heart Failure Treated with Angiotensin-Converting Enzyme Inhibitors. *J Am Coll Cardiol*, **36**, 523-8.

SHORE, A.C. (1996). Vascular biology and physiology. In: *A Textbook of Vascular Medicine*, Ch.2, ed. Tooke, J.E. & Lowe, G.D.O., Churchill Linvingstone, London.

SIDDHANTA, U., WU, C., ABU-SOUD, H.M., ZHANG, J., GHOSH, D.K. & STUEHR, D.J. (1996). Heme Iron Reduction and Catalysis by a Nitric Oxide Synthase Heterodimer Containing One Reductase and Two Oxygenase Domains. *J Biol Chem*, **271**, 7309-12.

SIDDHANTA, U., PRESTA, A., FAN, B., WOLAN, D., ROUSSEAU, D.L. & STUEHR, D.J. (1998). Domain Swapping in Inducible Nitric-Oxide Synthase. Electron Transfer Occurs between Flavin and Heme Groups Located on Adjacent Subunits in the Dimer. *J Biol Chem*, **273**, 18950-8.

SIMON, J. & KASSON, B.G. (1995). Identification of Vasopressin mRNA in Rat Aorta. *Hypertension*, **25**, 1030-3.

SINGAL, P.K., KHAPER, N., PALACE, V. & KUMAR, D. (1998). The Role of Oxidative Stress in the Genesis of Heart Disease. *Cardiovasc Res*, **40**, 426-32.

SINGER, H.A. & PEACH, M.J. (1983). Endothelium-Dependent Relaxation of Rabbit Aorta. I. Relaxation Stimulated by Arachidonic Acid. *J Pharmacol Exp Ther*, **226**, 790-5.

SMITH, J.A., SHAH, A.M. & LEWIS, M.J. (1991). Factors Released from Endocardium of the Ferret and Pig Modulate Myocardial Contraction. *J Physiol (Lond)*, **439**, 1-14.

SMITH, P.J.W. (1996). An investigation into the pathogenesis of Raynaud's disease: the role of the endothelium. *PhD Thesis (Edinburgh)*.

SMITH, C.J., SUN, D., HOEGLER, C., ROTH, B.S., ZHANG, X., ZHAO, G., XU, X.B., KOBARI, Y., PRITCHARD, K., JR., SESSA, W.C. & HINTZE, T.H. (1996). Reduced Gene Expression of Vascular Endothelial No Synthase and Cyclooxygenase-1 in Heart Failure. *Circ Res*, **78**, 58-64.

SPRATT, J.C.S., GODDARD, J., LABINJOY, C. ET AL. (1999). The haemodynamic effects of systemic endothelin A receptor antagonism in healthy humans *in vivo*. *Br J. Clin. Pharmacol.*, **47**, 576.

STAMLER, J.S., SIMON, D.I., OSBORNE, J.A., MULLINS, M.E., JARAKI, O., MICHEL, T., SINGEL, D.J. & LOSCALZO, J. (1992). S-Nitrosylation of Proteins with Nitric Oxide: Synthesis and Characterization of Biologically Active Compounds. *Proc Natl Acad Sci U S A*, **89**, 444-8.

STAMLER, J.S., LOH, E., RODDY, M.A., CURRIE, K.E. & CREAGER, M.A. (1994). Nitric Oxide Regulates Basal Systemic and Pulmonary Vascular Resistance in Healthy Humans. *Circulation*, **89**, 2035-40.

STATHOPULOS, P.B., LU, X., SHEN, J., SCOTT, J.A., HAMMOND, J.R., MCCORMACK, D.G., ARNOLD, J.M. & FENG, Q. (2001). Increased L-Arginine Uptake and Inducible Nitric Oxide Synthase Activity in Aortas of Rats with Heart Failure. *Am J Physiol Heart Circ Physiol*, **280**, H859-67.

STEIN, B., ESCHENHAGEN, T., RUDIGER, J., SCHOLZ, H., FORSTERMANN, U. & GATH, I. (1998). Increased Expression of Constitutive Nitric Oxide Synthase III, but Not Inducible Nitric Oxide Synthase II, in Human Heart Failure. *Journal of the American College of Cardiology*, **32**, 1179-86.

STONE, J.R. & MARLETTA, M.A. (1994). Soluble Guanylate Cyclase from Bovine Lung: Activation with Nitric Oxide and Carbon Monoxide and Spectral Characterization of the Ferrous and Ferric States. *Biochemistry*, **33**, 5636-40.

STROES, E., HIJMERING, M., VAN ZANDVOORT, M., WEVER, R., RABELINK, T.J. & VAN FAASSEN, E.E. (1998). Origin of Superoxide Production by Endothelial Nitric Oxide Synthase. *FEBS Letters*, **438**, 161-4.

STUEHR, D.J., KWON, N.S., GROSS, S.S., THIEL, B.A., LEVI, R. & NATHAN, C.F. (1989). Synthesis of Nitrogen Oxides from L-Arginine by Macrophage Cytosol: Requirement for Inducible and Constitutive Components. *Biochem Biophys Res Commun*, **161**, 420-6.

STUEHR, D.J. & GRIFFITH, O.W. (1992). Mammalian Nitric Oxide Synthases. *Adv Enzymol Relat Areas Mol Biol*, **65**, 287-346.

STUEHR, D.J. (1999). Mammalian Nitric Oxide Synthases. *Biochim Biophys Acta*, **1411**, 217-30.

SUN, X., WEI, S., SZABO, C. & DUSTING, G.J. (1997). Depression of the Inotropic Action of Isoprenaline by Nitric Oxide Synthase Induction in Rat Isolated Hearts. *European Journal of Pharmacology*, **320**, 29-35.

SUTTON, G.C. & COWIE, M.R. (1997). Epidemiology of heart failure in Europe. In: *Heart failure. Scientific principles and clinical practice.* p 617 – 633, ed. Poole-Wilson, P.A., Colucci, W.S., Massie, B.M., Chatterjee, K. & Coates, A.L.S., Churchill Livingtone, London.

SUZUKI, S., SATO, H., SHIMADA, H., TAKASHIMA, N. & ARAKAWA, M. (1993a). Comparative Free Radical Scavenging Action of Angiotensin-Converting Enzyme Inhibitors with and without the Sulfhydryl Radical. *Pharmacology*, **47**, 61-5.

SUZUKI, T., KUMAZAKI, T. & MITSUI, Y. (1993b). Endothelin-1 is Produced and Secreted by Neonatal Rat Cardiac Myocytes *in vitro*. *Biochem Biophys Res Commun*, **191**, 823-30.

SWYNGHEDAUW, B. (1999). Molecular Mechanisms of Myocardial Remodeling. *Physiol Rev*, **79**, 215-62.

SZABO, C., ZINGARELLI, B. & SALZMAN, A.L. (1996). Role of Poly-Adp Ribosyltransferase Activation in the Vascular Contractile and Energetic Failure Elicited by Exogenous and Endogenous Nitric Oxide and Peroxynitrite. *Circ Res*, **78**, 1051-63.

SZATALOWICZ, V.L., ARNOLD, P.E., CHAIMOVITZ, C., BICHET, D., BERL, T. & SCHRIER, R.W. (1981). Radioimmunoassay of Plasma Arginine Vasopressin in Hyponatremic Patients with Congestive Heart Failure. *N Engl J Med*, **305**, 263-6.

TAKASE, H., MOREAU, P. & LUSCHER, T.F. (1995). Endothelin Receptor Subtypes in Small Arteries. Studies with Fr139317 and Bosentan. *Hypertension*, **25**, 739-43.

TANAKA, Y., AIDA, M., TANAKA, H., SHIGENOBU, K. & TORO, L. (1998). Involvement of Maxi-K(Ca) Channel Activation in Atrial Natriuretic Peptide-Induced Vasorelaxation. *Naunyn Schmiedebergs Arch Pharmacol*, **357**, 705-8.

TEERLINK, J.R., GRAY, G.A., CLOZEL, M. & CLOZEL, J.P. (1994). Increased Vascular Responsiveness to Norepinephrine in Rats with Heart Failure Is Endothelium Dependent. *Circulation*, **89**, 393-401.

TEWARI, K. & SIMARD, J.M. (1997). Sodium Nitroprusside and cGMP Decrease Ca^{2+} Channel Availability in Basilar Artery Smooth Muscle Cells. *Pflugers Arch*, **433**, 304-11.

THOENES, M., FORSTERMANN, U., TRACEY, W.R., BLEESE, N.M., NUSSLER, A.K., SCHOLZ, H. & STEIN, B. (1996). Expression of Inducible Nitric Oxide Synthase in Failing and Non-Failing Human Heart. *Journal of Molecular & Cellular Cardiology*, **28**, 165-9.

TIMMS, A.D. & DAVIES, S.W. (2000). *Heart failure*, Grower Medical Publishing.

TITHERADGE, M.A. (1999). Nitric Oxide in Septic Shock. *Biochim Biophys Acta*, **1411**, 437-55.

TODOKI, K., OKABE, E., KIYOSE, T., SEKISHITA, T. & ITO, H. (1992). Oxygen Free Radical-Mediated Selective Endothelial Dysfunction in Isolated Coronary Artery. *Am J Physiol*, **262**, H806-12.

TORRE-AMIONE, G., KAPADIA, S., LEE, J., BIES, R.D., LEBOVITZ, R. & MANN, D.L. (1995). Expression and Functional Significance of Tumor Necrosis Factor Receptors in Human Myocardium. *Circulation*, **92**, 1487-93.

TORRE-AMIONE, G., KAPADIA, S., BENEDICT, C., ORAL, H., YOUNG, J.B. & MANN, D.L. (1996a). Proinflammatory Cytokine Levels in Patients with Depressed Left Ventricular Ejection Fraction: A Report from the Studies of Left Ventricular Dysfunction (Solvd). *J Am Coll Cardiol*, **27**, 1201-6.

TORRE-AMIONE, G., KAPADIA, S., LEE, J., DURAND, J.B., BIES, R.D., YOUNG, J.B. & MANN, D.L. (1996b). Tumor Necrosis Factor-α and Tumor Necrosis Factor Receptors in the Failing Human Heart. *Circulation*, **93**, 704-11.

TORRE-AMIONE, G., VOOLETICH, M.T. & FARMER, J.A. (2000). Role of Tumour Necrosis Factor-α in the Progression of Heart Failure: Therapeutic Implications. *Drugs*, **59**, 745-51.

TRAYLOR, T.G. & SHARMA, V.S. (1992). Why No? *Biochemistry*, **31**, 2847-9.

VANBAVEL, E., GIEZEMAN, M.J., MOOIJ, T. & SPAAN, J.A. (1991). Influence of Pressure Alterations on Tone and Vasomotion of Isolated Mesenteric Small Arteries of the Rat. *J Physiol (Lond)*, **436**, 371-83.

VARIN, R., MULDER, P., RICHARD, V., TAMION, F., DEVAUX, C., HENRY, J.P., LALLEMAND, F., LEREBOURS, G. & THUILLEZ, C. (1999). Exercise Improves Flow-Mediated Vasodilatation of Skeletal Muscle Arteries in Rats with Chronic Heart Failure. Role of Nitric Oxide, Prostanoids, and Oxidant Stress. *Circulation*, **99**, 2951-7.

VEJLSTRUP, N.G., BOULOUMIE, A., BOESGAARD, S., ANDERSEN, C.B., NIELSEN-KUDSK, J.E., MORTENSEN, S.A., KENT, J.D., HARRISON, D.G., BUSSE, R. & ALDERSHVILE, J. (1998). Inducible Nitric Oxide Synthase (iNOS) in the Human Heart: Expression and Localization in Congestive Heart Failure. *Journal of Molecular & Cellular Cardiology*, **30**, 1215-23.

VENEMA, R.C., JU, H., ZOU, R., RYAN, J.W. & VENEMA, V.J. (1997). Subunit Interactions of Endothelial Nitric-Oxide Synthase. Comparisons to the Neuronal and Inducible Nitric-Oxide Synthase Isoforms. *J Biol Chem*, **272**, 1276-82.

VILA-PETROFF, M.G., YOUNES, A., EGAN, J., LAKATTA, E.G. & SOLLOTT, S.J. (1999). Activation of Distinct cAMP-Dependent and cGMP-Dependent Pathways by Nitric Oxide in Cardiac Myocytes. *Circ Res*, **84**, 1020-31.

WANG, J., YI, G.H., KNECHT, M., CAI, B.L., POPOSKIS, S., PACKER, M. & BURKHOFF, D. (1997). Physical Training Alters the Pathogenesis of Pacing-Induced Heart Failure through Endothelium-Mediated Mechanisms in Awake Dogs. *Circulation*, **96**, 2683-92.

WANG, Q.D., LI, X.S. & PERNOW, J. (1994). Characterization of Endothelin-1-Induced Vascular Effects in the Rat Heart by Using Endothelin Receptor Antagonists. *Eur J Pharmacol*, **271**, 25-30.

WEBER, K.T. (1997). Extracellular Matrix Remodeling in Heart Failure: A Role for De Novo Angiotensin Ii Generation. *Circulation*, **96**, 4065-82.

WEI, C.M., LERMAN, A., RODEHEFFER, R.J., MCGREGOR, C.G., BRANDT, R.R., WRIGHT, S., HEUBLEIN, D.M., KAO, P.C., EDWARDS, W.D. & BURNETT, J.C., JR. (1994). Endothelin in Human Congestive Heart Failure. *Circulation*, **89**, 1580-6.

WEIGERT, A.L., HIGA, E.M., NIEDERBERGER, M., MCMURTRY, I.F., RAYNOLDS, M. & SCHRIER, R.W. (1995). Expression and Preferential Inhibition of Inducible Nitric Oxide Synthase in Aortas of Endotoxemic Rats. *J Am Soc Nephrol*, **5**, 2067-72.

WERNER-FELMAYER, G., WERNER, E.R., FUCHS, D., HAUSEN, A., REIBNEGGER, G. & WACHTER, H. (1990). Tetrahydrobiopterin-Dependent Formation of Nitrite and Nitrate in Murine Fibroblasts. *J Exp Med*, **172**, 1599-607.

WEVER, R.M., LUSCHER, T.F., COSENTINO, F. & RABELINK, T.J. (1998). Atherolsclerosis and the two faces of endothelial nitric oxide synthase, *Circulation*, **97**, 108 -12

WILDHIRT, S.M., DUDEK, R.R., SUZUKI, H., PINTO, V., NARAYAN, K.S. & BING, R.J. (1995). Immunohistochemistry in the Identification of Nitric Oxide Synthase Isoenzymes in Myocardial Infarction. *Cardiovascular Research*, **29**, 526-31.

WILSON, R.A., DI MARIO, C., KRAMS, R., SOEI, L.K., WENGUANG, L., LAIRD, A.C., THE, S.H., GUSSENHOVEN, E., VERDOUW, P. & ROELANDT, J.R. (1995). *In vivo* Measurement of Regional Large Artery Compliance by Intravascular Ultrasound under Pentobarbital Anesthesia. *Angiology*, **46**, 481-8.

WINLAW, D.S., SMYTHE, G.A., KEOGH, A.M., SCHYVENS, C.G., SPRATT, P.M. & MACDONALD, P.S. (1994). Increased Nitric Oxide Production in Heart Failure. *Lancet*, **344**, 373-4.

WOLFF, D.J., PAPOIU, A.D., MIALKOWSKI, K., RICHARDSON, C.F., SCHUSTER, D.I. & WILSON, S.R. (2000). Inhibition of Nitric Oxide Synthase Isoforms by Tris-Malonyl-C(60)-Fullerene Adducts. *Arch Biochem Biophys*, **378**, 216-23.

WRAY, G.M., MILLAR, C.G., HINDS, C.J. & THIEMERMANN, C. (1998). Selective Inhibition of the Activity of Inducible Nitric Oxide Synthase Prevents the Circulatory Failure, but Not the Organ Injury/Dysfunction, Caused by Endotoxin. *Shock*, **9**, 329-35.

WU, C.C., CHEN, S.J., SZABO, C., THIEMERMANN, C. & VANE, J.R. (1995). Aminoguanidine Attenuates the Delayed Circulatory Failure and Improves Survival in Rodent Models of Endotoxic Shock. *Br J Pharmacol*, **114**, 1666-72.

WU, X., SOMLYO, A.V. & SOMLYO, A.P. (1996). Cyclic Gmp-Dependent Stimulation Reverses G-Protein-Coupled Inhibition of Smooth Muscle Myosin Light Chain Phosphate. *Biochem Biophys Res Commun*, **220**, 658-63.

XIA, Y., ROMAN, L.J., MASTERS, B.S. & ZWEIER, J.L. (1998a). Inducible Nitric-Oxide Synthase Generates Superoxide from the Reductase Domain. *J Biol Chem*, **273**, 22635-9.

XIA, Y., TSAI, A.L., BERKA, V. & ZWEIER, J.L. (1998b). Superoxide Generation from Endothelial Nitric-Oxide Synthase. A Ca^{2+}/Calmodulin-Dependent and Tetrahydrobiopterin Regulatory Process. *J Biol Chem*, **273**, 25804-8.

XIE, Q.W., CHO, H.J., CALAYCAY, J., MUMFORD, R.A., SWIDEREK, K.M., LEE, T.D., DING, A., TROSO, T. & NATHAN, C. (1992). Cloning and Characterization of Inducible Nitric Oxide Synthase from Mouse Macrophages. *Science*, **256**, 225-8.

YAMAKAGE, M., HIRSHMAN, C.A. & CROXTON, T.L. (1996). Sodium Nitroprusside Stimulates Ca^{2+} -Activated K^+ Channels in Porcine Tracheal Smooth Muscle Cells. *Am J Physiol*, **270**, L338-45.

YANAGISAWA, M., KURIHARA, H., KIMURA, S., TOMOBE, Y., KOBAYASHI, M., MITSUI, Y., YAZAKI, Y., GOTO, K. & MASAKI, T. (1988). A Novel Potent Vasoconstrictor Peptide Produced by Vascular Endothelial Cells. *Nature*, **332**, 411-5.

YEN, M.H., CHEN, S.J. & WU, C.C. (1995). Comparison of Responses to Aminoguanidine and N^{ω}-Nitro-L-Arginine Methyl Ester in the Rat Aorta. *Clin Exp Pharmacol Physiol*, **22**, 641-5.

YOKOYAMA, T., VACA, L., ROSSEN, R.D., DURANTE, W., HAZARIKA, P. & MANN, D.L. (1993). Cellular Basis for the Negative Inotropic Effects of Tumor Necrosis Factor-α in the Adult Mammalian Heart. *J Clin Invest*, **92**, 2303-12.

YOSHIZUMI, M., PERRELLA, M.A., BURNETT, J.C., JR. & LEE, M.E. (1993). Tumor Necrosis Factor Downregulates an Endothelial Nitric Oxide Synthase mRNA by Shortening Its Half-Life. *Circ Res*, **73**, 205-9.

YUCEL, D., AYDOGDU, S., CEHRELI, S., SAYDAM, G., CANATAN, H., SENES, M., CIGDEM TOPKAYA, B. & NEBIOGLU, S. (1998). Increased Oxidative Stress in Dilated Cardiomyopathic Heart Failure. *Clinical Chemistry*, **44**, 148-54.

YUE, T.L., CHENG, H.Y., LYSKO, P.G., MCKENNA, P.J., FEUERSTEIN, R., GU, J.L., LYSKO, K.A., DAVIS, L.L. & FEUERSTEIN, G. (1992). Carvedilol, a New Vasodilator and Beta Adrenoceptor Antagonist, Is an Antioxidant and Free Radical Scavenger. *J Pharmacol Exp Ther*, **263**, 92-8.

ZELIS, R., DELEA, C.S., COLEMAN, H.N. & MASON, D.T. (1970). Arterial Sodium Content in Experimental Congestive Heart Failure. *Circulation*, **41**, 213-6.

ZEMBOWICZ, A., HATCHETT, R.J., JAKUBOWSKI, A.M. & GRYGLEWSKI, R.J. (1993). Involvement of Nitric Oxide in the Endothelium-Dependent Relaxation Induced by Hydrogen Peroxide in the Rabbit Aorta. *Br J Pharmacol*, **110**, 151-8.

ZHOU, X.B., RUTH, P., SCHLOSSMANN, J., HOFMANN, F. & KORTH, M. (1996). Protein Phosphatase 2a Is Essential for the Activation of Ca^{2+}-Activated K^{+} Currents by cGMP-Dependent Protein Kinase in Tracheal Smooth Muscle and Chinese Hamster Ovary Cells. *J Biol Chem*, **271**, 19760-7.

British Journal of Pharmacology (2000) 131, 29–36
www.nature.com/bjp

Inducible nitric oxide synthase-derived superoxide contributes to hypereactivity in small mesenteric arteries from a rat model of chronic heart failure

[1]Alyson A. Miller, [1]Ian L. Megson & *,[1]Gillian A. Gray

[1]Endothelial Cell Biology and Molecular Cardiology Section, Centre for Cardiovascular Science, Department of Biomedical Sciences, University of Edinburgh, Hugh Robson Building, George Square, Edinburgh, EH8 9LD

1 The aims of this study were to (a) determine whether inducible nitric oxide synthase (iNOS) is expressed in small mesenteric arteries from rats with chronic heart failure (CHF), (b) investigate the functional significance of this potential source of nitric oxide (NO) on vascular responsiveness and (c) investigate the role that superoxide plays in modulating vascular function in these arteries.

2 CHF was induced in male Wistar rats by coronary artery ligation (CAL). In sham-operated rats the ligature was not tied but pulled under the artery. Six weeks after surgery CAL rats had left ventricular (LV) infarctions and elevated LV end-diastolic pressures.

3 Immunoreactive iNOS was found in endothelial cells, vascular smooth muscle cells and in the adventitia of small mesenteric arteries from CAL rats but not those from sham-operated rats.

4 Third order mesenteric arteries (300–350 μm) were mounted in a small vessel pressure myograph. Endothelium-intact arteries from CAL rats were more responsive to phenylephrine (PE) than arteries from sham-operated rats (pD_2 value, CAL, 6.2 ± 0.1; sham-operated, 5.9 ± 0.1, $P<0.05$).

5 Both the selective iNOS inhibitor, N-(3-(Aminomethyl) benzyl) acetamidine dihydrochloride (1400W; 10^{-6} M) and the superoxide dismutase mimetic, Mn [III] tetrakis [1-methyl-4-pyridyl] porphyrin, (MnTMPyP; 10^{-4} M) reversed the hyperresponsiveness (pD_2 values, 1400W, 5.9 ± 0.1; MnTMPyP, 5.81 ± 0.1, $P<0.05$). The NOS substrate, L-arginine (10^{-3} M), reduced responsiveness of endothelium-denuded small mesenteric arteries from CAL rats ($P<0.01$). None of these drugs altered responses to PE in arteries from sham-operated rats.

6 In summary, this study demonstrates that iNOS is expressed in mesenteric arteries from rats with CHF. However, instead of generating large quantities of NO, iNOS appears to be generating superoxide, perhaps because of a deficiency in its substrate, L-arginine. Increased superoxide generation from iNOS contributes to the hyperresponsive nature of endothelium-intact small mesenteric arteries from rats with CHF.

British Journal of Pharmacology (2000) **131,** 29–36

Keywords: Nitric oxide; inducible nitric oxide synthase; superoxide; L-arginine; endothelium; rat mesenteric arteries; heart failure

Abbreviations: ANOVA, analysis of variance; CAL, coronary artery ligation; CHF, chronic heart failure; CRC, concentration response curve; eNOS, endothelial nitric oxide synthase; iNOS, inducible nitric oxide synthase; LV, left ventricle; LVEDP, left ventricular end-diastolic pressure; MnTMPyP, Mn [III] tetrakis [1-methyl-4-pyridyl] porphyrin; N-(3-(Aminomethyl) benzyl) acetamidine dihydrochloride; NO, nitric oxide; PE, phenylephrine; SOD, superoxide dismutase; VSM, vascular smooth muscle; 1400W, N-(3-(Aminomethyl) benzyl) acetamidine dihydrochloride

Introduction

Endothelium-derived nitric oxide (NO) plays a vital role in the regulation of vasomotor tone and arterial blood pressure (for review see Moncada *et al.*, 1991). Evidence is accumulating to suggest that impaired NO-mediated vasodilatation contributes to increased peripheral vascular resistance associated with chronic heart failure (CHF). In clinical and experimental CHF it has been established that endothelium-dependent relaxation in response to acetylcholine is impaired (Drexler *et al.*, 1992; Ramsey & Jones, 1994; Bauersachs *et al.*, 1999). In contrast, data on basal release of NO in CHF is controversial. Some studies suggest that basal release of NO is preserved or may even be enhanced in CHF (Drexler *et al.*, 1992; Habib *et al.*, 1994; Winlaw *et al.*, 1994), while other studies show that it is impaired (Elsner *et al.*, 1991; Teerlink *et al.*, 1994). The aetiology of endothelial dysfunction associated with CHF is unclear and is likely to be complex.

*Author for correspondence; E-mail: gillian.gray@ed.ac.uk

The inducible isoform of nitric oxide synthase (iNOS) is expressed in the vasculature in response to inflammatory cytokines and pathogens (Moncada *et al.*, 1991). Inflammatory cytokines such as tumour necrosis factor-α are elevated in the plasma of patients with CHF (Katz *et al.*, 1994). Furthermore, iNOS has been reported by some investigators to be present in the myocardium (Fukuchi *et al.*, 1998; Vejlstrup *et al.*, 1998) and skeletal muscle (Adams *et al.*, 1997) of patients with CHF. The role of iNOS in the vasculature has not been directly addressed in CHF. It has been suggested, however, that iNOS may be responsible for increased basal production of NO in CHF (Carville *et al.*, 1998).

Irrespective of its source, increased basal production of NO should counteract compensatory constrictor mechanisms and thus reduce peripheral vascular resistance. Increased superoxide production is associated with CHF (Belch *et al.*, 1991). Superoxide scavenges NO (Gryglewski *et al.*, 1986), therefore, a reduction in NO bioavailability may well explain why

peripheral vascular resistance remains elevated in CHF despite a preserved or enhanced basal release of NO.

The aims of the present study were to determine if iNOS is expressed in isolated small mesenteric arteries from a rat model of CHF, to determine the functional significance of this potential source of NO on vascular responsiveness and to investigate the role that superoxide plays in modulating vascular function in these arteries.

Methods

Coronary artery ligation model of CHF

All experiments were carried out in accordance with the Animals (Scientific Procedures) Act 1986. Myocardial infarction was induced in 5 week old male Wistar rats (250–300 g, Charles River) by coronary artery ligation (CAL), as previously described (Pfeffer *et al.*, 1979). In brief, rats were anaesthetized (sodium pentobarbitol; 60 mg kg^{-1}, i.p.), the thoracic cavity was opened and the heart exteriorized. Using a silk ligature, the left anterior descending coronary artery was tied. In control sham-operated rats, the ligature was not tied but pulled through under the coronary artery. After closure of the chest, animals were allowed to recover and were maintained on standard chow and water *ad libitum*.

Six weeks after surgery, rats were anaesthetized (sodium pentobarbitol; 60 mg kg^{-1}, i.p.), the right carotid artery was isolated and a Millar pressure transducer-tipped catheter (2F, model SPR 407, Millar Instruments, Inc., Houston, TX, U.S.A.) introduced into the artery for measurement of arterial blood pressure. The catheter was then advanced into the left ventricle (LV) for measurement of left ventricular end-diastolic pressure (LVEDP) as an index of left ventricular function.

Following exsanguination, the mesenteric bed was excised, the gut removed and the remaining vascular bed placed into cold, oxygenated (95% O_2, 5% CO_2), Krebs-Henseleit solution (composition, in mM: NaCl 118, KCl 4.7, $CaCl_2$ 2.5, $MgSO_4$ 1.2, KH_2PO_4 1.2, $NaHCO_3$ 25 and glucose 5.5) for functional studies. Sections of the mesenteric bed from both CAL and sham-operated rats were placed in 10% neutral phosphate buffered formalin for fixation. The hearts and lungs were removed and weighed. Hearts were bisected, fixed in formalin as above for detection of mature collagen in the infarcted zone and measurement of infarct size.

Immunohistochemistry

Formalin fixed mesenteric arteries from both CAL and sham-operated rats were processed in ethanol and embedded in paraffin wax. Three-μm sections were taken from blocks, dewaxed in xylene (10 min), rehydrated through a descending alcohol series (100, 90 and 70% alcohol; 3 min each) and washed in water (15 min). To expose antigenic sites, arteries were treated with 0.1% trypsin (diluted in Tris-buffered saline; pH 7.8; 15 min). Arteries were then treated with anti-iNOS monoclonal antibody for 24 h (4°C), washed in phosphate buffered saline (PBS; pH 7.6; 10 min) and treated with alkaline phosphatase-conjugated goat anti-rabbit IgG for 30 min (room temperature). To detect iNOS within arteries, sections were treated with an alkaline phosphatase substrate and red fuchsin as a chromogen (~20 min). Negative controls were treated with an antibody of the same immunoglobulin class but not directed against the iNOS epitope. Tissues were counterstained with Harris' haematoxylin (BDH, Poole, U.K.).

Measurement of infarct size

Hearts were processed as above and 3 μm sections taken from paraffin blocks. After dewaxing and rehydration, hearts were treated with Van Gieson's stain for detection of collagen formation in infarctions. Infarct size was measured in sections as previously described (Mulder *et al.*, 1998). Sections were placed under a CCD video camera module (Sony, U.K.) attached to a microscope with a ×20 lens. The endocardial and epicardial circumferences of the infarcted tissue and of the LV were determined with image analysis software (Imaging Associates, U.K.). Infarct size was calculated as a percentage [endocardial + epicardial circumference of the infarcted LV (mm)/endocardial + epicardial circumference (mm)] of the whole LV.

Preparation of arteries from mesenteric bed

Third order branches of the mesenteric artery (~3 mm length, internal diameter; 300–350 μm) were dissected free of the bed and mounted between two microcannulae in a small vessel pressure myograph (Living Systems Instrumentation Inc., Burlington, U.S.A.). Arteries were constantly superfused with warm (37°C), oxygenated (95% O_2, 5% CO_2) Krebs-Henseleit solution. The intraluminal pressure of the vessel was raised to 60 mmHg and maintained at this level with a pressure servo unit without further intraluminal perfusion. A pressure of 60 mmHg was chosen because it has been estimated that vessels of this size would experience pressures approximately 50% of mean arterial pressure *in vivo* (Halpern & Kelley, 1991). Luminal diameter was measured using a video dimension analyser (Living Systems Instrumentation Inc., Burlington, U.S.A.) and a calibrated hand micrometer, when the optical dimension analyser was unable to detect differences in optical density at smaller lumen diameters.

After an equilibration period of 60 min, arteries were exposed twice in succession, separated by washout, to modified Krebs-Henseleit solution containing 60 mM KCl (equimolar replacement of NaCl by KCl) to obtain maximal constriction. Arteries were then exposed twice to a supramaximal concentration of phenylephrine (PE; 10^{-5} M). In all arteries the endothelial integrity was tested by measuring ACh-induced relaxation (10^{-5} M) of PE-induced tone (10^{-5} M), with maximal relaxation indicating the presence of an intact endothelium. In some arteries, the endothelium was removed by passing an air bubble through the vessel lumen by a method previously described (Falloon *et al.*, 1993), and successful denudation verified by loss of ACh-induced relaxation (10^{-5} M). After sufficient washout and re-equilibration, arteries were constantly superfused in a closed system with a total volume of 30 ml warm (37°C), oxygenated (95% O_2, 5% CO_2) Krebs-Henseleit solution. All drugs used throughout this study were applied to this 30 ml reservoir, removing 1 ml of Krebs-Henseleit solution and replacing with the drug being added (as previously described, Mickley *et al.*, 1997). Responses were recorded 5 min after addition of drug in order to allow time for responses to reach equilibrium. Four arteries were isolated from each CAL and sham-operated rat and the following experiments carried out in a random order.

Experimental protocols

Vascular responsiveness of arteries from coronary artery ligation and sham-operated rats To assess vascular responsiveness of small mesenteric arteries from CAL and sham-operated rats to adrenoceptor stimulation, cumulative concentration response

curves (CRC) to PE (1×10^{-9} to 3×10^{-5} M) were constructed in endothelium-intact ($n=8$) and endothelium-denuded ($n=6$) arteries. Following completion of CRCs all vessels were repeatedly washed and allowed to re-equilibrate before further experiments.

Effect of iNOS inhibition on vascular responsiveness To investigate the role of iNOS in modulating vascular responsiveness, endothelium-intact mesenteric arteries were exposed to the iNOS inhibitor, N-(3-(Aminomethyl) benzyl) acetamidine dihydrochloride (1400W; 10^{-6} M, $n=8$) for 30 min prior to repeating cumulative CRCs to PE (1×10^{-9} to 3×10^{-5} M). At this concentration, 1400W has been shown to inhibit the activity of iNOS in isolated rat aortic rings treated with lipopolysaccharide, without modifying the release of NO from endothelial NOS (eNOS) (Garvey *et al.*, 1997). 1400W was present in the superfusate throughout the CRC.

Effect of superoxide quenching on vascular responsiveness To investigate the role that superoxide plays in modulating vascular responsiveness, endothelium-intact mesenteric arteries were exposed to the superoxide dismutase (SOD) mimetic, Mn [III] tetrakis [1-methyl-4-pyridyl] porphyrin (MnTMPyP; 10^{-4} M, $n=8$) for 30 min prior to repeating cumulative CRCs to PE (1×10^{-9} to 3×10^{-5} M). At a concentration of 10^{-4} M, MnTMPyP has been shown to protect endothelial-derived NO from destruction by superoxide in an *in vitro* model of oxidative stress (MacKenzie & Martin, 1998). MnTMPyP was present in the superfusate throughout the CRC.

Effect of combined iNOS inhibition and superoxide quenching on vascular responsiveness To further investigate the role of iNOS and superoxide in modulating vascular responsiveness, endothelium-intact mesenteric arteries were exposed to the iNOS inhibitor, 1400W (10^{-6} M, $n=8$) and the SOD mimetic, MnTMPyP (10^{-4} M, $n=8$) for 30 min prior to repeating cumulative CRC's to PE (1×10^{-9} to 3×10^{-5} M). Both drugs were present in the superfusate throughout the CRC.

Effect of NOS substrate on vascular responsiveness To investigate the effect of the NOS substrate, L-arginine, on vascular responsiveness, endothelium-denuded mesenteric arteries were exposed to a supramaximal concentration (Schott *et al.*, 1993) of L-arginine (10^{-3} M, $n=6$) for 30 min prior to repeating cumulative CRCs to PE (1×10^{-9} to 3×10^{-5} M). L-arginine was present in the superfusate throughout the CRC.

Assessment of endothelium-dependent relaxations in arteries from coronary artery ligation and sham-operated rats in the presence and absence of the SOD-mimetic, MnTMPyP To assess endothelium-dependent relaxations in mesenteric arteries from CAL and sham-operated rats ACh-mediated relaxations were measured in PE-constricted arteries. A submaximal concentration of PE ($\sim EC_{50}$), as determined from PE CRCs, was used to induce arterial tone. Cumulative CRCs to ACh (1×10^{-10} to 3×10^{-6} M, $n=7$) were then obtained in the absence and presence of the SOD-mimetic MnTMPyP (10^{-4} M, $n=6$).

Materials

Anti-iNOS monoclonal antibodies were obtained from Affiniti Laboratories (Exeter, U.K.) and alkaline phosphatase-conjugated goat anti-rabbit IgG from Vector Laboratories (Peterborough, U.K.). IgG antibodies were purchased from Vector Laboratories (Peterborough, U.K.). New Fuchsin Substrate System was purchased from Dako Corporation (Carpinteria, U.S.A.).

Phenylephrine hydrochloride, acetylcholine chloride and L-arginine were obtained from Sigma (Poole, U.K.), were diluted in Krebs-Henseleit solution to give a stock solution of 10^{-1} M and frozen (−20°C) in aliquots until use on day of experiment. 1400W (N-(3-(Aminomethyl) benzyl acetamidine dihydrochloride) was obtained from Calbiochem (Nottingham, U.K.) and subsequently diluted in saline (0.9% NaCl) under argon to give a stock solution of 10^{-3} M. Aliquots were then frozen (−20°C) and stored under argon. Further dilutions were made in Krebs-Henseleit solution. MnTMPyP (Mn [III] tetrakis [1-methyl-4-pyridyl] porphyrin) was obtained from Alexis (Nottingham, U.K.) and diluted in Krebs-Henseleit solution immediately prior to experimentation.

Analysis of data

All results were expressed as means ± s.e.mean. Where maximal values were obtained for cumulative CRCs, the negative logarithm of the agonist concentration that results in a half-maximal constriction or relaxation (pD_2) was calculated. Two-tailed *t*-tests, one-way analysis of variance (ANOVA) with Bonferroni multiple comparisons post-test and two-way repeated measures ANOVA were used as indicated in the text. $P<0.05$ was considered to be statistically significant.

Results

Effect of left coronary artery ligation

All the animals that survived the first 24 h after CAL surgery (76%) were still alive 6 weeks later. There were no significant differences between rat weights for CAL and sham-operated groups at 6 weeks after surgery (Table 1). Heart weights (corrected for body weight) for CAL rats were significantly greater than those of sham-operated rats despite the presence of large infarcts ($P<0.05$, two-tailed unpaired *t*-test, Table 1), indicating that hearts from CAL rats had undergone compensatory hypertrophy as a result of left ventricular infarction. There were no significant differences between groups with respect to lung weights and arterial blood pressures (Table 1). LVEDPs measured from CAL rats were significantly greater than those for sham-operated rats ($P<0.05$, two-tailed unpaired *t*-test, Table 1). CAL rats had left ventricular infarctions averaging 60 ± 3% of the LV free wall. Additionally there was histological evidence for mature collagen scar formation within the infarcted zone (not shown).

Table 1 Summary of all parameters measured from coronary artery ligation (**CAL**) and sham-operated (**SHAM**) rats

Parameter	***CAL*** ($n>8$)	***SHAM*** ($n>8$)
Rat weight (g)	473.9 ± 9.7	495.7 ± 22.3
Heart weight (g kg^{-1} body weight)	3.3 ± 0.2*	2.7 ± 0.1
Lung weight (g kg^{-1} body weight)	4.3 ± 0.5	3.3 ± 0.1
Left ventricular end-diastolic Pressure (mmHg)	15.4 ± 1.5**	6 ± 1.1
Arterial pressure (mmHg)	78.2 ± 5.7	94.8 ± 6.2

All values are given as mean ± s.e.mean. *$P<0.05$, **$P<0.001$ for CAL rats compared with sham-operated rats (two-tailed unpaired *t*-test).

Immunohistochemistry

Immunoreactive iNOS was found in endothelial cells, vascular smooth muscle (VSM) cells and in the adventitia of small mesenteric arteries from CAL rats (Figure 1). No immunoreactivity was found in mesenteric arteries from sham-operated rats (Figure 1) or in negative controls using IgG antibodies (not shown).

KCl, PE maximal constrictions and endothelial integrity

There were no significant differences between endothelium-intact and endothelium-denuded small mesenteric arteries from CAL and sham-operated groups with respect to internal diameters at rest and in response to KCl (60 mM; Table 2). However, maximal constriction to PE was significantly greater in endothelium-denuded than in endothelium-intact mesenteric arteries from both CAL and sham-operated rats ($P<0.05$, one-way ANOVA with Bonferroni post-test, Table 2). All endothelium-intact small mesenteric arteries studied had functional endothelium (CAL, $101.3\pm4\%$; sham-operated, $95.9\pm3\%$ relaxations to ACh) and no significant differences in maximal relaxations were found between CAL and sham-operated groups (Table 2).

Assessment of vascular responsiveness to adrenoceptor stimulation in coronary artery ligation and sham-operated rats

In both endothelium-intact and endothelium-denuded small mesenteric arteries from CAL and sham-operated rats, cumulative additions of PE (1×10^{-9} to 3×10^{-5} M) resulted in concentration-dependent constrictions (Figure 2a,b). In endothelium-intact arteries from CAL rats, cumulative CRCs to PE were shifted significantly to the left when compared with responses in sham-operated groups, indicating that arteries from CAL rats were more responsive to PE than those from sham-operated rats ($P<0.05$, two-way ANOVA, Figure 2a). Indeed, pD_2 values for PE CRCs in arteries from CAL rats were significantly greater than those in sham-operated rats (CAL, 6.2 ± 0.1; sham-operated, 5.9 ± 0.1, $P<0.05$, two-tailed unpaired t-test). There was no significant difference between maximal constrictions observed in arteries from CAL and sham-operated rats (Figure 2a).

In endothelium-denuded arteries no significant differences were found between CAL and sham-operated rats with respect to PE CRCs (Figure 2b). In addition, there were no significant

Table 2 Internal luminal diameters of endothelium-intact (+end) and -denuded (–end) arteries from coronary artery ligation (**CAL**) and sham-operated (**SHAM**) rats

	CAL (μm)		*SHAM* (μm)	
	+end ($n=11$)	*–end* ($n=9$)	*+end* ($n=8$)	*–end* ($n=8$)
Resting	330 ± 9	310 ± 10	319 ± 15	310 ± 13
60 mM KCl	125 ± 9	110 ± 10	118 ± 15	105 ± 10
10^{-5} M PE	120 ± 5**	85 ± 5	117 ± 5*	88 ± 10
10^{-5} M ACh	335 ± 10	95 ± 5	305 ± 15	107 ± 20

Internal diameters of arteries at rest, after exposure to KCl, phenylephrine (PE) and acetylcholine (ACh) (arteries pre-contracted with 10^{-5} M PE) are given as mean values±s.e. mean. *$P<0.05$ as compared with sham-operated endothelium-denuded arteries, **$P<0.01$ as compared with CAL endothelium-denuded arteries (one-way ANOVA with Bonferroni post-test).

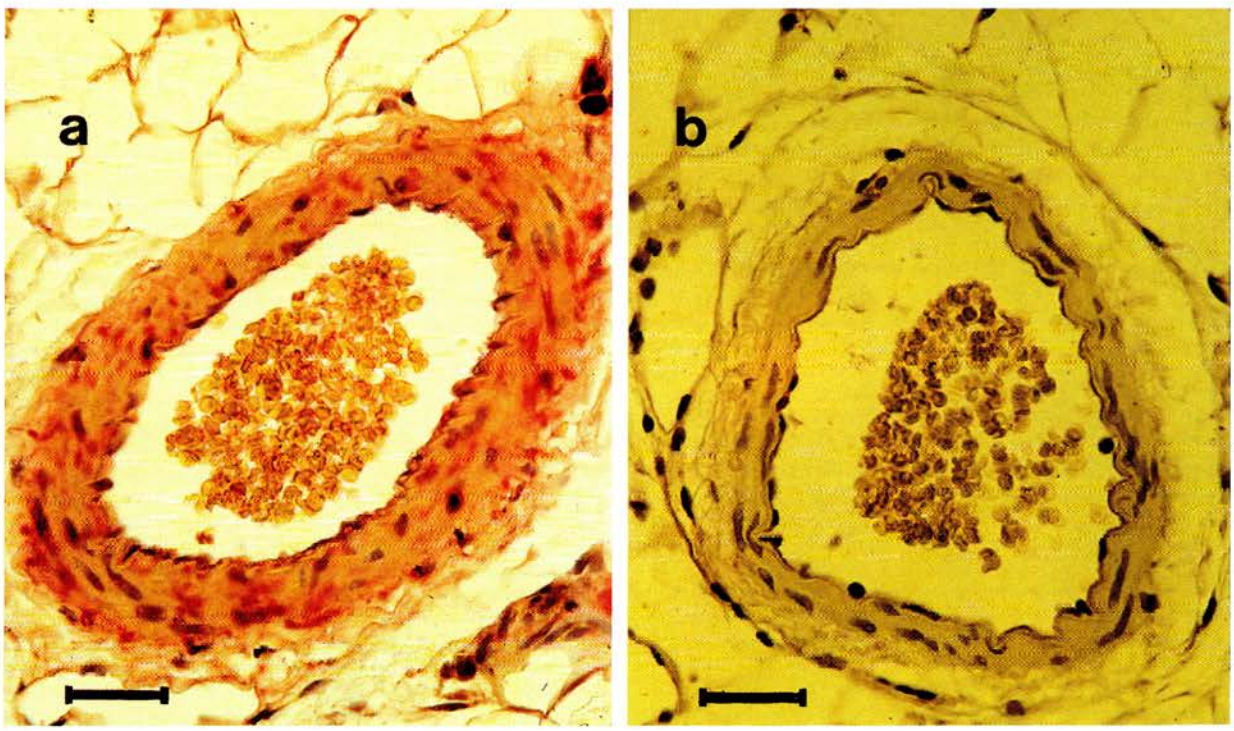

Figure 1 Localization of iNOS by immunohistochemical staining in mesenteric arteries from coronary artery ligation and sham-operated rats. (a) Showing immunoreactive iNOS (pink staining) in endothelial cells, vascular smooth muscle cells and in the adventitia of mesenteric arteries from rats following coronary artery ligation. (b) Showing absence of immunoreactive iNOS in arteries from sham-operated rats. Nuclei are stained with Harris' Haematoxylin (purple staining). Magnification ×400, scale bar = 30 μm.

differences between pD_2 values (CAL, 6.3±0.3; sham-operated, 5.9±0.2) and maximal % constrictions (Figure 2b).

Effect of 1400W and MnTMPyP on vascular responsiveness

Treatment of endothelium-intact arteries from CAL rats with 1400W (10^{-6} M) or MnTMPyP (10^{-4} M) shifted PE CRCs to the right with respect to responses in untreated arteries ($P<0.05$ for both, two-way ANOVA, Figure 3a), indicating a reduction in responsiveness to PE. pD_2 values were significantly decreased in the presence of 1400W or MnTMPyP when compared with untreated arteries (untreated, 6.3±0.1; 1400W, 5.9±0.1; MnTMPyP, 5.8±0.1, $P<0.05$, one-way ANOVA with Bonferroni post-test). Responses to PE in arteries from CAL rats treated with 1400W or MnTMPyP were not significantly different from those in sham-operated arteries (Figure 3a). Responses to PE in endothelium-intact arteries from sham-operated rats were unaffected by 1400W (10^{-6} M) or MnTMPyP (10^{-4} M) (Figure 3b).

In a similar fashion to those arteries treated with 1400W (10^{-6} M) or MnTMPyP (10^{-4} M) alone, combined treatment with both drugs resulted in significant reduction in responsiveness of arteries from CAL rats to PE ($P<0.01$ two-way ANOVA, Figure 3a). pD_2 values were significantly decreased in the presence of 1400W and MnTMPyP when compared with

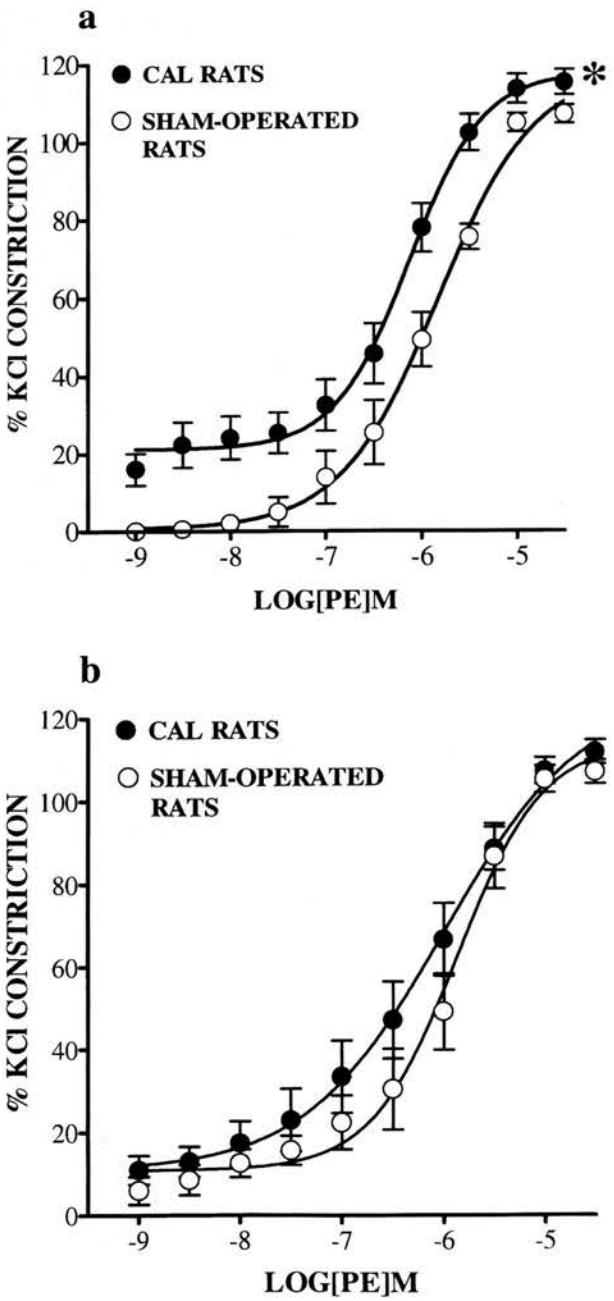

Figure 2 Cumulative concentration response curves (CRC) showing contractile responses to phenylephrine (PE; 1×10^{-9} to 3×10^{-5} M) in (a) endothelium-intact ($n=8$) and (b) endothelium-denuded ($n=6$) small mesenteric arteries from coronary artery ligation (CAL) and sham-operated rats 6 weeks post-surgery. Values are given as means±s.e.mean. *$P<0.01$ as compared with CRCs in sham-operated arteries (two-way ANOVA).

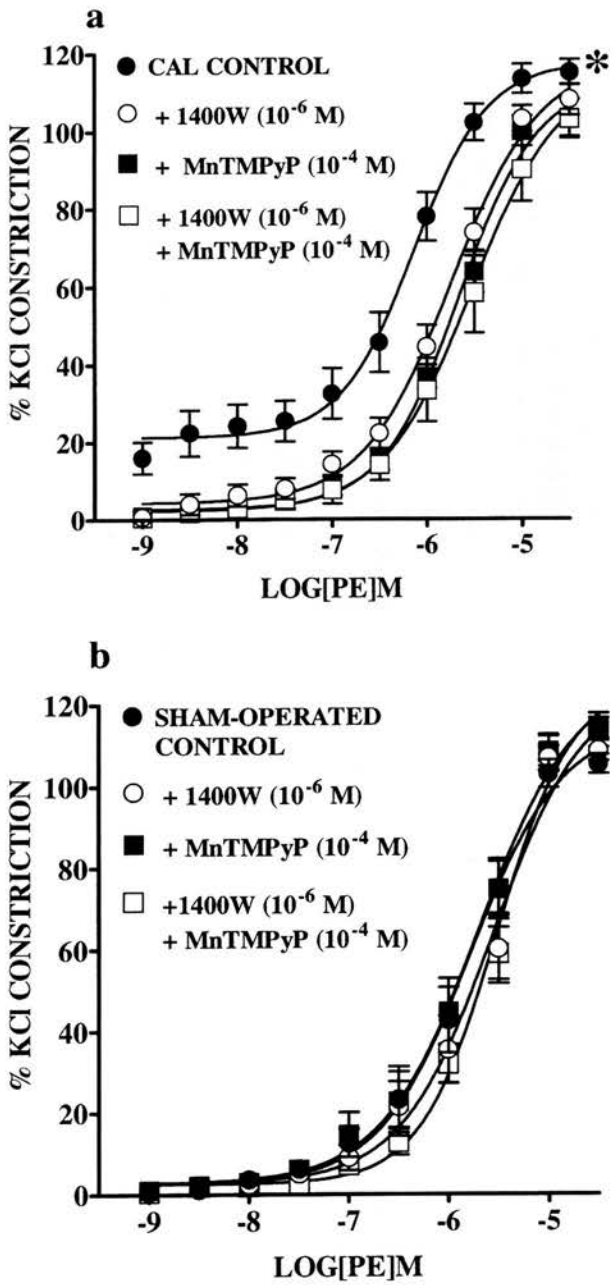

Figure 3 Effect of 1400W (10^{-6} M) and MnTMPyP (10^{-4} M), on their own or together on cumulative concentration response curves (CRC) to phenylephrine (PE; 1×10^{-9} to 3×10^{-5} M) in endothelium-intact small mesenteric arteries from (a) coronary artery ligation (CAL; $n=8$) and (b) sham-operated ($n=8$) rats 6 weeks post-surgery. Values are given as means±s.e.mean. *$P<0.01$ for CRCs in untreated arteries compared with CRCs in 1400W, MnTMPyP treated arteries from CAL rats (two-way ANOVA).

untreated arteries (untreated, 6.3±0.1; 1400W+MnTMPyP, 5.7±0.2, $P<0.01$, one-way ANOVA with Bonferroni post-test). However, no differences were found when compared with responses in arteries treated with 1400W alone. In arteries from sham-operated rats, combined treatment had no significant effect on responses to PE (Figure 3b).

Effect of L-arginine on vascular responsiveness

Treatment of endothelium-denuded arteries from CAL rats with the NOS substrate, L-arginine (10^{-3} M) for 30 min shifted PE CRCs to the right with respect to untreated arteries ($P<0.05$, two-way ANOVA, Figure 4a), indicating that in the presence of L-arginine arteries are less responsive to PE. pD_2 values could not be calculated as maximal constrictions were not reached. L-arginine had no significant effect on PE responses in arteries from sham-operated rats (Figure 4b).

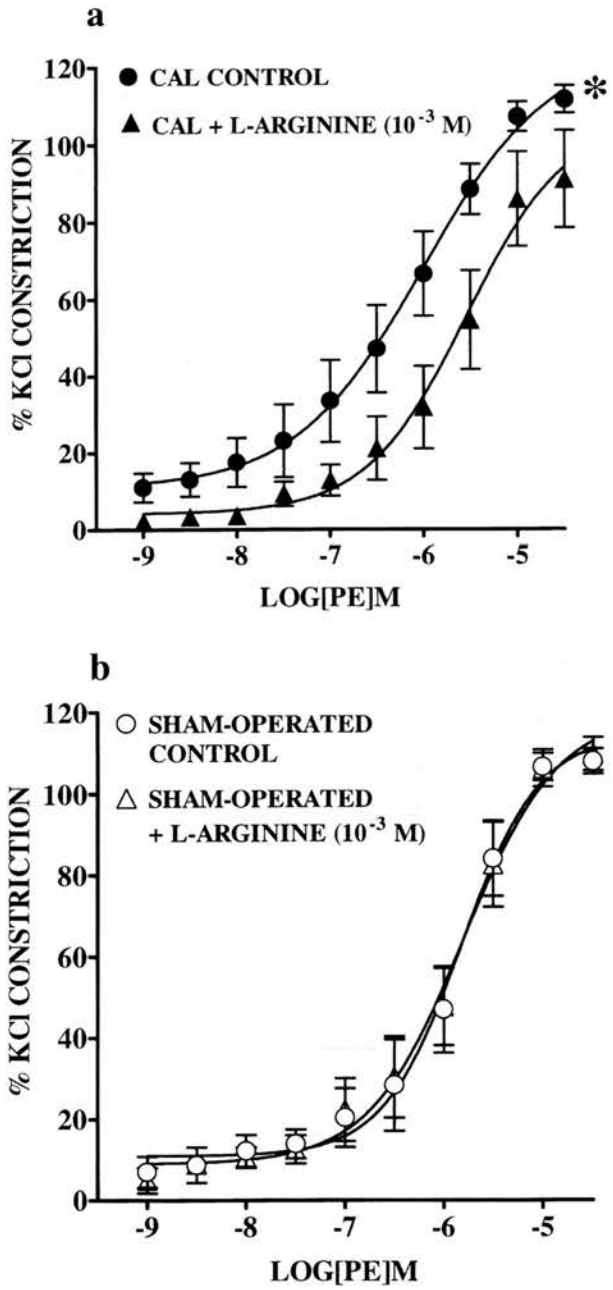

Figure 4 Effect of L-arginine (10^{-3} M) on cumulative concentration response curves (CRC) to phenylephrine (PE; 1×10^{-9} to 3×10^{-5} M) in endothelium-denuded small mesenteric arteries from (a) coronary artery ligation (CAL; $n=6$) and (b) sham-operated ($n=6$) rats 6 weeks post-surgery. Values are given as means±s.e.mean. *$P<0.01$ as compared with CRCs in untreated arteries (two-way ANOVA).

Endothelium-dependent relaxations: effect of superoxide quenching

Following induction of PE-induced tone (CAL, 49.1±2.3%; sham-operated, 52.6±2.4% of maximal PE constriction) in endothelium-intact arteries from CAL and sham-operated rats, cumulative additions of ACh (1×10^{-10} to 3×10^{-6} M) resulted in concentration-dependent relaxations. pD_2 values for cumulative CRCs in arteries from CAL rats were significantly lower than those in sham-operated rats, indicating that endothelium-dependent relaxations were blunted in small mesenteric arteries from CAL rats (CAL, 7.4±0.1; sham-operated, 7.9±0.2, $P<0.05$, two-tailed unpaired t-test). Maximum relaxations to ACh were achieved in most arteries at a concentration of 3×10^{-6} M and no significant differences were found between CAL and sham-operated groups (CAL, 104.1±3.5%; sham-operated, 102.4±2.4%).

In the presence of MnTMPyP (10^{-4} M), relaxations to ACh in arteries from CAL rats were significantly enhanced, with a significant increase in pD_2 values (untreated 7.4±0.1; MnTMPyP, 7.9±0.2, $P<0.05$, two-tailed paired t-test). Treatment of arteries from sham-operated rats with MnTMPyP had no significant effect on ACh CRCs.

Discussion

The salient finding of this study is that iNOS is expressed in mesenteric arteries from rats with CHF. However, despite the presence of iNOS, endothelium-intact small mesenteric arteries from CHF rats were found to be more responsive to phenylephrine that those from sham-operated rats. Hyperesponsiveness of endothelium-intact arteries from CAL rats was reversed by the iNOS inhibitor, 1400W and by the SOD-mimetic, MnTMPyP. Furthermore, supplementation of endothelium-denuded arteries from CAL rats with the NOS substrate resulted in a significant reduction in responsiveness to phenylephrine. These results suggest that substrate deficient, iNOS-derived superoxide may be responsible for the vascular dysfunction associated with this model of CHF.

Increased cytokine levels may serve as a stimulus for iNOS expression in CHF (Katz *et al.*, 1994). Indeed, iNOS is expressed in the myocardium (Fukuchi *et al.*, 1998; Vejlstrup *et al.*, 1998) and skeletal muscle (Adams *et al.*, 1997) in clinical CHF. In the present study, iNOS was expressed in endothelial cells, VSM cells and in the adventitia in small mesenteric arteries from rats with CHF, but not in arteries from sham-operated rats. This is the first study to demonstrate iNOS expression in the peripheral vasculature in experimental CHF. These findings are in contrast to a recent study, which failed to detect iNOS in thoracic aortae from rats 8 weeks after myocardial infarction (Bauersachs *et al.*, 1999). Differences in vessel type may explain this discrepancy. Moreover, rats used in the present study had larger infarcts than those used in the aforementioned study, perhaps suggesting that the severity of the model influences iNOS expression.

During endotoxemia, expression of iNOS in the vasculature, and the subsequent production of NO, plays an important role in the vascular hyporeactivity to vasoconstrictors (for review see Thiemermann, 1994). Therefore, in this model of CHF, increased production of NO from iNOS would be expected to reduce vascular responsiveness to phenylephrine. Somewhat paradoxically, endothelium-intact small me-

senteric arteries from CHF rats were more responsive to phenylephrine than arteries from sham-operated rats. There was no significant difference between responses to phenylephrine in endothelium-denuded arteries from CHF or sham-operated rats, demonstrating that this vascular dysfunction is dependent on the presence of the endothelium. Basal NO from eNOS serves to dampen the effects of vasoconstrictors. One could speculate, therefore, that decreased basal release of NO is responsible for the hyperesponsiveness to phenylephrine. Teerlink *et al.* (1994) showed increased adrenergic responsiveness of thoracic aortic rings from rats with CHF, which was dependent on the presence of the endothelium. Furthermore, their study demonstrated that impaired basal release of NO from the endothelium was responsible for this vascular dysfunction.

To investigate the role that iNOS plays in modulating vascular function in this model of CHF we used a novel selective iNOS inhibitor, 1400W, and the NOS substrate, L-arginine. 1400W is an irreversible inhibitor of iNOS that is at least 1000 fold more selective for iNOS than eNOS in rats (Garvey *et al.*, 1997). Furthermore, 1400W is effective in abolishing iNOS activity and attenuating hypotension associated with endotoxemia in rats (Wray *et al.*, 1998). In the present study we show, somewhat surprisingly, that inhibition of iNOS with 1400W reversed, rather than potentiated, the hyperesponsiveness of small mesenteric arteries from CHF rats. These results suggest that induction of iNOS does not result in the expected increase in NO generation. Instead, expression of the enzyme appears to be a major contributory factor in the hyperresponsive nature of endothelium-intact CHF arteries. In experimental endotoxemia addition of the NOS substrate, L-arginine, to isolated blood vessels increases NO production from iNOS and potentiates hyporesponsiveness to vasoconstrictors (Julou-Schaeffer *et al.*, 1990). Here we show that supplementation of endothelium-denuded small mesenteric arteries from CHF rats, but not sham-operated rats, with a supramaximal concentration of L-arginine results in a reduction in responsiveness to phenylephrine, presumably through production of NO from iNOS. These results suggest that although iNOS is present in small mesenteric arteries from CHF rats, it is unable to synthesize NO because there is insufficient substrate. Recent studies have shown that iNOS, when deficient in its substrate/cofactors, produces superoxide rather than NO (Xia & Zweier, 1997; Xia *et al.*, 1998). Therefore, in this model of CHF, it is possible that a deficiency in L-arginine will not only prevent iNOS from generating NO but will also result in the enzyme producing superoxide. Increased scavenging of NO by superoxide would result in a reduction in the bioavailability of endothelium-derived NO, which may explain the marked increase in responsiveness of endothelium-intact arteries from CHF rats to phenylephrine.

To determine if increased superoxide production plays a role in modulating vascular function in this model of CHF, we used the cell permeable metalloporphyrin SOD mimetic, MnTMPyP. In a similar fashion to 1400W, MnTMPyP reversed the hyperesponsiveness of endothelium-intact small mesenteric arteries from CHF rats. This implies that mesenteric arteries from CHF rats are indeed generating superoxide, which is responsible for the marked elevation in responsiveness to phenylephrine. Numerous studies have demonstrated increased superoxide production in CHF (McMurray *et al.*, 1990; Belch *et al.*, 1991; Bauersachs *et al.*, 1999). NADH/NADPH oxidases (Bauersachs *et al.*, 1999), autoxidation of catecholamines, increased arachidonate metabolism and inflammatory cytokines have all been suggested as possible sources of superoxide in CHF (for review see Givertz & Colucci, 1998). In the present study, however, both inhibition of iNOS and superoxide quenching reverses the hyperresponsiveness to phenylephrine suggesting that iNOS is the source of superoxide in this model of CHF. Indeed, there were no significant differences between responses to phenylephrine in arteries treated with 1400W alone and those treated with both 1400W and MnTMPyP.

Although MnTMPyP has been shown to protect SOD-null *E. coli* against oxidant stress (Faulkner *et al.*, 1994), recent studies provide evidence that MnTMPyP may actually scavenge NO itself and directly inhibit the activity of eNOS (Pfeiffer *et al.*, 1998; Mackenzie *et al.*, 1999). Mackenzie *et al.* demonstrated an augmentation of phenylephrine-induced constrictions by MnTMPyP in isolated rat aortic rings that is reversed by inhibition of eNOS. However, in the present study MnTMPyP reduced responsiveness to phenylephrine in endothelium-intact small mesenteric arteries from CHF rats and had no significant effect on responses in arteries from sham-operated rats. We are convinced, therefore, that the effects of MnTMPyP in the present study are a direct consequence of its SOD-mimetic properties.

This study presents an interesting new facet to the impact of iNOS in CHF. In this model of CHF, instead of generating large quantities of NO, iNOS appears to be generating superoxide, perhaps because of a deficiency in its substrate, L-arginine. Moreover, this increase in superoxide production is responsible for the hyperresponsive nature of endothelium-intact small mesenteric arteries from rats with CHF. The precise mechanism and time course by which superoxide results in arteries being hyperresponsive is unclear from these experiments alone. However, the fact that the hypereactivity is dependent on the endothelium suggests that increased scavenging of basal, eNOS-derived NO by superoxide is responsible. In addition to impaired basal release of NO, we also show that ACh-mediated endothelium-dependent relaxations are impaired in arteries from rats with CHF. Moreover, relaxations to ACh were improved in the presence of MnTMPyP.

In summary, the present study suggests that substrate deficient, iNOS-derived superoxide is responsible for increased responsiveness of endothelium-intact mesenteric arteries, possibly as a result of impaired release of endothelial-derived NO. While it remains to be established if this study mirrors clinical CHF, our findings may represent an important mechanism for the endothelial dysfunction and raised peripheral resistance associated with CHF.

A.A. Miller is the recipient of an MRC PhD studentship. This study was supported, in part, by the British Heart Foundation (FS/95061). We gratefully acknowledge the help of Dr Pauline McEwan and Mr Lorcan Sherry in the establishment of immunohistochemical techniques.

References

ADAMS, V., YU, J., MOBIUS-WINKLER, S., LINKE, A., WEIGL, C., HILBRICH, L., SCHULER, G. & HAMBRECHT, R. (1997). Increased inducible nitric oxide synthase in skeletal muscle biopsies from patients with chronic heart failure. *Biochem. Mol. Med.*, **61**, 152–160.

BAUERSACHS, J., BOULOUMIÉ, A., FRACCAROLLO, D., HU, K., BUSSE, R. & ERTL, G. (1999). Endothelial dysfunction in chronic myocardial infarction despite increased vascular endothelial nitric oxide synthase and soluble guanylate cyclase expression. Role of enhanced vascular superoxide production. *Circulation*, **100**, 292–298.

BELCH, J.J.F., BRIDGES, A.B., SCOTT, N. & CHOPRA, M. (1991). Oxygen free radicals and congestive heart failure. *Br. Heart J.*, **65**, 245–248.

CARVILLE, C., ADNOT, S., SEDIAME, S., BENACERRAF, S., CASTAIGNE, A., CALVO, F., DE CREMOU, P. & DUBOIS-RANDÉ, J.-L. (1998). Relation between impairment of nitric oxide pathway and clinical status in patients with congestive heart failure. *J. Cardiovasc. Pharmacol.*, **32**, 562–570.

DREXLER, H., HAYOZ, D., MUNZEL, T., HORNIG, B., JUST, H., BRUNNER, H.R. & ZELIS, R. (1992). Endothelial function in chronic congestive heart failure. *Am. J. Cardiol.*, **69**, 1596–1601.

ELSNER, D., MUNTZE, A., KROMER, P. & RIEGGER, A. (1991). Systemic vasoconstriction induced by inhibition of nitric oxide synthesis is attenuated in conscious dogs with heart failure. *Cardiovasc. Res.*, **25**, 438–440.

FALLOON, B.J., BUND, S.J., TULIP, J.R. & HEAGERTY, A.M. (1993). In vitro perfusion studies of resistance artery function in genetic hypertension. *Hypertension*, **22**, 486–495.

FAULKNER, K.M., LIOCHEV, S.I. & FRIDOVICH, I. (1994). Stable Mn(III) porphyrins mimic superoxide dismutase *in vitro* and substitute for it *in vivo*. *J. Biol. Chem.*, **269**, 23471–23476.

FUKUCHI, M., HUSSAIN, S.N. & GIAID, A. (1998). Heterogeneous expression and activity of endothelial and inducible nitric oxide synthases in end-stage human heart failure. Their relation to lesion site and beta-adrenergic receptor therapy. *Circulation*, **98**, 132–139.

GARVEY, E.P., OPLINGER, J.A., FURFINE, E.S., KIFF, R.J., LASZLO, F., WHITTLE, B.J.R. & KNOWLES, R.G. (1997). 1400W a slow, tight binding, and highly selective inhibitor of inducible nitric-oxide synthase *in vitro* and *in vivo*. *J. Biol. Chem.*, **272**, 4959–4963.

GIVERTZ, M.M. & COLUCCI, W.S. (1998). New targets for heart-failure therapy: endothelin, inflammatory cytokines, and oxidative stress. *Lancet*, **352** (Suppl I), 34–38.

GRYGLEWSKI, R.J., PALMER, R.M.J. & MONCADA, S. (1986). Superoxide anion is involved in the breakdown of endothelium-derived vascular relaxing factor. *Nature*, **320**, 454–456.

HABIB, F., DUTKA, D., CROSSMAN, D., OAKLEY, C.M. & CLELAND, J.G.F. (1994). Enhanced basal nitric oxide production in heart failure: another failed counter-regulatory vasodilator mechanism? *Lancet*, **344**, 371–373.

HALPERN, W. & KELLEY, M. (1991). In vitro methodology for resistance arteries. *Blood Vessels*, **28**, 245–251.

JULOU-SCHAEFFER, G., GRAY, G.A., FLEMING, I., SCHOTT, C., PARRATT, J.R. & STOCLET, J.C. (1990). Loss of vascular responsiveness induced by endotoxin involves the L-arginine pathway. *Am. J. Physiol.*, **259**, H1038–H1043.

KATZ, S.D., RAO, R., BERMAN, J.W., SCHWARTZ, M., DEMOPOLOUS, L., BIJOU, R. & LEJEMTEL, T.H. (1994). Pathophysiology correlates of increased serum tumour necrosis factor in patients with congestive heart failure. Relation to nitric oxide-dependent vasodilation in the forearm circulation. *Circulation*, **90**, 12–16.

MACKENZIE, A., & MARTIN, W. (1998). Loss of endothelium-derived nitric oxide in rabbit aorta by oxidant stress: restoration by superoxide dismutase mimetics. *Br. J. Pharmacol.*, **124**, 719–728.

MACKENZIE, A., FILIPPINI, S. & MARTIN, W. (1999). Effects of superoxide dismutase mimetics on the activity of nitric oxide in rat aorta. *Br. J. Pharmacol.*, **127**, 1159–1164.

MCMURRAY, J., MCLAY, J., CHOPRA, M., BRIDGES, A. & BELCH, J.J. (1990). Evidence for enhanced free radical activity in chronic congestive heart failure secondary to coronary artery disease. *Am. J. Cardiol.*, **65**, 1261–1262.

MICKLEY, E.J., GRAY, G.A. & WEBB, D.J. (1997). Activation of endothelin ET_A receptors masks the constrictor role of endothelin ET_B receptors in isolated small mesenteric arteries. *Br. J. Pharmacol.*, **120**, 1376–1382.

MONCADA, S., PALMER, R.M.J. & HIGGS, E.A. (1991). Nitric oxide: physiology, pathophysiology and pharmacology. *Pharmacol. Rev.*, **43**, 109–141.

MULDER, P., RICHARD, V., BOUCHART, F., DERUMEAUX, O., MUNTER, K. & THUILLEZ, C. (1998). Selective ET_A receptor blockage prevents left ventricle remodelling and deterioration of myocardial function in experimental heart failure. *Cardiovasc. Res.*, **39**, 600–608.

PFEFFER, M.A., PFEFFER, J.M., FISHBEIN, M.C., FLETCHER, P.J., SPADARO, J., KLONER, R.A. & BRAUNWALD, E. (1979). Myocardial infarct size and ventricular function in rats. *Circ. Res.*, **44**, 503–512.

PFEIFFER, S., SCHRAMMEL, A., KOESLING, D., SCHMIDT, K. & MAYER, B. (1998). Molecular actions of a Mn(III)Porphyrin superoxide dismutase mimetic and peroxynitrite scavenger: reaction with nitric oxide and direct inhibition of NO synthase and soluble guanylyl cyclase. *Mol. Pharmacol.*, **53**, 795–800.

RAMSEY, M.W. & JONES, C.J. (1994). Large arteries are more than just passive conduits. *Br. Heart J.*, **72**, 3–4.

SCHOTT, C., GRAY, G.A. & STOCLET, J.-C. (1993). Dependence of endotoxin-induced vascular hyporeactivity on extracellular L-arginine. *Br. J. Pharmacol.*, **108**, 38–43.

TEERLINK, J.R., GRAY, G.A., CLOZEL, M. & CLOZEL, J.-P. (1994). Increased vascular responsiveness to norephinephrine in rats with heart failure is endothelium dependent. Dissociation of basal and stimulated nitric oxide release. *Circulation*, **89**, 393–401.

THIEMERMANN, C. (1994). The role of the L-arginine: nitric oxide pathway in circulatory shock. *Adv. Pharmacol.*, **28**, 45–79.

VEJLSTRUP, N.G., BOULOUMIE, A., BOESGAARD, S., ANDERSEN, C.B., NIELSEN-KUDSK, J.E., MORTENSEN, S.A., KENT, J.D., HARRISON, D.G., BUSSE, R. & ALDERSHVILE, J. (1998). Inducible nitric oxide synthase (iNOS) in the human heart: expression and localisation in congestive heart failure. *J. Mol. Cell. Cardiol.*, **30**, 1215–1223.

WINLAW, D.S., SMYTHE, G.A., KEOGH, A.M., SCHYVENS, C.G., SPRATT, P.M. & MACDONALD, P.S. (1994). Increased nitric oxide production in heart failure. *Lancet*, **344**, 373–374.

WRAY, G.M., MILLAR, C.G., HINDS, C.J. & THIEMERMANN, C. (1998). Selective inhibition of the activity of inducible nitric oxide synthase prevents the circulatory failure, but not the organ injury/dysfunction, caused by endotoxin. *Shock*, **9**, 329–335.

XIA, Y. & ZWEIER, J.L. (1997). Superoxide and peroxynitrite generation from inducible nitric oxide synthase in macrophages. *Proc. Natl. Acad. Sci. U.S.A.*, **94**, 6954–6958.

XIA, Y., ROMAN, L.J. MASTERS, B.S.S. & ZWEIER, J.L. (1998). Inducible nitric-oxide synthase generates superoxide from the reductase domain. *J. Biol. Chem.*, **273**, 22635–22639.

(Received April 14, 2000
Revised June 12, 2000
Accepted June 12, 2000)